Dissecting the Role of microRNAs in the Radiation Response of Human Prostate Cancer

Thesis

DISSECTING THE ROLE OF microRNAs IN THE RADIATION RESPONSE OF HUMAN PROSTATE CANCER

Rihan El Bezawy, Degree in Medical Biotechnology

Thesis submitted to the Open University for the degree of

Doctor of Philosophy

School of Life, Health and Chemical Sciences

April 2018

Fondazione IRCCS Istituto Nazionale dei Tumori

Milan, Italy


بسم الله الرحمن الرحيم

ABSTRACT

Radiotherapy is one of the gold standard treatments for non-metastatic prostate cancer (PCa), although development of radioresistance limits its effectiveness. Mounting evidence supports the ability of microRNAs to interfere with different radioresistance-associated pathways, suggesting their potential as radiosensitizers.

To identify miRNAs likely to be involved in influencing PCa radiation response, we first performed miRNA-profiling analysis of PCa cell lines exposed to photon irradiation. Based on their modulation upon radiation exposure, and their role in regulating pathways associated with radiation response we singled-out and characterized miR-23a-3p and miR-24-3p as potential radiosensitizer molecules in PCa, unrevealing a central role of miR-23a-3p-IL-6 axis.

In the framework of miRNAs downregulated in PCa and known to regulate genes relevant to radiation, miR-875-5p and miR-205 were identified.

Reconstitution of miR-875-5p, the expression of which directly correlates with that of E-cadherin, was able to enhance radiation response in PCa cell lines and xenografts through EGFR direct targeting. Consistent with the established role of EGFR in sustaining epithelial-to-mesenchymal transition (EMT) and promoting DNA repair following radiation, we found that miR-875-5p reconstitution in PCa cells counteracted EMT and impaired DNA lesion clearance, mainly via impairment of EGFR-ZEB1 axis.

Restoration of miR-205 was able to significantly enhance PCa sensitivity to radiation, in both cell and animal models. Specifically, we found that miR-205 radiosensitizing effect was imputable to the downregulation of PKC-ε. Consistent with PKC-ε well-established role in DNA damage repair, we found that pEGFR and, consequently, pDNA-PK levels were significantly reduced by

miR-205 reconstitution, thus suggesting that miR-205 enhances PCa radiation response via disruption of PKC-ε−EGFR−DNA-PK axis.

Overall, the results of this project support the clinical interest in developing novel therapeutic approaches based on miRNA reconstitution (miR-23a-3p, miR-875-5p and miR-205) to enhance PCa response to radiotherapy.

A Papà

ACKNOWLEDGEMENTS

I apologize to the reader for preferring to write the acknowledgements in my native language (Italian). This is to make sure that all the acknowledged persons could fully understand.

Dedico questa tesi, tutto il percorso di dottorato, e tutta la mia vita a mio Papà. A Te dedico questo momento cui avresti voluto assistere, certa che in qualche modo tu lo stia facendo, e garantendoti che in questo, come in tutti i giorni della mia vita, sei e sarai sempre con me. Sono felice di essere qui oggi a dedicarti la mia tesi, dicendoti che ho mantenuto la promessa e, come da tuo desiderio, sto ottenendo il dottorato prima di intraprendere l'importante passo del matrimonio. Sono orgogliosa di avercela fatta e di non aver deluso le tue aspettative, spero che lo sia anche Tu. A Te dedico il percorso di dottorato per cui mi hai sempre spronata e incoraggiata, e Ti dedico ogni successo e ogni conquista, piccola e grande, di ogni giorno. Ti ringrazio per avermi trasmesso sicurezza e determinazione, e per avermi insegnato a credere in me stessa. Ti ringrazio per avermi donato la tua positività e forza nell'andare avanti e affrontare ogni sfida con il sorriso, il tuo regalo più grande. Ti ringrazio per essere il Papà migliore che sia mai esistito.

Ringrazio la mia Famiglia, per aver sempre creduto in me e per avermi incoraggiata a dare sempre il meglio di me stessa, supportandomi nei momenti di sconforto e assecondando le mie volontà ed inclinazioni. Ti ringrazio Mamma per la dolcezza e la comprensione con cui mi hai insegnato ad essere una Donna tenace e determinata, nella vita come nel lavoro. Ti ringrazio per avermi sempre sostenuta e spronata nel mio percorso di studi, permettendomi di raggiungere livelli sempre più alti di istruzione e aiutandomi a coltivare ambizione e determinazione. Spero con questo importante traguardo di renderti ancora più orgogliosa della piccola donna che hai cresciuto. Ringrazio mia sorella, Rasha, per avermi accompagnata nei momenti più importanti del mio percorso. Grazie per avermi indicato questo percorso e per avermi sostenuta nella sua realizzazione, e grazie per avermi

sempre aiutata a crescere e tirare fuori il meglio di me in tutte le situazioni. Ringrazio mio fratello, Kariim, per avermi insegnato, senza saperlo, forza e caparbietà, aiutandomi a non mollare mai, affermandomi e credendo in me stessa ancor prima che lo facessero gli altri. Ringrazio Adham, il mio piccolo eroe, che, pur essendo nella mia vita da poco più di un anno, con il suo affetto e il suo immancabile sorriso è già così importante da regalarmi entusiasmo e serenità nei momenti di sconforto e di difficoltà.
Grazie per essere la Famiglia più bella che potessi desiderare.

Ringrazio te Haithm, mio fidanzato e compagno di vita, che da sempre credi in me e mi fai sentire unica e speciale. Grazie di cuore per tutte le volte che mi hai aiutata a rialzarmi e ritrovare forza, serenità e solarità, sostenendo e proteggendo la mia visione positiva e sognatrice della vita, che ogni giorno mi permette di essere quello che sono, e che mi ha permesso di affrontare in un modo meraviglioso questo percorso. Il desiderio di renderti orgoglioso di me è una delle mie più forti motivazioni, e la consapevolezza di essere sempre la migliore ai tuoi occhi, come non smetti mai di dirmi, è la mia carica più grande. Ti prometto qui, ora e per sempre, che non smetterò mai di inseguire il sogno di renderti un marito orgoglioso di sua moglie e della mamma dei suoi figli. Grazie per tutto quello che sei e che mi regali.

Grazie al fantastico gruppo di lavoro che ha reso piacevole anche i momenti più difficili e sfidanti.
Grazie a te Vale, sia per avermi aiutata concretamente nella realizzazione di questo progetto, sia e soprattutto per avermi sempre supportata con i tuoi consigli e con l'affetto di una collega che in realtà è un'amica speciale.
Grazie Marta e grazie Fede per esserci sempre con una lealtà e un sorriso che hanno la forza di trasformare il lavoro in passione. Grazie per i momenti di sfogo e di condivisione senza i quali ora non sarei qui e non sarei quello che sono.
Grazie Paolo per il tuo indispensabile contributo nella realizzazione di questo progetto e di questo percorso, e per i tuoi consigli che mi aiutano a crescere

ogni giorno, e grazie per essere per noi un modello di ricercatore da ammirare e seguire.
Grazie Marco per gli insegnamenti che mi hai trasmesso e per i consigli e suggerimenti che hanno reso migliore questo percorso di studi e di vita.
Grazie Stefano per rendere accessibile anche a me e a noi il mondo altrimenti incomprensibile della bioinformatica e della statistica, rendendoti sempre disponibile per confronti e chiarimenti.
Grazie a tutti per aver reso questo posto una seconda casa, realizzando il sogno di andare a lavoro con il sorriso.

Grazie Dottoressa Zaffaroni, che è ben più di un capo e di un supervisor. Grazie per avermi consentito ed avermi incoraggiata ad intraprendere il PhD e per avermi costantemente aiutata a crescere professionalmente in tutti gli aspetti che fanno parte di questo percorso. La ringrazio per aver sempre rispettato l'importanza del dottorato, dando sempre la priorità al mio PhD e consentendomi di cogliere tutte le opportunità di formazione e crescita che questo programma ha offerto. Grazie per tutti gli insegnamenti e i consigli che porterò sempre con me e per l'umanità e la comprensione che ha mostrato nei miei confronti nei momenti più difficili e importanti.

Grazie Dottoressa Tagliabue, mia supervisor, per essersi sempre dimostrata disponibile a incontri e confronti durante questi anni, e per avermi incoraggiata nel mio percorso.
Grazie al nostro coordinatore PhD, Luca, per il tuo impegno quotidiano che sta rendendo sempre migliore non solo il programma di dottorato ma anche noi studenti, stimolandoci e aiutandoci ad essere ricercatori critici e consapevoli.
Grazie Daniela per i tuoi preziosissimi consigli che hanno reso migliore il mio inglese e la mia scrittura. Grazie per la tua disponibilità e la tua presenza su cui ho sempre potuto contare. E soprattutto grazie per avermi sostenuta aiutandomi a scoprire e coltivare la mia passione per la comunicazione, offrendomi occasioni di crescita e di miglioramento.

ACKNOWLEDGEMENTS

Grazie Dottoressa Mezzananica e grazie Dottor Castellano, per aver mostrato interesse e disponibilità nel ricoprire il ruolo di examiner nel momento conclusivo del mio percorso di PhD. E grazie per l'impegno e il tempo che dedicherete alla lettura e al miglioramento di questa tesi.

Grazie a tutti coloro che hanno partecipato a questo progetto.

Grazie

LIST OF ABBREVIATIONS

ABBREVIATION	DESCRIPTION
ADT	Androgen Deprivation Therapy
AR	Androgen Receptor
AS	Active Surveillance
ATM	Ataxia Telangiectasia Mutated
CDH1	Cadherin 1
cDNA	Complementary DNA
CFRT	Conventionally Fractionated Radiation Therapy
CHK1	Checkpoint Kinase 1
CNAO	Centro Nazionale di Adroterapia Oncologica
CRPC	Castration-Resistant Prostate Cancer
CT	Computered Tomography
CTNNB1	Catenin B
DE	Differential Expression
DNA-PK	DNA-Dependent Protein Kinase
DSB	Double Strand Break
EGFR	Epidermal Growth Factor Receptor
EMT	Epithelial to Mesenchymal Transition
FC	Fold Change
FDR	False Discovery Rate
γ–H2AX	Phosphorylated H2A Histone Family Member X
GAPDH	Glyceraldehyde-3-Phosphate Dehydrogenase
GO	Gene Ontology
H2AX	H2A Histone Family Member X
HR	Homologous Recombination
IL-6	Interleukin-6
IL-6R	Interleukin-6 Receptor
IR	Ionizing Radiation
LAMP3	Lysosomal Associated Membrane Protein 3
LIN7C	Lin-7 Homolog C
miR-Mask	microRNA masking
miRNA	microRNA
mRNA	Messenger RNA
NHEJ	Non Homologous End Joining
Pca	Prostate Cancer
PE	Plating Efficiency
pEGFR	Phosphorylated Epidermal growth factor receptor
PKC-ε	Protein Kinase C Epsilon
PSA	Prostate Specific Antigen
qRT-PCR	Quantitative Real-Time Polymerase Chain Reaction
RAB27A	Member RAS Oncogene Family
RBE	Realtive Biological Effectiveness
RIN	RNA Integrity Number
RQ	Relative Quantity
RT	Radiotherapy
SCID	Severe Combined Immunodeficiency
SD	Standard Deviation
siRNA	Small Interfering RNA
STAT1	Signal Transducer And Activator Of Transcription 1
UTR	Untranslated Region
ZEB1	Zinc Finger E-box Binding Homeobox 1

TABLE OF CONTENTS

LIST OF FIGURES

INTRODUCTION

1. INTRODUCTION

1.1 PROSTATE CANCER

1.1.1 Epidemiology

The prostate (from Ancient Greek prostates (aden), literally "one who stands before, leader, guardian") is an exocrine gland of the male reproductive system. The size of a healthy prostate gland is about that of a chestnut and its weight ranges from 7 to 16 grams. The prostate is located directly below the bladder and above the muscles of the pelvic floor. Its location with respect to the bladder, if seen from below, justifies the etymology of its name, as it "stands before" the bladder (Fig. 1.1) [1].

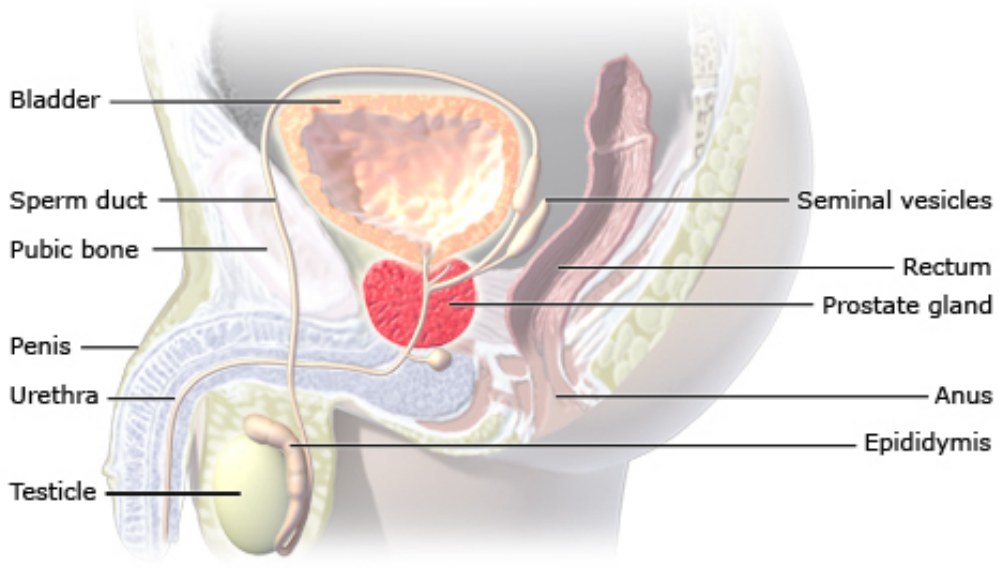

Figure 1.1 Location of the prostate gland

The main function of the prostate is to secrete an alkaline fluid that constitutes approximately 30% of the semen volume, along with sperm cells from the testicles and seminal vesicle fluid. The alkalinity of semen helps neutralize the acidity of the vaginal tract, prolonging the lifespan of sperm. The prostatic fluid is expelled in the first ejaculate fractions, together with most of the spermatozoa. The muscles of the prostate also ensure that the semen is forcefully pressed into the urethra and then expelled outwards during ejaculation [1].

Among the components of the prostatic fluid there is a particular protein called Prostate Specific Antigen (PSA), which is a biomarker used for the detection of prostate cancer [2].

Prostate cancer (PCa) is the first cancer for incidence and second for mortality, according to the data provided from Cancer Statistics 2018 (Fig.1.2) [3].

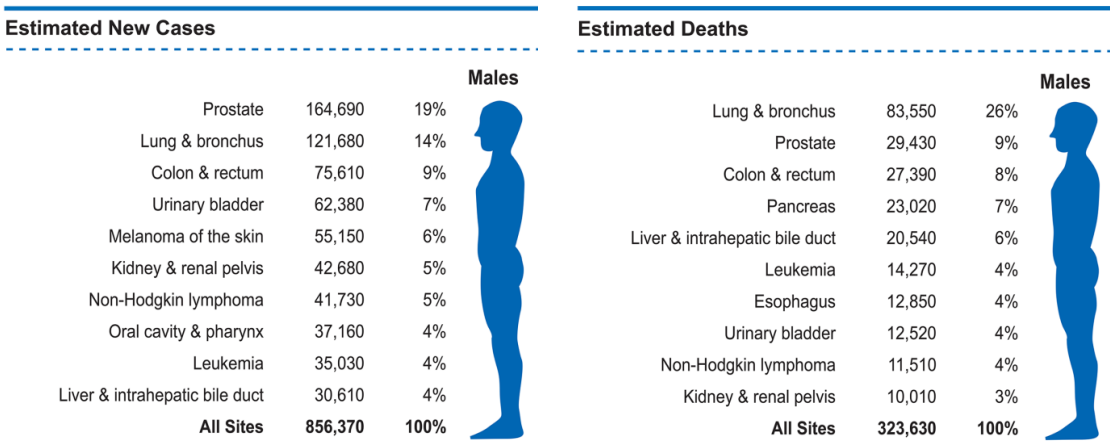

Figure 1.2 Ten Leading Cancer Types for the Estimated New Cancer Cases and Deaths by Sex, United States, 2018 (Adapted from Siegel et al. Cancer Statistics, 2018).

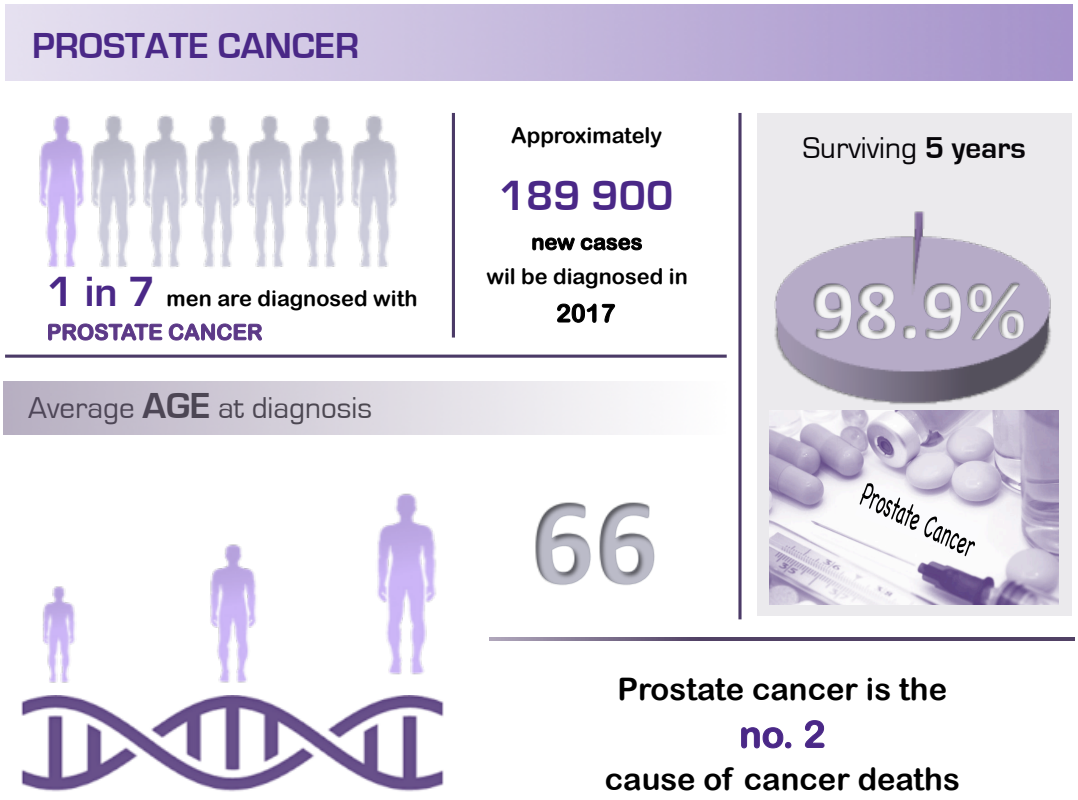

Figure 1.3 Schematic summary of PCa epidemiology

Prostate cancer diagnosis is very common in industrialized countries for two main reasons: i) the great development of techniques that allow an early diagnosis and ii) the increased aging of population. Nowadays, the factors that determine the risk of developing prostate cancer are not totally understood although there is increasing evidence for a possible link between nutrition and prostate cancer development [4]. For example, in a recent case–control study from Italy it was observed that a diet rich in animal products such as red meat, dairy products and refined cereals and sugars appears to have an unfavourable role on prostate cancer [5]. Another main risk factor for prostate cancer is age. The probability of developing the tumour increases from 0.005% in men younger than 39 years to 13.7% in men between 60 and 79 years [6]. Prostate cancer appears to be linked to hereditary factors in a minority of cases (<15%).

The risk of developing the tumour is twice as high for those with a relative (father, brother, etc.) affected by the disease compared to those not having any tumour case in their family. Moreover, the presence of mutations in specific genes such as BRCA1 and BRCA2, already involved in promoting the onset of breast and ovarian cancers, may increase the risk of developing prostate cancer [7].

Lastly, studies that establish a correlation between the prostate cancer and chronic or recurrent prostate inflammation are constantly increasing, yet only few epidemiological studies have confirmed this data. Although the cause of this inflammatory reaction is still unknown, some studies have shown that viruses, bacteria or toxic substances introduced into the body can play a decisive role. However, although microorganisms are thought to cause prostatitis or sexually transmitted infections, their role in the development of prostate cancer is still unknown [8].

1.1.2 Diagnosis

Over the years, many markers have been used for the diagnosis and follow-up of prostate cancer. Until recently, prostate-specific antigen (PSA) was considered the most reliable marker for prostate cancer detection.

PSA, a kallikrein-like serine protease, is a glycoprotein produced by the prostate gland. As long as the prostate grows, blood levels of PSA get higher. In 1994, the FDA approved the use of PSA test in conjunction with a digital rectal exam (DRE) for asymptomatic prostate cancer diagnosis. Specifically,

blood PSA levels higher than 4.0 ng/mL are considered an indication of prostate cancer [9]. However, yet being organ-specific, PSA is not a cancer specific marker. Indeed, other conditions within the prostate have an elevation of serum PSA levels as a consequence, such as benign prostate hyperplasia (BPH), prostatitis and urinary tract infection. For this reason, PSA screening has fallen under controversy. Indeed, out of the men that display elevated PSA levels in the blood, only 25% are associated with prostate cancer [10].

At present, diagnosis of PCa is based on examination of histopathological specimens from the organ, usually obtained by transrectal or transperineal ultrasound guided core biopsies.

Prostate adenocarcinoma is graded according to the Gleason Pattern Score. This histopathologic grading system was developed by Donald F. Gleason in the 1960s and 1970s.

The system is based on the architectural patterns of the tumour where the Gleason score is the sum of two scores, each varying from 1 (well-differentiated) to 5 (undifferentiated), representative of the most prevalent and the second most prevalent differentiation grade within the tumour, respectively (Fig. 1.4). To be counted, a pattern needs to occupy more than 5% of the biopsy specimen [11].

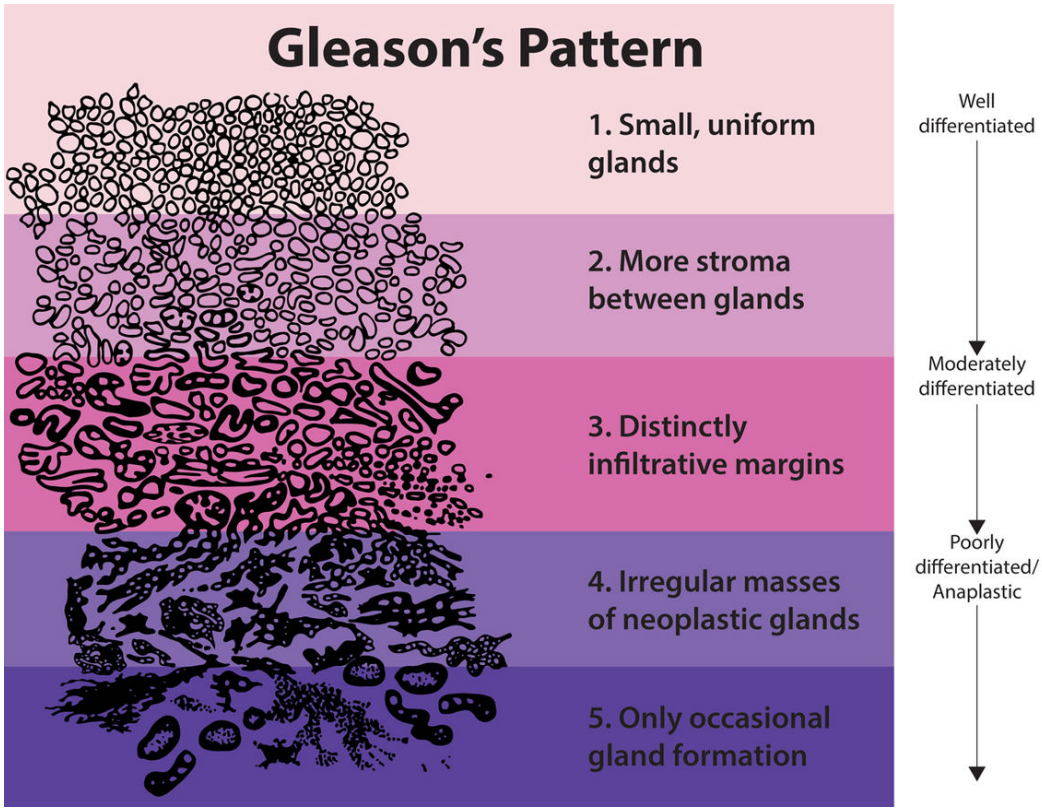

Figure 1.4 Architectural patterns of the Gleason System

The original Gleason grading system was modified in 2005 during a consensus conference of the International Society of Urological Pathology (ISUP) [12]. The ISUP 2005 modifications included changes to the morphologic criteria to include poorly formed glands as Gleason pattern 4 and restricted criteria to distinguish cribriform pattern 4 vs. cribriform pattern 3, as well as recommendations on how to grade the different variants of prostate cancer and on how to report the Gleason grading in needle biopsies and radical prostatectomies. However, after the 2005 modifications, several aspects of the grading system continued to be unresolved [11]. Another consensus of 2014 generated several further modifications to the original scheme proposed by Gleason, resulting in a current grading system that is dramatically different from the original one. According to the new grading system, certain patterns of Gleason score 6 are now

considered pattern 7, and therefore, the contemporary Gleason score 6-cancer has a better prognosis than the historic one. Moreover, scores 2–5 are no longer in use, therefore a scale from 2–10 is no longer applicable. The last updated grading system consists of five groups: grade group 1 (Gleason score ≤6), grade group 2 (Gleason score 3 + 4 = 7), grade group 3 (Gleason score 4 + 3 = 7), grade group 4 (Gleason score 4 + 4 = 8), and grade group 5 (Gleason score 9–10) (Table 1.1). With the current grading system, Epstein has addressed the deficiencies of the previous application of the Gleason system, mainly by differentiating the different subgroups associated woth Gleason score 7. For instance, a Gleason score 7 can represent mostly well-differentiated cancer with a lesser component of more poorly differentiated cancer (Gleason 3 + 4 = 7) or mostly poorly differentiated cancer with a smaller component of well-differentiated cancer (4 + 3 = 7). Treatment decisions using a simplified single Gleason score of 7 fail to recognize that 3 + 4 = 7 and 4 + 3 = 7 are very different from a prognostic point of view. The introduction of the new grading system, distinguishes between these two groups separating them into grade group 3 and 4, respectively [13,14].

New grading system	Gleason score	Histologic definition
Grade group 1	≤3 + 3 = 6	- Only individual discrete well-formed glands
Grade group 2	3 + 4 = 7	- Predominantly well-formed glands with lesser component of poorly formed/fused/cribriform glands
Grade group 3	4 + 3 = 7	- Predominantly poorly formed/fused/cribriform glands with lesser component of poorly formed glands[a]
Grade group 4	8	- Only poorly formed/fused/cribriform glands - Predominantly well-formed glands and a lesser component lacking glands[b] - Predominantly lacking glands and lesser component of well-formed glands
Grade group 5	9–10	Lack of gland formation (or with necrosis) with or without poorly formed/fused/cribriform glands[a]

Figure 1.5 New PCa grading system (adapted from Epstein et al, Eurol 2015)

Prostate cancer, as with all other types of cancer, is also classified by TNM system. The TNM classification system was developed as a tool to stage different types of cancer based on certain, standardized criteria: T refers to the size and extent of the main tumour; N refers to the number of nearby lymph nodes that present cancer; M refers to whether the cancer has metastasized, meaning that the cancer has spread from the primary tumour to other parts of the body. For example, patients with a tumour localized to the prostate are

characterized by the absence of extensions to the prostatic capsule (T1/T2), without lymphatic invasion (N0) and without metastasis (M0). Whereas, patients with disseminated prostate cancer are characterized by the extension of the tumour beyond seminal vesicles (T4), lymphatic invasion (N1) and/or metastasis (M1).

1.1.3 Therapy

The treatment of prostate cancer proposes different goals, depending on various factors such as the anatomy extension and the aggressiveness of the disease, but also the life expectancy of the patient and the presence of comorbidities that may present a higher mortality than that associated with the prostatic neoplasia itself.

Indeed, it is necessary to remember that a considerable portion (about 40%) of patients diagnosed with prostate cancer is destined to die “with” and not “for” their tumour.

After this essential premise, today many options of prostate cancer treatment are available, each with specific benefits and side effects: active surveillance, surgery, radical prostatectomy, radiotherapy, hormone therapy and chemotherapy.

1.1.3.1 Active surveillance

For many men, prostate cancer treatment are likely to produce effects far worse than their cancer ever would. In some cases the patient, under medical advice, can decide not to undergo immediate surgery or radiation therapy and monitor the course of the disease, with the possibility of intervening in case of tumour progression.

This particular approach is called "active surveillance" (AS) and is proposed to patients with a low risk or limited life expectation. AS is a way of monitoring slow-growing prostate cancer, rather than treating it straight away. The aim is to avoid unnecessary treatment, or delay treatment and the possible side effects. Treatment objective is to observe the course of tumour in patients who will probably never develop cancer related symptoms [15].

If there is evidence of increased risk of disease progression from the results of periodic monitoring, it will be proposed to reconsider a treatment with a radical intent to cure the tumour. AS is based on the assumption that the clinical development of low-risk cancer progression is so slow that, while postponing treatment at the time of the first signs of a major risk, it is possible to maintain high chances of healing. It is important to keep in mind that the patient can still decide, for whatever reason and at any time, to stop AS and undergo treatment without any difficulties or delays.

This option might be a good choice for elder men (>75 years old) with limited life expectancy that are in no state to tolerate side effects of the traditional cancer therapy.

The main challenge for AS is the definition of the inclusion criteria. The basic concept underlying AS is that Gleason 6 prostate cancer is a pseudo-disease, part of the ageing process, a condition that develops normally in men and does not pose a significant threat to their lives. However, a minority of such patients harbour higher grade cancer that does pose a significant threat. Therefore, the definition of suitability for AS depends on the identification of “insignificant tumour”. The ideal active surveillance programme should identify patients at a very low risk of prostate cancer progression, as well as those who harbour more aggressive disease early after diagnosis. A commonly used stratification is the ‘Epstein criteria’. According to Epstein criteria, characteristics of indolent tumors include: Gleason 6 or less on biopsy, no more than two positive cores, no involvement of more than 50% of a core and PSA density less than 0.15. Around 75% of such patients had a ‘clinically insignificant’ disease, and 25% had intermediate risk disease and about 90% can be expected to have organ-confined disease [16].

Once a patient is selected for AS, the schedule of clinical examinations and monitoring visits includes:

- every 3 months: dosage of PSA (possibly always performed from the same laboratory);
- at least every 6 months: urological visit with rectal exploration to evaluate the prostate (shape, size, texture);
- after 1 year (and then after 4 and 7 years): a prostate biopsy.

In case of positivity to the examinations, indicating tumour upgrading or upstaging, patients are redirected to treatment.

1.1.3.2 Surgery

In prostate cancer patients, surgery represents, together with radiotherapy, the therapeutic option that provides the highest efficacy in terms of healing from the disease. The surgery intervention is called radical prostatectomy and consists of the complete removal of prostate, seminal vesicles and lymph nodes present in the regions surrounding the prostate and the pelvis. Until a few years ago, radical prostatectomy was performed "open-air", through an incision between navel and pubis. Today, this practice has been supplemented by the mini invasive radical prostatectomy that allows operating by 4-5 small incisions on the abdomen, minimizing invasiveness.

Afterwards, robotic surgery, and in particular the use of Robot da Vinci, has led the practice of mini-invasive radical prostatectomy to a higher level and today it is considered a valid and well established alternative [17].

Because the nerves that regulate erection run very close to the gland and part of the urethra passes inside, two possible consequences of prostatectomy may be the deficiency of erection and urinary incontinence. However, in recent years, “nerve sparing” techniques have been developed to help maintain erectile function. As for urinary incontinence, it is a disorder that manifests itself in the vast majority of patients immediately after surgery, but often regresses within three months.

1.1.3.3 Radiotherapy

Together with prostatectomy, radiotherapy (RT) is a gold standard treatment for organ confined prostate cancer. Radiotherapy used in first line ensures comparable therapeutic success with respect to prostatectomy, displaying a different toxicity that can result beneficial based on patient conditions. For this reason, the choice between prostatectomy and radiotherapy is concerted between the patient and the physician. As in almost all tumours, radiotherapy can be also used as adjuvant treatment after prostatectomy. In these cases RT is delivered immediately post-operation in patients with adverse pathological features, when the tumour extends beyond the prostatic capsule thus increasing the risk of local relapse.

Radiotherapy is delivered through the generation of high-energy beams of ionizing radiation produced by linear accelerators (external beam radiotherapy) or emitted by radioactive substances (brachytherapy).

The main goal of external beam RT is to reach the maximum radiation dose at the target organ with less adjacent tissue damage. Because the prostate is influenced by both bowel and bladder filling, and thus mobile within the pelvis, the conventional RT had larger planning margin that results in underdosing of the target and overdosing of surrounding normal tissues. Consequently, three-dimensional conformal radiotherapy (3D-CRT) and intensity modulated external-beam radiotherapy (IMRT) technics were developed for the high-dose treatment of PCa [18]. These high-precision radiotherapy techniques have improved the treatment of many types of cancer, including prostate cancer [19].

Brachytherapy is a type of radiotherapy where tiny radioactive seeds are put into the prostate. It is a treatment option highly recommended for patients with an early-stage localised disease, being a minimally invasive treatment that is performed in day-surgery, characterized by a low rate of complications and guarantees a high preservation of life quality [20].

Most curative radiotherapy regimens consist of daily fractions in the range of 1.8 to 3 Gy per day over a period of 5 to 8 weeks. Using modern planning techniques, doses up to about 75 Gy to the tumour can usually be achieved without causing severe side effects.

1.1.3.4 Hormone therapy

Hormones are part of the endocrine system and are our body's chemical messengers. Testosterone and dihydrotestosterone (DHT) have an important role in the proliferation, development, maintenance, differentiation and physiology of the prostate [21]. Hormone therapy, also called "androgen deprivation therapy" (ADT), seeks to counteract this action by slowing or blocking the synthesis of these hormones. Although most tumour cells respond to the deprivation, some proliferate independently of hormonal stimulation and do not respond to the treatment. The amount of these resistant cells can increase over time, making the disease "resistant to castration".

The level of testosterone can be surgically reduced by orchiectomy or by administration of drug similar to the hormones produced by the body, which control the growth and activity of the cells. Hormone therapy may be used before, during or after surgery or radiotherapy. Unlike surgical removal, the effects of this therapy can be reversible.

The main drugs used for hormone prostate therapy are:

- **super agonists of LHRH** (or **GnRH**): They are analogs of the natural LH-RH. These drugs act more upstream than other hormone drugs because they block the production of luteinizing hormone (LH), produced by the pituitary gland and able to stimulate the activity of the testes. They suppress the function of the testicles, thus ceasing to produce hormones. The main drugs of this category are Triptorelina, Leuprorelina, Buserelin e Goserelin.

- **Antiandrogen**: Testosterone stimulates the replication of prostate cancer cells by binding to specific receptors on the surface of the tumour cells. Antiandrogens are drugs that block the interaction between male sexual hormone and these receptors, thus inhibiting tumour growth. They cause less erectile dysfunction but more pain in the breast than LHRH agonists. The main drugs of this category are: ciproterone acetate, cicalutamide, futamide and enzalutamide.

  Among antiandrogens is abiraterone acetate, an androgen biosynthesis inhibitor used in the management of CRPC. Abiraterone is an oral, well-tolerated drug that targets a newly elucidated paradigm of continued AR activation in CRPC. It is approved in CRPC patients who have received docetaxel (chemotherapy), and recent data suggest that the drug will also be effective and utilized in the pre-chemotherapy setting [22].

The most common side effects of this therapy are hot flashes, muscle mass reduction, anemia, osteoporosis, libido loss and erectile dysfunction.

1.1.3.5 Chemotherapy

Although ADT is one of the first line treatment for prostate cancer, some patients develop resistance to treatment and the tumour is called "castration-resistant prostate cancer (CRPC)". In these cases, the tumour is still able to grow and progress ever in the presence of low doses of circulating testosterone.

Currently, the first line drug used in these conditions is docetaxel, general associated with prednisone, which has been shown to contribute with increased survival of several months in treated patients. It is administered intravenously with cycles to be performed every three weeks in the hospital. Docetaxel is able to bind the tubulins that constitute the microtubules, stabilizing them and preventing their disassembly. Through this treatment, morphological changes lead the tumour cell into apoptosis.

Recent studies have shown that cabazitaxel, a semi-synthetic derivative of taxol, is able to increase the survival of patients with CRPC who do not respond to chemotherapy with docetaxel [23].

Bone is the predominant prostate cancer metastasis site. Bone tissue treatments use drugs such as bisphosphonates, among which the most powerful currently available on the market is zometa.

The most common side effects of chemotherapy include fatigue, hair loss, diarrhea, nausea and vomiting. These effects can be more or less controlled by drugs such as antiemetics.

The new frontier for the treatment of tumour is based on the use of anti-tumour vaccines or immunomodulatory antibodies, such as anti PD1-PDL1, able to

stimulate the immune system. This method of treatment is called "immunotherapy" and aims to improve the immune response by making it able to selectively destroy cancer cells. Immune checkpoint inhibitors act by blocking the inhibition of T cells, also attacking patient's own cells, thus possibly giving rise to autoimmune reactions. The main side effects associated to autommunity can manifest as moderate systemic side effects such as fatigue, decreased appetite, fever, but also as serious effects affecting gastrointestinal and respiratory system.

Although this therapy is still at an early stage, "Sipuleucel-T" is the first vaccine approved in the United States in 2010, so it is expected that these treatments can be recognized also in Italy [24].

1.2 RADIOTHERAPY

1.2.1 Photon Radiotherapy

1.2.1.1 Ionizing Radiation

Ionizing radiations are emitted in the decay process of unstable nuclei or by de-excitation of atoms and their nuclei in nuclear reactors, X-ray machines, cyclotrons and other devices. Ionizing radiation may be divided into directly and indirectly ionizing for the understanding of biological effects. When ionizing radiations traverse through matter, they lose energy gradually through various interaction processes along the length of their path. The density of energy deposition in a material such as tissue is called the Linear Energy Transfer (LET) of the radiation. LET essentially indicates the quality of different types of radiation and is important because the biological effect of a type of radiation (its relative biological effectiveness, RBE) depends on its average LET [25].

The biochemical changes produced by ionizing radiations are the fundamental events leading to radiation damage in tissues. Radiation is measured either as exposure or as absorbed dose. The absorbed dose is the amount of energy absorbed in a system and generally regarded as the best way to quantify the irradiation absorption. The amount of energy absorbed per mass is known as radiation dose. Specifically, radiation dose is the energy (Joules) absorbed per unit mass of tissue and has the (S.I.) units of Gray (1 Gy = 1 J/ kg). In the past the rad (radiation absorbed dose) was used, where 100 rad = 1 Gy (1 rad = 1 cGy) [26].

Most of the particulate types of radiation are directly ionizing i.e. individual particles with adequate kinetic energy can directly disrupt the atomic structure of the absorbing medium through which they pass producing chemical and biological damage to the molecules. In contrast, electromagnetic radiations, namely, X and γ rays, are indirectly ionizing because they do not produce chemical and biological damage themselves but produce secondary electrons (charged particles) after energy absorption in the material. Ionization is the process of removing one or more electrons from atoms by the incident radiation leaving behind electrically charged particles (an electron and a positively charged ion), which may subsequently produce significant biological effects in the irradiated material (Figure 1.5) [25].

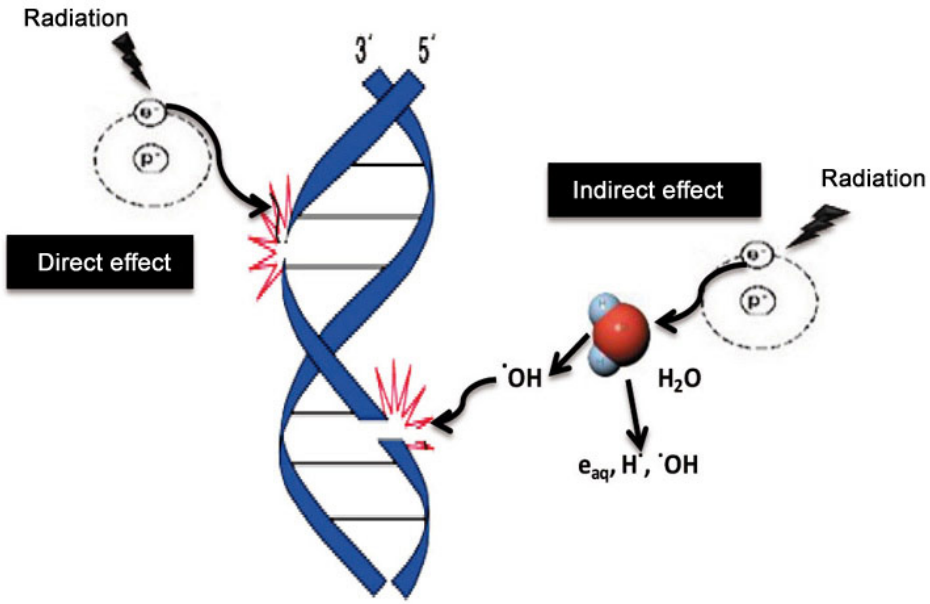

Figure 1.6 Direct and indirect effects of ionizing radiation on DNA

The ionized or excited atom or molecule may either fragment producing free radicals. Free radicals are fragments of molecules having unpaired electrons,

which have high reactivity with cellular molecules. These radicals react with neighbouring molecules and produce secondary DNA or lipid radicals by reaction with another neighbouring molecule. Chain reactions may also occur, particularly in lipids, and may play a role in damage to cell membranes. Free radicals are known to play a major role in radiation effects on biological tissues and organisms.

1.2.1.2 Radiation induced DNA damage

Radiation causes a wide range of lesions in DNA such as single strand breaks in the phosphodiester linkage, double strand breaks on opposing sites or displaced, base damage, protein-DNA crosslinks and protein-protein crosslinks involving nuclear proteins such as histones and non-histone proteins. The numbers of lesions induced in the DNA of a cell by a dose of 1-2 Gy are approximately: base damages > 1000; single strand breaks (SSBs) ~1000; double strand breaks (DSBs) ~40 [27]. DSBs play a critical role in cell killing, since they are the most difficult damages to repair, and are the major responsible for radiation-induced cell death. There are experimental data showing initially-produced DSBs to correlate with radiosensitivity and survival at low dose, and unrepaired or mis-repaired DSBs to correlate with survival after higher doses [27].

It is possible to observe and measure the damage caused by the DSB by different methods including **comet assay** or **immunostaining** of specific protein. For example, DSB can be observed by immunostaining of the protein γH2AX, the phosphorylated form of the H2AX histone, that is considered one of

the earliest markers of the DSB signalling. H2AX is phosphorylated within 1 to 3 minutes after DSB and the number of H2AX molecules phosphorylated increases linearly with the severity of the damage [28]. Phosphorylated H2AX (γH2AX) is rapidly concentrated in chromatin domains around DSBs after the action of ionizing radiation or chemical agents and at stalled replication forks during replication stress. γH2AX foci could be easily detected in cell nuclei using immunofluorescence microscopy that allows to use γH2AX as a quantitative marker of DSBs in various applications [29]. To assess DNA damage at single cell level, the most common method is comet assay. The assay depends on the relaxation of supercoiled DNA in agarose-embedded nucleoids, which allows the DNA to be drawn out towards the anode under electrophoresis, forming comet-like images as seen under fluorescence microscopy. The relative amount of DNA in the comet tail indicates DNA break frequency [30].

1.2.1.3 DNA damage repair

Since cells cannot tolerate DNA damage, the evolution has selected the best systems to restore the lost information depending to the type of damage inflicted to the genome. There are multiple enzymatic mechanisms of DNA repair in cells that act on different types of lesions. For double strand breaks there are two primary repair pathways, non-homologous end joining (NHEJ) and homologous recombination (HR). NHEJ repair operates on blunt ended DNA fragments resulting from broken phosphodiester linkages. There is a requirement for Ku70/Ku80 repair proteins to recognize the lesion termini,

binding of the Ku-heterodimer to DNA-PK (protein kinase), and activation of the XRCC4 ligase enzyme by this complex for final religation of the fragments after enzymatic “cleaning up” of the broken ends of the DNA molecule, by a variety of other recruited proteins, so that ligation can occur [31]. Repair by NHEJ operates throughout the cell cycle but dominates in G1/S-phases. The process is error prone because it does not rely on sequence homology. DSB repair by homologous recombination (HR) utilizes sequence homology with an undamaged copy of the broken region and hence can only operate in late S- or G2- phases of the cell cycle. It starts by nucleolytic resection of blunt ends, binding of NBS/MRE11/rad50 protein complex to the DNA termini, followed by strand exchange facilitated by attachment of rad51/XRCC2 protein [32]. Then there is DNA synthesis of the missing nucleotides on the undamaged templates and ligation. This creates a complex strand crossover between the damaged and undamaged strands known as a Holliday junction, which is finally resolved before the repair process is complete. Other DNA repair mechanisms such as base excision repair (BER), mismatch repair (MR) and nucleotide excision repair (NER) respond to damage such a base oxidation, alkylation, and strand intercalation [32].

Cells are generally regarded as having been “killed” by radiation if they have lost reproductive integrity. Loss of reproductive integrity can occur by apoptosis, necrosis, mitotic catastrophe or proliferative senescence. The accepted gold standard for measuring the radiosensitivity of a cell population is the retention of reproductive integrity or mitotic intactness i.e. the ability of a cell to undergo more than 5-6 cell divisions (and produce a viable colony containing at least 50 cells). This is referred to as cell survival and survival fraction after irradiation is calculated by correcting for the ‘plating efficiency’ of not-irradiated cells.

There are many molecules that have been found to increase the radiosensitivity of cells, including molecules that enhance the persistence of DNA damage, such as inhibitors of DNA repair, modifiers of cell cycle checkpoints and microRNAs [33,34].

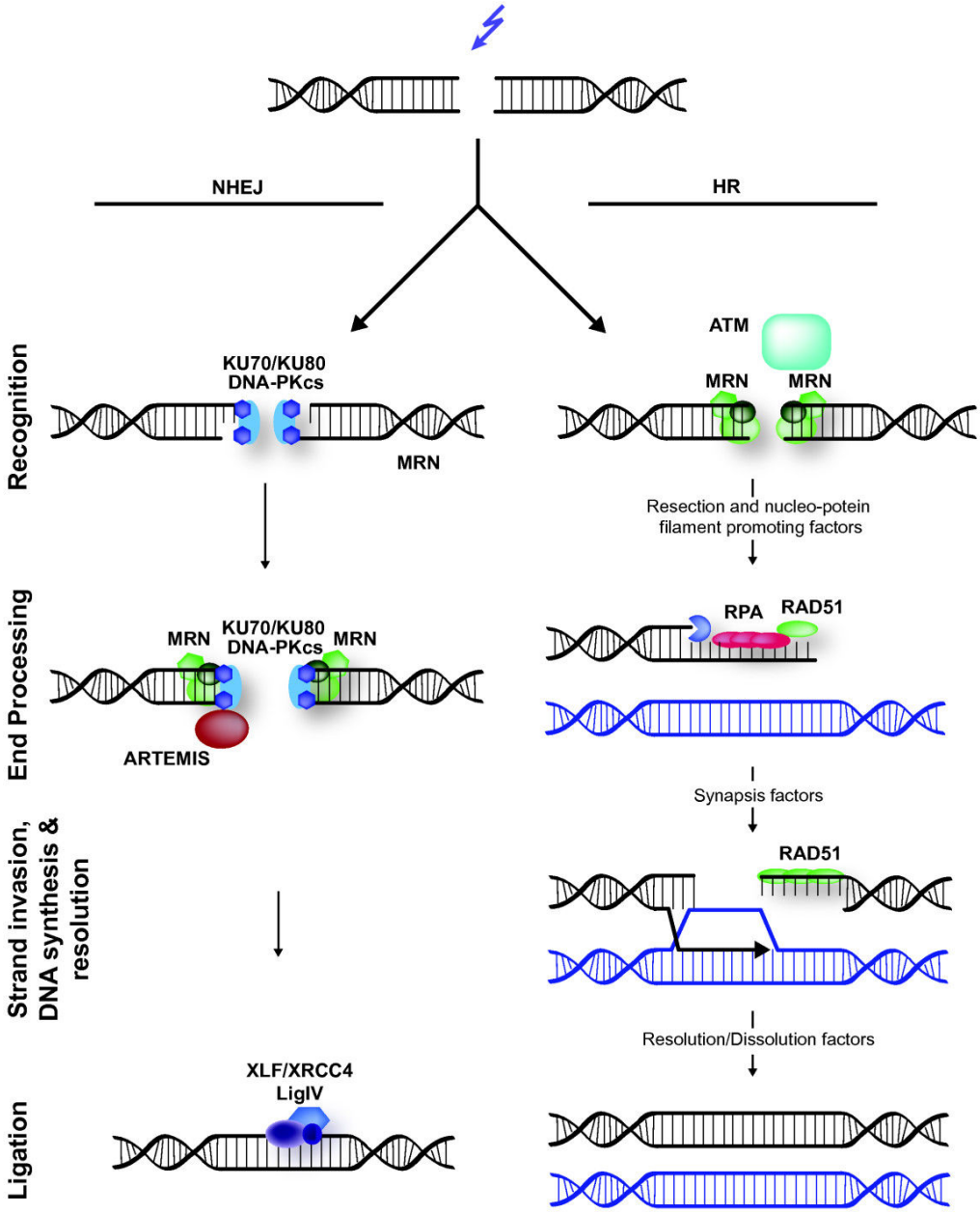

Figure 1.7 Mammalian double-strand break (DSB) repair. Schematic representation of non-homologous end-joining (NHEJ) and homologous recombination (HR). (Adapted from ATP-dependent chromatin remodeling in the DNA-damage response. Hannes Lans et all. [30])

1.2.2 Hadrontherapy

In radiotherapy the key problem is to deliver the dose in such a way that ideally the intended target volume (covering the tumour region) receives 100% of the planned dose needed to kill all cancer cells in the tumour, while the surrounding normal tissue does not receive any dose. This can not be achieved in practice because of the unavoidable dose deposited in the entrance channel of the irradiation, but in the past 60 years significant progress has been made to better understand the biological effectiveness of radiation and to improve the dose deposition towards the ideal and to increase thereby the tumour control rate for potentially curable cases.

Charged particles (protons, heavy ions) have a physical advantage because they can give improved depth-dose distributions for deep-seated tumours. Much of their energy is deposited in tissue at the end of particle tracks (i.e., in the region of the Bragg peak). Bragg peak is the major physical advantage of heavy charged particles. Whereas the photon dose decreases exponentially with penetration depth according to the absorption law for electromagnetic radiation, the depth-dose profile of heavy charged particles exhibits a flat plateau region with low dose and a distinct peak near to the end of range of the particles, the so-called 'Bragg peak'. This characteristic allows the delivery of a high radiation dose to the target, yet significantly spearing surrounding normal tissues, which is the major challenge in radiotherapy [25].

Another important aspect of the use of heavy charged particles is the possibility of nuclear fragmentation. For instance, ^{12}C may break up into three α-particles in nuclear reactions, thus producing lighter fragments at high energies. The projectile-fragments continue travelling with nearly the same velocity and

direction. As a consequence of nuclear fragmentation a rather complex radiation field is produced and leads to significant alterations.

Another important advantage of ion beams is their elevated biological effectiveness (RBE). The factor RBE was introduced to measure the relative effectiveness of ion beams with respect to X-ray. Specifically, the RBE is defined as ratio between X-ray dose and ion dose that are required to produce the same effect:

$$\mathbf{RBE} = \frac{D_x}{D_{ion}}\ \text{Isoeffect}$$

The elevated biological effectiveness of ion beams is of greatest importance for therapy applications and has to be correctly implemented into the treatment planning procedures [25].

Proton and carbon ion beam therapy require powerful accelerators in order to reach clinically relevant particle ranges in tissue up to 30 cm. Today most therapy facilities offering exclusively protons are operated with cyclotrons, while all facilities with ^{12}C ions are using synchrotron accelerators. Cyclotrons are considered as easy to operate, highly reliable, and compact machines. They offer continuous beam (ideal for beam scanning) and extremely stable and regulable intensities, but no energy variation, i.e. only by means of passive degraders in the beam line. Synchrotrons, on the other hand, offer fast energy variation (from pulse to pulse), but need an injector and a delicate extraction system and are more complex in operation. Particle beams provided by cyclotron or synchrotron accelerators are typically narrow, pencil-like beams centred at the axis of the beam tube. Since the beams, and consequently the Bragg peaks, are relatively narrow, the irradiation of extended target volumes

requires the superposition of a number of Bragg curves in order to move the position of the Bragg peak in depth over the whole target volume (Fig 1.7).

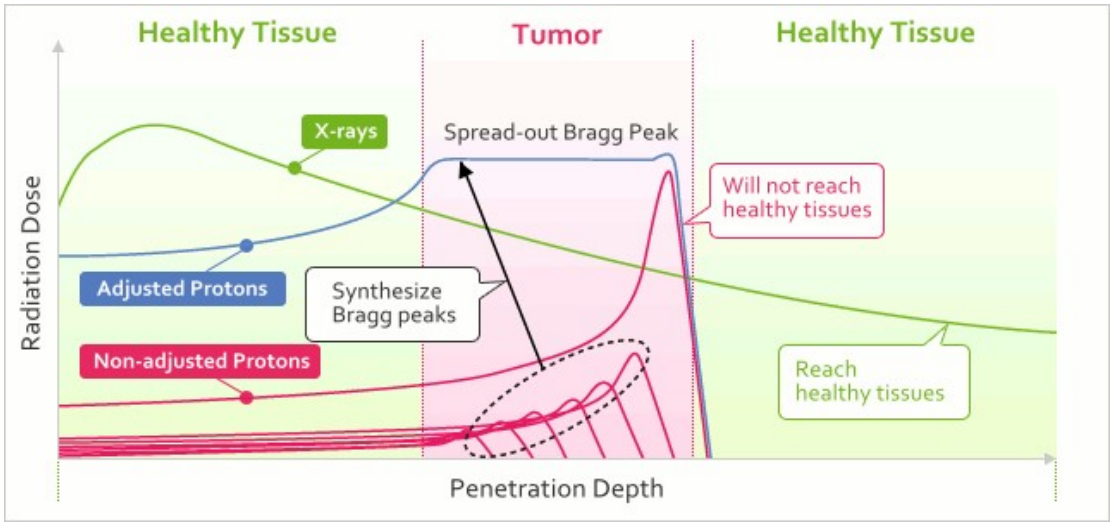

Figure 1.8 Dose distribution curves of heavy ion beams compared to x-rays

1.3 microRNAs

microRNAs (miRNAs) are a class of small non-coding RNAs, naturally occurring small (~22 nucleotide long) non-coding RNA molecules involved in the regulation of gene expression. Through the binding of complementary sequences mostly situated in the 3'-untranslated region (3'-UTR) of target mRNAs, they negatively regulate protein expression mainly by inducing mRNA cleavage or translational repression [35]. Each miRNA is predicted to target hundreds of transcripts, and each transcript, in turn, can be subjected to the regulation of several miRNAs [36]. The ability of miRNAs to simultaneously regulate multiple genes, make them key regulators of various fundamental biological processes, including pathways responsible of tumour initiation and progression. The other way around, increasing evidence shows that the expression of miRNAs is markedly deregulated in cancer [36]. Due to their implication in regulating several cancer hallmarks, including tumour response to conventional treatments, miRNAs are promising candidates to be exploited as sensitizer molecules able to enhance cancer response to radiotherapy.

1.3.1 Biogenesis of miRNAs

miRNAs are generally expressed by genes located in non-coding regions of the genome [35] and are often embedded in fragile chromosomal regions that are susceptible to translocations, microdeletions and amplifications [37]. Most miRNAs are encoded in independent transcription units. However, approximately one quarter of human miRNAs, including mirtrons, are within introns of mRNAs with the same orientation, suggesting that they are not transcribed from their own promoters but processed from introns by the splicing machinery. Other miRNAs are clustered in the genome and transcribed as polycistronic primary transcripts, suggestive of their functional relationships [35].

RNA polymerase II contributes to the synthesis of a 5'-capped and 3'-polyadenylated primary miRNA transcript (pri-miRNA) (Figure 1.8). This is then cleaved in the nucleus by an RNase III enzyme Drosha in association with its cofactor DGCR8 in humans, to generate a 70–90 nt long precursor miRNA (pre-miRNA) that folds into an imperfect stem–loop hairpin structure. Pre-miRNA is then exported into the cytosol through the complex exportin-5/Ran-GTP [38]. RNase III Dicer is involved in the further remodelling of pre-miRNA in the cytoplasm, converting it into a mature double-stranded RNA, with two nucleotide-long 3' overhangs at both ends. The miRNA is then separated into two single stranded molecules: the antisense strand is incorporated in the multiproteic RNA-induced silencing complex (RISC) through its interaction with Argonaute proteins, whereas the other strand, usually referred to as star miRNA (miRNA*), is degraded (Figure 1.8).

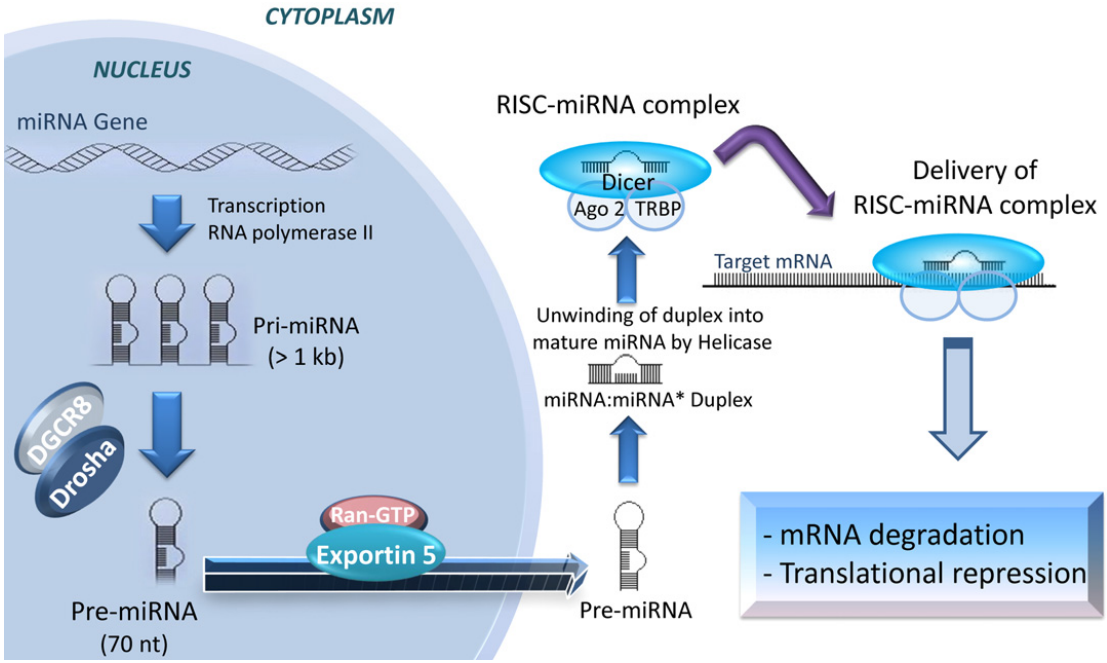

Figure 1.9 Schematic representation of miRNA Biogenesis

Conserved base-pairing between the 3'-UTR of a mRNA and the "seed sequence" located in the 5' end of the miRNA seems to have a major role in the selection of target mRNAs by miRNAs. Through evaluation of the minimal requirements for miRNA:mRNA interactions, Brennecke et al. [39] identified two broad categories of target sites: 5' dominant and 3' compensatory sites. The first have sufficient complementarity to the miRNA 5' end to function with little or no support from pairing to the miRNA 3' end. They can be further classified in two subtypes: "canonical" sites, which pair well at both the 5' and 3' ends, and the "seed" sites, which require little or no 3' pairing support. Targets in the second category, in contrast, have insufficient 5' pairing and require strong 3' pairing for function. Specifically, these authors showed that i) complementarity of seven or more bases to the 5' end miRNA is sufficient to confer regulation, even if the target 3'-UTR contains only a single site; ii) sites with weaker 5' complementarity require compensatory pairing to the 3' end of the miRNA in

order to confer regulation; and iii) extensive pairing to the 3' end of the miRNA is not sufficient to confer regulation on its own without a minimal element of 5' complementarity. Moreover, they demonstrated that, although all site types are used to mediate regulation by miRNAs, canonical sites are likely to be more effective than other site types because of their higher pairing energy, and may function when only one copy is present. In general, however, multiple sites in the 3'-UTR of the targeted mRNA confer better regulation than a single site. Cooperation and spacing between these sites are also important factors that determine the effectiveness of miRNA binding.

The number of base pair mismatches between the miRNA and its target is fundamental in dictating the end result. If perfect complementarity exists, then generally the target mRNA is cleaved. In contrast, imperfect matches tend to result in the inhibition of protein translation, even if it is plausible that they can also reduce the amount of the mRNA target (Fig. 1.9).

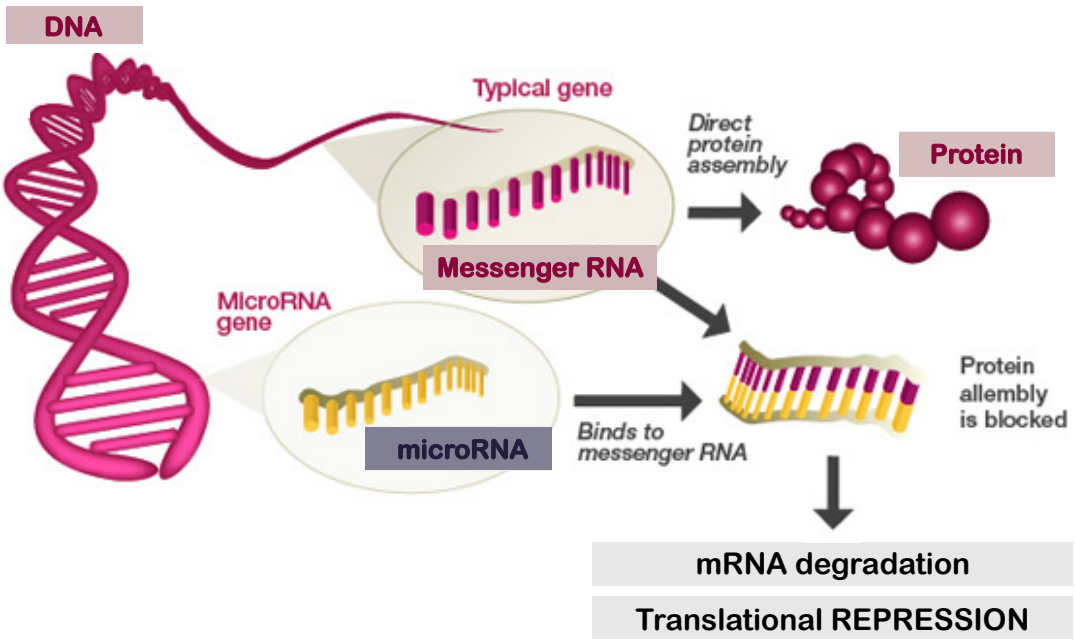

Figure 1.10 Schematic representation of miRNA target regulation

Few years ago, it has been shown that miRNAs also direct rapid deadenylation of target mRNAs, leading to rapid mRNA decay and reduction of transcript levels [40]. Since in animal cells miRNAs generally match complementary targets with a partial homology, the repression of translation represents their prevalent mechanism of regulating gene silencing [35,41].

Several hundreds of miRNAs are estimated to be encoded within the human genome but many are still to be identified [42]. This reflects the complexity of their structural and functional characteristics, including low and variable expression levels and the heterogeneity of coding genes. A further level of complexity in miRNA-mediated gene silencing is introduced by the fact that each miRNA can interact with different mRNAs and a single mRNA can be targeted by diverse miRNAs, thus making it possible for a small number of miRNAs to concurrently regulate multiple factors involved in the same cellular pathway. Regulation by miRNAs guarantees rapid and reversible changes in protein synthesis without altering the transcription of the target mRNAs and is even more refined by the tissue- and time-dependent expression/functionality of miRNAs [43]. This is obtained by transcriptional (e.g., co-transcription of miRNAs with their target genes or binding of transcriptional factors to miRNA promoters) or post-transcriptional mechanisms [44], such as differential processing of primary or precursor transcripts to mature miRNAs [45], sequestration of miRNAs within specific cell compartments [46] or degradation events. Accessibility of target mRNAs can be also modulated by sequestration into P-bodies [47] or binding of specific proteins (i.e., Dnd1 [48]). In general, the numerous biochemical mechanisms that govern miRNA function are dependent on the availability of local regulatory factors [49].

It is estimated that up to one-third of protein-coding genes are susceptible to miRNA regulation [50] and, as a consequence, several miRNAs seem to play pivotal roles in crucial biological processes, such as development, differentiation, cell proliferation and apoptosis [35]. It is thus conceivable that the deregulation of miRNA expression may result in the onset of disease.

1.3.2 miRNAs and cancer

The first connection between miRNAs and cancer emerged from a study by Calin and colleagues [51], who showed that two clustered miRNAs, namely miR-15a and miR-16-1, were the targets of homozygous and heterozygous deletions and translocations at 13q14.3 in human B-cell chronic lymphocytic leukemias (B-CLL). Interestingly, the same group successively showed that this cluster of miRNAs is endowed with tumour-suppressive functions, as it negatively regulates the expression of B-cell lymphoma gene-2 (Bcl-2), a well-known inhibitor of apoptosis [52]. As a consequence of deletions at the 13q14.3 locus, miR-15a and miR-16-1 expression levels are reduced in a high percentage of B-CLL patients, and Bcl-2 is up-regulated, thus resulting in a global antiapoptotic and oncogenic effect. Altogether, these studies suggested a possible direct involvement of miRNAs in the pathogenesis of cancer, as abnormal expression of these molecules may result in a deregulation of their target genes. Hypothetically, overexpression of miRNAs that target tumour suppressor genes may have a pro-tumorigenic effect, which may also arise from the down-regulation of miRNAs targeting oncogenic factors. In this context,

deregulation of miRNA expression has been reported in a wide variety of solid and haematopoietic tumours, compared to normal tissues. For example, cancer-specific miRNA fingerprints were identified in B-CLL [53], breast carcinoma [54], primary glioblastoma [55], hepatocellular carcinoma [56], papillary thyroid carcinoma [57], lung cancer [58], colon carcinoma [59] and endocrine pancreatic tumours [60].

Recent evidence also supports the ability of miRNAs to regulate several steps during neoplastic cell transformation. Many aspects of tumorigenesis, defined also as a hallmark of cancer [61], are common to almost all, if not all, tumours: 1) selfsufficiency of tumour cells, 2) insensitivity to antigrowth signals, 3) abnormal apoptosis, 4) limitless replicative potential, 5) induction and sustained angiogenesis, and 6) invasion and metastasis. For several miRNAs, a specific involvement in sustaining these features has been functionally validated in experimental models [62].

The origins of abnormalities in miRNA expression are multiple. Many miRNAs reside in genomic regions that are prone to alterations in cancer, including minimal regions of loss of heterozygosis, minimal amplicons, or breakpoint cluster regions [63]. The last are preferential sites of sister chromatid exchange, translocation, deletion, amplification. Recent findings indicate that epigenetic aberrations may also influence miRNA expression. In this context, it has been shown that half of miRNA genes are associated with CpG islands, thus suggesting that miRNAs may be targets of DNA methylation machinery. For instance, decreased miR-124a expression in colon, breast and lung carcinomas was attributed to DNA hypermethylation [64].

Changes in miRNA expression can arise from alterations in miRNA processing as well. Due to the short length of miRNA genes, mutations and polymorphisms

located in mature miRNA, pre-miRNA, or in adjacent genomic regions are rare, yet they have been described [65]. More frequently, defects in miRNA processing arise from aberrations in components of the processing machinery, namely Drosha [66] or Dicer [67], or from the binding of specific proteins, such as Lin-28 [45].

Given that binding of specific transcription factors has been proven for several miRNA promoters, as is the case of p53 for miR-34a [68] or c-myc for miR-17-92 cluster [69], changes in miRNA expression may also arise from aberrant transcriptional programmes.

1.3.3 microRNA in Prostate Cancer

In an attempt to investigate the role of miRNA deregulation in determining the onset and progression of PCa many studies analysed miRNA expression profiles in prostate cancer versus normal tissues [70–76]. In these studies, several miRNAs have been found to be differentially expressed in prostate cancer specimens compared to normal counterparts, suggesting an involvement of such miRNAs in the disease status. According to these findings, other studies investigated the causal role of miRNAs in the progression of prostate cancer, by studying the biological effect exerted by specific miRNAs upon their up- or down-regulation. Sun et al. demonstrated that up-regulation of miR-221 was involved in reprogramming the androgen receptor (AR) signalling promoting the transition to castration- resistant PCa (CRPC) [77]. More recently, the downregulation of miR-221/222 cluster was demonstrated to enhance migration and invasion in PCa cells thus leading to CRPC [78]. In another study, Spahn et al. demonstrated that down-regulation of miR-221 in 92 PCa patients was associated with clinicopathological parameters, including the Gleason score and the clinical recurrence [79]. In 2009, Tong et al examined the miRNA expression profile of 40 prostatectomy specimens, finding out that miR-23b, -100, -145, -221 and -222) were significantly downregulated in neoplastic tissues compared to non-involved areas of each specimen. Ectopic expression of these miRNAs significantly reduced PCa cell growth, suggesting that an altered miRNA expression signature in associated with prostate cancer progression [71].

miR-21 is one of the most over-expressed oncogenic miRNAs in many cancer types, including prostate cancer. The majority of miR-21 targets are related to angiogenesis and tumour invasiveness. Li et al. reported a positive correlation of miR-21 expression with poor biochemical recurrence-free survival and the risk of biochemical recurrence in patients with prostate cancer after radical prostatectomy, thus proposing miR-21 as a biomarker to predict prostate cancer progression [80].

Another microRNA that have been extensively associated with prostate cancer is miR-205. In 2009 our lab (Gandellini et al.) demonstrated that restoring the expression of miR-205 in prostate cancer cells resulted in counteracting the epithelial-to-mesenchymal transition by directly targeting protein kinase Cepsilon, thus ascribing to miR-205 an oncosuppressive role in PCa [81]. Later, Bhatnagar et al. reported that downregulation of miR-205 and miR-31 confers resistance to chemotherapy-induced apoptosis in advanced prostate cancer. Accordingly, Verdoodt et al. demonstrated that miR-205 promotes apoptosis in prostate cancer cells in response to DNA damage by cisplatin and doxorubicin by targeting the anti-apoptotic protein Bcl2 [82].

Several different studies reported that the expression levels of miRNAs, including miR-224 [83,84], miR-18a [85], miR-126 [86], miR-34b [87] and miR-15/16 [88], correlate with clinical outcome, thus suggesting a possible role of such miRNAs as novel prognostic biomarkers and therapeutic targets [89].

1.3.4 miRNAs and Radiation Response

As previously reported, due to their capacity to simultaneously regulate multiple targets thus disrupting several biological processes, including cell development, metabolism, proliferation, cell-cycle and apoptosis, miRNAs can play a pivotal role in contributing to the onset of pathological conditions, including cancer. Strong evidence suggests that miRNAs can take part in pathways sustaining all the diverse hallmarks of cancer and therefore actively contribute to determine tumour progression, also by affecting tumour response to conventional treatments, including radiotherapy.

In this context, miRNAs have been demonstrated to be involved in the IR response network, as many of them directly regulate the expression of genes belonging to cellular pathways relevant to radioresponsiveness [90,91]. However, the causal role exerted by individual miRNAs in determining tumour response to radiation need to be better elucidated [34].

It has been widely reported and corroborated that miRNAs play a pivotal role in contributing to cancer cell sensitivity by regulating several cell stress-related pathways.

One approach to identify miRNAs that could be implicated in radiation response is to analyse their modulation upon radiation exposure [92,93]. Mounting evidence demonstrates that exposure to radiation can significantly alter miRNA expression profile in cancer cells including PCa [94–96]. Leung et al. identified 6 miRNAs upregulated (miR-9, miR-22, miR-25, miR-30a, miR-550a and miR-548h) and 16 miRNAs downregulated (let-7c/d/e, miR-15a, miR-17, miR-30d, miR-92a, miR-125a, miR-197, miR-221, miR-320b, miR-342, miR-361, miR-

374a, miR-501 and miR-671) after exposure to 10 Gy of radiation, suggesting such miRNAs as candidates in contributing to radiosensitivity and proposing them as biomarkers for radiotherapy [97].

Using a miRNA microarray assay, Li et al. screened 132 tumour miRNAs in LNCaP cells in response to radiation treatment and reported that miR-106b was downregulated in PCa cells upon radiation exposure. Functionally, ectopic expression of miR-106b was able to suppress radiation-induced p21 activation, overriding radiation-induced cell cycle arrest and cell growth inhibition check points and finally resulting in a transient reduction of radiation-induced growth inhibition. These findings suggest miR-106b as a potential therapeutic target in those prostate cancer types whose radiation resistance is likely due to consistently elevated levels of the microRNA [98].

A recent study of Gong et al. reported that miR-145 modulates tumour sensitivity to radiation in prostate cancer. miR-145 was already known to reduce chemoradioresistance in glioblastoma and suppress prostate cancer proliferation, migration and invasion. By performing miRNA expression profile analyses in 30 prostate tumour tissue biopsies taken prior to neoadjuvant radiotherapy, they found miR-145 to be significantly upregulated in PCa patients demonstrating good response to neoadjuvant radiotherapy. Consistently, same specimens revealed a significantly decreased expression levels of miR-145-regulated DNA repair genes, suggesting a possible mechanism for miR-145 in modulating radiosensitivity, potentially through down regulating of DNA repair processes. Consistently, the ectopic reconstitution of the microRNA in prostate cancer cell models demonstrated that miR-145 significantly sensitized cells to radiation, by reducing the efficiency of the repair

of radiation-induced DNA double-strand breaks, as suggested by the increased percentage of γ-H2AX foci and the enhanced mitotic catastrophe observed in miR-145 expressing cells. These findings supported a potential role of miR-145 as a therapeutic target to enhance prostate cancer response as well as a novel clinical biomarker of radiation response [99].

Another screening study reported a different miRNA modulation upon fractionated radiation compared to single-dose radiation in LNCaP, PC3 and DU145 prostate cancer cells. Specifically, miR-17-92 cluster was found to be downregulated in p53 positive LNCaP cells. Whereas miR-34a and let-7 miRNAs were upregulated by fractionated radiation in both p53 -positive and –null cell lines, indicating that radiation-induced miRNA expression may be regulated in a p53 independent manner [100].

The above studies provided solid evidence that the expression of several miRNAs is affected by radiation in prostate cancer models. However, the modulation of specific miRNAs upon radiation does not directly imply a functional involvement of such microRNAs in regulating cell response to radiation the other way around.

With the final purpose to identify miRNAs that are actively responsible of modulating cell sensitivity profile to radiation treatment, the artificial modulation of candidate miRNAs, by the use of miRNA mimetics or inhibitors, was performed in different functional studies.

In 2008, Josson et al. identified several miRNAs altered in response to radiation response of prostate cancer cells. In particular, cell exposure to radiation causes significant changes in miR-521 and miR-34c. To investigate a functional role of such miRNAs in modulating radiation response, they transiently overexpressed miR-521 and observed a significant sensitization of prostate

cancer cells to radiation treatment. Conversely, inhibition of miR-521 resulted in radiation resistance of prostate cancer cells. Interestingly, they showed that the expression levels of CSA, a DNA repair protein, inversely correlated with the levels of the microRNA, suggesting CSA as the possible mediator of miR-521-induced radiosensitizing effect [101].

In 2015, Hatano et al. screened a library of 810 miRNA mimetics for the ability to modulate cellular sensitivity to ionizing radiation. They found that a large percentage of miRNA mimetics was able to increase PCa cell sensitivity to IR. Specifically, they reported that miR-890 and miR-744-3p significantly delayed IR induced DNA damage repair, and that both miRNAs were able to inhibit the expression of multiple components of DNA damage response and DNA repair, acting as radiosensitizer factors [102].

Several miRNAs have been associated with cell proficiency in recovering from radiation-induced injury, by targeting genes involved in DNA damage repairing.

It is widely recognized that c-Myc is reduced when cells are exposed to DNA damaging agents such as ionizing radiation. In their study, Mao et al. recerntly demonstrated that miR-449a enhances radiosensitivity of LNCaP cells both in vitro and in vivo by targeting c-Myc. Specifically, they found that miR-449a was upregulated and c-Myc was downregulated in LNCaP irradiated cells. Consistently, overexpression of miR-449a or knockdown of c-Myc promoted the sensitivity of LNCaP cells to IR. Furthermore, miR-449a enhanced radiation-induced G2/M phase arrest by directly targeting c-Myc which controls the Cdc2/CyclinB1 cell cycle signal by modulating Cdc25A [103].

The miR-99 family has been shown to play ain important role in regulating DNA damage response by targeting SWI/SNF chromatin remodelling factors in different cell line models [104]. In their recent study, Rane at al. demonstrated

that miR-99a and miR-100 are downregulated in radioresistant prostate cancer stem cells and castration-resistant prostate cancer cells. Interestingly, they found that the upregulation of the two microRNAs, induced by the androgen receptor inhibitor Mifepristone, resulted in the sensitization of prostate cells to radiation [105].

Another strategy widely used for the identification of miRNAs to be investigated for their ability to affect radiation response in prostate cancer, consists of exploiting the knowledge of their involvement in cell stress-related pathways, including cell proliferation, DNA damage repair, autophagy, and hypoxia.

It is well known that cancer cells undergoing hypoxia are prompted to trigger adaptive changes in cellular metabolism, such as altering autophagy. This might be a cause of enhanced radioresistance in some types of cancer, including prostate cancer, where mounting evidence suggests that irradiation-induced autophagy acts as a protective mechanism.

In 2016, Gu et al., by investigating hypoxia-responsive miRNAs in DU145 and PC3 cell lines, reported that hypoxia induces downregulation of miR-124 ad miR-144. Moreover, the overexpression of such miRNAs can inhibit hypoxia-induced autophagy and enhance radiosensitivity, at least in part, by downregulating PIM1, a common target of the two microRNAs [106].

Consistent with this link between autophagy and radiosensitivity, another study reported that miR-301-a and -b overexpression results in elevated autophagy and increased radioresistance in LNCaP cells, by targeting NDRG2 [107].

Similarly, Wang et al. demonstrated that ectopic expression of miR-205 substantially reduced the survival fraction of both DU145 and LNCaP cells to radiation, by directly targeting TP53INP1 and inhibiting irradiation induced-autophagy [108].

In another study, it was found that miR-32 was able to induce autophagy resulting in a decreased radiosensitivity of prostate cancer cells. Specifically, they showed that miR-32 mimics enhanced tumour cell survival leading to radioresistance, which was reversed by a miR-32 inhibitor. More significantly, the overexpression of miR-32 enhanced autophagy in the IR-treated PCa cells, regulating the expression of varius autophagy related protein, such as DAB2IP, Beclin 1 and LC3β I/II [109].

Among the several pathways that have been hugely correlated with radiation response, is the epithelial to mesenchymal transition (EMT), a phenotypic switch that promotes the acquisition of a fibroblastoid-like morphology by epithelial tumour cells, resulting in enhanced tumour cell motility/invasiveness, increased metastatic potential and treatment resistance [110].

In this context, cumulative evidence has recently reported that specific miRNAs which are able to repress the EMT switch can act as radiosensitizers in different tumour types. Specifically, ectopic expression of such miRNAs targeting the EMT-inducing transcription factor zinc-finger E-box binding homeobox 1 (ZEB1), which also promotes homologous recombination-mediated DNA repair, results in increased tumour radiosensitivity, at least in part, as a consequence of a reduced clearance of treatment-induced DNA damage [111,112]. Zhang et al. found that miR-205 promotes radiosensitivity and is downregulated in radioresistant breast cancer cells, and that loss of miR-205 is highly associated with poor relapse-free survival in breast cancer patients. In particular, they demonstrated that radiation suppresses miR-205 expression through ataxia telangiectasia mutated (ATM) and zinc finger E-box binding homeobox 1 (ZEB1). Moreover, miR-205 inhibits DNA damage repair by targeting ZEB1. In this study they identified miR-205 as a radiosensitizing miRNA further

supporting the relevance of repressing EMT in order to increase sensitivity to radiation treatment [113].

1.3.5 Clinical applications of miRNAs

Over the past years, it has become clear that alterations in miRNA expression are a widespread phenomenon in human cancer, thus suggesting a role for these molecules in tumourigenesis [114]. In some instances, the expression of selected miRNAs or miRNA profiles were found to correlate with diverse clinico-pathological parameters and to predict patient clinical outcome or response to treatment [114]. Overall, these findings have highlighted the potential of miRNAs as new diagnostic or prognostic biomarkers. In addition, the evidence that specific miRNAs are endowed with oncogenic or tumour-suppressive functions has emerged from several studies conducted in experimental models, pointing to a possible role as novel targets or tools for anticancer therapy.

1.3.5.1 miRNAs as diagnostic tools

Evidence that miRNAs may represent new diagnostic markers for human cancer is rapidly accumulating. In fact, the expression profile of a number of miRNAs significantly differs between tumour and normal tissues of diverse histotype. For example, in tumour specimens of patients with lung cancer, a reduced expression of let-7 (a miRNA able to repress the proto-oncogene RAS) [115,116] and an increase in miR-155 expression levels [54] have been observed, as compared to adjacent normal tissue. Similarly, a reduced expression of miR-143 and miR-145 has been observed in precancerous and neoplastic lesions of colorectal tissue [59]. In papillary tumours of thyroid, miR-221, miR-222 and miR-146 are highly up-regulated compared to normal tissue and their expression levels inversely correlate with KIT mRNA and protein expression levels [57]. These and other studies paved the way for studies aimed at investigating the potential of miRNA profiles in classifying tumour from normal tissues. In this context, a milestone was the study by Lu and colleagues [70], who showed that hierarchical clustering based on miRNA expression profiles can actually classify tumours of different developmental lineages (epithelial vs haematopoietic; tumours from the gastrointestinal tract vs other tissues) or differentiation states and distinguish between tumour and normal tissues with higher efficiency compared with that based on mRNA profiling. Actually, whereas mRNAs must be translated into proteins to have a biological effect, mature miRNA expression levels represent more closely the functional level of a gene. Rosetta Genomics recently showed that a classifier based on 48 miRNAs, constructed by profiling 400 samples from 22 different tumour

tissues and metastases, had the potential to classify tumour type with an accuracy >90%. This finding has an impact for the identification of tissue of origin in metastatic cancers of unknown primary, which account for 3-5% of all new cancer cases in US [117]. As for cancer-specific diagnostic signatures, by analysing 76 breast carcinomas and 10 normal breast samples, Iorio and colleagues identified 29 miRNAs whose expression was significantly deregulated in tumours and a smaller set of 15 miRNAs (including miR-125b, miR-145, miR-21 and miR-155) that were able to correctly predict the nature of the sample analysed (i.e., tumour or normal breast tissue) with 100% accuracy [54]. In another study, a set of 21 over-expressed and 4 down-regulated miRNAs was reported to correctly classify pancreatic adenocarcinoma from benign tissue [60].

MiRNA expression profiling was also used to distinguish tumour subtypes or histotypes. An unsupervised analysis of miRNA expression profiles in a set of 38 estrogen receptor (ER)-positive primary breast tumours of patients with lymph node-negative disease identified three subgroups predominantly driven by three miRNA signatures: an ER-driven luminal B-associated miRNA signature, a stromal miRNA signature (composed of miRNAs predominantly expressed in stromal fibroblasts and endothelial cells and marginally in the epithelial breast cancer cell lines), and an overexpressed miRNA cluster (miR-515–522) located on chromosome 19q23, though these intrinsic miRNA signatures were not associated with tumour aggressiveness [118].

By profiling miRNAs in 10 normal mucosa samples and 49 stage II colon cancers differing with regard to microsatellite status, Schepeler and colleagues [119] showed that several miRNAs were differentially expressed between normal tissue and tumour microsatellite subtypes, with miR-145 showing the

lowest expression in cancer relative to normal tissue. Microsatellite status could be correctly predicted based on miRNA expression profiles for the majority of cases. In a similar effort, a molecular signature consisting of 27 differentially expressed genes, comprising mRNAs and miRNAs, was reported to correctly distinguish colon cancers with and without microsatellite instability, thus suggesting that combining mRNA and miRNA expression profiling data may represent a further method to improve the molecular classification of cancer [120].

In some instances, single miRNAs, rather than miRNA profiles, have been proven to have a strong classification power. This is the case of miR-205, which was reported to be a highly specific marker for squamous cell lung carcinoma: the expression of this miRNA, measured using quantitative RT-PCR (qRT-PCR) reached a sensitivity of 96% and a specificity of 90% in discriminating squamous cell lung carcinoma from adenocarcinoma [121]. Similarly, in esophageal squamous cell carcinoma, the expression of selected miRNAs was shown to correlate with gross pathological classification (fungating vs medullary), as is the case of miR-335, miR-181d, miR-25, miR-7 and miR-495, or with grade (miR-25 and miR-130b) [122].

Overall, these studies suggested miRNA profiles or single miRNAs as possible future markers for cancer diagnosis and classification. The development of biomarkers that help detect cancer at an early stage is important since early detection has a direct impact on prognosis and clinical outcome. MiRNAs show great stability and maintain their expression profiles in archival formalin-fixed paraffin-embedded (FFPE) samples [123], due to their small size. In contrast, mRNAs tend to be fragmented in archival tissues. This represents a huge advantage over mRNA profiling and enables studies to take advantage of the

vast resources in routine diagnostic archives. Thanks to the recent advances in qRT-PCR methods, which can detect miRNAs starting from a few nanograms of total RNA, miRNA expression levels can be also measured in fine-needle aspiration biopsy samples [124]. In addition, the small size, relative stability and resistance to RNase degradation make the miRNAs superior molecular markers than mRNAs for the setting-up of non-invasive diagnostic tests, such as those on blood, plasma or serum. In this context, Mitchell et al. [73] demonstrated that both serum and plasma samples are suitable for investigations of miRNAs as blood-based biomarkers, as miRNAs can be detected in both compartments and the results correlate. Ng and colleagues examined the expression of miRNAs in plasma from a series of colorectal cancer patients and controls and showed that the expression of miR-92 could discriminate tumour patients from healthy individuals with 70% specificity and 89% sensitivity [125]. Similarly, eight miRNAs were found to be differentially expressed in sera from ovarian cancer patients compared to those from healthy individuals, with miR-21, miR-92 and miR-93 being overexpressed in three patients with normal pre-operative CA-125 (the current marker used to assess the risk of having ovarian cancer) levels [126]. It is worth mentioning that most patients enrolled in these studies presented advanced stage tumours. At present it not clear whether cancer-associated miRNAs can be detected in the blood only when the disease has already metastasised, thus being potentially used only for the diagnosis of advanced cancers, or if they are released into the circulation also in the presence of an early stage tumour. It is also still to be elucidated whether circulating miRNAs are mainly released from cells by lysis or whether they are encapsulated in small (40-100 nm) membrane vesicles of endocytoc origin referred to as exosomes. Exosomes are secreted by most cell types in vitro and

are also found in body fluids, such as blood, urine, malignant ascites, amniotic fluid and breast milk. Although their biological role is still to be clarified, it is conceivable that they can mediate communication between cells. Taylor and Gercel-Taylor [127] compared miRNA profiles of ovarian tumours to those of tumour exosomes isolated from the same patients and found that the levels of 8 miRNAs (miR-21, miR-141, miR-200a, miR-200c, miR-200b, miR-203, miR-205 and miR-214) were similar between cellular and exosomal miRNAs. In addition, whereas EpCAM-positive exosomes were detectable in both patients with benign ovarian disease and ovarian cancer, exosomal miRNA from ovarian cancer patients exhibited similar profiles, which were significantly distinct from profiles observed in benign disease. The same group showed that circulating exosomes are significantly more abundant in lung adenocarcinoma patients than in a control group, with a higher mean exosomal miRNA concentration in cancer patients [128]. In addition, they found that there is a close correlation between circulating miRNAs of tumour-derived exosomes and tumour miRNAs, confirming that miRNA expression in peripheral blood could be a surrogate of miRNA expression in the tumour biopsy. Overall, the evidence collected on miRNAs would suggest that combining the miRNA diagnostic biomarkers with other available screening tests may improve diagnostic accuracy.

1.3.5.2 MiRNAs in cancer prognosis

The clinical utility of miRNAs in oncology extends beyond diagnostics, as different reports showed correlation between the expression of specific miRNAs with i) bio-pathological features of the tumour that are commonly used for

prognostication, ii) clinical outcome and iii) response to therapy. For example, in breast cancer, Iorio and colleagues showed that the expression of a number of miRNAs correlated with the expression of estrogen and progesterone receptors, tumour stage, nodal status, proliferation index and vascular invasion [54]. Similarly, Slaby et al. reported that miR-21 overexpression in colorectal cancer has a strong correlation with established prognostic factors, such as nodal stage, metastatic disease and stage [129].

In lung adenocarcinomas, including those classified as disease stage I, miRNA expression profiles were reported to correlate with patient's survival [58]. Specifically, Kaplan-Meier survival estimates showed that patients with either high miR-155 or reduced let-7a-2 expression had a poorer survival than the patients with low miR-155 or high let-7a-2 expression, respectively. Using a multivariate Cox proportional hazard regression analysis, the same authors found that high miR-155 expression was a significantly unfavourable prognostic factor independent of other clinicopathological factors, such as age, sex, and smoking history [58]. Interestingly, 143 lung cancer cases that had undergone potentially curative resection could be classified into two major groups according to let-7 expression in unsupervised hierarchical analysis, showing significantly shorter survival after potentially curative resection in cases with reduced let-7 expression. Multivariate COX regression analysis showed this prognostic impact to be independent of disease stage [130].

As far as squamous cell lung carcinoma is concerned, miR-146b alone was found to have a strong prediction accuracy (78%) in stratifying prognostic groups of patients and miRNA signatures were reported to be superior in predicting overall survival than a previously described 50-gene prognostic signature [131].

Expression profiling of 157 miRNAs in 35 primary neuroblastoma tumours indicated that 32 were differentially expressed in favourable and unfavourable tumour subtypes. Many of these miRNAs were significantly underexpressed in tumours with MYCN amplification, which have particularly poor prognoses [132]. In some instances, miRNA expression was reported to correlate to response to therapy, as is the case of let-7g and miR-181b in colorectal cancer, which were identified as significant indicators of chemoresponse to chemotherapy with 5-fluorouracil-based antimetabolite S-1 [133].

In hepatocellular carcinomas, patients whose tumours had low miR-26 expression levels, a miRNA whose abundance was found to be reduced in hepatic cancer compared to paired noncancerous tissue, had shorter overall survival but a better response to interferon therapy than did patients whose tumours had high expression of the miRNA [134]. Mishra and colleagues [135] identified the miR-24 binding site in the dihydrofolate reductase 3'-UTR as the target of a single nucleotide polymorphism (SNP), previously described as associated with methotrexate resistance in childhood leukemia and lymphoma patients [135]. Functionally, this SNP was demonstrated to impair miR-24 binding to dihydrofolate reductase mRNA, with a consequent overexpression of the enzyme and increase of methotrexate resistance [136]. In this context, recent studies showed that SNPs in miRNA target sites may not only affect response to treatment but also cancer predisposition. For example, a SNP in a let-7 complementary site in the KRAS 3'-UTR was reported to be significantly associated with a 1.4- to 2.3-fold increased risk for non-small cell lung cancer among moderate smokers [137].

1.3.5.3 MiRNAs in cancer therapy

Because of the clinical and biological significance of miRNAs in cancer, the management of miRNAs with altered expression in tumours should be considered as a therapeutic strategy. The rationale for using miRNAs as potential therapeutic targets comes from the several studies that have documented, through loss- or gain-of-function approaches, oncogenic or tumour suppressive functions of selected miRNAs in different human cancers [138].

The function of over-expressed oncogenic miRNAs has been successfully antagonized in experimental models using chemically modified antisense oligonucleotides, such as 2'-O-methyl-antisense oligonucleotides or 'locked' nucleic acids (LNA). The latter, which exhibit the highest affinity and specificity for complementary target RNA and show properties of cellular uptake and biodistribution adequate for being used in vivo [139], proved to efficiently inhibit the expression of specific miRNAs [140]. Similarly, intravenous injection of antagomirs, 2'-O-methyl-antisense oligonucleotides conjugated with a cholesterol moiety at the 3' end, produced a long-lasting inhibition of specific miRNAs in mice [141]. In contrast, restoration of expression of down-modulated tumour-suppressive miRNAs is usually achieved using synthetic double-stranded RNA molecules resembling precursor miRNAs or expression vectors carrying miRNA genes packed into lentiviral systems [141].

Given that the role of a miRNA in the development cancer has to be preliminary ascertained by functional studies, the reconstitution of tumour-suppressive miRNAs or the knockdown of over-expressed, oncogenic miRNAs could offer an extraordinary opportunity to regulate the expression of disease-relevant

genes. Efficient in vivo delivery of miRNA precursors and miRNA-specific antisense oligonucleotides or antagomirs is a crucial factor for the development of successful miRNA-based treatment modalities. In this context, it is noteworthy that efficient reconstitution of miR-15a and miR-16-1 expression has been achieved by injecting a lentiviral vector expressing miRNA precursor into prostate tumour xenografts in mice [142]. In addition, a proof-of-concept of the antagomir treatment has been successfully demonstrated, as tumour growth in a neuroblastoma mouse model was abolished by the injection of antagomiR-17-5p [143].

As miRNAs have the potential to simultaneously modulate a cohort of cancer-relevant gene networks, they might become therapeutically relevant in a 'one-hit multitarget' context against cancer, including PCa. However, the multi-specific nature of miRNA-based gene regulation is both a strength and a weakness as interfering with miRNA expression might give rise to unpredictable off-target effects on unintended mRNA targets and elicit immune-activating 'danger signals'. This makes imperative i) the precise definition and validation of the genes targeted by a given miRNA in relevant cell types and tissues, as well as ii) the development of approaches to deliver miRNA-modulating agents specifically to the cells of interest. As far as the first issue is concerned, it is noteworthy that the identification of putative target genes is still problematic, since each miRNA can interact with several mRNAs and each mRNA can be targeted by several miRNAs. Prediction of miRNA/mRNA pairs is usually accomplished using dedicated software, which perform computational predictions based on a two-step process. In the first step potential miRNA binding sites are searched within the 3'-UTR of several genes, according to

specific base-pairing rules. Parameters that are usually evaluated by widely used target prediction software include the complementarity with miRNA seed, the binding-energy threshold and several empirically determined binding rules, so that each programme can predict different putative target genes for the same miRNA. In the second step, programmes implement cross-species conservation requirements, in order to predict only the target sites which are under selective pressure to preserve their sequence and their functionality. Each programme prioritises some specific requirements, thus furnishing predictions that rarely fit together. For this reason, a common practice is intersecting the results obtained on different platforms to increase the probability to find true miRNA-mRNA pairs. In addition, gene expression profiling [144] and proteomic analysis [145] associated to loss- and gain-of-function studies in in vivo or in vitro models might contribute to a better understanding of miRNA controlled cellular networks in a given disease and identify biologically relevant targets. In vivo knock-out or knock-in models should be helpful to understand the pathways that are affected by miRNA manipulations.

As for the delivery of small RNAs, the two main strategies currently being developed rely on the use of viral vectors and non-viral, lipid-based complexes, such as liposomes and nanoparticles [146]. In our opinion, the use of delivery systems displaying carrier-defined specificity (as, for example, cell-specific immunoliposomes, which have been already used successfully to deliver small interfering RNAs by target-specific cell-surface receptors [147]) might represent a reliable approach for controlled delivery of miRNA-modulating agents to relevant tissues/organs, thereby avoiding cytotoxic side effects. In this context, prostate-specific membrane antigen (PSMA), which is specifically expressed on

prostate epithelial cells and strongly upregulated in PCa, has been proven to be a suitable surface molecule to drive PCa-specific delivery of small RNAs [148].

The interference with cancer related miRNAs, besides producing a possible direct anticancer effect, could be exploited to increase the sensitivity of tumour cells to conventional anticancer agents. In this context, it has been recently reported that specific miRNAs can contribute to chemoresistance in various cancer cell lines [149] and that antisense oligonucleotide-mediated inhibition of miR-21 and miR-200b was able to enhance the sensitivity of cholangiocarcinoma cells to the chemotherapeutic agent gemcitabine [150]. Again, ectopic expression of members of the let-7 family of miRNAs in lung cancer cells increased their in vitro radiation response [95]. Based on this evidence, the possibility to rationally design therapeutic approaches combining conventional treatments and specific miRNA modulators could be envisaged to improve therapeutic response.

STUDY AIMS & EXPERIMENTAL DESIGN

2. STUDY AIMS AND EXPERIMENTAL DESIGN

2.1. Study Aims

Radiotherapy is a standard treatment for organ-confined prostate cancer (PCa). Although treatment technical optimization has greatly improved local tumour control, approximately 30% of patients still undergo recurrence. Thus, new strategies to increase radiotherapy effectiveness are needed.

Radioresistance is a complex phenomenon that can arise as a result of various genetic and epigenetic abnormalities. microRNAs (miRNAs) are endogenous small non-coding RNAs that negatively regulate gene expression. Their documented dysregulation in cancer together with their potential to simultaneously regulate multiple oncogenic-oncosuppressive pathways, has aroused interest in defining a functional association between miRNAs and tumour radiation response. The few preclinical studies carried out thus far in PCa (mainly in cellular models) provided controversial results.

The final goal of the project was to identify specific miRNAs acting as radiosensitizers in PCa that can be potentially exploited for designing novel strategies aimed at increasing radiotherapy effectiveness. To achieve this goal, we proposed to 1) identify miRNAs involved in radiation response and ii) dissect the underlying molecular mechanisms in order to substantiate their functional involvement in determining PCa response to radiation treatment.

2.2 Experimental Design

To address the first aim of the study, consisting of the identification of specific miRNAs potentially contributing to radiation response in PCa, the very first step of this study consisted of the definition of the possible strategies to follow to select miRNAs related to radiation response. In order to consider all the miRNAs potentially matching our query, we followed two complementary approaches of miRNA sorting. The first approach is based on the identification of miRNAs modulated upon radiation exposure, since modulation in response to radiation stimulus could likely reflect an involvement in radiation response processes. However, it is worth noting that miRNA modulation upon radiation does not *per se* imply that such miRNAs play an active role in influencing radiation response. To investigate whether singled out miRNAs were functionally involved in the response, taking advantage of a panel of PCa cell lines and of subcutaneous PCa xenografts, miRNA expression was artificially modulated in PCa cells by transfection with specific miRNA modulators (i.e.: miRNA mimics) and transfected cells were exposed to radiation in order to check whether miRNA modulation induce changes in sensitivity profiles of both cell and animal PCa models. Taking advantage of an established collaboration with CNAO (Pavia), PCa cell lines exposed to photons were also exposed to carob ions in order to compare the effects induced by conventional radiotherapy and hadrontherapy, respectively.

As a second approach of miRNA identification, we focused on miRNAs that i) are downregulated in PCa and ii) target genes belonging to pathways relevant to radiation response. This strategy is based on the evidence that miRNA

downregulation in PCa compared to normal prostate suggests a possible oncosuppressive function of the miRNA, which is compatible with a role of this molecules in making cells susceptible to a specific treatment. As for the second criterion, the evidence that a specific miRNA targets pathways relevant to radiation response support its putative role in influencing cell sensitivity to radiation. The intersection of these two criteria should accrue the reliability of miRNA sorting for the evaluation of their radiosensitizing effect.

Once miRNAs were selected, by either the first or the second approach, their radiosensitizing effect was studied in order to dissect the underlying molecular mechanisms. To this aim, we sought to figure out, for each selected miRNA, the target genes that could be relevant to radiation response. Top targets were validated as actually implicated in mediating the radiosensitizing effect ascribed to the respective miRNA.

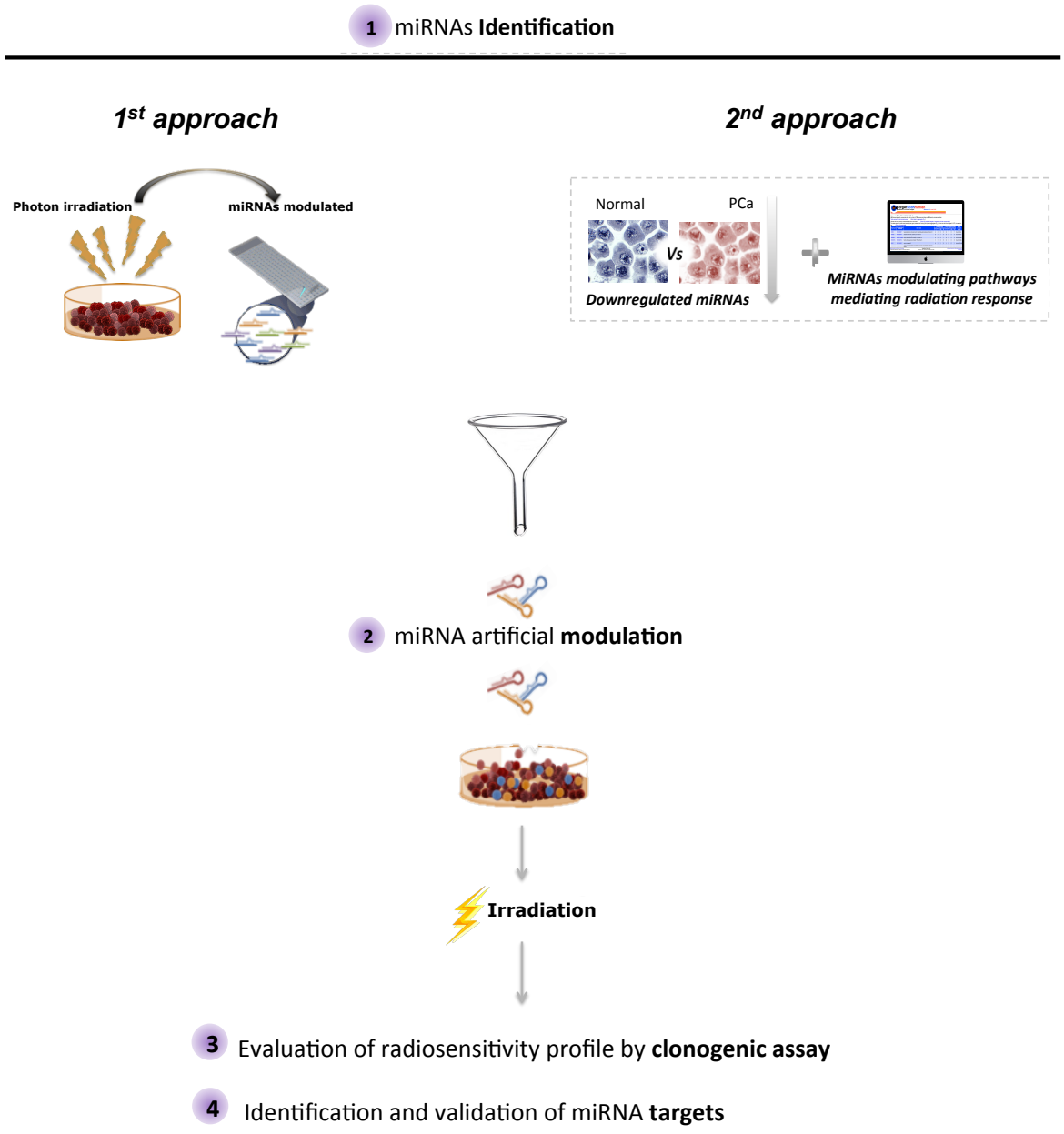

Figure 2.1 Schematic representation of the experimental design of the study

MATERIALS & METHODS

3. MATERIALS AND METHODS

3.1. Cell culture

3.1.1 Cell lines

The following human prostate cancer cell lines were used: DU145, PC-3, LNCaP, 22Rv1, which represent the gold standard of PCa cell lines [151]. All cell lines have been purchased from American Type Tissue Culture Collection (ATCC, VA, USA). DU145 cell line derives from a brain metastasis of a Caucasian 69-year-old carcinoma patient and displays an epithelial morphology. According to the information provided by ATCC, DU145 cell line is not hormone sensitive and does express neither androgen receptor nor the prostate specific antigen (PSA). The doubling time is approximately 30 hours (h), therefore a subcultivation ratio of 1:5 was observed twice a week. PC-3 cell line derives from a bone metastasis of a grade IV prostatic adenocarcinoma from a 62-year-old Caucasian patient. As for DU145 cell line, it is hormone insensitive and presents no AR or PSA. This epithelial cell line has a doubling time of approximately 24 h, thus needing a subcultivation rate of 1:6 two times a week. Both DU145 and PC-3 cells are able to form adenocarcinoma when injected into nude mice. LNCaP cell line was isolated from the left supraclavicular lymph node of a 50-year-old Caucasian male with confirmed diagnosis of metastatic prostate carcinoma. Unlike the first two cell lines, LNCaP are characterised by a slow growth, doubling every 48-60 h, thus implying a subcultivation rate of 1:3 and a very modest success rate upon

xenograft transplantation. 22Rv1 cell line was isolated from the xenograft CWR22R derived from a patient with bone metastasis. The main characteristic of 22Rv1 is the presence of the AR-V7 variant, a splicing variant of the androgen receptor that results in a constitutive activation of the receptor in a ligand independent manner. 22Rv1 doubling time ranges from 36–40 h, needing a subcultivation rate of 1:4 twice a week. All cell lines were maintained in RPMI-1640 medium supplemented with 10% fetal bovine serum (FBS), at 37°C and 5% CO_2. Cell lines were authenticated and periodically monitored by genetic profiling using short tandem repeat analysis (AmpFISTR Identifiler PCR amplification kit, Thermo Fisher Scientific Inc, Waltham, MA, USA).

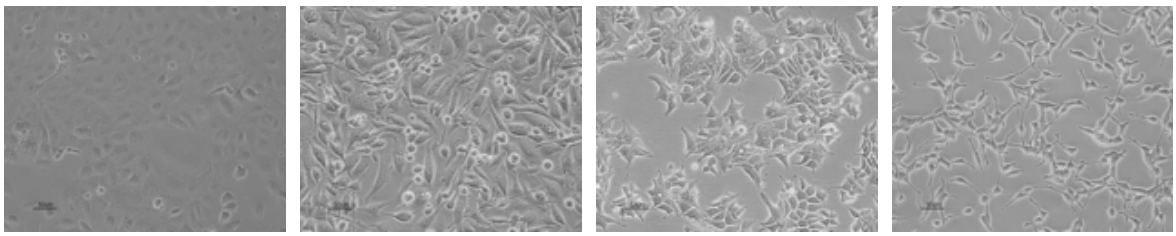

CELL LINE	DERIVATION	MUTATIONAL STATUS			ANDROGEN SENSITIVITY
		p53	PTEN	AR	
PC-3	Vertebral metastasis	Del/Mut	Del/Del	-	Insensitive
DU145	Brain metastasis	Mut/Mut	Wt/Del	-	Insensitive
LNCaP	Lymph Node	Wt	Del/Mut	+	Sensitive
22Rv1	CWR22R xenograft line	TS-Mut	Wt	+ (mut)	Sensitive

Figure 3.1 PCa cell lines morphology (up) and characteristics (down)

3.1.2 Cell transfection

Cell transfection was performed to vehicle miRNA, siRNA and target protector molecules into the host cells (DU145 and PC-3). The expression of the miRNAs of interest was ectopically modulated by transfecting cells with respective miRNA mimics, small, chemically modified double-stranded RNAs that mimic endogenous miRNAs and enable miRNA functional analysis by up-regulation of miRNA activity. miRNA mimics were purchased from Thermo Fisher Scientific (Waltham, MA, USA) and resuspended in sterile RNase-free water, diluted to the appropriate stock solution (10 μM) and stored at −20 °C until use.

siRNAs sequences were selected using the online siMAX design tool (www.eurofinsdna.com). A BLAST search for siRNA sequences was carried out to exclude any alignment with other sequences in the human genome. Control siRNAs made of mismatched sequences (with no significant homology to any known human mRNA) were included. SiRNAs were manufactured by Eurofins MWG Operon (Ebersberg, Germany) as pre-formed and purified duplexes, made of 19 bp-long RNA oligonucleotides with two extra-thymidine bases forming a 3′ overhang on both strands. Each siRNA was resuspended in sterile RNase-free water, diluted to the appropriate stock solution (10 μM) and stored at −20 °C until use.

For miRNA and siRNA experiments, cells were transfected for 4 h at 37°C with 20 nM mirVana miRNA mimic molecules (Thermo Fisher Scientific) or with 20 nM siRNA molecules using Lipofectamine 2000 (Thermo Fisher Scientific), respectively. Specifically, cells were let to grow until reaching 80% confluence and then the medium was replaced with Opti-MEM medium (Thermo Fisher

Scientific), a reduced serum medium supplemented with hypoxanthine, thymidine, sodium pyruvate, L-glutamine, trace elements, and growth factors, thus resulting ideal to be used during cationic lipid transfections since the presence of serum inhibits transfection efficiency by reducing the amount of lipid DNA complexes associating with the target cells [152]. Transfection mix is composed by 2 solutions where the miRNA molecule and the lipofectamine, respectively, are diluted in Optimem. For each condition two mixes were prepared containing miRNA mimic and Lipofectamine RNAiMAX, rispectively. To allow miRNA-lipofectamine complex formation the two solutions were mixed and incubated for 15 minutes at room temperature, added to host cells and incubated for 4 h at 37 °C in 5% CO_2. After incubation cells were washed with 0.9% saline solution and serum supplemented medium was added in order to stop transfection and cells were incubated at 37 °C in 5% CO_2 for further processing. Control experiments were performed in parallel by transfecting cells with 20 nM miRNA/siRNA negative controls. miR-875-5p synthetic mimic is referred to as miR-875-5p, miR-205 as miR-205, negative mock control oligomer as Neg, EGFR or PKCε miScript Target Protector as miR-Mask, ZEB1 siRNA as siZEB1, PKCε siRNA as siPKCε, LAMP3 siRNA as siLAMP3 and RAB27A siRNA as siRAB27A.

For target protection experiments, the target protector molecules (hereafter referred to as “miR-Mask”) were designed as “miScript Target Protectors” (Qiagen, Hilden, Germany) on Qiagen website, by indicating the REFseq ID of the target gene of interest (EGFR for miR-875-5p and PKCε for miR-205) and the seed region of the miRNA. The specific miR-Mask sequences were automatically generated and the respective custom product turned available for

purchase. Each miR-Mask was resuspended in sterile RNase-free water, diluted to the appropriate stock solution (10 μM) and stored at −20 °C until use. In order to allow the physical interaction between the target and the miR-Mask preventing its binding to the miRNA, a cotransfection with the miRNA mimic of interest and the miR-Mask was performed. Twenty nM EGFR or PKCε-miScript Target Protector (Qiagen, Hilden, Germany) were used alone or in cotransfection with miR-875-5p or miR-205 mimic, respectively.

For the generation of a DU145 cell clone overexpressing miR-875-5p, pEZX-MR04 vector (GeneCopoeia, Rockville, MD, U.S.A) carrying the 230 bp DNA region encompassing the 76 bp miR-875-5p precursor sequence was used to stable transfect DU145 cell line. The plasmid containing a scramble sequence was used as negative control and referred to as Null. Cells were transfected according to Lipofectamine 3000 protocol (Thermo Fisher Scientific Inc). Briefly, cells were seeded in 6-well plate (5 x 10^5 cells/well) and 24 h later transfected with vectors (10 pg). After 72 h, cells were selected using 0.3 mg/ml puromycin for 5 weeks. Stable transfectants were stored in liquid nitrogen at 196° C. When cultured, transfected cells were maintained in presence of 0.3 mg/ml of puromycin. As for the DU145 cell clone stably overexpressing miR-205, a clone previously established in the lab for a prior study on miR-205 has been used [153].

For IL-6 levels restoration in miR-23a-3p transfected DU145 cells, recombinant human IL-6 was purchased from Peprotech (Rocky Hill, NJ) and used at 50 ng/ml as a single-supplementation.

3.1.3 Clonogenic assay

To evaluate radiation-induced late effect, consisting of disrupting cell capacitiy to proliferate indefinitely upon DNA damage induction, cell clonogenicity was assessed by clonogenic assay. Transfected cells were exposed to increasing doses of radiation (2- 8 Gy) delivered as a single dose using the ^{137}Cs γ-irradiator IBL-437 (dose rate 5.2 Gy/min). Cell suspensions at increasing cell densities (500 to 8000 cells/well) were prepared to allow colony formation even at the higher doses of radiation (Fig. 3.2).

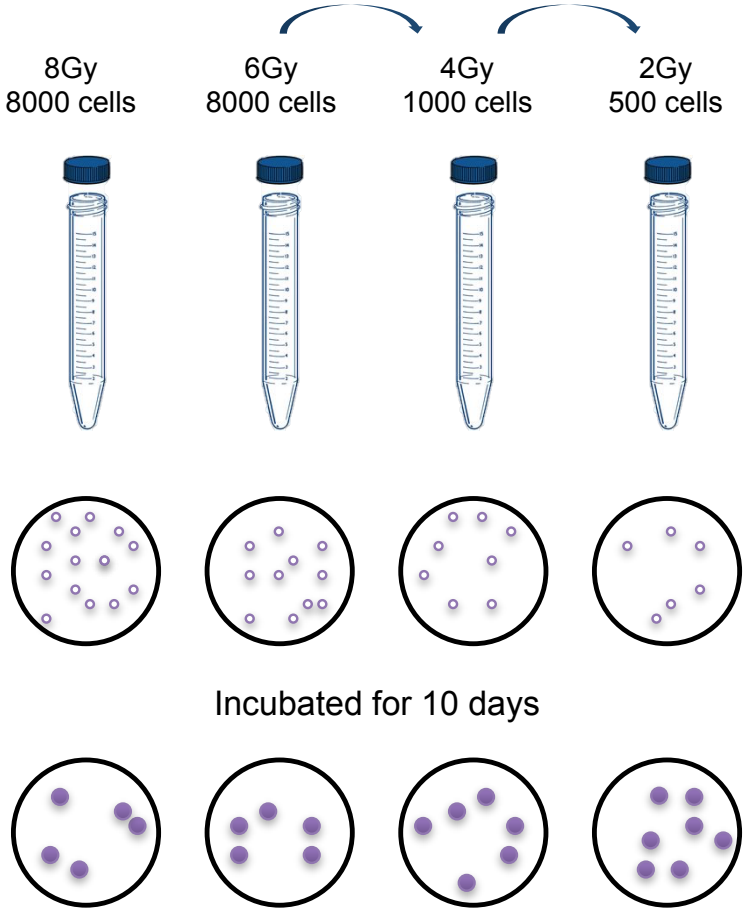

Figure 3.2 Schematic representation of clonogenic assay

Different cell suspensions were seeded in triplicate in RPMI medium containing 10% FBS and let to form colonies for several days according to cell doubling time (approximately 8 days for DU145 and 12 days for PC-3), since a colony is defined to consist of at least 50 cells, and each cell line took different days to undergo the number of cell duplications needed to reach this cell number. Once colony formation occurred, colonies were fixed with 70% ethanol, stained with crystal violet in 70% ethanol, and counted. The colony plating efficiency (PE) was calculated as the ratio of the number of colonies to the number of single cells seeded. The surviving fraction (SF) was calculated as the ratio of the colony-forming efficiency of the irradiated sample to that of the non-irradiated one.

Plating Efficiency (PE) = $\text{Number of counted colonies} / \text{Number of seeded cells}$

Surviving Fraction (SV) = $\text{PE of irradiated cells} / \text{PE of non irradiated cells}$

3.1.4 In vivo experiments

All animal experiments were approved by the Ethics Committee for Animal Experimentation of Fondazione IRCCS Istituto Nazionale dei Tumori.

For the xenotransplantation of DU145 cells stably expressing the miRNA of interest (miR-875 and miR-205), SCID mice were used for subcutaneous injection.

Specifically, ten million DU145 cells (negative control and stably expressing miR-875-5p/miR-205 clones) were injected into the right flank of eight-week-old male SCID mice, and when tumors reached ~300 mm^3 ($Width^2$ x Length/2) for miR-875-5p experiments and 100 mm^3 for miR-205, mice were randomly assigned to control or radiation treatment groups (n=8). Mice received 5 Gy single dose irradiation using a micro-CT/microirradiator (225Cx, Precision X-ray) capable of image-guided radiation delivery at the small-animal.

Specifically, mice were anesthetized with an intraperitoneal injection of a solution containing ketamine (100 mg/kg) and xylazine (5 mg/kg). After approximately 20 minutes, anesthetized mice were placed on the carbon-fibre support platform, which is under the control of stepper motors used to precisely drive the stage in the correct position, where the tumour to be irradiated is centred by the gantry. The first imaging acquisition aimed at positioning both the stage and the gantry was done with a photon energy of 40 kVp, 1 mA, and a resolution of 0.2 mm. To select the desired targeting location, and plan the treatment, CBCT images were acquired with the animal in the treatment position, by using SmART Plan software, which is an executable program on a Linux-based platform. The CBCT images were imported in the CT upload module and cropped and resized, reconstructing the 3D image by integrating the imaging information deriving from each dimension (axial, sagittal and lateral). A specific contouring of the target area to be irradiated was done and, once the target was selected, an appropriate irradiation protocol was designed, starting from a beam-definition step, which includes isocentre definition, and beam angles and size setting. Dose distribution and treatment parameters were automatically calculated by the software, based on Monte Carlo calculation algorithms. In particular, to administer 5 Gy single dose to the xenografts, 2

opposing (angle=180°) beams of 2.5 Gy each were set in order to minimize the dose absorbed by the surrounding normal tissues yet delivering the desired dose to the target tumour. According to the restrained volume of the tumour, a rectangular collimator of 1.0 cm×1.0 cm was used in order to precisely sharpen the beams towards the target by limiting radiation scattering. Once radiotherapy is delivered, mice are retrieved from the irradiator stage and placed in their cages under controlled conditions [154].

At day of the treatment (31 and 20 for miR-875-5p and miR-205, respectively) and after ~50 and 40 days (for miR-875-5p and miR-205, respectively), representative X-ray images were collected. In order to perform *ex vivo* evaluations, tumour specimens were removed from 4 additional mice 24 h after irradiation and immediately disaggregated for *ex-vivo* clonogenic assay and RNA/protein collection or fixed in 10% buffered formalin for immunohistochemical analysis.

3.2 Molecular biology analyses

3.2.1 RNA isolation

To perform miRNA and gene expression analysis, total RNA was extracted by using miRNeasy mini kit (Qiagen, Valencia, CA, U.S.A.), which combines phenol/guanidine-based lysis of cell samples and silica-membrane–based purification of total RNA, including miRNAs.

Specifically, cell pellets were disrupted and homogenised by resuspension with 700µl of QIAzol Lysis Reagent (Qiagen), a monophasic solution of phenol and

guanidine thiocyanate, designed to facilitate lysis of fatty tissues and inhibit RNases and also to remove most of the cellular DNA and proteins from the lysate by organic extraction. The homogenate was incubated at room temperature for 5 minutes. Subsequently 140 µl of chloroform were added and the homogenate was separated into aqueous and organic phases by centrifugation (15 minutes at 12000 x g at 4°C). RNA partitions to the upper aqueous phase, while DNA remains in the interphase and proteins in the lower, organic phase. The upper aqueous phase was transferred to a new collection tube avoiding transferring any interphase. 1.5 volumes of 100% ethanol were added and mixed thoroughly by pipetting in order to precipitate RNA from the aqueous phase. Then, 700 µl of each sample, including any precipitate, were transferred into an RNeasy Mini column in a 1.5 ml collection tube, and then centrifuged at ≥ 8000 x g at room temperature for 15 seconds.

The flow-through was discarded and 700 µl of Buffer RWT were added to the columns and centrifuged for 15 seconds at ≥ 8000 x g at room temperature. Then the columns were washed with 500 µl of Buffer RPE by two centrifugation steps. Finally, columns were transferred to a new 1.5 ml tube and 30 µl of RNase-free water were pipetted directly into the column membrane and centrifuged for 1 minute at ≥ 8000 x g to elute RNA.

The total amount of RNA was quantified through Nanodrop, a spectrophotometer that allows nucleic acid quantification, by a modification of the Beer-Lambert equation. The determination of nucleic acid concentrations is based on the absorbance at 260 nm, corrected for the extinction coefficient specific for RNA (=40 ng-cm/µL). Moreover, purity ratios were verified for each sample, by considering as “pure” a value of ~ 2.0 for 260/280 ratio (indicative of the presence of protein, phenol or other contaminants that absorb strongly at or

near 260 nm) and 1.8-2.0 for 260/230 ratio (the presence of residual phenol, guanidine, magnetic beads, carbohydrates or proteins). Quantified RNA samples were stored at -20° C until use.

3.2.2 Reverse Trancription

Conversion of RNA to cDNA was performed by using miScript II RT kit (Qiagen).

For reverse transcription, miRNAs and other noncoding RNAs (ncRNAs) included in the total RNA are polyadenylated by poly(A) polymerase and converted into cDNA by reverse transcriptase with oligo-dT priming. mRNAs are converted into cDNA by reverse transcriptase using both oligo-dT and random priming. Detection of mature miRNAs and mRNAs was performed using specific assays. Detection of mature miRNA, precursor miRNA, other ncRNA, and mRNA can be performed using the appropriate assays (Fig. 3.3).

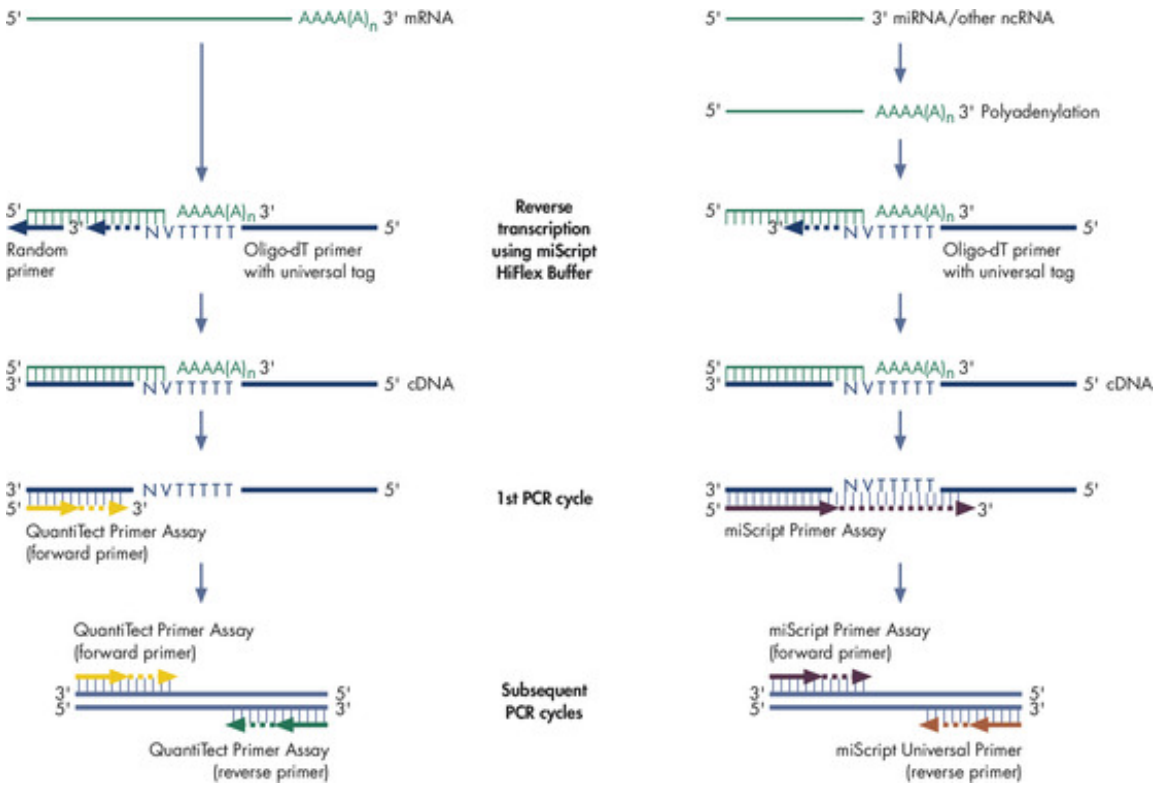

Figure 3.3 Reverse transcription of mRNAs and miRNAs using miScript II RT kit

For each sample, a total amount of 1 µg of RNA was reverse transcribed in the reverse-transcription master mix containing all components required for first-strand cDNA synthesis, except template RNA. The master mix was prepared as following: 4 µl of 5x miScript HiFlex Buffer, 2 µl of 10x miScript Nucleic Mix, 1 µl of Reverse Transcriptase, 3 µl RNase-free water to a final volume of 10 µl (volumes for 1 reaction).

A thermal cycler was used to perform the retrotranscription reaction using the conditions: 60 minutes at 37°C followed by 5 minutes at 95° to inactivate miScript Reverse Transcriptase. cDNA was stored ad -20°C until use.

3.2.3 miRNA and mRNA expression analysis

Quantification of miR-875-5p or miR-205 expression levels was assessed by qRT-PCR using miScript SYBR Green PCR kit (Qiagen), which includes the QuantiTect SYBR Green PCR Master Mix and the miScript Universal Primer, a reverse primer that allows detection of miRNAs in combination with the following specific miScript Primer Assays:

Detector	**Assay ID**
miR-875-5p	Hs_miR-875-5p_1
miR-205	Hs_miR-205_1
RNU6	Hs_RNU6-2_11

Table 3.1 SYBR Green PCR Assays

RNU6 was used as endogenous control, as it is an ncRNA that show a relatively constant expression level across a variety of cells and tissues. An ideal endogenous reference RNA for normalisation of data in real-time PCR quantification of miRNA should have the following features:

- A constant expression level across all samples in the study
- A similar small size as the miRNA under study
- A similar expression level in the sample as the miRNA under study
- Should not be regulated under the experimental conditions.

The mix was prepared using: 12.5 µl of master mix (QuantiTect SYBR Green PCR Master Mix), 2.5 µl of universal primer (10x miScript Universal Primer), 2.5 µl of specific primer, 2.5 µl of diluted cDNA and 5 µl of water (volumes for 1

reaction). The amplification reaction was performed by 7900HT Fast Real-Time PCR System as following: 95°C for 15 minutes followed by 40 cycles of denaturation at 94°C for 15 seconds, annealing at 55°C for 30 seconds and extension at 70°C for 30 seconds.

For gene expression analyses, qRT-PCR was assessed using the specific following TaqMan gene expression assays (Thermo Fisher Scientific):

Detector	**Assay ID**
CDH1	Hs00170423_m1
CTNNB1	Hs00355045_m1
EGFR	Hs01076078_m1
ZEB1	Hs00232783_m1
PKCε	Hs00178455_A1
LAMP3	Hs01111316_m1
RAB27A	Hs00608302_m1
GAPDH	Hs02786624_g1

Table 3.2 TaqMan Gene Expression Assays

GAPDH was used as endogenous control. For each gene, a mix was prepared in 1.5 ml tubes using: 5 µl of Taqman master mix (TaqMan Fast universal master mix, Applied Biosystems), 0.5 µl of specific primer, 2.5 µl of diluted cDNA and 2 µl of water (volumes for 1 reaction). The amplification reaction was performed as following: 95°C for 15 minutes, 40 cycles of denaturation at 95°C for 15 seconds and annealing at 55°C for 30 seconds, and a final step of extension at 72°C for 30 seconds. Amplifications were run on the 7900HT Fast

Real-Time PCR System. Data were analyzed by SDS 2.2.2 software (Thermo Fisher Scientific Inc) and reported as relative quantity with respect to a calibrator sample using the $2^{-\Delta\Delta Ct}$ method. The $2^{-\Delta\Delta Ct}$ method is a comparative method that relies on comparing the differences in CT (threshold cycles) values obtained with normal (negative control) versus experimental (transfected) samples. Specifically, the CT for each sample was determined. Next, the ΔCT value was calculated as the difference between the CT value of the target miRNA and the CT value of the endogenous control (RNU6/GAPDH).

ΔCT = CT (target) - CT (endogenous control)

In the next steps, the ΔΔCT value and the normalized target expression were calculated:

ΔΔCT = ΔCT (sample [i.e.: transfected cells]) - ΔCT (calibrator [e.g., negative control cells])

The relative quantification (RQ), which allows to analyse changes in miRNA/gene expression in the sample of interest relative to the reference sample, is calculated as $2^{-\Delta\Delta CT}$.

3.3 Biochemical analyses

3.3.1 Western blotting

Western blotting analysis was performed to evaluate protein expression levels upon different transfection and irradiation conditions. The total protein content was considered for all the experiments except for the assessment of phospho-DNA-PK, phospho-ATM, and the subcellular localization of EGFR upon

irradiation, where a sub-fractionation was performed. For the assessment of EGFR nuclear translocation, DU145 cells were transfected with miR-875-5p or miR-205 mimic and the respective negative control as described. Twenty-four hours after transfection, cells were irradiated at 4 Gy and harvested for subcellular protein distribution by Subcellular Protein Fractionation Kit (ThermoFisher Scientific) after 30 minutes and 60 minutes from irradiation. As for ATM and DNA-PK evaluation, 48 h after transfection, cells were irradiated at 4 Gy and harvested at 0.5, 2 and 4 h later for subcellular protein fractionation.

As for the western blotting analysis where the fractionation was not needed, total proteins were extracted from DU145 cells at different time points after radiation. Pellets were washed in ice PBS (Lonza) and homogenized in 4 mL Laemli lysis buffer mix composed as in table 3.3:

Reagent	Quantity
TRIS HCL 0,5 M PH 6.8	1 ml
SDS 10%	2 ml
Leupeptina	4 µl
Pepstatina	4 µl
A protein	4 µl
PMSF 100 nM	40 µl
H20	948 µl

Table 3.3 Composition of Laemli lysis buffer.

Lysed samples were cooled in ice and stored at -20° C.

For both total and fractionated contents, protein concentration was determined using spectrophotometer POLARstar OPTIMA at a wavelength of 562 nm using Pierce BCA Protein Assay Kit as colorimetric assay. To perform protein quantification, the Bovine Serum Albumin according to scale of dilutions from 0.01 µg/µl to 0.05 µg/µl was used as a standard reference. Quantification was performed using the spectrophotometer.

After quantisation, samples were prepared to be resolved on polyacrylamide gel and then transferred into Hybond nitrocellulose membranes (Amersham, Pittsburgh, PA). 30 µg of protein were loaded into the gel. Running buffer was prepared using: Tris-glycine 100 ml, SDS 10% 10 ml and water to a final volume of 1 L. The electrophoretic run was performed at 110 V for the time necessary to allow the separation of proteins.

Then the gel was transferred to the nitrocellulose filter using transfer buffer composed by: Tris-glycine 100 ml, methanol (96%) 200 ml and water to a final volume of 1 L. The presence and the integrity of the extract in the nitrocellulose were verified by treatment with Red Ponceau making proteins visible upon direct binding. Filters were blocked in PBS-Tween/0,5% skim milk and probed overnight with the appropriate primary antibodies (table 3.4):

Antibody	Company	Code
RAB27A	Abcam	Ab55667
LAMP3	Abcam	Ab83659
PKC-ε	Santa Cruz	Sc-1681
β actin	Abcam	Ab8226

Table 3.4 Primary Antibodies.

The filters were then incubated with the respective secondary peroxidase-linked whole antibodies (Life Technologies) 1 h at room temperature. Bound antibodies were detected using the Novex ECL, HRP Chemiluminescent substrate Reagent Kit (Life Technologies) and filters were autoradiographed. For the preparation of figures, the original western blots were cropped to generate the figure panels with the relevant lanes. Cropped images were then subjected to uniform image enhancement of contrast and brightness. Molecular weights were determined using the colorimetric Precision Plus Protein Standard (Bio-Rad) and standard protein bands were removed from the chemoluminescent blot image.

3.3.2 Immunofluorescence

To perform immunofluorescence analysis, cells were immobilized on a solid support that is optically suitable for microscopy. For this purpose, we prepared a cellular solution of 300.000 cells/ml.

Then slides and filters were placed into appropriate slots in the cytospin with the cardboard filters facing the centre of the cytospin and we subsequently aliquoted 200 µl of cellular solution for each sample. Centrifugation was performed at 8000 rpm for 3 minutes.

Slides were carefully removed from cytocentrifuge and cells were fixed with 4% formaldehyde and permeabilised with cold methanol/acetone solution. Cells were probed with primary antibodies for phospho-Histone H2A.X (ab11174, Abcam) and with Alexa Fluor488-labeled secondary antibodies (Thermo Fisher Scientific Inc.) for 1 hour at room temperature. Nuclei were stained with DAPI (Thermo Fisher Scientific Inc) and images were acquired by Nikon Eclipse E600 microscope using ACT-1 software (Nikon). For each sample, only the cells with at least 10 γH2AX nuclear foci were counted at different time points from irradiation (0, 1, 4 and 8 hours).

3.3.3 Immunohistochemistry

To assess distribution and localisation of specific cellular components (γ-H2AX and ZEB1) within cells and within their proper histological context, immunohistochemical analysis was performed. Briefly, tumours were removed, formalin-fixed and paraffin-embedded. Tumour sections of 4-μm were deparaffinized in xylene, rehydrated through graded alcohols to water, and subjected to immunohistochemical analysis using the following antibodies: anti-ZEB1, rabbit polyclonal antibody (H102, Santa Cruz) at the dilution of 1:100 and the anti-phospho-H2AX (Ser139), mouse monoclonal antibody (clone JBW301, Millipore) at the dilution of 1:1200, respectively. Nuclei were counterstained with hematoxylin.

3.3.4 Comet assay

To assess DNA-damage at the level of a single cell, the alkaline Comet assay was performed. Comet assay is a microgel electrophoresis technique where a small number of cells suspended in a thin agarose gel on a microscope slide are lysed, electrophoresed, and stained with a fluorescent DNA-binding dye. Indeed, comet assay allowed the detection of DNA breaks induced by radiation, based on the different migration of damaged DNA compared to intact one when submitted to electrophoresis migration. For instance, cells with increased DNA damage display an increased DNA migration from the nucleus toward the anode, resembling the shape of a comet (Fig. 3.4). Specifically, 4 h upon irradiation at 4 Gy, transfected DU145 cells were resuspended in low-melting

agarose, layered on microscope slides and treated with a hypertonic lysis solution to disrupt and remove cell membranes, cytoplasm, and nucleoplasm and dissolve nulceosomes releasing their DNA content. Subsequently, the leftover nucleoid was treated with high alkaline solution, and let to migrate by electrophoresis for 10 minutes at 1 V/cm. Migration under alkaline conditions led to DNA unwinding and consequent exposure of alkali sites of DNA breaks. Such breaks migrated towards the anode when exposed to current during electrophoresis thereby producing the aforementioned 'comet'-like appearance. The extent of such a comet is proportional to the extent of DNA damage. To visualise comets, DNA was stained with SYBR Green and comets were imaged using a fluorescence microscope equipped with a video camera (Jai Pulnix, Sunnyvale, CA), and quantitative assessment of DNA damage was obtained using the Comet Assay IV software (Perceptive Instruments, Suffolk, UK). To estimate the extent of DNA damage, length and intensity of the comet tail were measured and the tail moment was calculated as the product of tail length and tail intensity. Tail moment was determined by counting at least 200 comets.

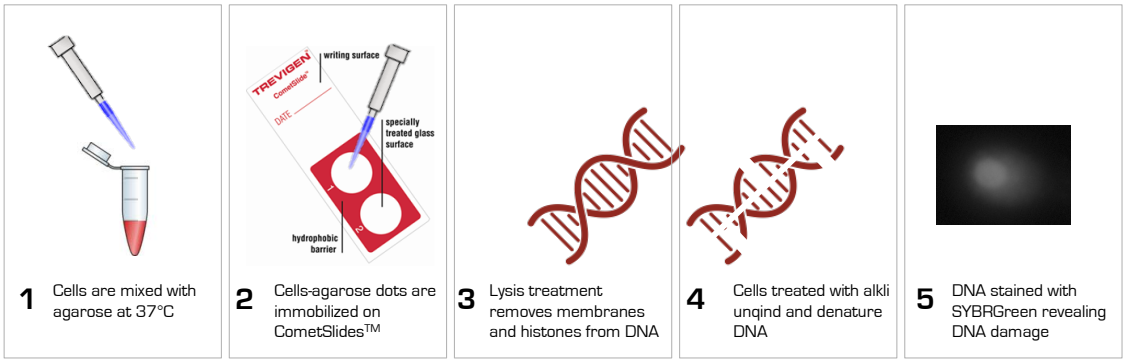

Figure 3.4 Schematic representation of Comet assay

3.3.5 Luciferase assay

To validate EGFR as a direct target of miR-875-5p, a luciferase assay was performed. Luciferase assay allows the validation of a specific target as a direct target of a miRNA of interest, as it relies on miRNA capacity to directly and specifically bind to the complementary sequence of the target mRNA. In the assay, a reporter activity is used as indicator of miRNA capacity to regulate the reporter expression *in vitro*. For instance, cells were cotransfected with the miRNA and a plasmid containing Firefly or Renilla luciferase coding sequence upstream of an mRNA 3'UTR from the gene of interest. If the mRNA 3'UTR is a target of the miRNA, the luminescence of the reporter will be altered, as a reflection of the changes in the transcript's stability and/or translation efficiency. Specifically, a 1285 nt-long portion of EGFR 3' UTR containing the predicted miR-875-5p binding site was amplified by PCR from cDNA obtained from DU145 cells, by using the following primers:

- *forward* 5'-AATTTCTAGACCACGGAGGATAGTATGAG-3'

- *reverse* 5'-AATTTCTAGAGCTACTGTCATTCGCACCT-3'.

PCR product was cloned into the XbaI site downstream of the FireFly luciferase gene carried in the pGL3-Basic. pGL3-Basic reporter plasmids (3.6 fmol) and pRL-Reporter (500 ng for normalization; Promega, Madison, Wisconsin, USA) were transfected with Lipofectamine 2000 (Thermo Fisher Scientific Inc) into DU145 cells (Fig. 3.5). Cells were collected after 24 h, lysed using Passive Lysis Buffer and the DLR Assay was performed according to the manufacturer's protocol (Promega E1910). For normalization, the ratio of Luciferase activity to

Renilla activity was measured. All experiments were performed in triplicate with data pooled from at least two independent experiments.

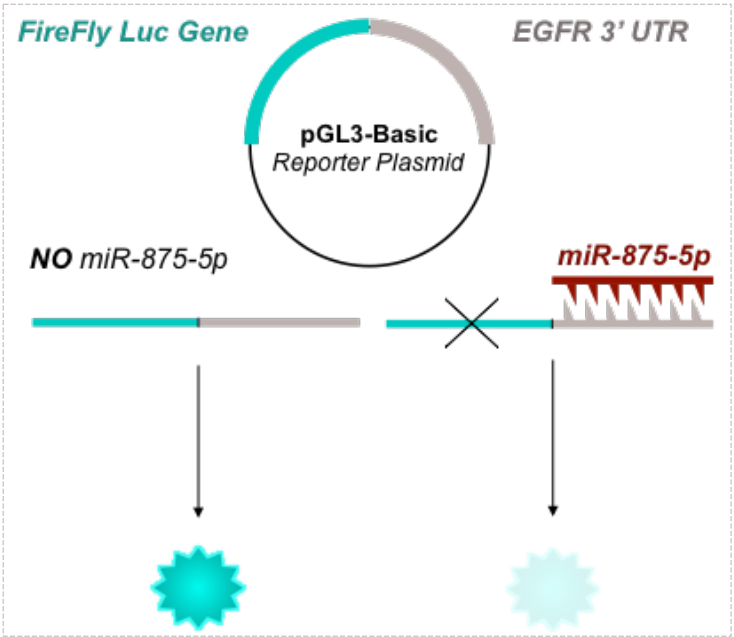

Figure 3.5 Schematic representation of Luciferase assay

3.4 Bioinformatics analyses

To assess miRNA expression in PCa tissues compared to normal matched tissues, normalised miRNA expression data of tumour and non-neoplastic prostate samples from prostate cancer patients were retrieved from GEO repository with accession number GSE76260. Data were filtered keeping only probes with a detection p-value < 0.01 in at least one sample and probes not associated to known mature miRNA transcripts were removed. Differentially expressed miRNAs between tumour and normal samples were identified using a moderated paired t-test as implemented in the limma package, considering only the 26 patients for which matched tumour and normal samples were available. miRNAs showing an FDR < 0.05 were considered significantly differentially expressed. The Pearson's correlation coefficient between miRNA and E-cadherin mRNA expression (as measured by qRT-PCR) was calculated for a subset of 44 samples (19 tumour and 25 normal), for which leftover RNA was available in the laboratory. miRNAs with a nominal p-value < 0.05 associated to the Pearson's correlation coefficient were selected.

To identify miRNAs modulated by radiation, as putative miRNAs related to radiation response, a miRNA expression profiling was performed. For photon irradiation experiment, all the 4 PCa cell lines were exposed to 10 Gy of irradiation and RNA was collected at various time points from treatment (4, 8 and 24 h). As for carbon ion irradiation, DU145 and LNCaP cells were exposed to 5 Gy of irradiation at CNAO and RNA was collected at 4, 8 and 24 h. Since intact RNA is a key element for successful microarray analysis, RNA integrity was assessed by the Agilent 2100 Bioanalyzer System, which generated RNA profiles allowing a visual inspection of RNA integrity, and generating ribosomal ratios. Briefly, using electrophoretic separation on microchips, RNA samples are separated and detected by fluorescence. The Bioanalyzer software generates a gel-like image and displays results including RNA concentration and the ribosomal ratio. Indeed, ribosomal ratio is an indicator of RNA degradation, since, as degradation proceeds, there is a decrease in the 18S to 28S ribosomal band ratio. However, although ribosomal ratios play an important role in determining the level of sample degradation in gel electrophoresis, a more standardized parameter called RNA Integrity Number (RIN) is used. The RIN system, by taking the entire electrophoretic trace into account, attributes an integrity score, ranging from 1 to 10, with 1 being the most degraded profile and 10 being the most intact. According to their RIN value, intact RNA samples were considered for microarray analysis, which was performed using Agilent Human miRNA Microarray System Release 19.0. Agilent's miRNA microarray is a highthroughput system based on direct labelling method, where 40–60-mer oligonucleotide probes are directly synthetized on the microarray surface (Fig. 3.6).

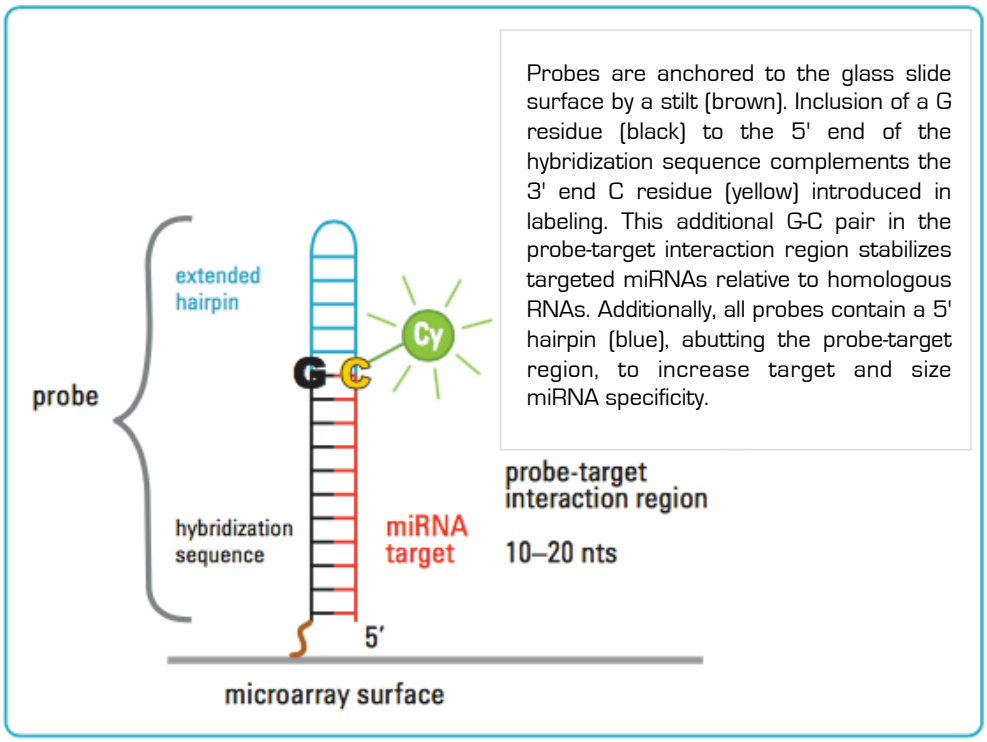

Figure 3.6 Agilent miRNA-microarray probe design

Raw intensity values obtained from the Agilent Feature Extraction (AFE) software, were processed using Robust Multi-array Average (RMA) algorithm for background correction. Data were then $\log_2$ transformed and quantile normalized. Based on detection information from the AFE software, only miRNA probes detected in at least 1 sample were considered for further processing. The remaining probe sets were mean summarised as a single miRNA expression value. Significant changes in miRNA profiles across time course were evaluated for each treatment (i.e., photons or carbon ions). To this end, we employed the linear model functions implemented within the limma package to compute log2 fold-changes and moderated t-statistics on pair-wise comparisons between time points. On continuation, we applied a Benjamini & Hochberg adjustment for multiple testing on each comparison. miRNAs with

log2 fold-changes >1.5 and adjusted p-value < 0.2 were considered as differentially expressed (DE).

To determine to which pathway the selected modulated miRNAs belong, functional over-overrepresentation of Gene Ontology (GO) Biological Process terms were generated for each set of predicted gene targets. Statistical significance of terms enrichment was determined by a hypergeometric test with Benjamini & Hochberg adjustment for multiple testing. For that purpose, we used the functions implemented within the clusterProfiler package in R. Enrichments with adjusted p-value <0.05 were considered significant. Construction of Circos plots was performed using the GOplot library.

To identify miR-875-5p and miR-205 relevant targets, the presence of putative miRNA binding sites in a given mRNA was predicted using MiRWalk (http://www.ma.uni-heidelberg.de/apps/zmf/mirwalk), which performs a comparison of the information produced by ten established miRNA target prediction programs. Only targets simultaneously predicted by at least three programs were considered as reliable. To sharpen the identification of miR-875-5p relevant targets, the list of predicted targets was then intersected with the list of genes found to be downregulated by a gene expression analysis performed on DU145 cells transfected with miR-875-5p and compared to Neg-transfected cells.

For gene expression profiling, RNA samples were processed for microarray hybridisation by the Functional Genomics core facility at Fondazione IRCCS Istituto Nazionale dei Tumori, Milan, Italy. Briefly, 800 ng of total RNA was reverse transcribed, labeled with biotin and amplified overnight (14 h) using the Illumina RNA TotalPrep Amplification kit (Thermo Fisher Scientific Inc)

according to manufacturer's protocol. One µg of the biotinylated cRNA sample was mixed with the Hyb E1 hybridization buffer containing 37.5% (w/w) formamide and then hybridized to Illumina HumanHT-12-v4 expression Bead Chip (Illumina, Inc., San Diego, CA, USA) at 58°C overnight (18 h). Arrays were washed with manufacturer's E1BC solution, stained with 1 µg/ml Cy3-streptavidine (Amersham Biosciences; GE Healthcare, Piscataway, NJ, USA) and eventually scanned with Illumina BeadArray Reader.

Raw expression data were collected from scanned images using Illumina BeadStudio v3.3.8 (Illumina) and processed using the lumi package from Bioconductor v3.0. Raw data were log2-transformed, normalized with Robust Spline Normalization and filtered, keeping only probes with a detection p-value < 0.01 in at least one sample. Multiple probes mapping to the same gene were collapsed selecting the probe with the highest detection rate, i.e., the percentage of samples in which the probe had a detection p-value < 0.01. In case of equal detection rates, the most variant probe according to interquartile range was selected. Gene expression data were deposited in the Gene Expression Omnibus repository (GEO) with accession number GSE68883. Differentially expressed genes were identified using the limma package. Multiple-testing correction was performed using the Benjamini-Hochberg false discovery rate (FDR) method. Genes with FDR < 0.05 and absolute fold-change (FC) ≥ 1.5 were considered significantly differentially expressed.

3.5 Statistical analyses

If not otherwise specified, data are presented as mean values ± SD from at least three independent experiments. Statistical analysis was performed by one-tailed Student's t test. Student's t test was chosen for statistical analysis since it is a statistical analysis technique used to test whether there is a significant difference between two independent sample means. Specifically, independent t-test was used, as in all cases the two groups under comparison were independent of each other. The test was applied to the compared groups by using the excel T.TEST function: T.TEST(array1,array2,tails,type), where Array 1 and 2 indicate the two data sets to be compared, tails specifies the number of distribution tails, referring to 1 tail if a specific direction (up or down) of the difference between the groups is expected. Specifically, all experiments in the study required a 1-tail test, as the effect of transfection/treatment was case-by-case expected to be more effective than the respective negative control, thus foreseeing the direction of the difference between the transfected/treated and the control group. Finally, type refers to the kind of T.TEST, with 2 being the independent T.TEST with equal variance between samples. Running the T.TEST function, a p-value was returned, a value that is defined as the probability, under the null hypothesis, of obtaining a result equal to or more extreme than what was actually observed, and that basically indicates the statistical significance of the difference observed between the compared groups. P-values <0.05 were considered statistically significant.

RESULTS

4. RESULTS I: miRNAs modulated in PCa cells upon radiation

With the aim of sorting miRNAs functionally involved in mediating PCa response to radiation, the very first step of this study was the definition of the possible strategies to follow in order to select miRNAs related to radiation response. In order to consider all the miRNAs potentially matching our query, we adopted two complementary approaches of miRNA identification. The first approach is based on the identification of miRNAs modulated upon radiation exposure, since they could represent a class of miRNAs that are responsive to radiation therefore displaying an involvement in radiation response processes. It is worth noting that miRNA modulation upon radiation does not indicate *per se* a functional role in radiation response, as miRNAs could be modulated upon radiation stimulus yet not having a functional role in influencing the response to the treatment. To investigate whether specific identified miRNAs actually play a functional role in determining cell responsiveness to radiation, their expression was artificially modulated in PCa cells by transfection with specific miRNA modulators (i.e.: miRNA mimics) and transfected cells were exposed to radiation in order to check whether miRNA modulation induced changes in cell sensitivity profiles.

To compare the effect induced by photon radiotherapy and hadrontherapy on miRNA profiling, PCa cell lines exposed to photon were also exposed to carbon ions and miRNA modulation was assessed.

4.1 miRNAs modulated upon photon irradiation

Following the first approach fort the identification of radiation response-related miRNAs, we evaluated the expression changes in the miRNome of PCa cells upon exposure to photon irradiation. Specifically, the 4 PCa cell lines available for the study (DU145, PC-3, 22Rv1 and LNCaP) were exposed to 10 Gy radiation delivered by the ^{137}Cs irradiator. For miRNA profiling, the total RNA, including miRNAs, from irradiated cells was isolated at different time points (4, 8 and 24 hours) from irradiation in order to obtain a kinetics of miRNA modulation.

4.1.1 RNA isolation

The use of an RNA extraction method in which small RNA species, including miRNAs, were conserved, was instrumental to start the miRNA expression analysis in PCa cells. For this purpose, RNA collected at 4, 8 and 24h from exposure to radiation was isolated using the miRNA isolation kit. Since the integrity of isolated RNA is a key element for successful microarray analysis, RNA integrity was verified by the Agilent 2100 Bioanalyzer System, which generated RNA profiles allowing a visual inspection of RNA integrity (Fig. 4.1).

A

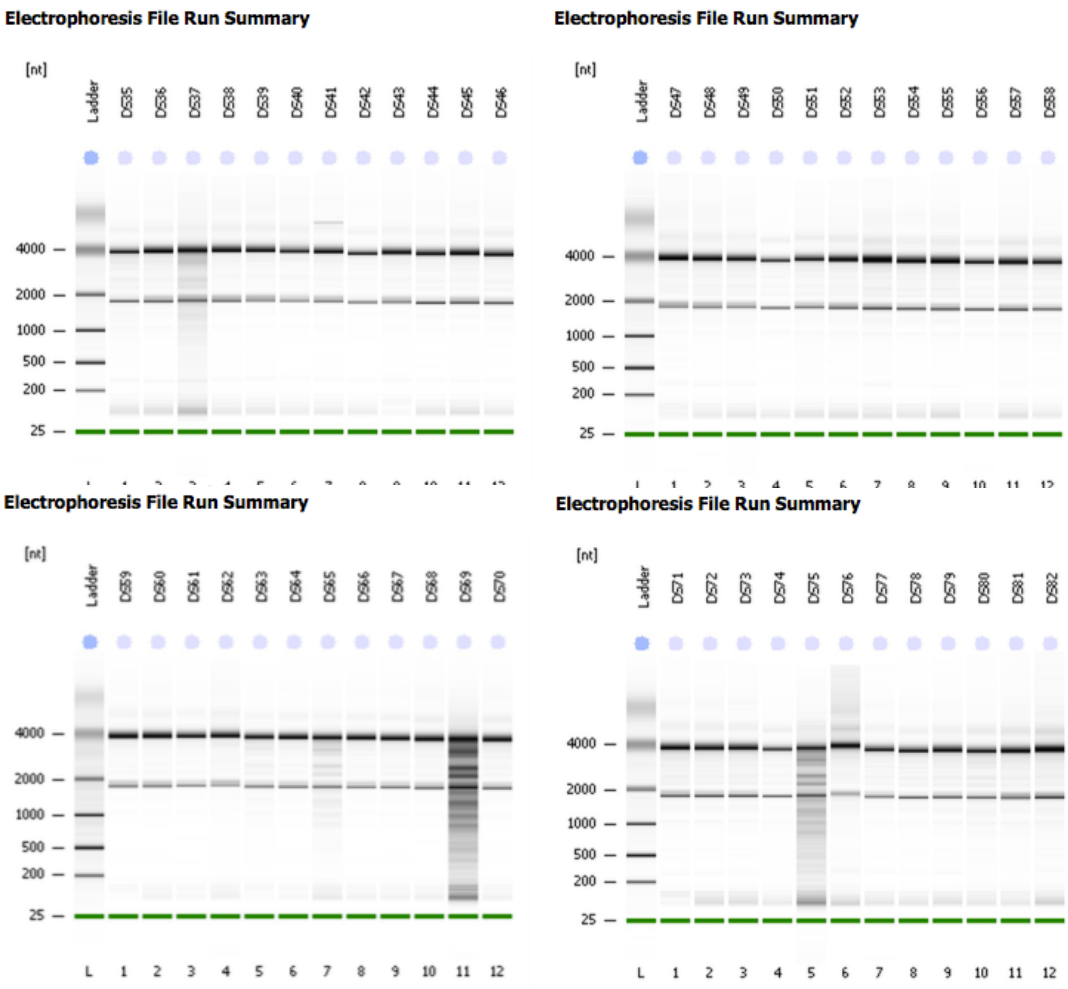
Electrophoresis File Run Summary
[nt]
Ladder
D535
D536
D537
D538
D539
D540
D541
D542
D543
D544
D545
D546
4000
2000
1000
500
200
25
Electrophoresis File Run Summary
[nt]
Ladder
D547
D548
D549
D550
D551
D552
D553
D554
D555
D556
D557
D558
4000
2000
1000
500
200
25
Electrophoresis File Run Summary
[nt]
Ladder
D559
D560
D561
D562
D563
D564
D565
D566
D567
D568
D569
D570
4000
2000
1000
500
200
25
L 1 2 3 4 5 6 7 8 9 10 11 12
Electrophoresis File Run Summary
[nt]
Ladder
D571
D572
D573
D574
D575
D576
D577
D578
D579
D580
D581
D582
4000
2000
1000
500
200
25
L 1 2 3 4 5 6 7 8 9 10 11 12

B

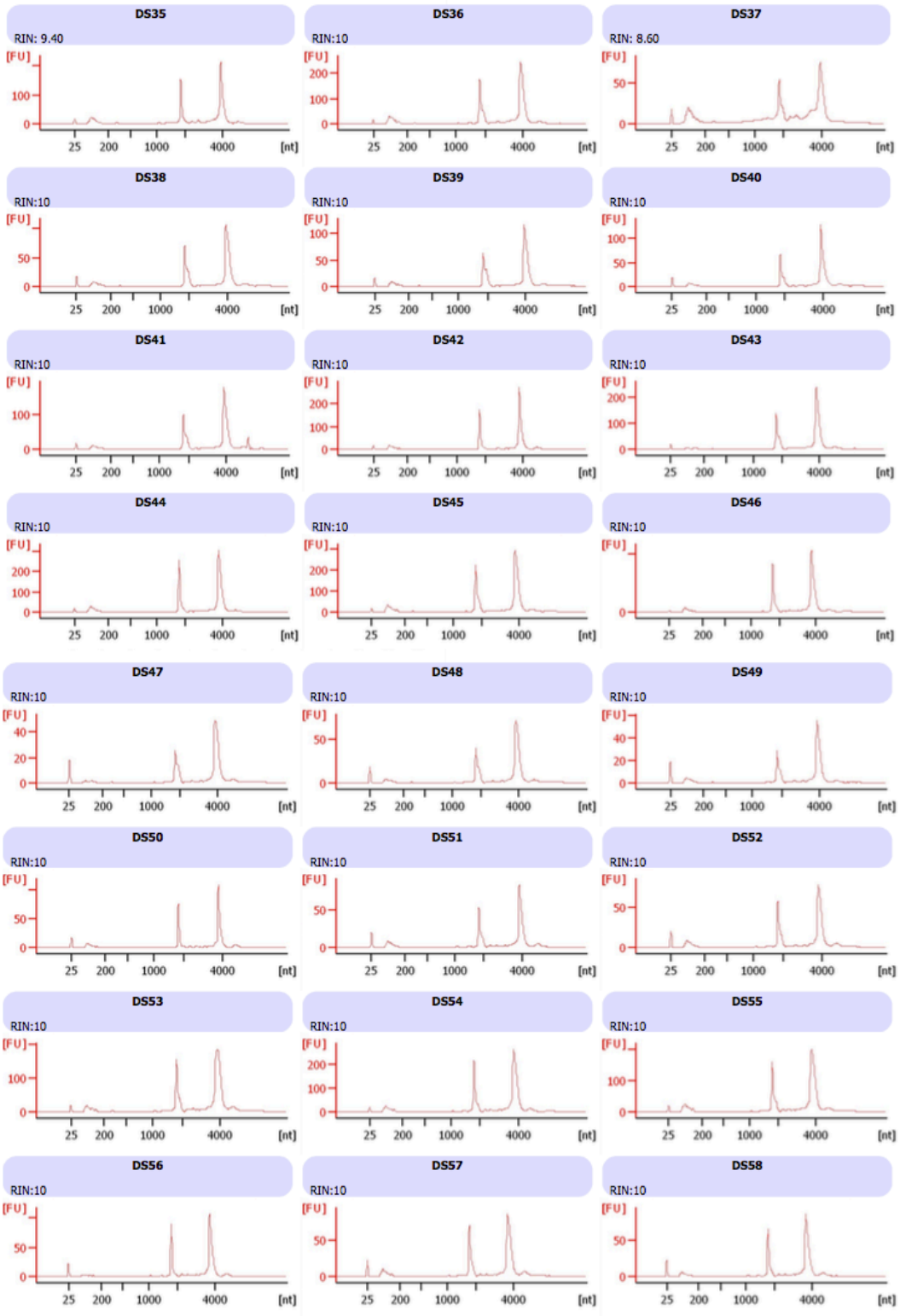
DS35
RIN: 9.40
DS36
RIN:10
DS37
RIN: 8.60
DS38
RIN:10
DS39
RIN:10
DS40
RIN:10
DS41
RIN:10
DS42
RIN:10
DS43
RIN:10
DS44
RIN:10
DS45
RIN:10
DS46
RIN:10
DS47
RIN:10
DS48
RIN:10
DS49
RIN:10
DS50
RIN:10
DS51
RIN:10
DS52
RIN:10
DS53
RIN:10
DS54
RIN:10
DS55
RIN:10
DS56
RIN:10
DS57
RIN:10
DS58
RIN:10
[FU]
[nt]
25
200
1000
4000

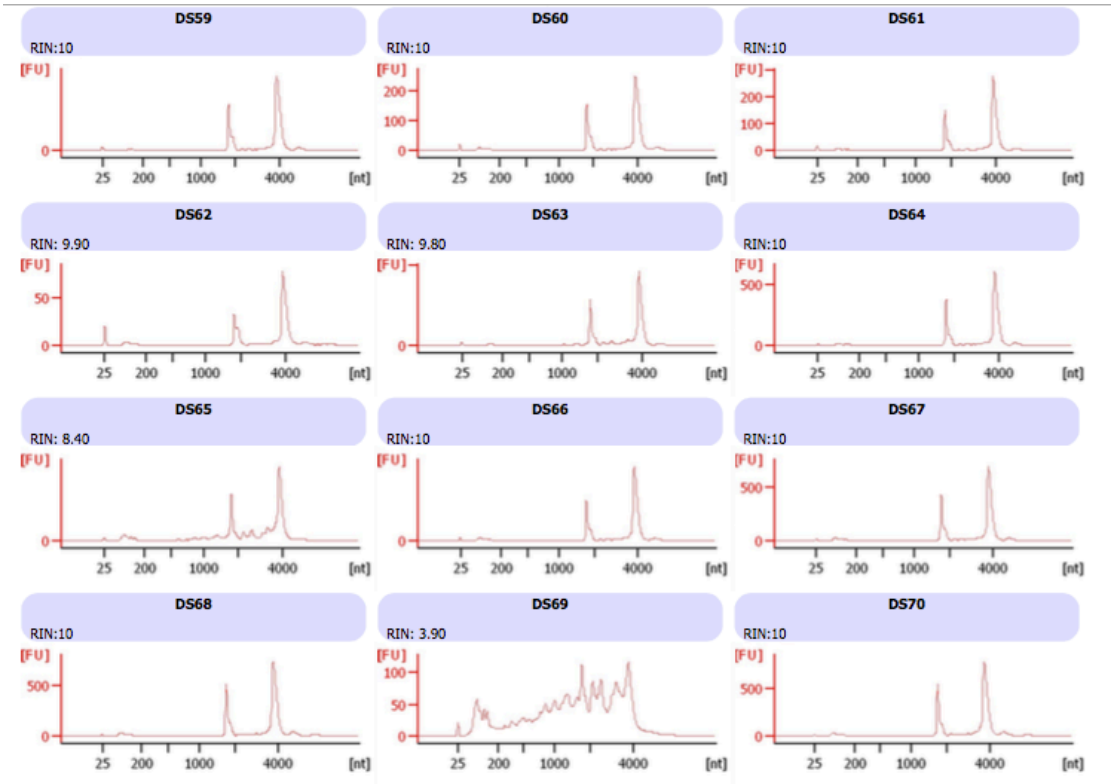
DS59
RIN:10
DS60
RIN:10
DS61
RIN:10
DS62
RIN: 9.90
DS63
RIN: 9.80
DS64
RIN:10
DS65
RIN: 8.40
DS66
RIN:10
DS67
RIN:10
DS68
RIN:10
DS69
RIN: 3.90
DS70
RIN:10
[FU]
[nt]
25
200
1000
4000

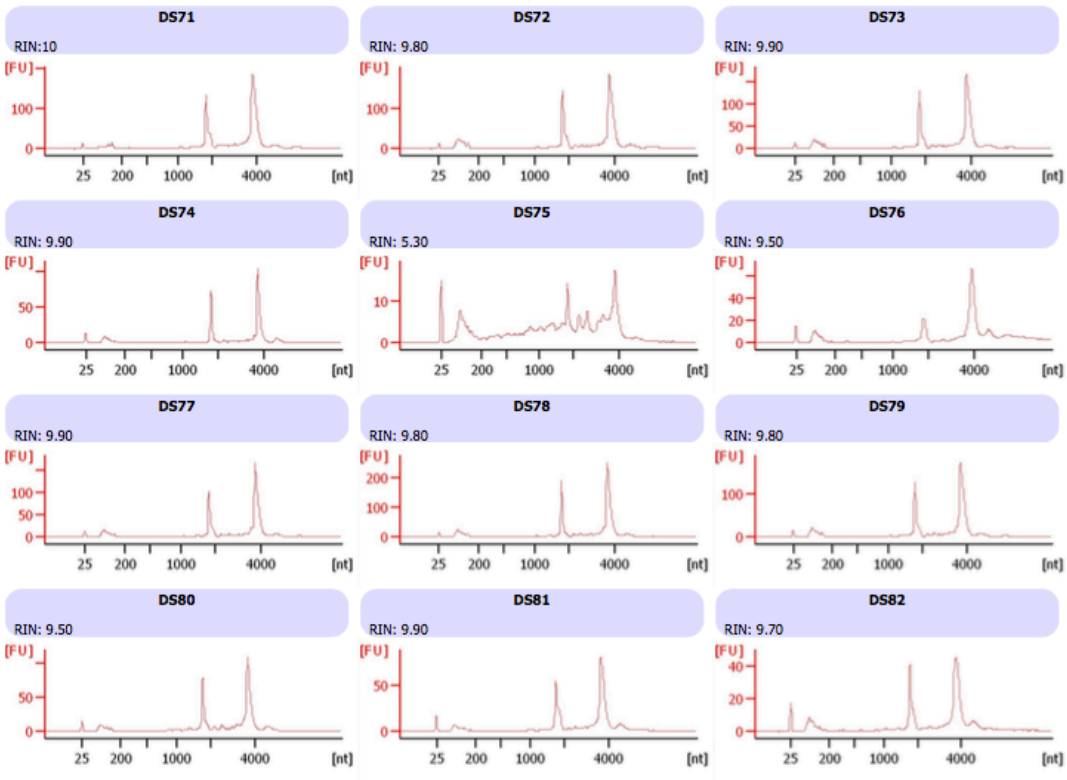

Figure 4.1 Integrity profiles of RNA isolated from PCa cell lines irradiated with photons. (A) Electrophoretic trace of the 48 samples of RNA isolated from DU145, PC-3, 22RV1 and LNCaP exposed to photon irradiation. The gel-like image reports the 18S to 28S ribosomal bands, which are indicative of RNA degradation presence, as in degraded RNA an increase in the baseline signal between the two ribosomal peaks and the lower marker is observable. Intact RNA shows a greater distance between ribosomal peaks and the lower marker. Samples were randomized into 4 groups of 12 samples/each. Each group was run on a different microarray chip taking into account intra-cell line variability. (B) RIN scores of RNA samples, ranging from 1 to 10, with 1 being the most degraded profile and 10 being the most intact. According to their RIN value, intact RNA samples were considered for microarray analysis, whereas non-intact RNA samples were replaced with new-isolated intact ones.

4.1.2 Microarray profiling

Quality-checked RNA was used for microarray analysis using Agilent platform and data were normalized and filtered as described in Materials and Methods section, thus generating a lists of miRNAs significantly up- and down-regulated, compared to non-irradiated cells, for each time point within each cell lines. In order to identify miRNA candidates responsive to irradiation, a differential expression analysis between different time points within each cell line was performed. Of importance, we detected two main miRNA subsets based on the temporal shift of expression changes along the whole-time series (i.e., at 4, 8 and 24 hours). For convention, we defined these subsets as “up-modulated”, characterized by bottom-up shift at 4 and 24 h, and “down-modulated”, characterized by a top-down shift at 4 and 24 h. To refine our analysis, we investigated which differentially expressed (DE) miRNAs in our initial lists are members of conserved miRNAs families (i.e., characterized by sharing a common conserved seed region).

4.1.2.1 Identification of miRNAs differentially expressed in each PCa cell line

DU145

With regards to the profile of temporally modulated miRNAs by photons in DU145, we found 66 miRNAs differentially expressed. From this list, 21 miRNAs were discovered to be up-modulated; while the remaining 45 miRNAs were down-modulated. The mapping against the data base of members of conserved miRNAs families (TargetScan) revealed 12 up-modulated and 19 down-modulated conserved miRNAs (Fig 4.2).

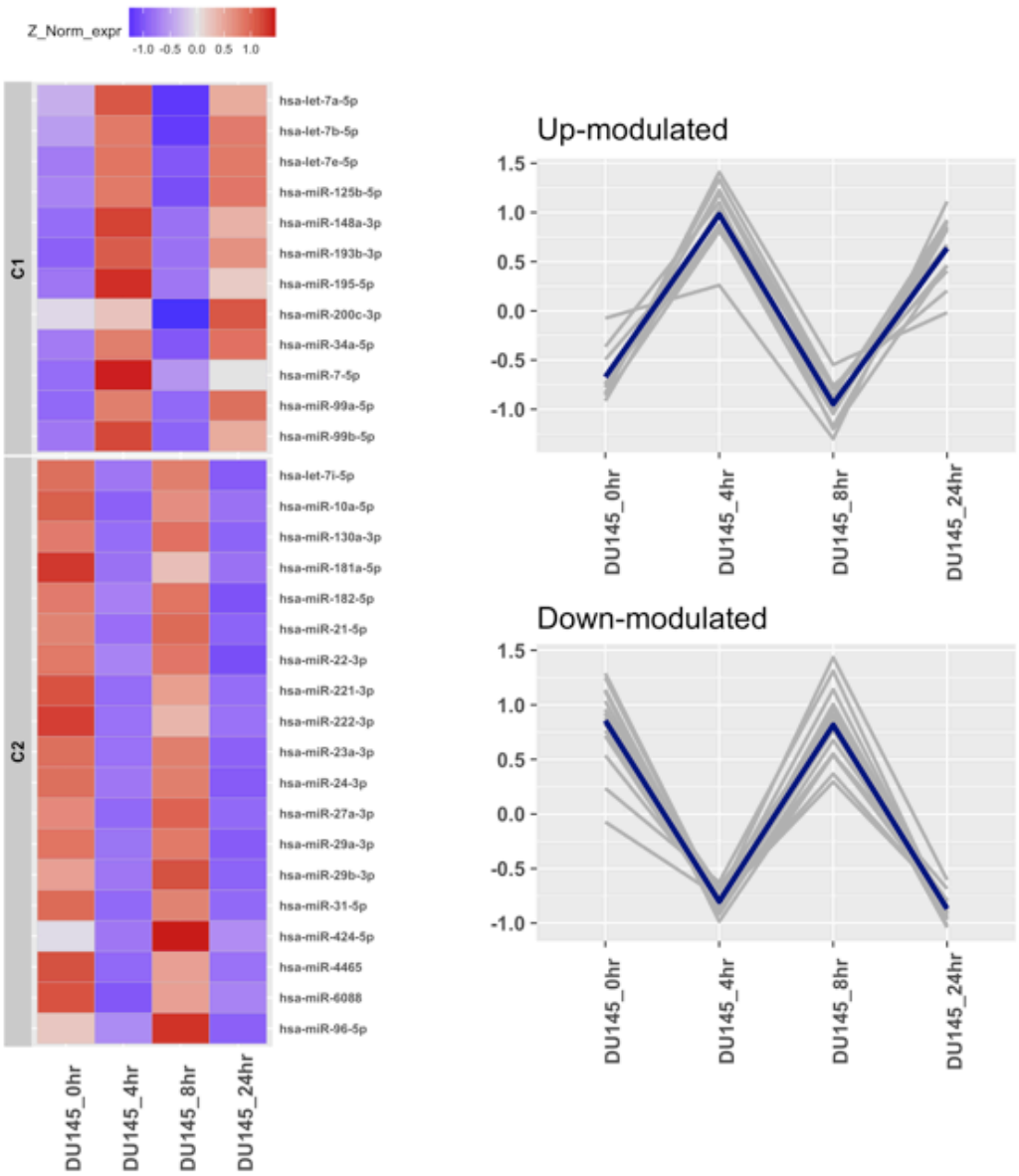

Figure 4.2 miRNAs in conserved miRNA families temporally modulated by photons in DU145 cells. (*Left*) Heatmap showing the expression levels of significantly modulated conserved miRNAs in DU145 along time, clustered according to their dynamic changes at 4, 8 or 24 h after photons irradiation as up-modulated (C1) or down-modulated group (C2). (*Right*) Line plots representing the average miRNA expression in the indicated group at each time point.

PC-3

The analysis for PC-3 cell line revealed only 16 miRNAs temporally affected by photon irradiation. As before, we clustered together these miRNAs based on their temporal shift across time and detected two main subsets. One of these subsets is composed of 10 Up-regulated miRNAs and is distinguished by a continuous increase in their expression at 4, 8 and 24 h. The second one is composed of 6 down-modulated miRNAs displaying a downward shift at 4 h, which gradually increases at 8 and 24 h (Fig 4.3). After the filtering process for conserved miRNAs, we obtained a final list of 6 up-modulated and 6 down-modulated miRNAs.

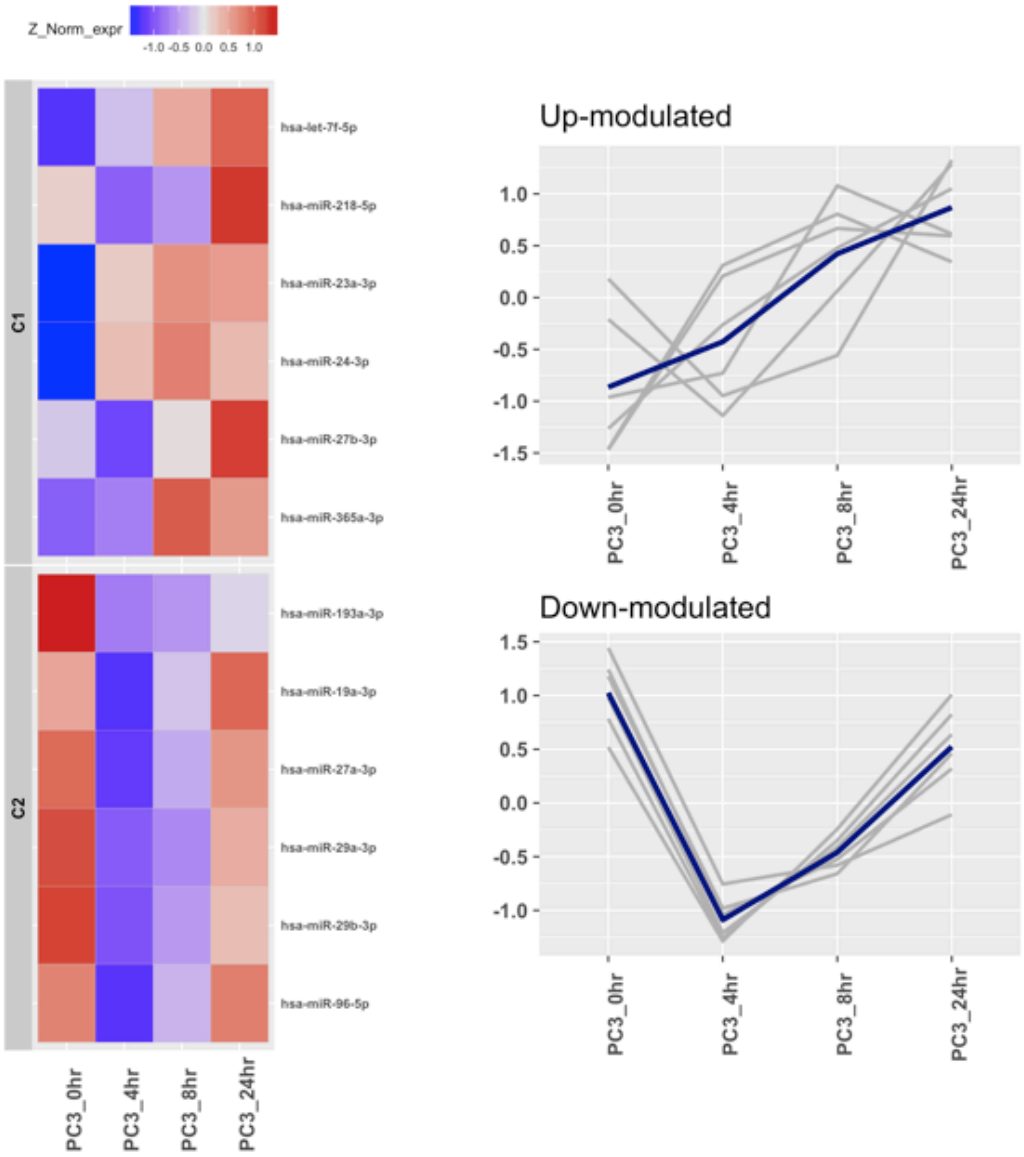

Figure 4.3 miRNAs in conserved miRNA families temporally modulated by photons in PC-3 cells. (Left) Heatmap showing the expression levels of significantly modulated conserved miRNAs in PC-3 cell line along time, clustered according to their dynamic changes at 4, 8 or 24 h after photons irradiation as up-modulated (C1) or down-modulated group (C2). (Right) Line plots representing the average miRNA expression in the indicated group at each time point.

22Rv1

Regarding the results for the 22RV1 cell line, we detected 67 miRNAs temporally regulated by photons. At defining the two main subsets of miRNAs based on the structure of their time-course expression, 35 up-modulate miRNAs showed a gradual increase at 4 ,8 and 24 h; while 32 down-modulated miRNAs showed a behaviour characterized by a top-down shift at 4 and 24 h. Following the filtering strategy to detect members of conserved miRNAs families, we detected 14 up-regulated and 7 down-modulated conserved miRNAs (Fig 4.4).

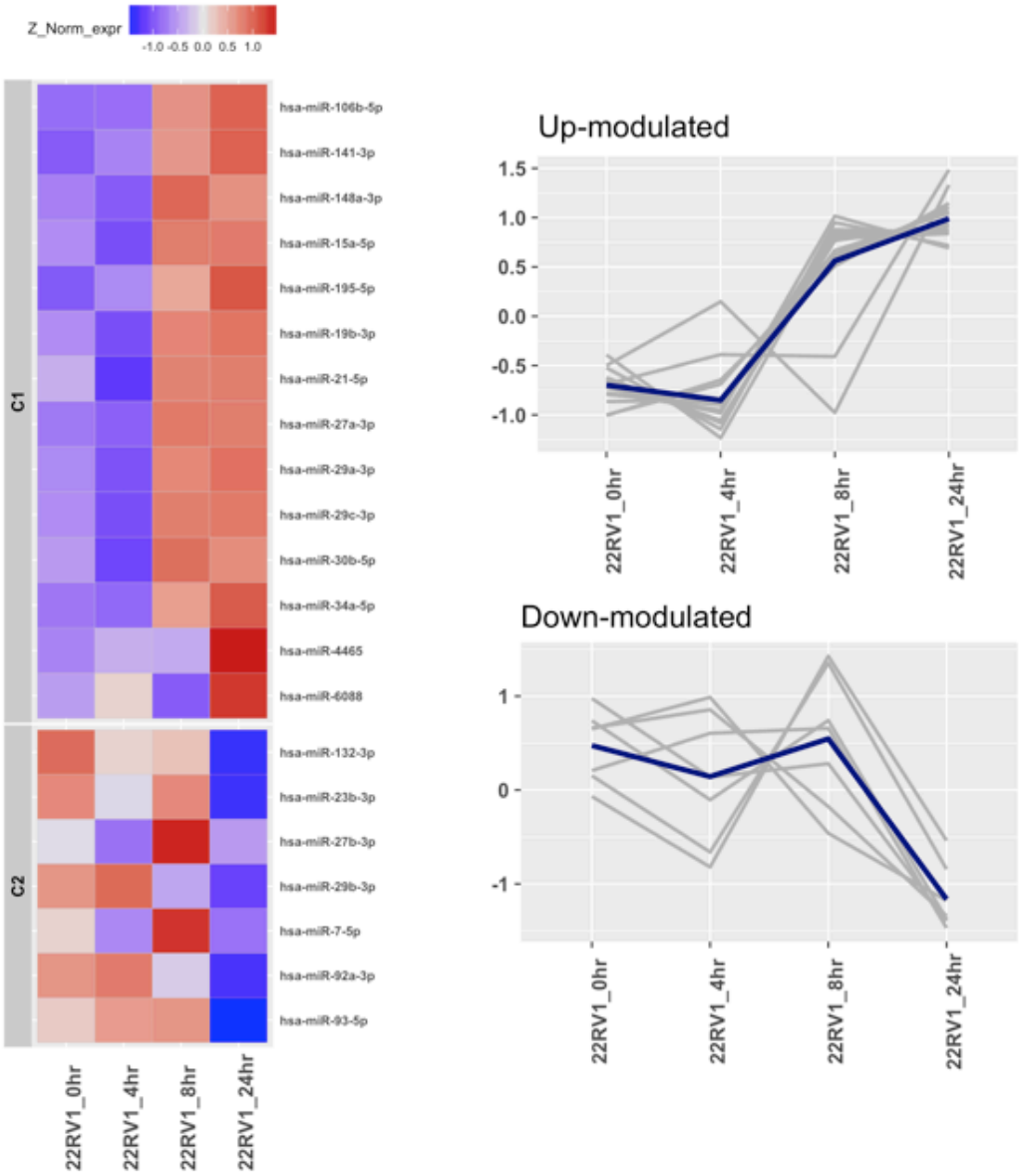

Figure 4.4 miRNAs in conserved miRNA families temporally modulated by photons in 22Rv1 cells. (*Left*) Heatmap showing the expression levels of significantly modulated conserved miRNAs in 22Rv1 cell line along time, clustered according to their dynamic changes at 4, 8 or 24 h after photons irradiation as up-modulated (C1) or down-modulated group (C2). (*Right*) Line plots representing the average miRNA expression in the indicated group at each time point.

LNCaP

Trough differential expression analysis between different time points in LNCaP, we were able to identify 109 miRNAs that were differentially expressed after cell irradiation. The “up-modulated” set was composed of 47 miRNAs, whereas the “down-modulated” was composed of 62 miRNAs. Among those, we identified 29 and 30 conserved miRNAs within the up-modulated and down-modulated subsets, respectively (Fig 4.5).

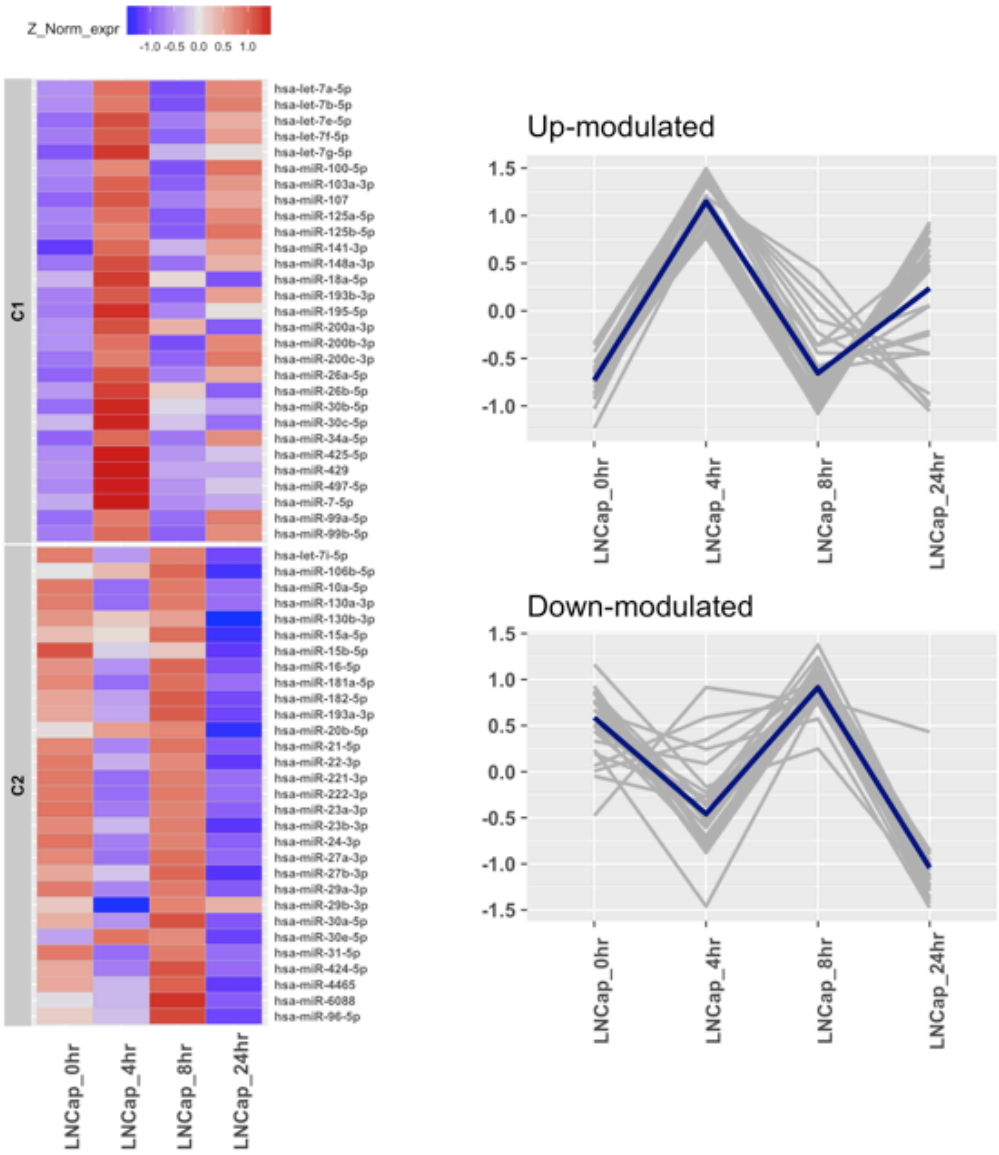

Figure 4.5 miRNAs in conserved miRNA families temporally modulated by photons in LNCaP cells. (*Left*) Heatmap showing the expression levels of significantly modulated conserved miRNAs in LNCaP cell line along time, clustered according to their dynamic changes at 4, 8 or 24 h after photons irradiation as up-modulated (C1) or down-modulated group (C2). (*Right*) Line plots representing the average miRNA expression in the indicated group at each time point.

4.1.2.2 Identification of miRNAs consistently modulated across PCa cell lines

In order to identify miRNAs modulated by radiation, we narrow our analysis on those miRNAs found to be consistently (up or down) modulated across cell lines, with the aim of obtaining a reliable list of potentially relevant miRNAs. Since we were looking for consistently modulated miRNAs, we compared all the miRNAs of the up-modulated sets or those of the down-modulated ones, separately.

With regards to the up-modulated miRNAs, no miRNAs were found to be regulated in all four cell lines. However, a great proportion of up-modulate miRNAs was found at the intersection between LNCaP and DU145 (9 miRNAs), making up 60% of all overlaps (Table 1). The comparison between down-modulated miRNAs among the different cell lines examined, revealed that 15 miRNAs follow a similar expression profile in LNCaP and DU145 (Table 4.1 and Fig. 4.6), which makes up 74% of all the overlapping subsets representing common regulated miRNAs among two or more cell lines.

Up_modulated	Down_modulated
hsa-let-7a-5p	hsa-let-7i-5p
hsa-let-7b-5p	hsa-miR-10a-5p
hsa-let-7e-5p	hsa-miR-130a-3p
hsa-miR-125b-5p	hsa-miR-181a-5p
hsa-miR-193b-3p	hsa-miR-182-5p
hsa-miR-200c-3p	hsa-miR-21-5p
hsa-miR-7-5p	hsa-miR-22-3p
hsa-miR-99a-5p	hsa-miR-221-3p
hsa-miR-99b-5p	hsa-miR-222-3p
	hsa-miR-23a-3p
	hsa-miR-24-3p
	hsa-miR-31-5p
	hsa-miR-424-5p
	hsa-miR-4465
	hsa-miR-6088

Table 4.1. List of conserved miRNAs temporally modulated in LNCaP and DU145

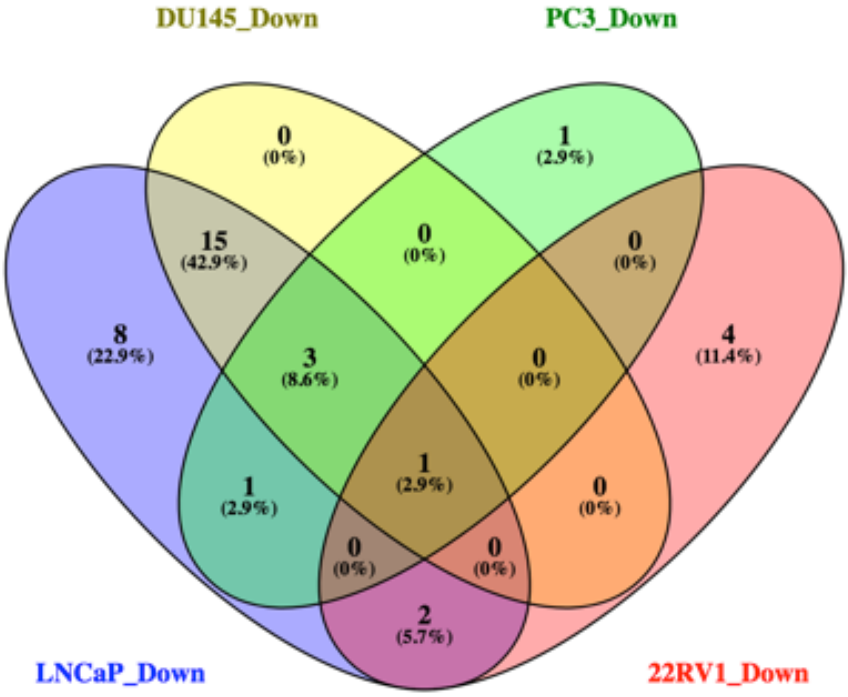

Figure 4.6 Venn diagram showing the intersection of conserved miRNAs down-modulated by photons in PCa cell lines

4.1.2.3 Identification of relevant modulated miRNAs

Based on these findings, we focused on miRNAs down-regulated by both DU145 and LNCaP in at least 2 time points. Specifically, considering the premise that miRNA modulation upon radiation does not per se imply a functional role of such miRNAs in radiation response, we sought to focus on those miRNAs that are known, from literature, to be involved in pathways related to radiation response. For this purpose, for each of the miRNAs belonging to the aforementioned intersection, we looked for their validated targets in order to identify which miRNAs regulate genes involved in processes relevant to radiation response. As a result, among miRNAs found to be downregulated in both DU145 and LNCaP cells, at 4 and 24h, we focused on miR-23a-3p and miR-24-3p, based on the evidence that they i) belong to the same miRNA cluster, and therefore are likely to be involved in the regulation of same cell processes, and ii) were reported to target genes linked to radiation response. In particular, according to literature data, we found that miR-23a-3p directly targets pathways known to be associated with PCa radioresistance, and that miR-24-3p, in turn, is indirectly regulated by miR-23a-3p [155]. Considering these data, we were prompted to study the role of miR-23a-3p and miR-24-3p in the radiation response of PCa cells.

4.1.3 Validation of microarray data

Before investigating the potential influence of miR-23a-3p and miR-24-3p on the radiosensitivity profile of PCa cells, we first validated the data obtained from microarray analysis to assess the reliability of our starting point. For this purpose, the expression of miR-23a-3p and miR-24-3p was evaluated by qRT-PCR. Overall, we observed a good correlation between the modulation on the array and the expression trend obtained by qRT-PCR, although to a different extent, thus confirming the reliability of microarray results and consequently demonstrating that our miRNA profiles were actually informative. For instance, we carried out both a technical and a biological validation, performing the qRT-PCR analysis on the same samples used for microarray and samples deriving from a different experiment, respectively (Fig. 4.7). In both cases we found that miR-23a-3p and miR-24-3p were downregulated in DU145 and LNCaP cells at 4 and 24 h upon irradiation, even if to a different extent compared to the modulation observed by microarray. Consistent with microarray results, the expression levels of both miRNAs were not decreased at 8h, recapitulating a trend of expression kinetics that has been previously observed in association with radiation, likely suggesting a failed attempt of the cell to contrast radiation-induced miRNA modulation.

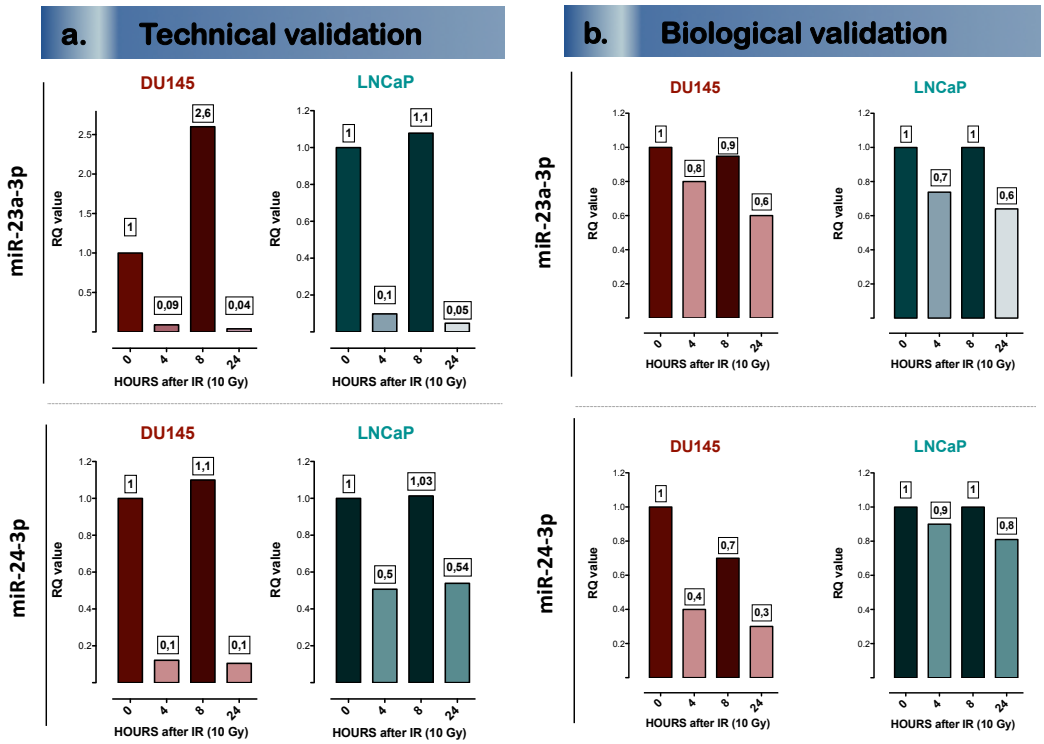

Figure 4.7 Validation of expression data obtained by microarray. The expression levels of miR-23a-3p and miR-24-3p upon irradiation of DU145 and LNCaP cells were evaluated by qrt-PCR. For technical validation (*left panel*) the RNA samples used for microarray analysis were tested to assess the reproducibility of the obtained data across different techniques. For biological validation (*right panel*) a new experiment was performed by exposing DU145 and LNCaP cells to 10 Gy of irradiation and collecting RNA in an independent setting. RNA collected at the same time points to microarray experiment (4, 8 and 24 h) was isolated and used for qrt-PCR analysis. Data are reported as RQ values with respect to Neg.

4.2 miR-23a-3p and miR-24-3p sensitize PCa cells to radiation

4.2.1 miR-23a-3p and miR-24-3p radiosensitize PCa cells

Considering the premises on the potential relevance of miR-23a-3p and miR-24-3p in determining the radiation response of PCa cells, we hypothesized that

the observed downregulation of such miRNAs upon radiation is functional for the cell to overcome radiation-induced injury, and that their reconstitution could in turn affect cell response to radiation.

To test the hypothesis that miR-23a-3p and miR-24-3p play a functional role in affecting cell response to radiation, the levels of miR-23a-3p and miR-24-3p were reconstituted in DU145 cells in order to evaluate their ability in enhancing cell radiation response. Specifically, DU145 cells were transfected with the mimic of miR-23a-3p or miR-24-3p and transfected cells were exposed to increasing doses of radiation (2 to 8 Gy) in order to test cell clonogenicity. Interestingly, both miRNAs showed a significant enhancement in DU145 cell sensitivity to radiation, as indicated by the reduced surviving fraction (Fig. 4.8).

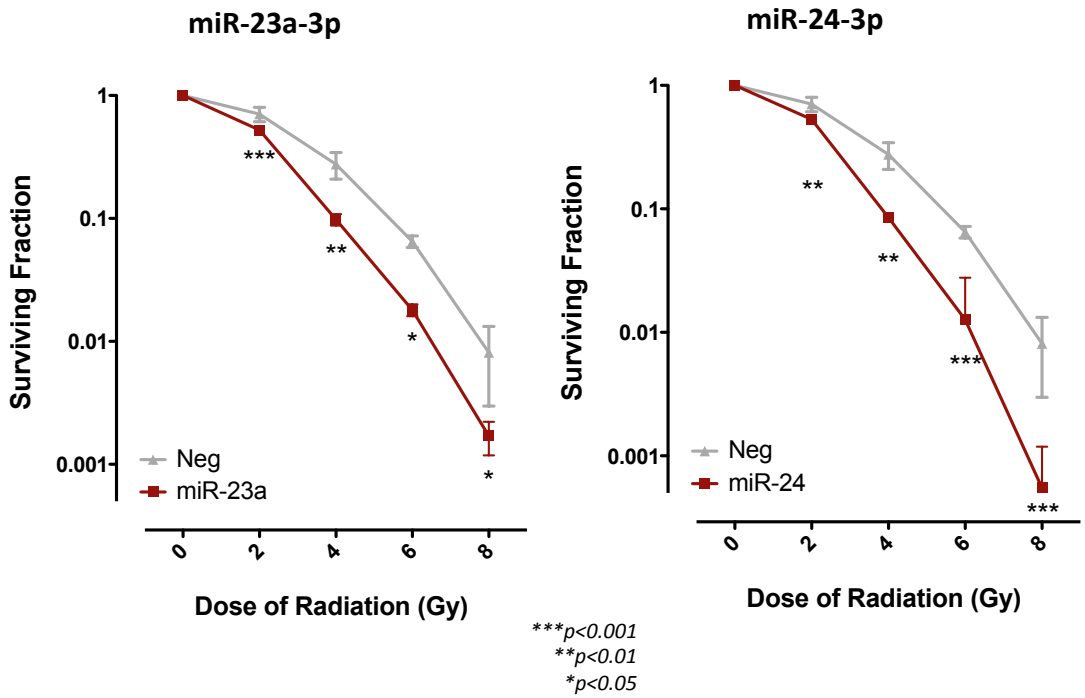

Figure 4.8 miR-23a-3p and miR-24-3p enhanced DU145 radiosensitivity. Clonogenic assay of DU145 cell transfected with miR-23a-3p (*left*) and miR-24-3p (*right*) mimic and respective negative controls. The surviving fractions following the indicated doses of irradiation are reported as mean ±SD, n=3.

An ideal radiosensitizer should exert an effect only when combined with the treatment towards which the sensitization is intended, without affecting *per se* cell viability. To assess whether the two miRNAs alone have an effect on cell clonogenicity, we evaluated cell plating in non-irradiated cells. As a result, miR-23a-3p did not show any effect on plating efficiency, thus allowing to conclude that the observed radiosensitizing effect is solely imputable to its role in enhancing radiation response, rather than inhibiting cell clonogenicity via other mechanisms (Fig. 4.9, *top*). In contrast, miR-24-3p was able to impact on cell clonogenicity even in absence of radiation exposure, as indicated by the significantly reduced plating efficiency (Fig. 4.9, *bottom*). This result suggests that the enhanced response to radiation observed upon miR-24-3p reconstitution, is not merely imputable to a radiosensitizing effect of miR-24-3p. It rather means that, at lest in part, the enhancement is due to an additive effect of transfection and treatment. For this reason, and for the central role of miR-23a-3p in the hypothesised axis, we focused our attention on miR-23a-3p as a putative promising radiosensitizer in PCa.

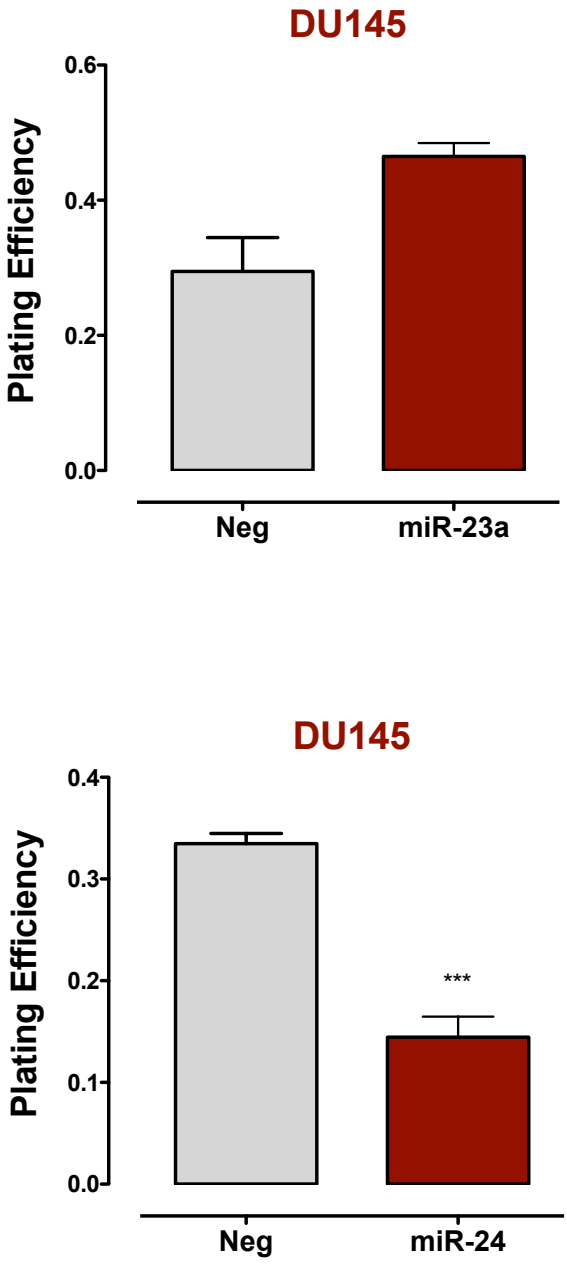

Figure 4.9 miR-23a-3p and miR-24-3p effects on DU145 cell plating efficiency. Plating efficiency of non-irradiated DU145 cells transfected with miR-23a (top) and miR-24-3p (bottom) was calculated as the ratio of the number of colonies counted to the number of cells seeded.

4.2.2 miR-23a-3p targets IL-6 pathway

The choice of investigating the role of miR-23a-3p in PCa radiation response was based on literature data reporting a role of the miRNA in targeting pathways known to be associated with radioresistance. Specifically, we found that miR-23a-3p negatively regulates the IL-6 pathway, known to be associated with radioresistance in PCa [156], by downregulating IL-6 receptor (IL-6R) in PCa cells [157], and directly targeting IL-6R in other tumour types [158]. As for miR-24-3p, it was reported to be upregulated as a consequence of IL-6 downregulation [155], thus prompting us to expect a positive correlation with the expression of miR-23-3p. To test our hypothesis, we assessed whether the hypothesized loop was verified in our models. As a first step, to confirm miR-23a-3p role in affecting IL-6 pathway, we reconstituted the miRNA in DU145 and PC-3 cells and assessed the expression levels of some of the main players belonging to IL-6 pathway (i.e.: IL-6, IL-6R, AKT and STAT1). In agreement with literature data, miR-23a-3p downregulated the expression levels of all the tested genes, even if to a different extent, in both DU145 and PC-3 cells (Fig. 4.10). Interestingly, the most downregulated were IL-6 and IL-6R, thus confirming miR-23a-3p reported role in regulating those two molecules.

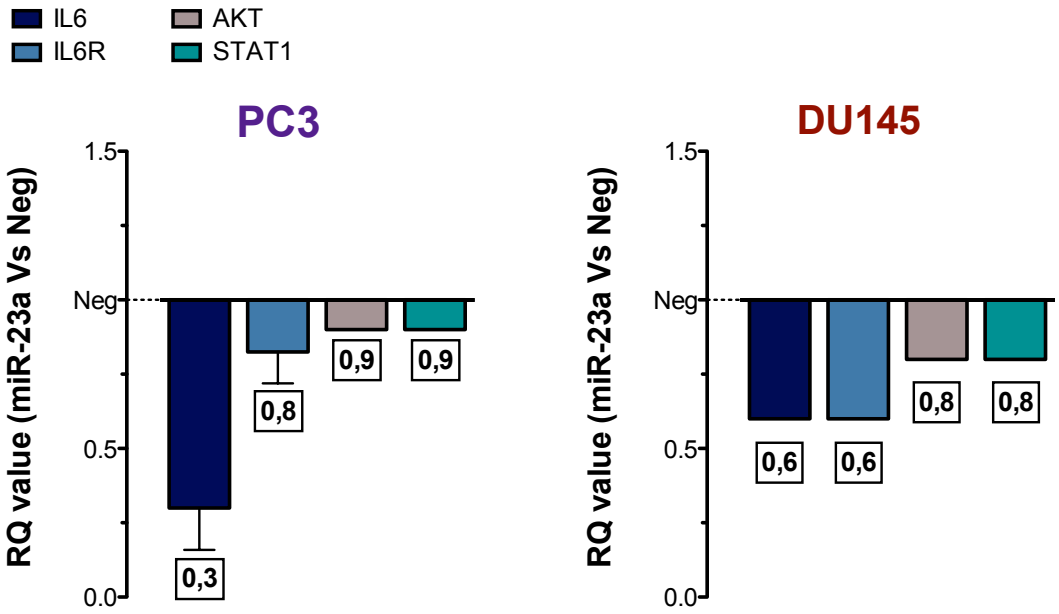

Figure 4.10 Expression levels of IL-6 pathway related genes upon miR-23a-3p reconstitution. miR-23a-3p downregulated the expression levels of IL-6, IL-6R, AKT and STAT1 as assessed by qRT-PCR. Data are reported as RQ values with respect to Neg.

IL-6R was validated as a direct target of miR-23a-3p [157]. In contrast, IL-6 is reported to be downregulated by the miRNA, yet not being a direct target. To investigate whether IL-6 was a predicted target of miR-23a-3p, we carried out *in silico* prediction tools as described in Materials and Methods section. Interestingly, IL-6 emerged as a potential target of miR-23a-3p, which is in line with our downregulation results, thus supporting the potential relevance of this miRNA in regulating IL-6 pathway.

4.2.3 miR-23a-3p induced radiosensitization relies on IL-6 targeting

Considering the already known and demonstrated role of IL-6 in determining radioresistance in PCa cells, and that, in our hands, miR-23a-3p was able to both radiosensitize PCa cells and to downregulate IL-6, we hypothesised that the radiosensitizing effect of the miRNA could rely, at least in part, on the induced downregulation of IL-6, thus disrupting its associated radioresistance and finally resulting in radiosensitization. To verify this hypothesis, we sought to counteract IL-6 downregulation induced by the miRNA by ectopically supplementing cells with recombinant IL-6, with the final aim of restoring IL-6 levels and evaluating whether the restoration was able to abrogate miR-23a-3p induced radiosensitization, which would indicate a central role of IL-6 downregulation in mediating such effect. For this purpose, 50 ng/ml IL-6 were added to DU145 cells transfected with miR-23a-3p. The concentration of recombinant IL-6 was established based on previous experiments of a different study run in the lab. DU145 cells with or without miR-23a-3p and/or IL-6 were exposed to increasing doses of radiation for clonogenic assay. Interestingly, the restoration of IL-6 levels was able to almost completely abrogate the radiosensitizing effect induced by miR-23a-3p, indicating that IL-6 downregulation is indeed crucial in mediating miR-23a-3p effect, thus confirming our hypothesis and providing insights on the mechanism underlying miR-23a-3p ability to enhance PCa cell sensitivity to radiation (Fig. 4.11).

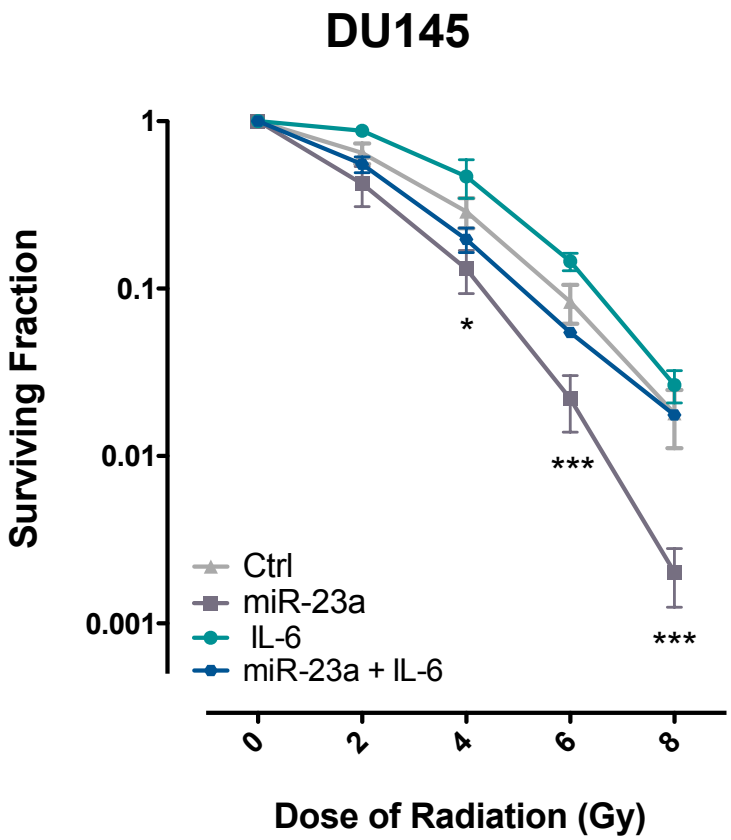

Figure 4.11 IL**-6 supplementation abrogated miR-23a-3p induced radiosensitivity.** Clonogenic assay of DU145 cells transfected with miR-23a-3p, with or without IL-6 supplementation and respective controls. The surviving fractions following the indicated doses of irradiation are reported as mean ±SD, n=3.

4.3 miRNA expression profiling upon carbon ions irradiation

Carbon ions are heavy charged particles that have the physical advantage of giving improved depth-dose distributions for deep-seated tumours. Much of their energy is deposited in tissue at the end of particle tracks (i.e., in the region of the Bragg peak). This characteristic allows the delivery of a high radiation dose to the target, yet significantly spearing surrounding normal tissues, which is the major challenge in radiotherapy.

Considering how promising are carbon ion beams in radiotherapy, and that almost nothing is known about their impact in modulating tumour miRNome, in this study we sought to investigate the miRNA expression profiling of PCa cells exposed to carbon ion irradiation. For this purpose, based on the results obtained by photon irradiation, DU145 and LNCaP cell lines were selected for carbon ions studies. In order to compare miRNA modulation following carbon ion irradiation to that induced by photons, the same treatment settings were maintained (relative dose and time points). Of importance, to have comparable doses, we considered the definition of RBE, based on the knowledge that different radiation sources need different doses to produce the same biological effect. Taking this aspect into account, we irradiated DU145 and LNCaP cells at 5 Gy of carbon ions at CNAO (Pavia). For miRNA expression analysis, RNA was collected at the same time point of photon experiments (i.e.: 4, 8 and 24 h). As for photon irradiation analysis, we identified miRNAs differentially expressed upon radiation across time within each of the two cell lines.

4.3.1 Definition of carbon ions RBE by clonogenic assay

As previously pointed out, because of their specific physical carachteristics, carbon ions produce the same effect of photons at lower doses, thus requiring the implementation of RBE definition. Specifically, to determine the RBE between carbon ions and photons, a specific biological endpoint should be selected in order to find out at which doses the two radiation sources are able to cause the same effect. As radiation cell toxicity *in vitro* is conventionally evaluated in terms of cell clonogenicity impairment, by clonogenic assay, we sought to compare the reduction of clonogenic survival induced by photons and carbon ions in order to compute the RBE of carbon ions with respect to photons. As shown in Fig. 4.12, lower doses (≈ ½ of photon dose) of carbon ion radiation was able to induce a similar impairment of cell clonogenicity to that caused by photons, resulting in an RBE value of ≈ 2.8, which is very close to that known in literature (RBE=3). This data confirmed in our hands what was expected from literature, namely that, at comparable absolute doses, carbon ions display a greater biological effect than photons.

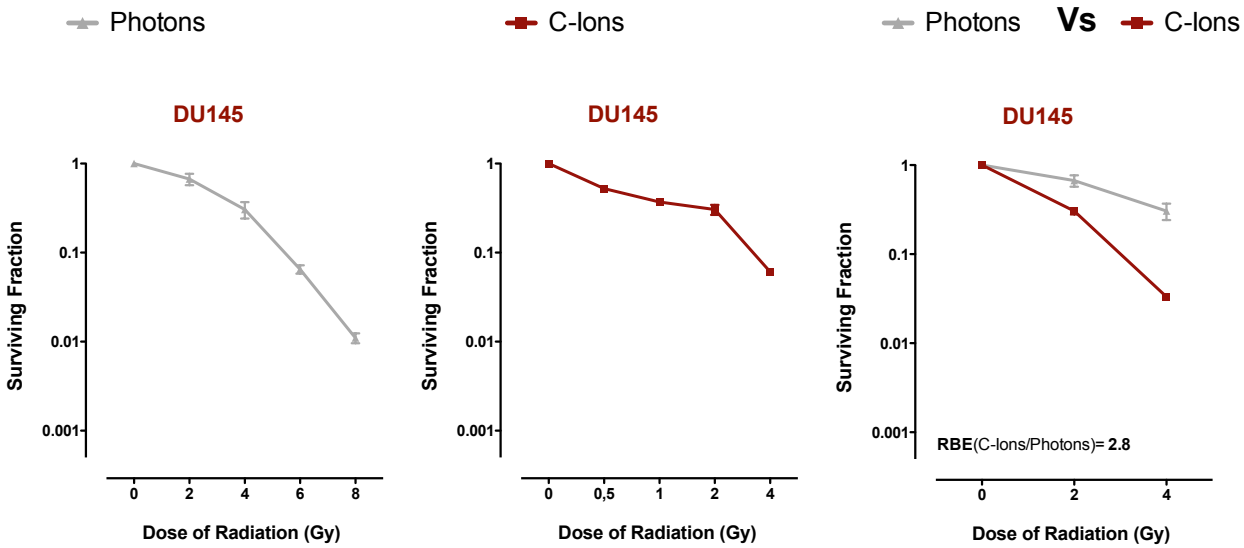

Figure 4.12 Clonogenic curves of DU145 exposed to increasing doses of carbon ions. (*Left*) Clonogenic curves of DU145 exposed to increasing doses (2, 4, 6 and 8 Gy) photon irradiation. (*Centre*) Clonogenic curves of DU145 exposed to increasing doses of carbon ions (0,5, 1, 2 and 4 Gy) (Right) Comparison between clonogenic curves of DU145 exposed to photons and carbon ions, and calculation of RBE of carbon ions to photons.

4.3.2 RNA isolation

As for RNA isolation from PCa cells exposed to photon irradiation, RNA collected at 4, 8 and 24h from exposure to radiation was isolated using the miRNA isolation kit and its integrity was verified by the Agilent 2100 Bioanalyzer System, which generated RNA profiles allowing a visual inspection of RNA integrity (Fig. 4.13).

A

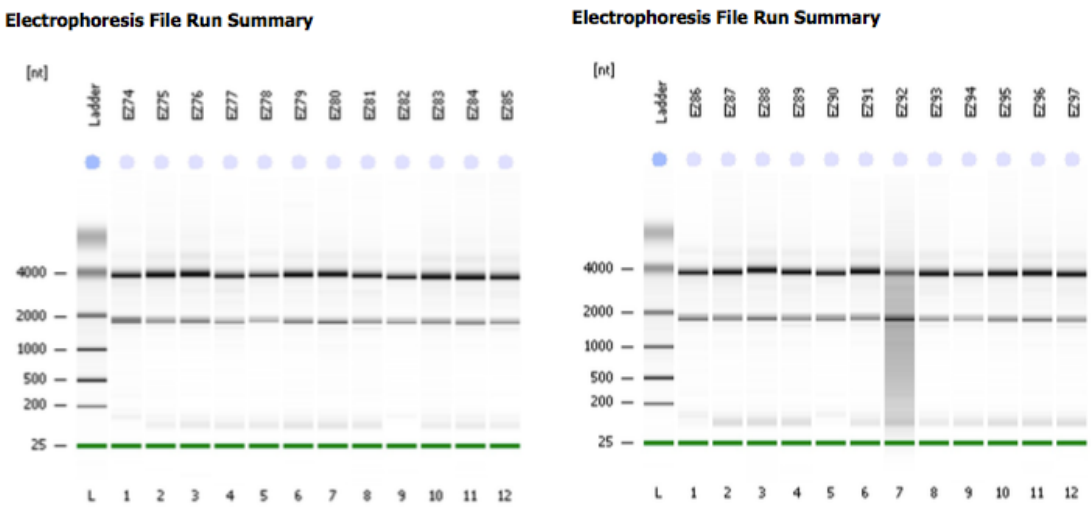

B

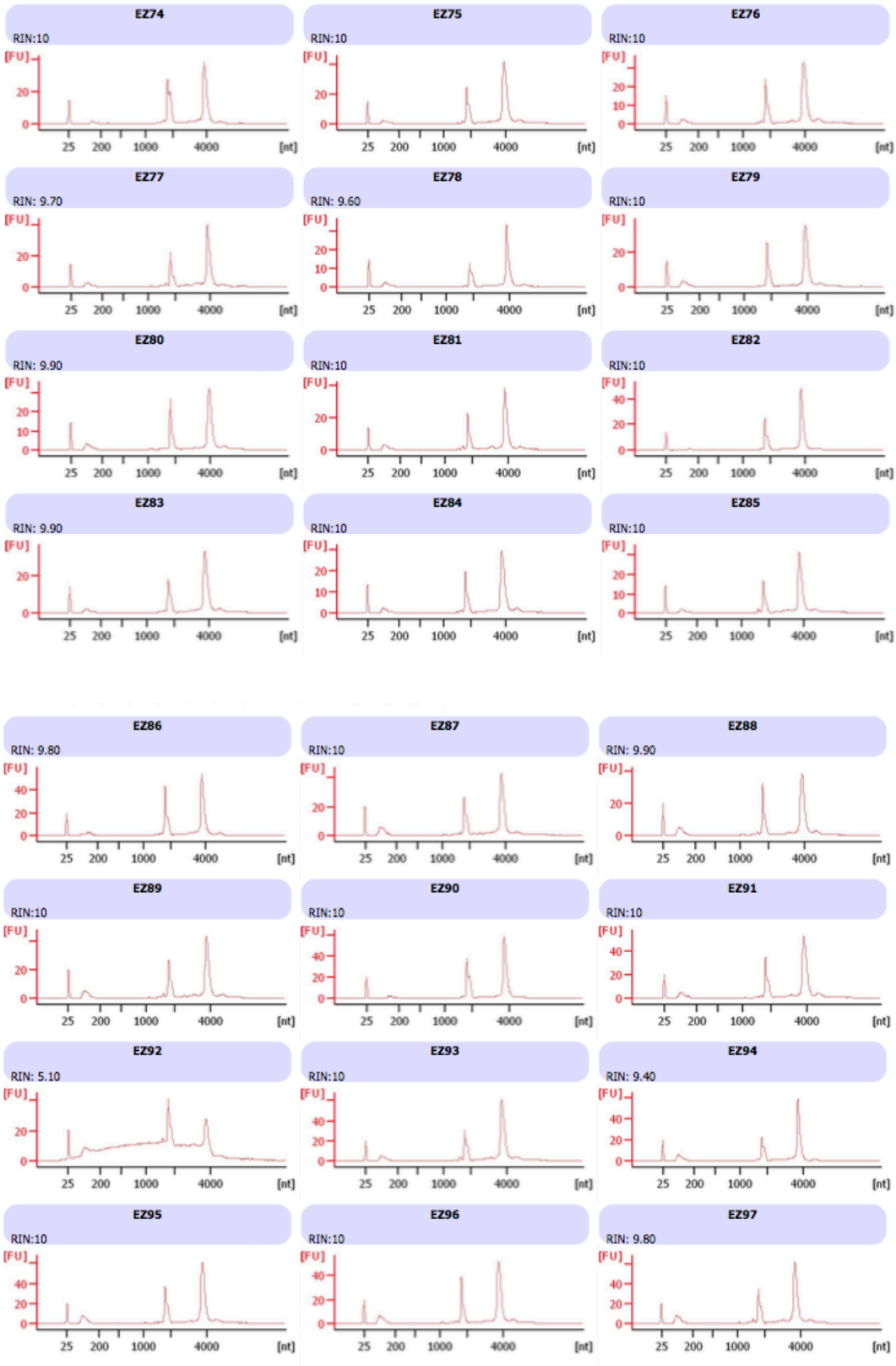
EZ74
RIN:10
EZ75
RIN:10
EZ76
RIN:10
EZ77
RIN: 9.70
EZ78
RIN: 9.60
EZ79
RIN:10
EZ80
RIN: 9.90
EZ81
RIN:10
EZ82
RIN:10
EZ83
RIN: 9.90
EZ84
RIN:10
EZ85
RIN:10
EZ86
RIN: 9.80
EZ87
RIN:10
EZ88
RIN: 9.90
EZ89
RIN:10
EZ90
RIN:10
EZ91
RIN:10
EZ92
RIN: 5.10
EZ93
RIN:10
EZ94
RIN: 9.40
EZ95
RIN:10
EZ96
RIN:10
EZ97
RIN: 9.80
[FU]
[nt]
25
200
1000
4000

Figure 4.13 Integrity profiles of RNA isolated from PCa cell lines irradiated with carbon ions. (A) Electrophoretic trace of the 48 samples of RNA isolated from DU145 and LNCaP exposed to carbon ion irradiation. The gel-like image reports the 18S to 28S ribosomal bands, which are indicative of RNA degradation presence, as in degraded RNA an increase in the baseline signal between the two ribosomal peaks and the lower marker is observable. Intact RNA shows a greater distance between ribosomal peaks and the lower marker. Samples were randomized into 2 groups of 12 samples/each. Each group was run on a different microarray chip taking into account intra-cell line variability. (B) RIN scores of RNA samples, ranging from 1 to 10, with 1 being the most degraded profile and 10 being the most intact. According to their RIN value, intact RNA samples were considered for microarray analysis, whereas non-intact RNA samples were replaced with new-isolated intact ones.

4.3.3 Identification of miRNA modulated upon exposure to Carbon Ions

DU145

With the purpose of following the temporal modulation of miRNAs by carbon ions, we performed a differential expression analysis to detect significant changes in miRNAs expression at 4, 8 and 24 h against 0 h, considered as the basal state. A total of 145 miRNAs showed significant changes at either time point. In order to identify miRNAs following a similar temporal pattern, we clustered miRNAs according to the temporal shift of expression changes along the whole-time series (i.e., at 4, 8 and 24 h). We discovered 73 up-modulated miRNAs, which show a bottom-up shift in expression at 4 h which slowly decreases at 8 and 24 h. The second subset we detected was composed of 72 down-modulated miRNAs. This subset, by contrast, follows a downward shift at 4 h, which continued to increase in a slowly manner until 24 h. The mapping against the database of members of conserved miRNAs families, revealed 46 up-modulated and only 14 down-modulated conserved miRNAs (Fig. 4.14).

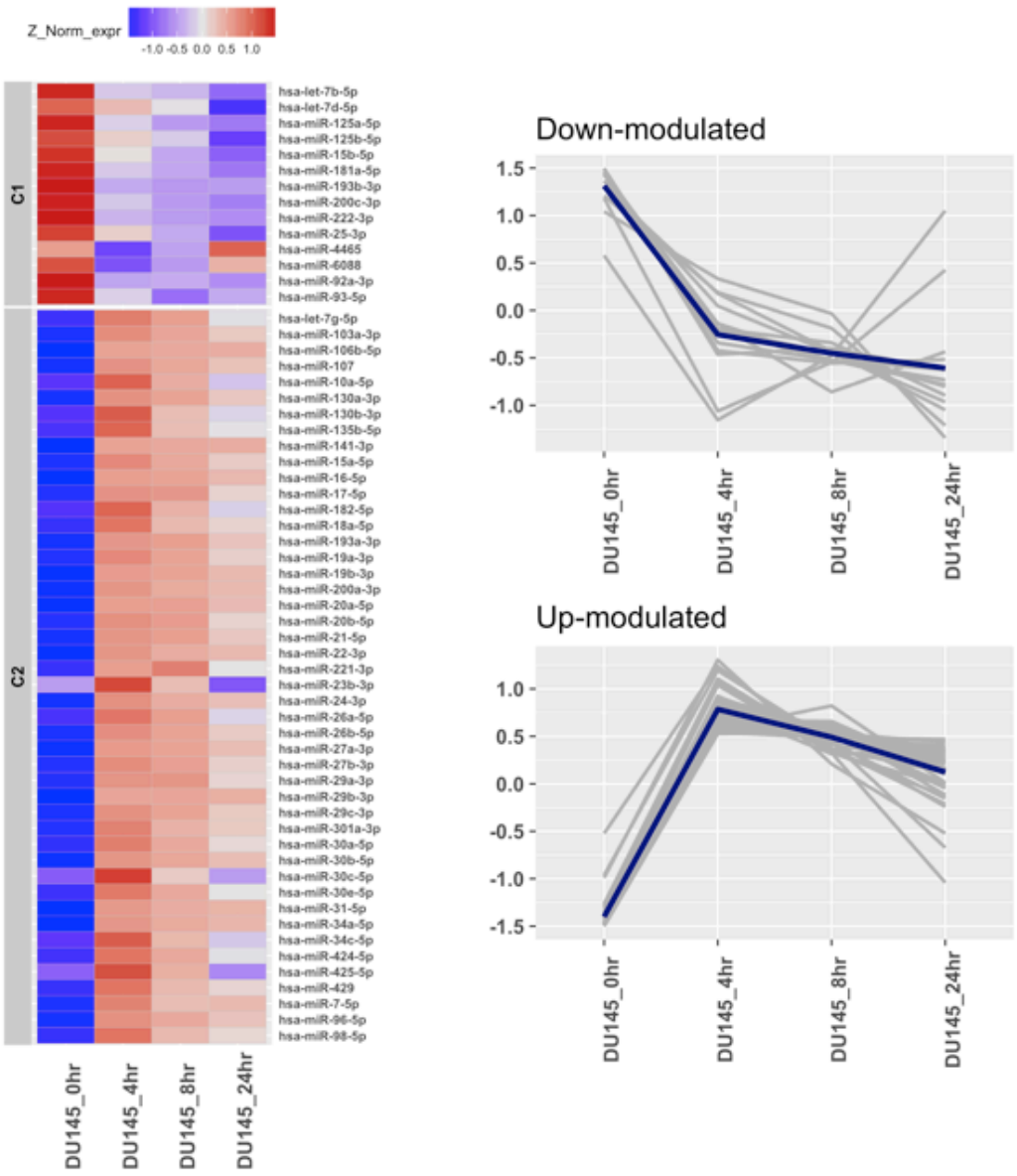

Figure 4.14 miRNAs in conserved miRNA families temporally modulated by carbon ions in DU145 cells. (*Left*) Heatmap showing the expression levels of significantly modulated conserved miRNAs in DU145 cell line along time, clustered according to their dynamic changes at 4, 8 or 24 h after carbon ions irradiation as up-modulated (C1) or down-modulated group (C2). Line plots on the right side represents the average miRNA expression in the indicated group at each time point.

LNCaP

In LNCaP cells, a total of 120 miRNAs showed significant changes at either time point. The subset of up-modulated miRNAs is composed of 40 up-modulated miRNAs and is characterized by an initial upward shift at 4 h, which remains sustained until the end of the time course. The second subset is composed of 80 down-modulated miRNAs and is distinguished by a marked top-down shift at 4 h, which gradually decrease until the 24 h point. Among those miRNAs we identified 40 conserved miRNAs within the up-modulated subset and 4 making part of the down-modulated subset (Fig. 4.15).

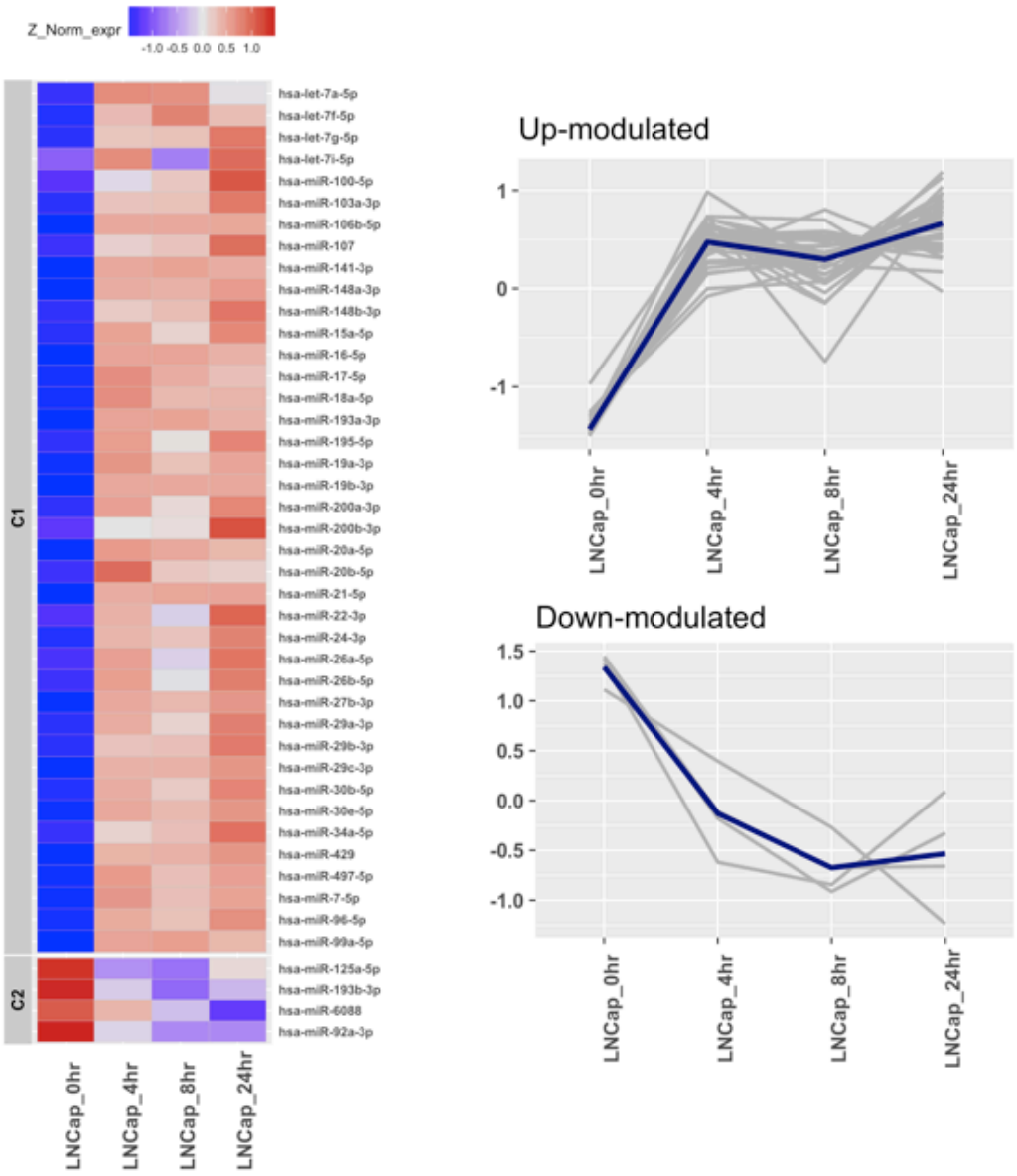

Figure 4.15 miRNAs in conserved miRNA families temporally modulated by carbon ions in LNCaP cells. (*Left*) Heatmap showing the expression levels of significantly modulated conserved miRNAs in LNCaP cell line along time, clustered according to their dynamic changes at 4, 8 or 24 h after carbon ions irradiation as up-modulated (C1) or down-modulated group (C2). Line plots on the right side represents the average miRNA expression in the indicated group at each time point.

4.3.4 Comparative analysis of miRNAs modulated by photons and carbon ions

With the aim of comparing miRNA expression changes induced by different radiation sources –a study never pursued in the available literature– and identify commonalities and differences, the PCa cell lines that were exposed to both photons and carbon ions, at RBE-adjusted comparable doses, were considered for comparative analysis. Specifically, we considered the lists of miRNAs significantly modulated upon photons and those modulated by carbon ions in DU145 and LNCaP cells, and compared them to investigate whether specific miRNA were jointly modulated by both sources.

To explore the commonalities, we compared the subsets of miRNAs consistently modulated by photons and carbon ions. As a result, we found that only 14 miRNAs were modulated by both radiation sources in the two considered PCa cell lines (Fig. 4.16). Noteworthy, miRNAs found in the intersection, still being modulated by both sources, are not consistently modulated. Almost all 14 miRNAs showed an opposite modulation direction (i.e. those up-modulated by photons were down-regulated by carbon ions and vice versa) (Fig. 4.17). Although it could seem unexpected that only few miRNAs are modulated by both sources, and that, moreover, those few miRNAs are inversely modulated by the two radiation modalities, indeed such partial overlap is likely reflecting the different relative biological effectiveness of photons and carbon ions. In keeping with this finding is that carbon ions display a greater

ionizing potential than photons, thus causing a more intense damage to the DNA helix and likely inducing different response mechanisms within the cell.

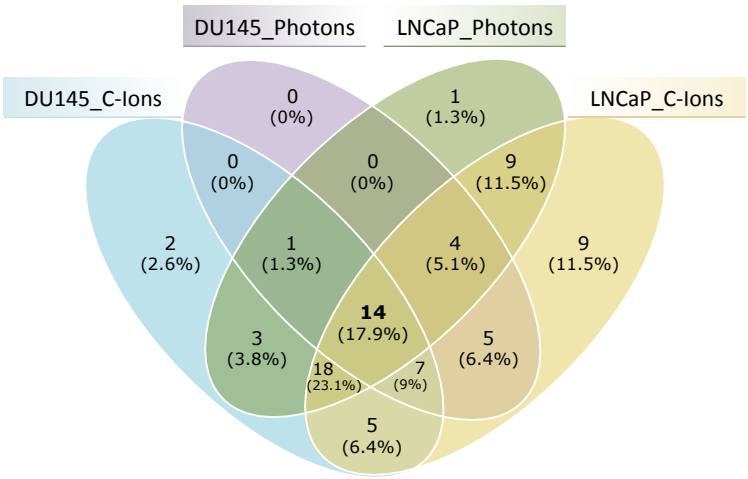

Figure 4.16 miRNAs modulated by photons and carbon ions. Venn diagram showing the intersection of miRNAs differentially expressed after photon (10 Gy) and carbon ion (5 Gy) irradiation, in DU!45 and LNCaP cells. Log2FC>1.5 and FDR<0.2 for any time point.

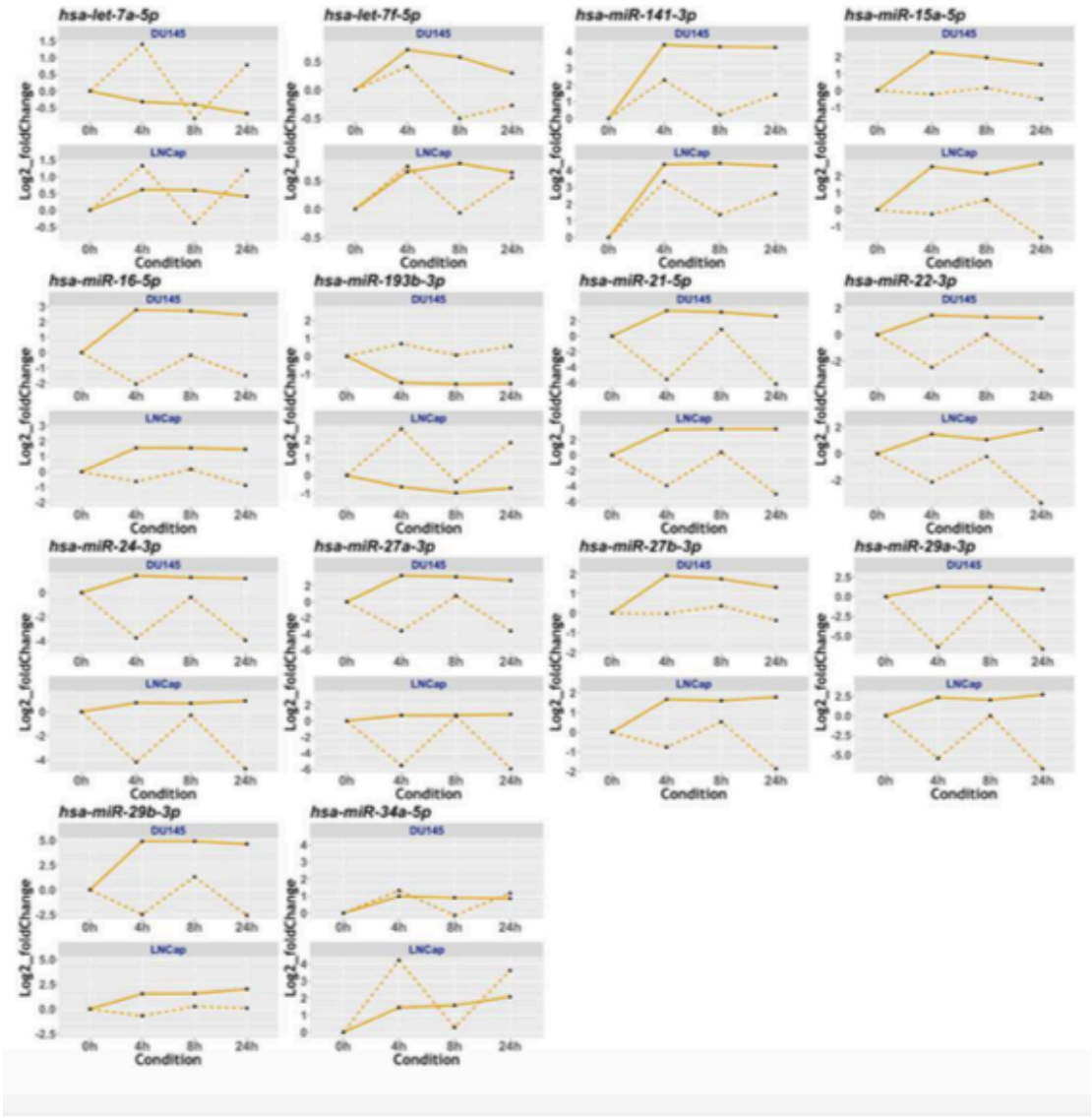

Figure 4.17 Dynamic expression changes of miRNAs modulated by either photons or carbon ions in DU145 and LNCaP. Log2 Fold changes (y-axis) relative to 0 h are plotted against time (x-axis). Photon treatment: dotted line; Carbon ions; continuous line.

4.3.5 Pathways modulated by both photons and carbon ions

To assess whether different pathways were triggered by the two different sources, we investigated the biological functions of the selected miRNAs. To that end, we searched for putative target genes and performed an over-representation analysis of GO biological processes. The top 10 enriched GO biological processes, which included negative regulation of amide metabolism, response to TGF-β and regulation of protein kinase activity (Fig. 4.18), revealed to be predominantly associated with 12 miRNAs, indicating a central role for this subgroup of radio-sensitive miRNAs in the regulation of such biological processes. Notably, among these is miR-24-3p, previously studied in the context of miRNAs modulated by photons.

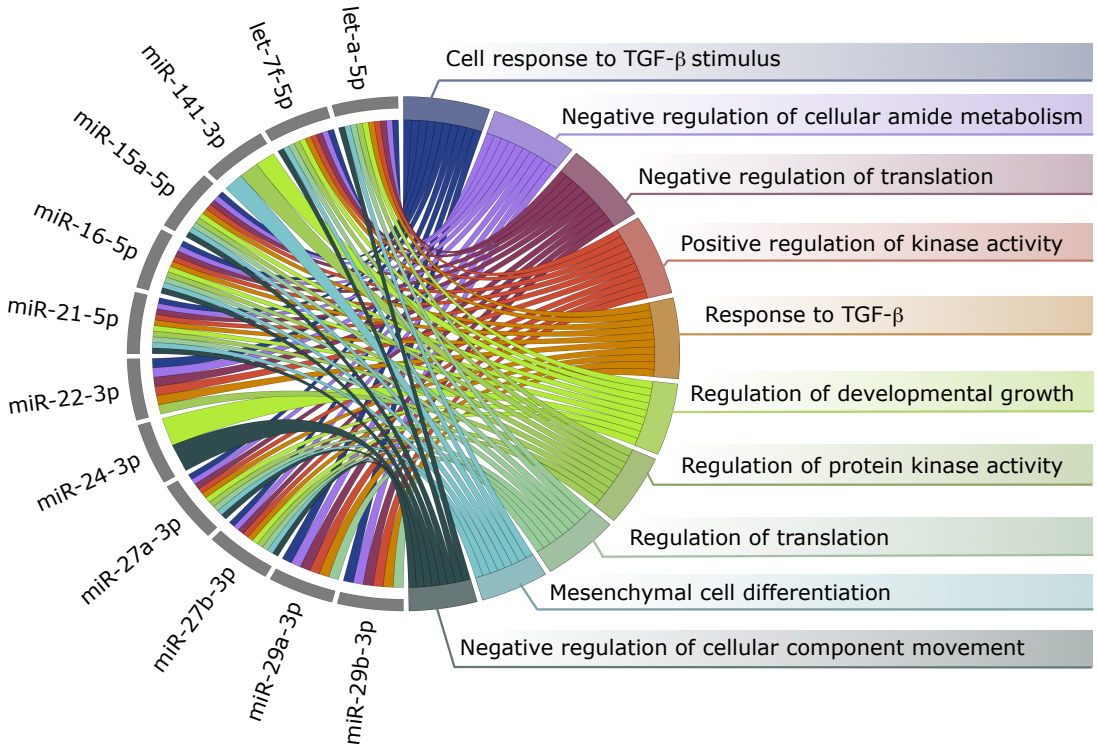

Figure 4.18 Top 10 GO biological process over-represented in target genes of 12 selected miRNAs. Over-representation analysis of GO biological processes in the set of miRNAs modulated by both photons and carbon ions. The Circos plot displays the relationship between the list of selected miRNAs and terms enriched within the set of target genes of the respective miRNA. Coloured ribbons link miRNAs with GO biological terms significantly enriched (adjusted p-value <0.1 from a hypergeometric test).

5. RESULTS II: the role of miR-875-5p in PCa radiation response

With the same aim of identifying miRNAs functionally involved in determining cell radiation response, we pursued a second strategy based on considering those miRNAs that i) are downregulated in PCa and ii) target genes involved in pathways relevant to radiation response. The strategy is based on the knowledge that the evidence of being downregulated in PCa suggests a possible oncosuppressive function of the miRNA, which is compatible with a role in making tumour cell susceptible to a specific treatment. As for the second criterion, focusing on miRNAs targeting pathways relevant to radiation response support their putative role in influencing cell sensitivity to radiation. The intersection of these two criteria should improve the reliability of miRNA selection for the evaluation of their radiosensitizing effect.

Following this strategy, we picked-up miR-875-5p. No information concerning its role in human tumours was available in the literature when we undertook this study. However, results from a miRNA expression profiling we carried out using the Agilent miRNA Microarray System in carcinoma and matched normal prostate samples obtained from 30 untreated PCa patients, showed reduced miR-875-5p expression in tumours with respect to normal counterparts (fold-change 0.706; adjusted P = 0.035) (Table 5.1). The possible relevance of the miRNA in PCa radiation response is based on the observation, coming from results obtained in our laboratory in the context of a previous independent study, that miR-875-5p showed a high positive correlation with E-cadherin, one of the main markers of the epithelial to mesenchymal transition (EMT), in clinical

specimens (Table 5.1). The relevance of such a correlation in supporting miR-875-5p interest as a possible radiosensitizer is given by the evidence that EMT is a phenotypic switch associated with radioresistance [159]. In support of this, is the story of miR-205, another miRNA highly correlated with E-Cadherin, that we previously demonstrated to exert a prominent role in repressing EMT in PCa cells [81] and that was successively found to act as a tumour radiosensitizer. The link between EMT and radiation response, further supported by the example of miR-205, prompted us to exploit such a correlation as a strategy to investigate miR-875-5p as a potential modulator of EMT and radiation response.

	Differential expression Tumor vs Normal		**Correlation with E-cadherin expression**	
miRNA	**logFC**	**p-value**	**Coefficient**	**p-value**
hsa-miR-875-5p	-0.66	0.013094	0.49	0.000736
hsa-miR-518b	-0.36	0.042304	0.45	0.002134
hsa-miR-149	-0.33	0.041602	0.40	0.007156
hsa-miR-1206	-0.14	0.026804	0.40	0.007405
hsa-miR-507	-0.22	0.004878	0.37	0.013232
hsa-miR-187	-1.36	0.006249	0.36	0.015330
hsa-miR-659	-0.33	0.004097	0.35	0.020540
hsa-miR-220a	-0.14	0.035549	0.33	0.026902
hsa-miR-548c-3p	-0.16	0.014834	0.33	0.027333
hsa-miR-30e*	-0.25	0.004097	0.32	0.036824
hsa-miR-222	-0.34	0.004410	0.31	0.037493

hsa-miR-296-5p	-0.63	0.014938	0.31	0.038876
hsa-miR-7-2*	-0.31	0.021906	0.30	0.048642
hsa-miR-1228	0.12	0.049020	-0.32	0.034506
hsa-miR-612	0.73	0.005305	-0.33	0.029485
hsa-miR-183*	0.59	0.007684	-0.34	0.022297
hsa-miR-1244	0.57	0.005204	-0.36	0.015390
hsa-miR-1245	0.34	0.030052	-0.40	0.007752

Table 5.1. miRNAs showing differential expression in tumors compared to matched normal tissues and correlated with *CDH1*. miRNAs differentially expressed in tumors compared to matched non-neoplastic tissues and also found positively or negatively correlated (Spearman correlation) with E-cadherin in clinical specimens.

5.1 miR-875-5p expression in PCa cell lines

To both check the suitability and reliability of our cell models for the following experiments and to further confirm miRNA downregulation in PCa, we tested miR-875-5p expression levels in PCa cell lines with respect to normal prostate tissues as a reference. As shown in Fig.5.1, miR-875-5p was found to be significantly downregulated in both PC-3 and DU145 cell lines, supporting the suitability of our cell models for pursuing the study of this miRNA.

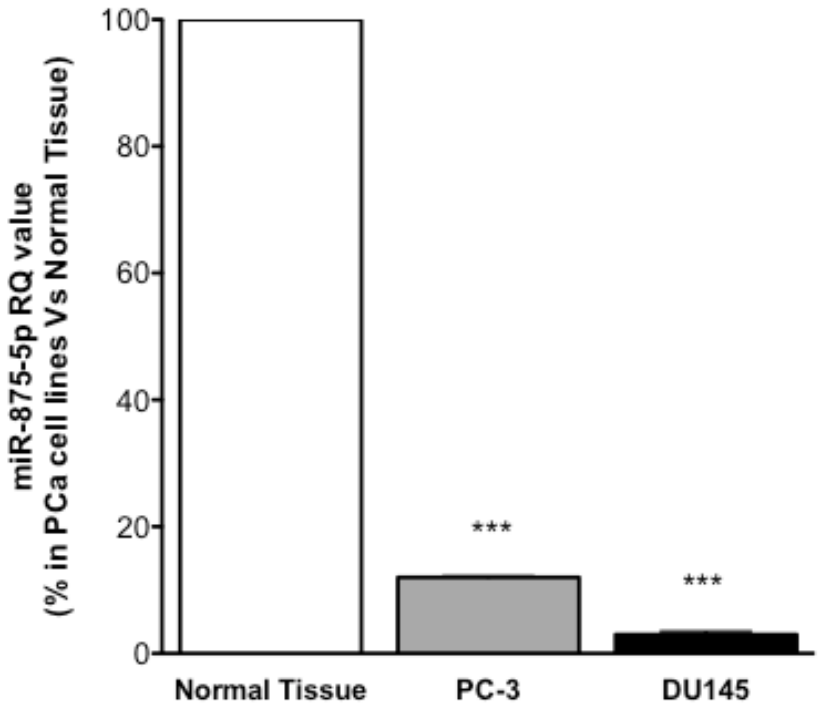

Figure 5.1 miR-875-5p is differentially expressed in normal and cancer tissues. miR-875-5p expression in PC-3 and DU145 tumor cell lines compared to normal prostate tissue. Expression was normalized to RNU48.

5.2 miR-875-5p reconstitution impairs EMT

5.2.1 miR-875-5p reconstitution resulted in marked morphological and cytoskeletal changes in DU145 cells

As suggested by the high correlation between miR-875-5p and E-Cadherin, and knowing that such epithelial gene is one of the most reliable markers of the EMT switch, we were prompted to postulate a role of miR-875-5p in regulating EMT. In particular, given that E-Cadherin is associated with the epithelial phenotype, which is more represented when EMT is reverted, we hypothesized that miR-875-5p could negatively affect EMT, counteracting the transition from a more epithelial to a mesenchymal phenotype. To test our hypothesis, we reconstituted miRNA levels in DU145 cells, and observed the biological effect exerted on transfected cells.

From a morphological point of view, we observed that miR-875-5p reconstituted cells display a more epithelial-like morphology, as suggested by the acquisition of polygonal, enlarged and packed-down appearance, and loss of filopodia and stress fibers, concomitant to a redistribution of F-actin to the subcortical level (Fig. 5.2).

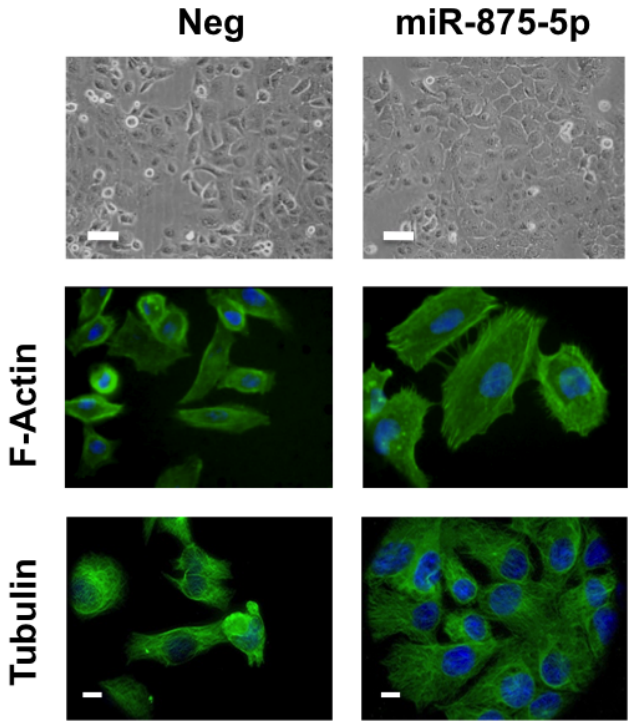

Figure 5.2 miR-875-5p reconstitution resulted in marked morphological and cytoskeletal changes in DU145 cells. Phase contrast microscopy (upper panel, scale bar 100 μm), phalloidin F-actin staining (middle panel, scale bar 10 μm) and tubulin immunostaining (lower panel, scale bar 10 μm) showing morphological changes and cytoskeleton architecture rearrangements in DU145 cells upon miR-875-5p reconstitution.

5.2.2 miR-875-5p increased E-cadherin and β-catenin expression levels

To further investigate miR-875-5p role in influencing the epithelial to mesenchymal switch, molecular analysis were performed in order to assess the expression levels of E-Cadherin and β-catenin, the two most important markers of EMT, associated with a more epithelial like phenotype. In accordance with the postulate role of miR-875-5p in promoting the epithelioid morphology, we found that the miRNA significantly increased the expression levels of the two markers, at both mRNA and protein levels (Fig. 5.3).

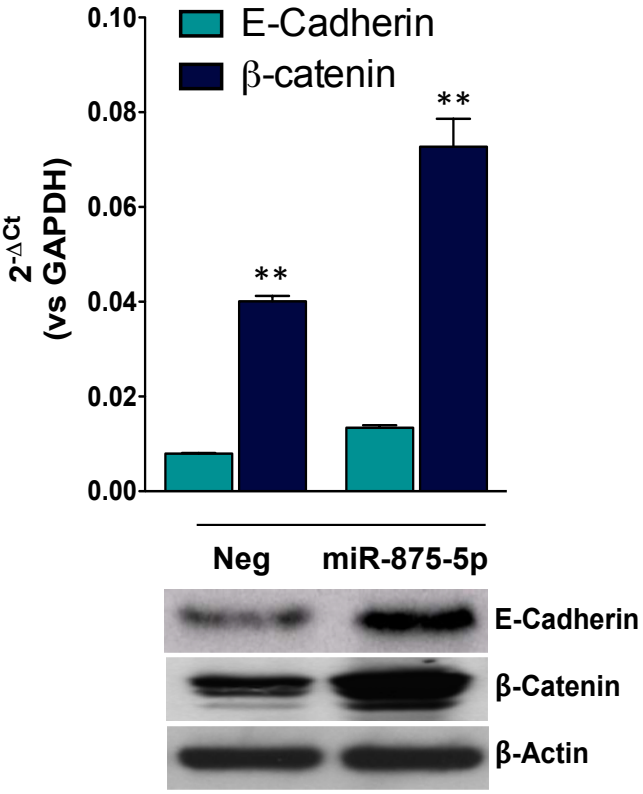

Figure 5.3 miR-875-5p reconstitution increased E-Cadherin and β-catenin levels. (Upper panel) Expression of the epithelial markers CDH1 and CTNNB1 assessed by qRT-PCR in DU145 cells transfected with miR-875-5p and negative control. Data are reported as relative quantity (RQ) ± SD with respect to Neg cells. (Lower panel) Western blot analysis showing E-cadherin and β-catenin protein levels upon miR-875-5p reconstitution in DU145 cells. Cropped images of selected proteins are shown. The level of significance was represented as *p<0.05, Student's t-test.

To explore such an effect at an *in situ* level, we performed an immunofluorescence analysis on transfected DU145 cells, to assess cell positivity to such markers. Consistent with previous results, we found that the presence of the miRNA is associated with an intense immunoreactivity for E-Cadherin and β-catenin staining, suggesting that miR-875-5p results in an upregulation of such markers. More interestingly, the immunostaining allowed us to appreciate cell localization of the proteins. Consistent with their role in

mediating cell-cell junction formation, the two markers were found to be co-localized at the cell membrane level, thus supporting a functional role of their upregulation mediated by the miRNA (Fig. 5.4).

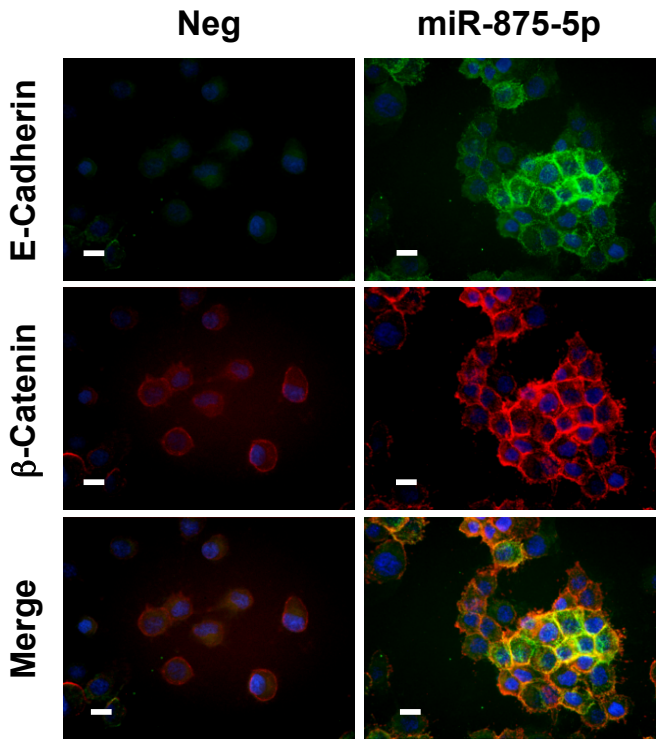

Figure 5.4 miR-875-5p promoted E-Cadherin and β-catenin co-localization at cell-cell adhesions. Immunofluorescence staining of E-cadherin (green) and β-catenin (red) in DU145 cells upon miR-875-5p ectopic expression. DAPI (blue) was used to stain nuclei. Scale bar 10 μm.

5.2.3 miR-875-5p decreased DU145 cell migration ability

Consistent with their role of leading cell migration and invasion, thus promoting tumour metastatization, mesenchymal cells display increased migration ability compared to their epithelioid counterpart. As a consequence, the evidence of the loss of such a migratory ability could reflect a reversion of the EMT switch. Compatible with miR-875-5p envisaged role of counteracting EMT, we hypothesised that miRNA reconstitution would result in a decreased migration potential. Migration ability could be recapitulated by cell capacity of healing a wound gap created by a scratch in the cell monolayer. Cells that are characterized by a high migration capacity, display a greater rate of gap healing. On the contrary, cells that are unable to “fill the gap” are likely showing an impairment of their migration potential. Reconstitution of miR-875-5p in DU145 cells showed a greater opening of the wound then negative cells, thus suggesting that the miRNA impairs cell migration (Fig. 5.5). Considering that this is a crucial property of mesenchymal cells, this result further supports the role of miR-875-5p in counteracting the EMT process, reverting the mesenchymal phenotype in a more epithelial-like one.

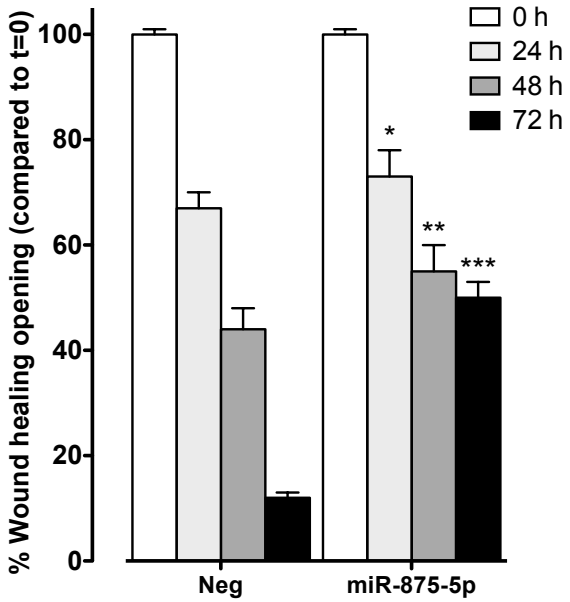

Figure 5.5 miR-875-5p decreased DU145 cell migration ability. Wound healing assay performed on miR-875-5p- and Neg-transfected DU145 cells, reported as wound opening percentage at different time points (24, 48 and 72 h) compared to t=0. The level of significance was represented as *p<0.05, Student's t-test.

5.3 miR-875-5p enhances radiosensitivity in PCa cells

5.3.1 miR-875-5p enhances radiosensitivity in vitro

Based on the finding that miR-875-5p counteracts EMT and considering the premises indicating that such transdifferentiation process is associated with an increased resistance to radiation, we were further encouraged to ascribe a putative radiosensitizing role to miR-875-5p. To explore this scenario, we assessed the sensitivity profile of miRNA reconstituted cells exposed to increasing doses of photon radiation and performed a clonogenic assay. Interestingly, miR-875-5p significantly enhanced the sensitivity of both PC-3 and DU145 cells to radiation with respect to negative control, as indicated by the markedly reduced surviving fractions (Fig. 5.6).

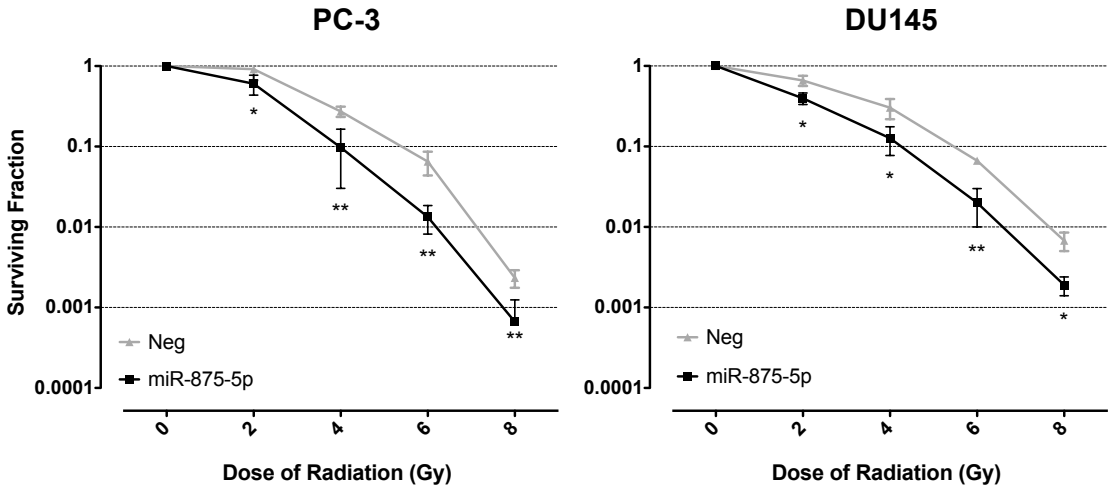

Figure 5.6 miR-875-5p enhanced PC-3 and DU145 cell sensitivity to radiation. Clonogenic cell survival of miR-875-5p- or Neg-transfected PC-3 and DU145 cells exposed to increasing doses of γ-irradiation (2, 4, 6 and 8 Gy). The surviving fraction is reported as mean±SD, n=3.

As previously done for the assessment of cell clonogenicity upon transfection with miR-23a-3p and miR-24-3p, we evaluated the effect of miR-875-5p alone on cell capacity to generate colonies, in order to exclude that the miRNA intrinsically displays a cytotoxic effect rather than a radiosensitizing one. Interestingly, the plating efficiency of both PC-3 and DU145 cells transfected with miR-875-5p compared to that of control cells (0.30 vs 0.28 and 0.21 vs 0.22, respectively) showed that the transfection did not modify the proliferative potential of PCa cells, confirming that the observed increased response to radiation exposure, actually relies on a miRNA-induced enhancement of susceptibility to the treatment, thus supporting the role of miR-875-5p as a promising radiosensitizer molecule.

5.3.2 miR-875-5p impairs radiation-induced DNA damage repair

The main lethal lesion induced by ionizing radiation consists of the generation of double strand breaks (DSBs). Radiosensitizing molecules are able to enhance the response to the treatment mainly by interfering with cell proficiency in repairing the lesion induced by radiation. To assess whether miR-875-5p-mediated radiosensitization is ascribable to such interference, we evaluated whether the persistence of radiation-induced injury was affected by the miRNA. For this purpose, we assessed the formation of DSBs through evaluation of γ-H2AX foci. H2AX is a histone variant that is phosphorylated on its Serine139-residue upon irradiation, accumulating in nuclear foci at the level of the DSBs. Actually, the phosphorylation of H2AX acts as a sensor of DNA damage that persists until activation of DNA-damage repair mechanisms. This role as an early player in the DNA damage response makes the phosphorylated form of the histone (γ-H2AX) one of the most reliable markers of DSBs formation and repair [29]. Therefore, the higher the number of unrepaired DSBs is, the higher will be the number of γ-H2AX foci. In light of this, we evaluated the kinetics of accumulation and resolution of γ-H2AX nuclear foci in miR-875-5p transfected cells compared to controls, in order to investigate whether the miRNA was able to interfere with the persistence of DNA damage. As appreciable in the immunofluorescence results shown in Fig. 5.7, control cells displayed a rapid accumulation of γ-H2AX foci, with almost 100% cells presenting more than 10 foci/nucleus at 1 hour from radiation exposure. Over time, the accumulation is markedly lost demonstrating rapid foci resolution, which suggests cell proficiency in repairing the radiation-induced DNA damage. In contrast, in miR-

875-5p cells the accumulation of γ-H2AX that is observed at 1 hour from irradiation persisted up to 8 hours, with a very low rate of foci resolution. This result indicates that miR-875-5p indeed interferes with cell capacity to repair the radiation-induced damage, thus justifying the enhanced susceptibility to radiation.

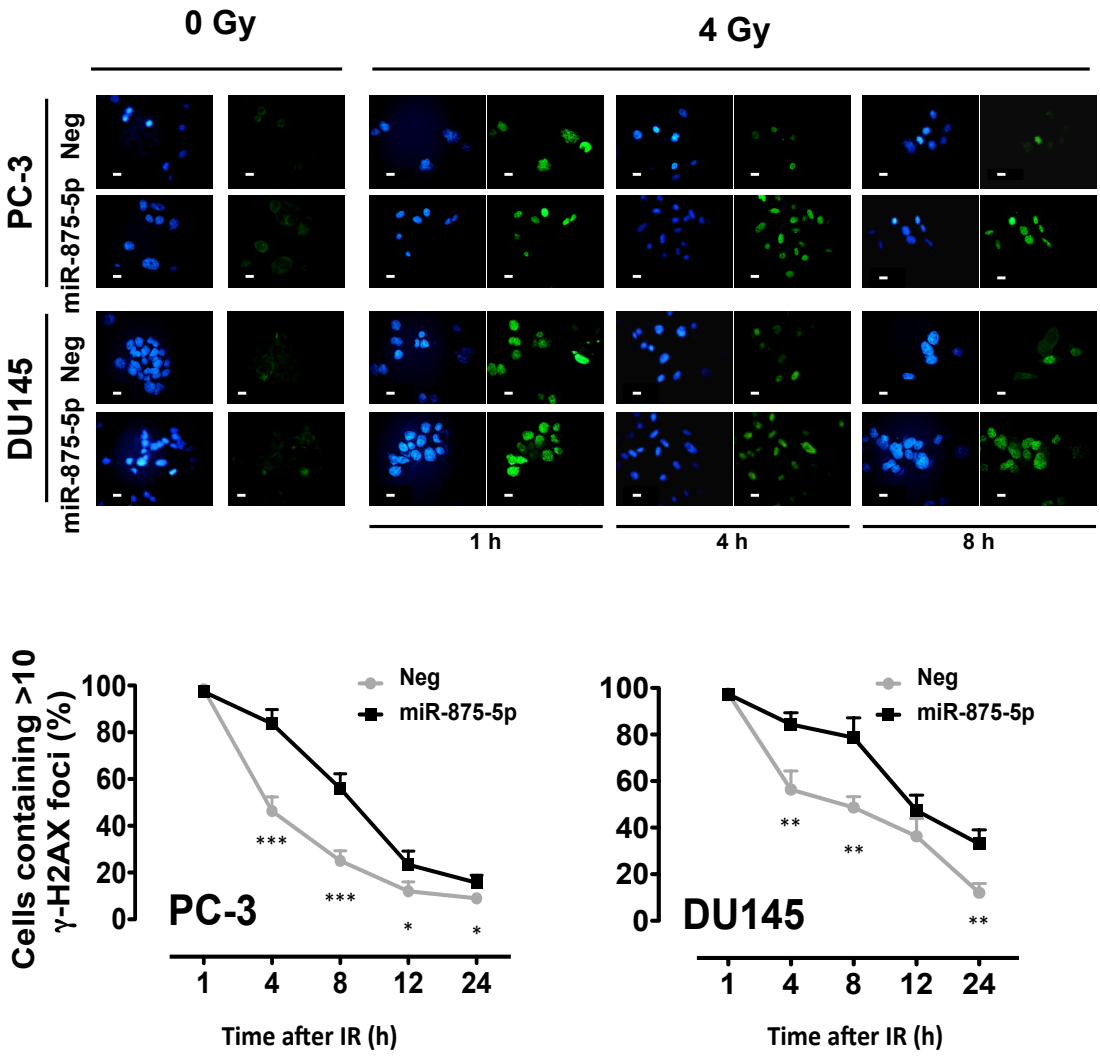

Figure 5.7 miR-875-5p impairs radiation-induced DNA damage repair. (Upper panel) Representative immunofluorescence images of nuclear γ-H2AX foci (cell nuclei: blue; γ-H2AX foci: green) in PC-3 and DU145 cells at 1, 4 and 8 h after exposure to 4 Gy of γ-irradiation. (Lower panel) Kinetics of γ-H2AX foci resolution in Neg- or miR-875-5p-reconstituted PC-3 and DU145 cells, calculated as mean number of cells containing >10 γ-H2AX foci at 1, 4, 8, 12 and 24 h after exposure to 4 Gy of γ-irradiation.

In addition, to directly assess DNA damage at a single cell level we performed experiments using the comet assay. Results indicated that the reconstitution of miR-875-5p allowed an increased extent of DNA damage at 4 h following radiation exposure. Indeed, in line with our hypothesis, miR-875-5p reconstitution resulted in an increased persistence of radiation-induced damage (Fig. 5.8).

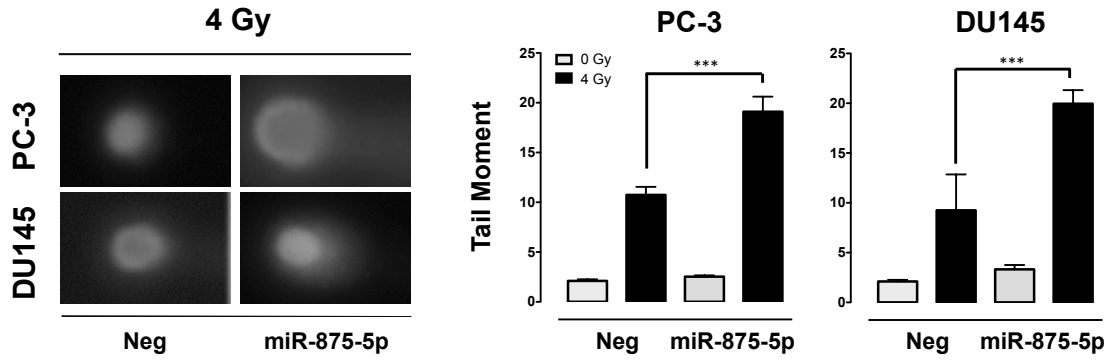

Figure 5.8 miR-875-5p increased radiation-induced DNA damage. *(Left panel)* Photomicrographs showing formation of Comets in Neg- or miR-875-5p-transfected PC-3 and DU145 cells at 4 h after exposure to 4 Gy of γ-irradiation. *(Right panel)* Quantification of tail moments counted in at least 100 cells per group, reported as mean±SD.The level of significance was represented as ***p<0.001, Student's t-test.

These findings suggest that miR-875-5p enhances cell susceptibility to radiation, by impairing cell-repair of treatment-induced DNA damage.

5.3.3 miR-875-5p enhanced PCa radiosensitivity in vivo

To further confirm these promising results supporting a role of miR-875-5p as a radiosensitizer in PCa, we carried out *in vivo* experiments aimed at verifying whether the radiosensitizing effect observed in PCa cells is also maintained in animal models. For this purpose, a DU145 clone stably expressing the miRNA was established. DU145 cells stably expressing the miRNA were subcutaneously injected into the right flank of SCID mice, and let to generate PCa tumours. When tumours reached ~300 mm^3, mice were exposed to 5 Gy single dose of irradiation by conformational radiotherapy, as detailed in Materials and Methods section. Tumour growth was monitored and tumour volumes were measured. As observed in Fig. 5.9, tumours deriving from cells expressing miR-875-5p and exposed to radiation showed a significantly enhanced tumour growth delay compared to irradiated control cell-derived xenografts. Interestingly, the presence of the miRNA alone (orange curve), in absence of treatment, did not impact on tumour growth, further confirming the in vitro findings and supporting the hypothesis that miR-875-5p is indeed a radiosensitizer as it acts enhancing the response to radiation, yet not displaying a cytotoxic effect *per se*.

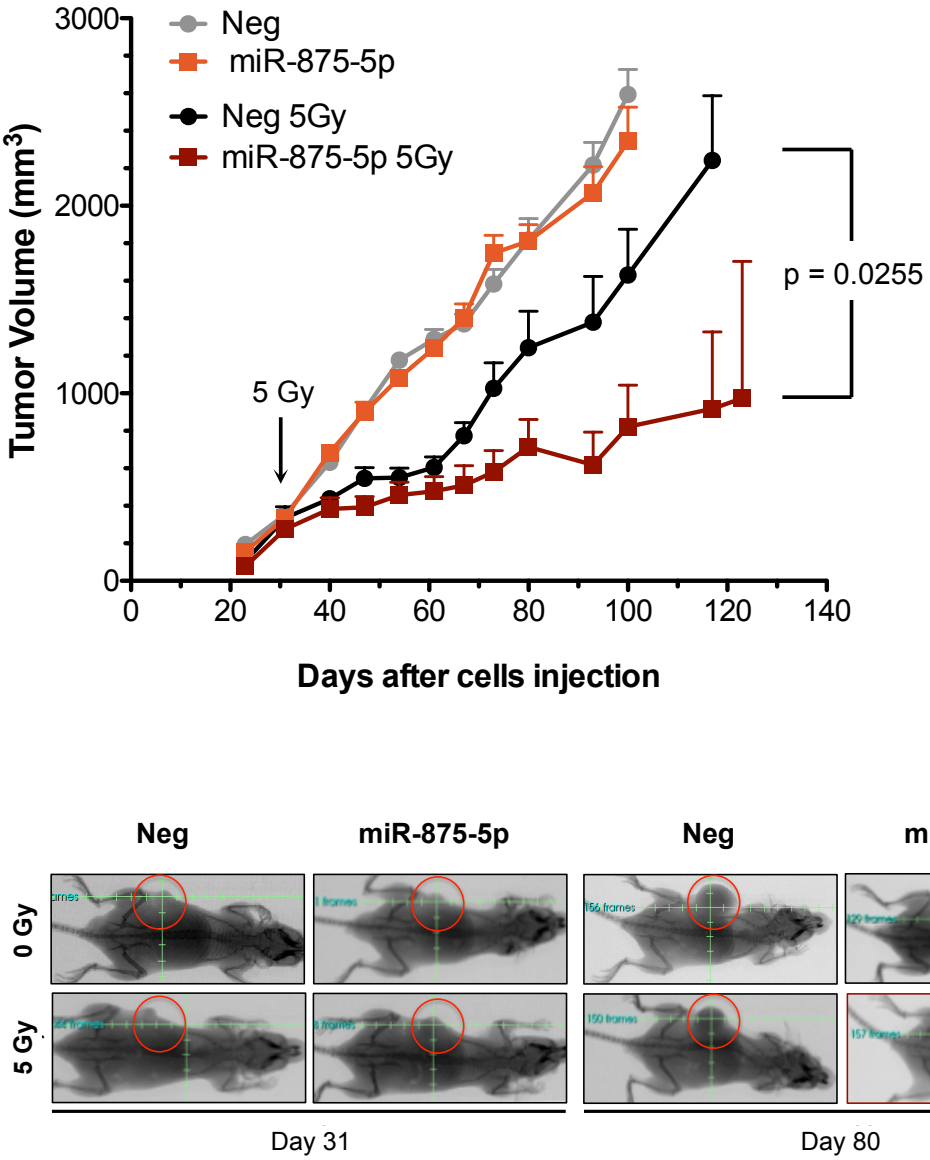

Figure 5.9 miR-875-5p significantly enhanced tumour growth delay induced by irradiation. DU145 cells stably transfected with miR-875-5p or Null vector were implanted subcutaneously into the right flank of SCID mice. When tumors reached ~300 mm^3, mice were randomly separated into four groups (8 mice/group) and were treated with 5 Gy single dose irradiation locally delivered to the tumor area. (*Upper panel*) Tumor growth volume (mm3) measured with a Vernier caliper on indicated days after cell injection. (*Lower panel*) Representative X-ray images of the subcutaneous tumour masses at the day of radiation treatment and after 50 days.

In agreement with tumour growth curves, miR-875-5p reconstitution significantly increased the time for DU145 xenografts to reach 1000 mm^3 tumour burden compared to control cell-derived xenografts (Fig. 5.10).

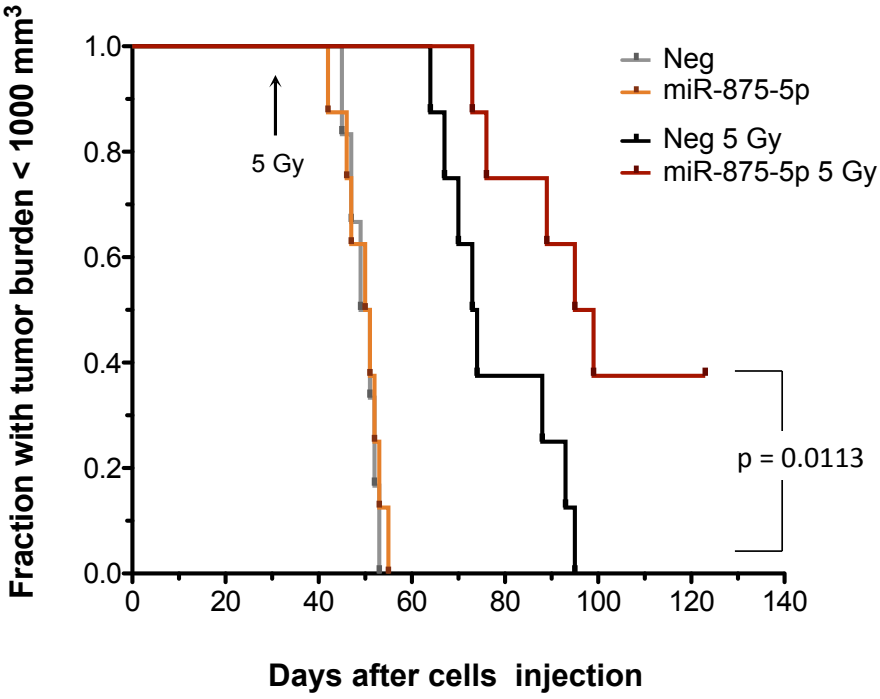

Figure 5.10 miR-875-5p significantly increased the time for DU145 xenografts to reach 1000 mm3 tumor burden. Kaplan-Meier plot of mouse tumor growth to 1000 mm3, n=8.

Moreover, to confirm that the effect associated with tumour growth delay is indeed ascribable to miRNA-induced radiosensitization, we performed en *ex vivo* clonogenic assay, with DU145 cells obtained from disaggregated tumours deriving from mice sacrificed 24 h upon irradiation. Tumour-derived cells were seeded and let to grow and form colonies, and the surviving fraction at 5 Gy (the single dose available from the *in vivo* treatment) was calculated. Strikingly, tumour-derived cells corroborated *in vitro* results. DU145 cells deriving from miR-875-5p-xenografts showed an enhanced radiation response, to an extent

superimposable to that observed in cell-lines assessment. This finding suggests that the enhancement observed in tumour growth delay actually relies on miR-875-5p ability to exert its radiosensitizing effect also in animal models. Moreover, the observation that the reduction in cell clonogenicity is almost superimposable to that observed *in vitro*, confirm that the *in vivo* effect fully recapitulates the behaviour of transfected cell model. This encouraged us to postulate that the molecular mechanism underlying miR-875-5p sensitization is maintained in animal models.

To further support this assumption, we also evaluated the levels of γ-H2AX in tumour sections obtained from miR-875-5p- xenografts (Fig. 5.11). In accordance with our hypothesis, the immunostaining revealed increased γ-H2AX levels compared to control xenografts, indicating that the radiosensitizing effect exerted *in vivo* is ascribable to an impairment of DNA damage repair as well as what has been observed to occur *in vitro*.

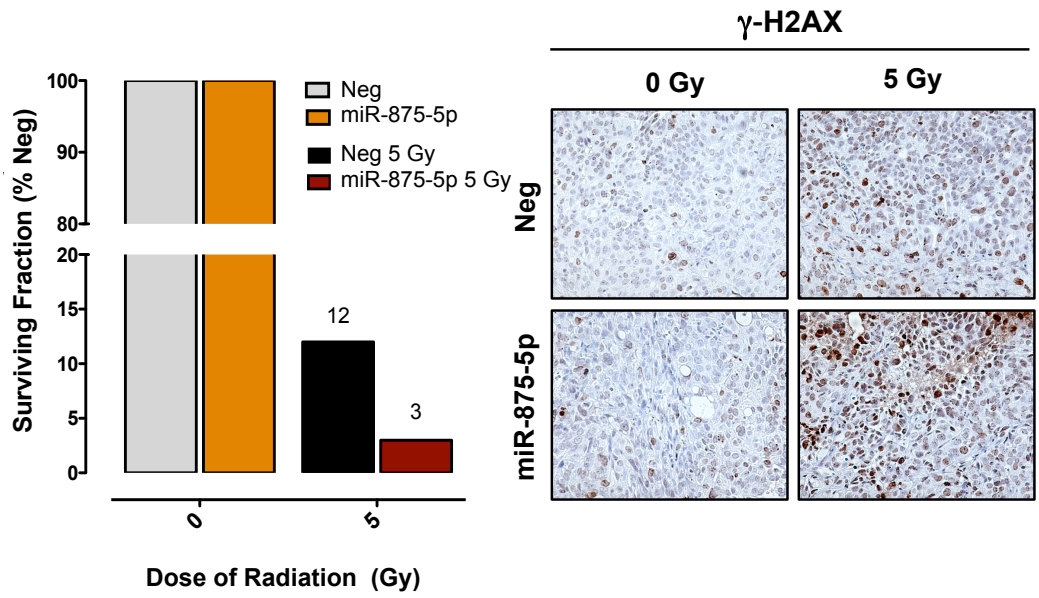

Figure 5.11 miR-875-5p reduced irradiated tumour-derived cell clonogenicity and increased γ-H2AX levels in irradiated xenografts. Ex-vivo clonogenic assay carried out in DU145 cells obtained through disaggregation of xenografts removed from SCID mice 24 h after exposure to 5 Gy or mock γ-irradiation. (E) Immunohistochemical staining of γ-H2AX shown in immunohistochemical analysis in tumor samples harvested 24 h after radiation treatment. Tumors were removed, formalin-fixed and paraffin-embedded. Tumor sections were subjected to immunohistochemical analysis using an anti-γ-H2AX (Ser139) mouse monoclonal antibody. Nuclei were counterstained with hematoxylin.

5.4 EGFR is a direct target of miR-875-5p

5.4.1 EGFR is a relevant predicted target of miR-875-5p

Once established that miR-875-5p is able to radiosensitize PCa both in cell and animal models, and that such effect relies on miRNA capacity to impair cell-proficiency in repairing radiation induced-DNA damage, the next step of the study was the dissection of the underlying molecular mechanisms. Specifically, known that miRNAs act by modulating the expression of specific target genes, to address this aim we focused on the identification of miR-875-5p targets that could be relevant in influencing radiation response, with the final aim to figure out the main mediator of the observed radiosensitization.

To narrow the list of putative mediator targets, we followed a strategy based on the intersection of:

- genes found to be downregulated in PCa cell lines transfected with miR-875-5p (as downregulation is compatible with miRNA targeting);
- genes predicted as miR-875-5p targets by using *in silico* prediction tools based on different algorithms.

According to this strategy, we first pursued the identification of genes downregulated in DU145 cells transfected with miR-875-5p compared to control transfectants, by performing gene expression analysis through microarray platform as described in Material and Methods section. Among differentially expressed genes, (FDR < 0.05 and FC ≥ 1.5) 195 were downregulated.

On the other hand, to identify miR-875-5p predicted targets, the presence of putative miR-875-5p binding sites in a given mRNA was predicted using MiRWalk algorithm, which performs a comparison of the information produced by ten established miRNA target prediction programs. Eighty-three targets simultaneously predicted by at least six programs were considered as reliable.

Once performed the described analysis separately, we merged the two gene sets and obtained a list of 19 genes (Table 5.2).

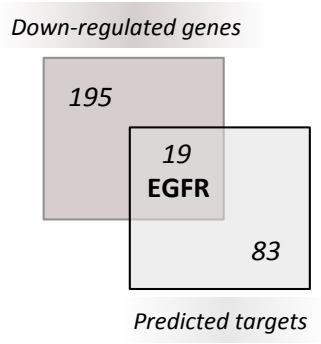

To further sharpen the selection of putative relevant targets, we reviewed the literature of the genes hunting those involved in any pathway known to be associated with radiation response. Interestingly, among possible relevant targets was EGFR, a tyrosine kinase receptor that, among its multiple functions, was also reported to be involved in influencing response to ionizing radiation, by activating DNA repair mechanisms following radiation exposure. Specifically, it has been demonstrated that, in response to radiation, EGFR is rapidly internalized and translocates to the nucleus, where it interacts with the DNA-

dependent protein kinase (DNA-PK) and increases the enzyme activity by stabilizing the phosphorylated form of DNA-PK catalytic subunit at the serine residue (S2056), which is essential for DNA double-strand break repair by non homologous end joining (NHEJ) pathway [160]. Therefore, the nuclear translocation of EGFR results in cell resistance to radiation. This link between EGFR and radiation response prompted us to pursue the hypothesis that miR-875-5p exerts its radiosensitizing effect by downregulating its target EGFR, thus interfering with EGFR-associated radioresistance.

Symbol	GeneName	logFC	FDR
NFE2L3	nuclear factor, erythroid 2-like 3	-1.52686	2.33E-12
MED20	mediator complex subunit 20	-1.27655	6.29E-12
USF2	upstream transcription factor 2, c-fos	-1.14178	4.04E-08
RAB11FIP2	RAB11 family interacting protein 2 (class I)	-1.11633	5.11E-11
SLC25A21	solute carrier family 25 (mitochondrial oxoadipate carrier), member 21	-1.0997	2.98E-11
WSB2	WD repeat and SOCS box containing 2	-0.91723	5.17E-06
EGFR	**epidermal growth factor receptor**	**-0.81115**	**6.62E-09**
DIRC2	disrupted in renal carcinoma 2	-0.76956	6.98E-08
SH3YL1	SH3 and SYLF domain containing 1	-0.76146	5.42E-07
NMT2	N-myristoyltransferase 2	-0.74431	5.82E-08
PM20D2	peptidase M20 domain containing 2	-0.72606	1.62E-05
DDX50	DEAD (Asp-Glu-Ala-Asp) box polypeptide	-0.69708	3.5E-06
HLTF	helicase-like transcription factor	-0.6863	1.97E-06
SH3D19	SH3 domain containing 19	-0.62052	2.26E-07
TAF5	TAF5 RNA polymerase II, TATA box binding protein (TBP)-associated factor,	-0.57288	3.73E-05

ZNF280B	zinc finger protein 280B	-0.56791	0.000113
LIN7C	**lin-7 homolog C (C. elegans)**	**-0.55586**	**0.004092**
SYPL1	synaptophysin-like 1	-0.54958	0.000205
CASD1	CAS1 domain containing 1	-0.50051	0.00038

Table 5.2. Putative *miR-875-5p* targets. List of genes arisen from the intersection between genes found to be downregulated in *miR-875-5p* cells (evaluated by microarray analysis performed in *miR-875-5p* reconstituted DU145 cells) with the list of genes predicted to be target of the miRNA by at least 6 different miRNA target prediction tools.

Notably, among the list of 19 genes was also LIN7C, which is known to favour the localization of EGFR at the baso-lateral membrane of epithelial cells [161,162]. The presence of two members of the same pathway in such a small list of 19 genes, further encouraged us to focus on EGFR for following investigation.

5.4.2 EGFR is a direct target of miR-875-5p

We found EGFR as a predicted target of miR-875-5p, however no validation data about its real direct targeting were available when we pursued the study. Hence, we assessed whether EGFR is directly bound and negatively regulated by miR-875-5p, by performing a luciferase assay. Specifically, we cloned a 1285 nt-long portion of EGFR 3' UTR containing the predicted miR-875-5p binding site downstream the FireFly luciferase gene. After 24 h from co-transfection with miR-875-5p, we evaluated Luciferase activity to assess

whether it was influenced by the presence of the miRNA. As showed in Fig. 5.12, luciferase activity was significantly reduced upon miR-875-5p co-transfection, indicating that the miRNA bound EGFR 3'UTR portion thus leading to the downregulation of luciferase expression and consequent activity. This result validated EGFR as a direct target of miR-875-5p.

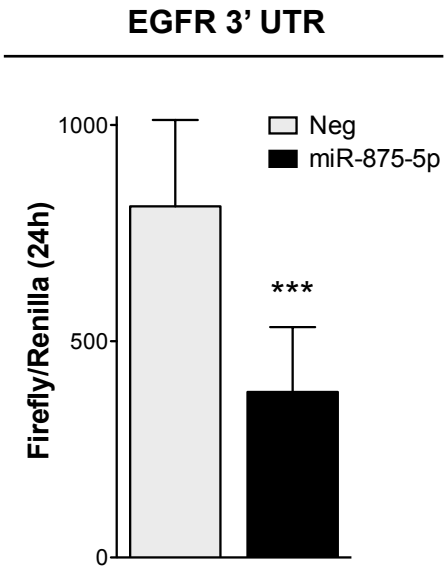

Figure 5.12 EGFR is a direct target of miR-875-5p. Luciferase assay confirming EGFR as a direct target of miR-875-5p. EGFR 3' UTR containing the predicted miR-875-5p binding site was amplified by PCR from cDNA obtained from DU145 cells and cloned in the reporter vector downstream of the FireFly luciferase gene. Cells were collected after 24 h and the luciferase activity was assessed. The ratio of FireFly activity to that of Renilla is reported as mean±SD.

5.4.3 EGFR is downregulated by miR-875-5p in PCa cells

Accordingly with the fact that miR-875-5p directly targets EGFR, we found that expression levels of EGFR were downregulated upon miRNA transfection with respect to control cells. Specifically, we evaluated the expression levels of EGFR transcript upon 24 h, a time point that allows detecting any change in transcription levels, and we found that indeed EGFR transcript was downregulated by miR-875-5p.

Moreover, we assessed the expression levels of EGFR protein, to confirm that a functional downregulation was occurring. Accordingly, EGFR levels were reduced also at protein levels, thus suggesting that miR-875-5p leads to a functional downregulation of EGFR in PCa cells (Fig. 5.13).

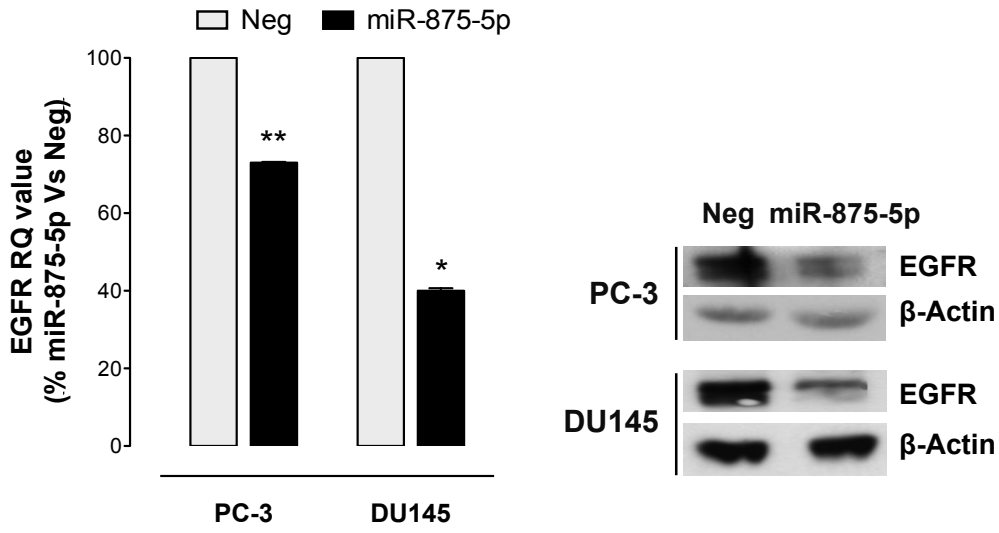

Figure 5.13 EGFR is downregulated by miR-875-5p. (*Left panel*) qRT-PCR showing EGFR mRNA amount in PC-3 and DU145 cells after miR-875-5p reconstitution, compared to control cells, normalized to GAPDH. Data are reported as a percentage of Neg-transfected cells. (*Right panel*) Western blot analysis showing EGFR protein amount in PC-3 and DU145 cells upon Neg- or miR-875-5p-transfection, normalized to β-Actin. Cropped images of selected proteins are shown.

Moreover, to appreciate EGFR downregulation at its cell site of localization, we performed an immunofluorescence staining along a wound healing assay. First of all, we could actually observe that EGFR is markedly downregulated upon miRNA transfection, as indicated by the low immunoreactivity (Fig. 5.14, *upper panel*). Interestingly, we could monitor EGFR localization and we found that miR-875-5p delocalizes EGFR from cellular invasive front, where it is normally highly expressed in control cells (Fig. 5.14, *lower panel*).

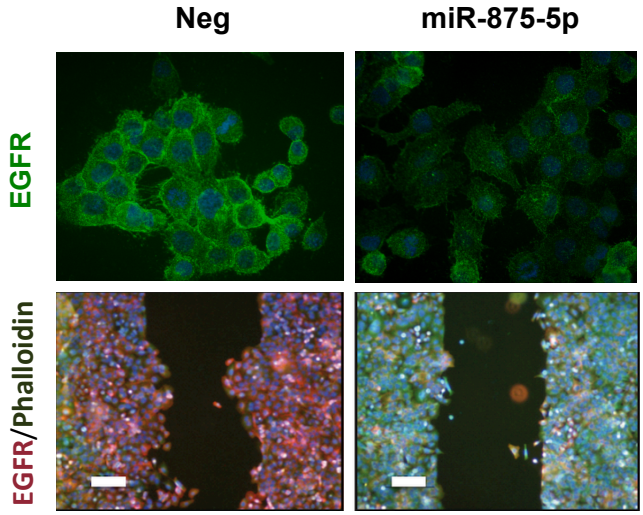

Figure 5.14 EGFR is downregulated and delocalized by miR-875-5p. *(Upper panel)* Images showing reduction of EGFR staining (green) and delocalization from the cell membrane in DU145 cells overexpressing miR-875-5p. DAPI (blue) was used to stain nuclei. (*Lower panel*) Representative images from a wound healing assay carried out in DU145 cells showing staining of EGFR (red), F-actin (green) and nuclei (blue) at 32 h following the scratch. Scale bar 100 μm.

Considering that EGFR was found to be delocalized upon miRNA transfection, and that among the 19 possible targets of miR-875-5p we also found LIN7C, we postulated that there might be a correlation between those two events. To verify our hypothesis we tested whether there was any modulation in LIN7C upon miR-875-5p reconstitution, which is expected based on gene expression analysis. In accordance with LIN7C gene downregulation upon gene expression, and in agreement with EGFR delocalization from the membrane, reduced mRNA and protein levels of LIN7C were found in miR-875-5p-overexpressing PC-3 or DU145 cells (Fig. 5.15), thus further supporting the relevance of the EGFR signalling pathway in mediating miR-875-5p biological effect.

.

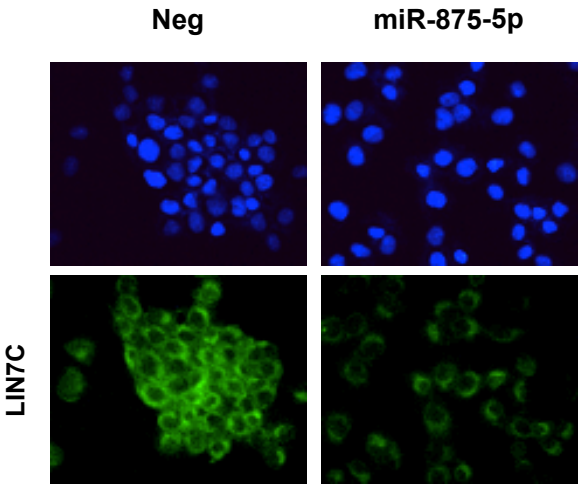

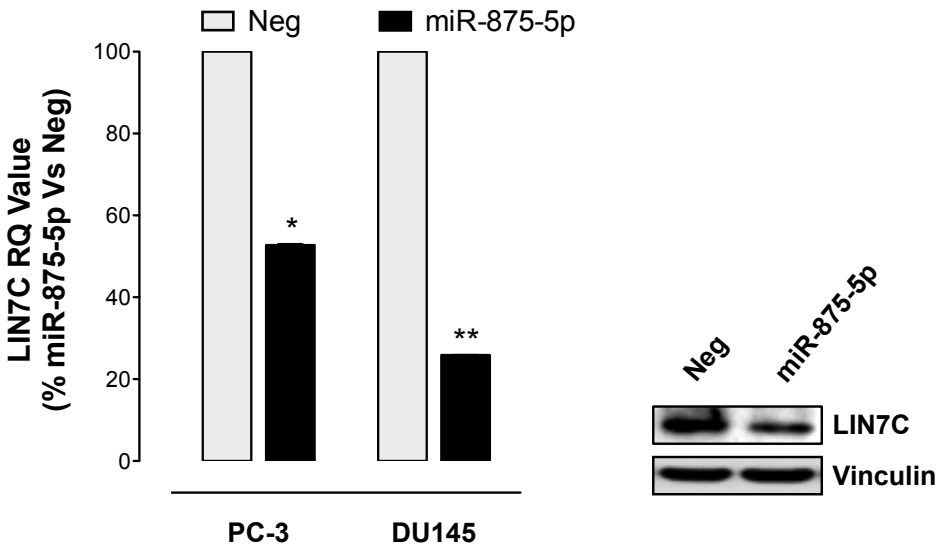

Figure 5.15 miR-875-5p down-regulates LIN7C. (*Upper panel, left*) qRT-PCR showing LIN7C mRNA amount in PC-3 and DU145 cells after miR-875-5p reconstitution, compared to control cells, normalized to GAPDH. Data are reported as a percentage of Neg-transfected cells. The level of significance was represented as *p<0.05, **p<0.01, Student's t-test. (*Upper panel, right*) Western blot analysis showing LIN7C protein amount in DU145 cells upon Neg- or miR-875-5p-transfection, normalized to Vinculin. Cropped images of selected proteins are shown. (*Lower panel*) Images showing reduction of LIN7C staining (green) in DU145 cells overexpressing miR-875-5p. DAPI (blue) was used to counterstain nuclei.

5.5 EGFR-ZEB1 axis mediates miR-875-5p radiosensitizing effect

5.5.1 EGFR contributes to mediate miR-875-5p-induced radiosensitization

The identification and validation of EGFR as a target that is known to play a role in radiation response, does not per se demonstrate that EGFR is actually responsible of miR-875-5p-radiosensitization. To investigate and provide evidence of EGFR involvement in miR-875-5p impact on radiation response, we performed a very specific experiment based on target protection strategy.

This approach consists of masking miRNA binding site within the target thus impeding the physical interaction between the miRNA and its target. To achieve this, we designed an oligonucleotide (miR-Mask) fully complementary to miR-875-5p binding site within EGFR 3'UTR, able to protect the site from miR-875-5p binding. First of all, we tested whether the designed miR-Mask was actually able to prevent miRNA-mRNA interaction, by evaluating EGFR expression levels upon co-transfection with both miR-875-5p and miR-Mask molecules. We found that the miR-Mask was able to significantly recover EGFR expression at both mRNA and protein level in miR-875-5p-reconstituted cells (Fig. 5.16). This result gave us the proof of masking ability to protect EGFR from miRNA targeting and consequent downregulation.

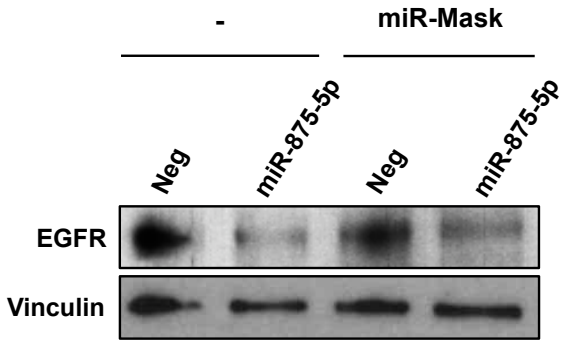

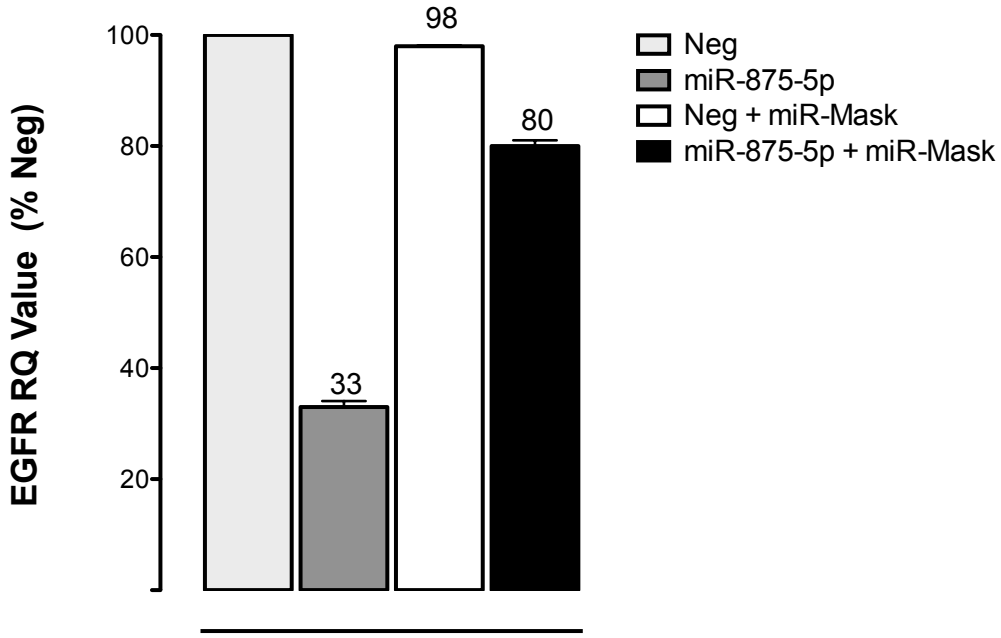

Figure 5.16 EGFR miR-Mask recovered EGFR expression levels in miR-875-5p cells. (*Upper panel*) Western blot analysis showing EGFR protein amount in DU145 cells upon Neg or *miR-875-5p* transfection, in presence or absence of EGFR miR-Mask, normalized to Vinculin. Cropped images of selected proteins are shown. *(Lower panel)* qRT-PCR showing *EGFR* mRNA amount in DU145 cells after *miR-875-5p* reconstitution in the presence or absence of miR-Mask, normalized to *GAPDH*. Data are reported as a percentage of Neg-transfected cells.

To examine whether EGFR is a key factor in determining the radiosensitizing effect induced by miR-875-5p, we transfected miRNA-reconstituted DU145 cells with the miR-Mask, with the aim of assessing whether the abrogation of EGFR downregulation influences miR-875-5p-induced effect. Strikingly, we found that miRNA mask was able to almost completely abrogate the radiosensitizing effect induced by miRNA reconstitution (Fig. 5.17). This result indicates that, upon EGFR recovering, the miR-875-5p is no longer able to influence cell sensitivity, suggesting that the downregulation of EGFR is a crucial step in the radiosensitizing process.

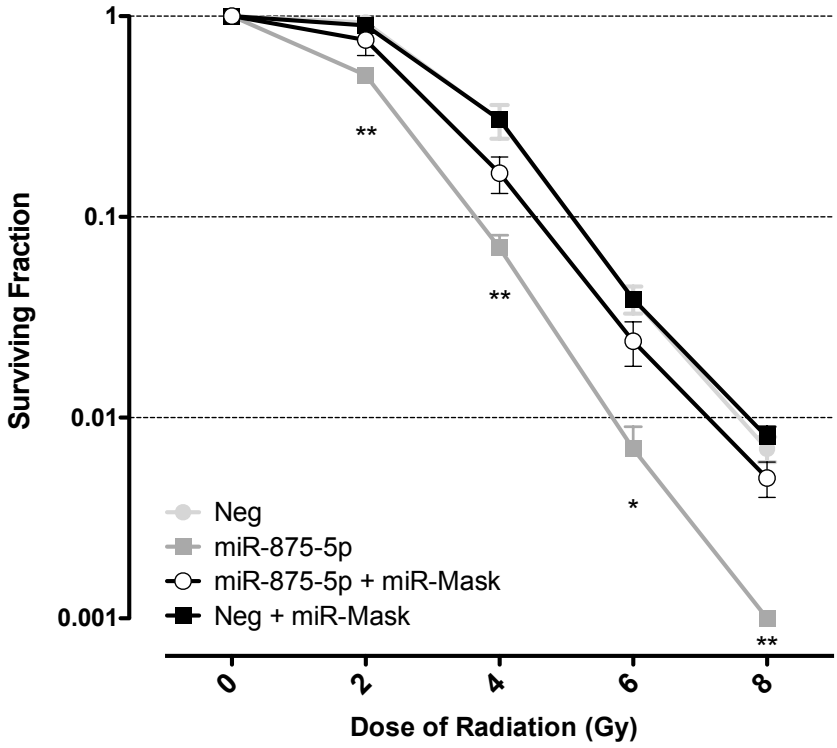

Figure 5.17 EGFR contributes to mediate *miR-875-5p*-induced radiosensitization. Clonogenic cell survival of DU145 cells transfected with *miR-875-5p* alone or co-transfection with miR-Mask. The surviving fractions following the indicated doses of radiation are reported as mean±SD, n=3. The level of significance was represented as *p<0.05, **p<0.01, Student's t-test.

5.5.2 miR-875-5p reduces DNA-PK activation via EGFR downregulation

As previously reported, EGFR role in radiation response relies on its internalization into the nucleus where it binds and activates DNA-PK, thus leading to NHEJ guided DNA-repair. The activation of DNA-PK occurs by phosphorylation of a specific residue (S2056), which is therefore considered a flag of DNA-PK active status. To verify whether EGFR mediates miR-875-5p effect by its participation to this pathway, we assessed EGFR levels in the nucleus with the purpose to monitor whether, following irradiation, a translocation has occurred.

According to the overall significantly reduced EGFR abundance, and the almost complete absence of the protein in the nuclear fraction observed in miR-875-5p-reconstituted DU145 cells under basal conditions, negligible EGFR levels were detected in the nucleus of these cells after 5 Gy irradiation (Fig. 5.18). In line with its role in influencing DNA damage-repair, miR-875-5p ectopic expression counteracted radiation-induced activation of ATM, as suggested by a slightly reduced activation of ATM as detected by the lower expression levels of the phosphorylated form of the enzyme at S1981 (ATM-S1981) (Fig. 15.19), which is consistent with previous results obtained in non-small cell lung cancer cells exposed to the EGFR inhibitor gefitinib before irradiation [163].

Surprisingly, any significant reduction in the activation of DNA-PK, assessed in terms of the phosphorylated form of the enzyme at S2056 (DNA-PK2056), was observed following irradiation of miR-875- 5p-reconstituted compared to control cells. This result prompted us to postulate the involvement of other effectors downstream EGFR, other than DNA-PK.

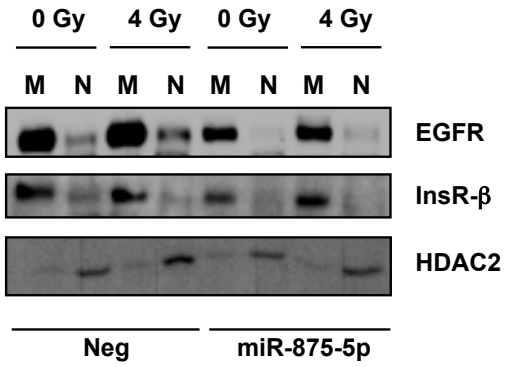

Figure 5.18 EGFR translocation to the nucleus is reduced upon miR-875-5p mediated downregulation. Western blot analysis showing EGFR subcellular localization in DU145 cells transfected with Neg or miR-875-5p. Forty-eight h after transfection, cells were irradiated at 4 Gy and 60 min later harvested for subcellular protein fractionation and Western blot assay. Insulin R-β and HDAC2 were used as control for membrane and nuclear fractionations, respectively. Cropped images of selected proteins are shown.

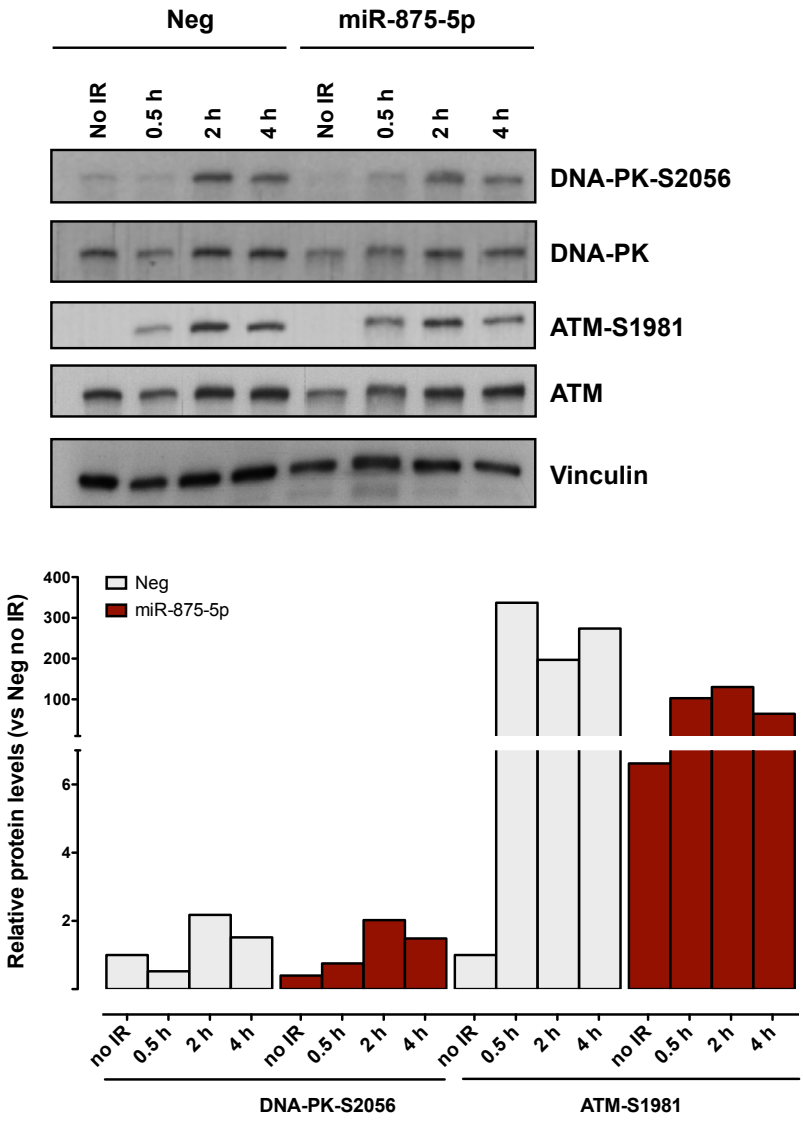

Figure 5.19 ATM and DNA-PK activation is reduced by miR-875-5p reconstitution. (Upper panel) Western blot analysis showing ATM and DNA-PK expression in DU145 cells transfected with Neg or miR-875-5p. Forty-eight hours after transfection, cells were irradiated at 4 Gy and harvested 0.5, 2 and 4h later harvested for Western blot assay. Vinculin was used as control for loading. (Lower panel) Quantification of protein expression levels of DNA-PK-S2056 and ATM-S1981 normilized to endougenous control (Vinculin) and to corresponding total protein (i.e. DNA-PK and ATM, respectively).

5.5.3 EGFR-mediated ZEB1 downregulation plays a main role in miR-875-5p-induced radiosensitization

Since, although present, the involvement of EGFR-DNA-PK pathway seemed to be almost neglectible with respect to the important effect induced by miR-875-5p, we were prompted to suppose that some other players were involved in determining the final effect.

As previously anticipated, recent results indicate that ZEB1 is associated with tumor radioresistance [159], and that its expression can be suppressed by EGFR inhibitors [164,165]. The merge of these findings fostered us to investigate a possible role of ZEB1 in miR-875-5p radiosensitizing effect of EMT-impairment, postulating that, yet not being a direct target of the miRNA, it could be indirectly downregulated via EGFR suppression. To test our hypothesis, we evaluated the expression levels of ZEB1 in miR-875-5p transfected cells. A significant reduction in ZEB1 protein expression was found in miR-875- 5p-reconstituted DU145 cells (Fig. 5.20, *left*). Moreover, taking advantage of tumour-sections of xenografts originating from DU145 cells stably expressing miR-875-5p, we could also appreciate such reduction in *ex vivo* tissues, thus confirming that ZEB1 downregultion is maintained in *in vivo* settings. (Fig. 5.20, *centre*). In addition, the recovery of ZEB1 expression observed when cells where transfected with the miR-Mask specifically blocking the interaction between miR-875-5p and EGFR mRNA suggests that, at least in part, the reduced ZEB1 expression in miRNA-reconstituted cells was consequent to miR-875-5p- induced EGFR down-regulation.

Recent data obtained in cell lines of tumor types other than PCa showed that ZEB1 induces radioresistance not only through EMT but also playing a direct role in homologous recombination-mediated repair of DNA breaks by regulating CHK1 expression levels [166]. Such a regulation is mediated by the interaction of ZEB1 with the deubiquitinase USP7, which promotes the enzyme ability to stabilize CHK1 protein [166].

In light of these findings, we tested the possible involvement of CHK1 in the cascade downstream of EGFR-ZEB1 axis. Interestingly, a reduced expression of CHK1 was found to parallel ZEB1 down-regulation in miR-875-5p-transfected cells (Fig. 5.20, *right*).

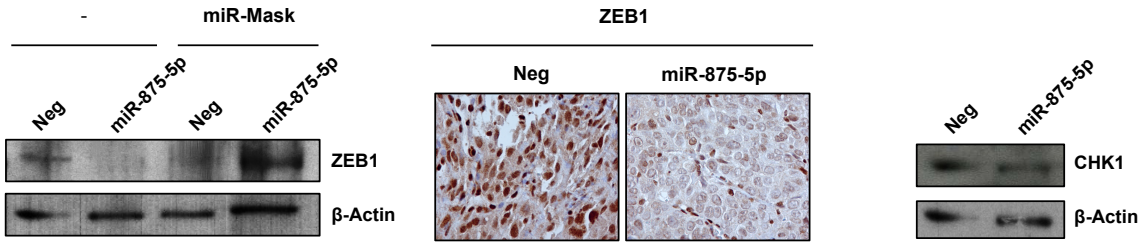

Figure 5.20 miR-875-5p induced ZEB1 repression via EGFR downregulation. (*Left panel*) Western blot analysis showing ZEB1 protein amount in DU145 cells upon Neg or miR-875-5p transfection, in presence or absence of EGFR miR-Mask, normalized to β-Actin. Cropped images of selected proteins are shown. (*Centre panel*) Expression and subcellular localization of ZEB1 in tumor xenografts of Null and miR-875-5p stably expressing DU145 cells grown in SCID mice, as assessed by IHC. Nuclei were counterstained with hematoxylin. (*Right panel*) Western blot analysis showing CHK1 protein expression levels in DU145 cells transfected with miR-875-5p- compared to Neg-transfected cells. β-actin was used for normalization. Cropped images of selected proteins are shown.

As we proceeded for demonstrating EGFR functional involvement in mediating miR-875-5p radiosensitization, we similarly wanted to assess the contribution of ZEB1 in determining the final effect on radiation response. Therefore, we transfected DU145 cells with a specific siRNA molecule against ZEB1, in order to evaluate whether ZEB1 silencing was able to phenocopy miR-875-5p in increasing cell sensitivity to radiation.

First of all, we compared the extent of ZEB1 inhibition by the two strategies (miRNA vs siRNA) in order to exclude that any difference in the evaluated effect could be due to a major/minor downregulation. Interestingly, the siRNA molecule was able to inhibit ZEB1 mRNA expression to an extent comparable to that observed following miR-875-5p reconstitution (Fig. 5.21). Strikingly, clonogenic assay results showed that ZEB1 silencing was able to fully reproduce the radiosensitizing effect induced by the miRNA (Fig. 6D), suggesting a main role of the EGFR-ZEB1-CHK1 axis inhibition in promoting PCa cell radiation response.

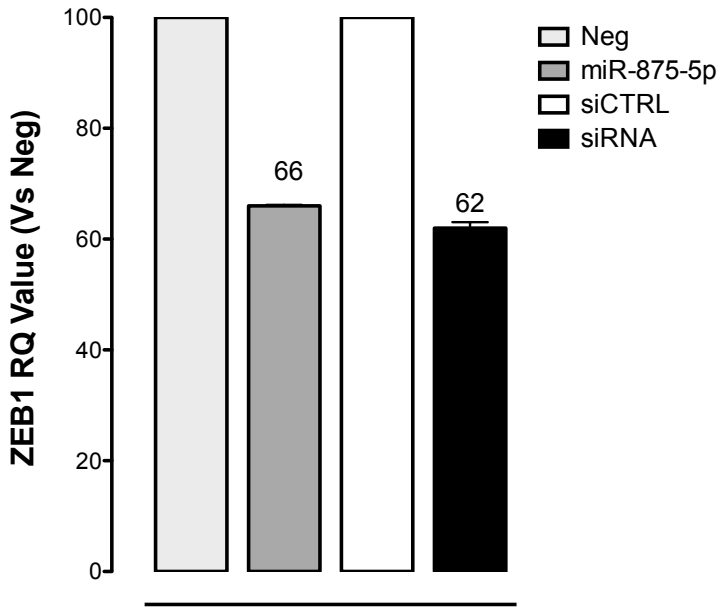

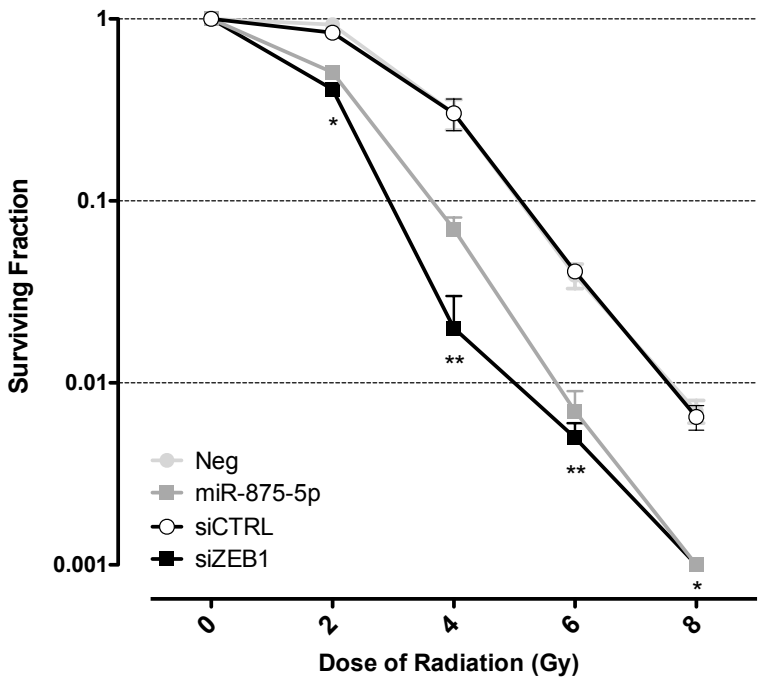

Figure 5.21 EGFR-mediated ZEB1 downregulation plays a main role in *miR-875-5p*-induced radiosensitization. (*Upper panel*) qRT-PCR showing *ZEB1* mRNA amount in DU145 cells after transfection with *miR-875-5p* or siZEB1 and respective controls, normalized to *GAPDH*. Data are reported as a percentage of Neg- or siCTRL-transfected cells, respectively. (*Lower panel*) Clonogenic cell survival of DU145 cells transfected with *miR-875-5p* or siZEB1 and respective negative controls. The surviving fractions following the indicated doses of γ-irradition are reported as mean±SD, n=3.

6. RESULTS III: the role of miR-205 in PCa radiation response

In the framework of miRNAs sorted by following the second approach, we singled out miR-205.

Previous studies undertaken by our group reported that miR-205 is a tumour-suppressor miRNA, the expression of which is reduced or lost in prostate tumours compared to normal tissues. We also found that miR-205 regulates pathways that are known to affect radiation response, such as autophagy and epithelial to mesenchymal transition (EMT). Specifically, we previously observed that restoration of miR-205 in DU145 cells was able to impair the autophagic flux by downregulating RAB27A and LAMP3 lysosome-associated proteins, thus resulting in an enhancement of cisplatin cytotoxic activity [153].

The possible relevance of the miRNA in PCa radiation response is also based on the well-established role of miR-205 in counteracting EMT, mainly by targeting ZEB1/2 EMT-transcription factors, as demonstrated by Gregory et al. [167] for the first time and, shortly after, by Gandellini et al. [81]. In particular, our group demonstrated that miR-205 plays a crucial role in EMT-regulation in the context of PCa, at least in part through the down-regulation of protein kinase Cepsilon (PKC-ε).

Interestingly, the relevance of PKC-ε in determining cell response to radiation-induced injury is also supported by the study of Wanner et al [168]. The authors demonstrated that the activation of PKC-ε stimulates DNA-repair by promoting the nuclear accumulation of EGFR, leading to activation of DNA-PK, a protein kinase essential for DNA-repair [169].

Based on this premises, to examine whether miR-205 is able to enhance PCa cells, presumably by regulating one of the mentioned target pathways, we first reconstituted miR-205 in PCa cells and investigated its impact on radiation response, and dissected the underlying molecular mechanism.

6.1 miR-205 reconstitution enhanced PCa cell response to radiation

6.1.1 Transient transfection of DU145 with miR-205 significantly increased miRNA expression levels

As a very first step of this part of the study, we reconstituted miR-205 in DU145 and PC-3 cells by transient transfection. To verify that transfection actually increased miR-205 levels in PCa cells, we assessed the kinetics of miR-205 expression levels over the course of 10 days (Fig. 6.1). As showed, in both DU145 and PC-3 cells, miR-205 was upregulated beginning at 24 h after transfection, with an expression peak at 48 h. Afterwards, miRNA levels gradually decreased, still maintaining a high expression at least up to 10 days from transfection. This data led us to assume that any biological effect observed within this time window can still be imputable to the verified upregulation of miR-205 in PCa cells.

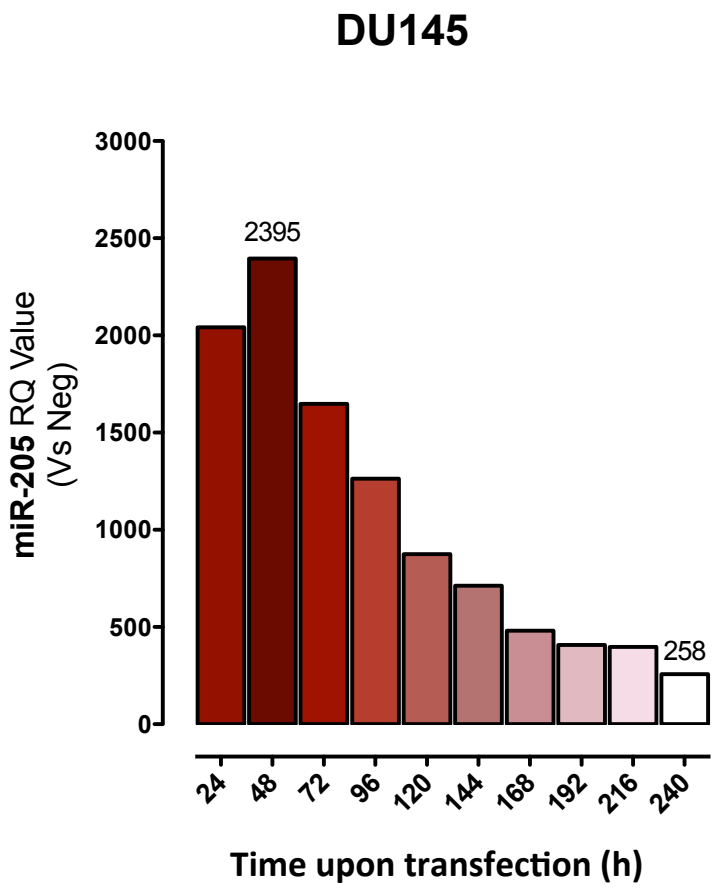

Figure 6.1 miR-205 was upregulated up to 10 days upon transient transfection. Expression of miR-205 assessed by qRT-PCR in DU145 cells transfected with miR-205 compared to negative control cells. Data are reported as relative quantity (RQ) ± SD with respect to Neg cells.

6.1.2 miR-205 enhances PCa cell response to radiation

Once verified that ectopic transfection allowed miR-205 overexpression to an extent sufficient to appreciate the biological effects exerted the miRNA, we exposed transfected cells to radiation and evaluated miR-205 capacity to influence cell sensitivity to the treatment. Remarkably, miR-205 reconstitution was able to significantly enhance radiation response of DU145 cells, as indicated by reduced clonogenic cell survival (Fig.6.2).

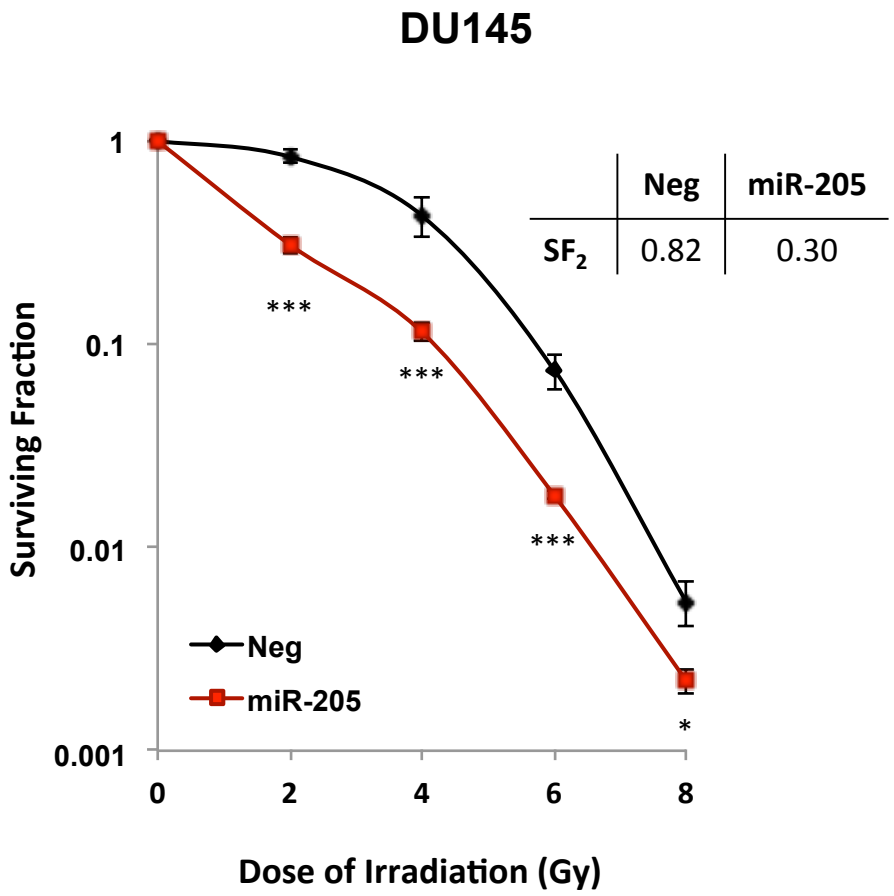

Figure 6.2 miR-205 enhanced DU145 cell sensitivity to radiation. Clonogenic cell survival of miR-205- or Neg-transfected DU145 cells exposed to increasing doses of γ-irradiation (2, 4, 6 and 8 Gy). The surviving fraction is reported as mean±SD, n=3.

Considering the established role of miR-205 in prostate cancer tumorigenesis, we wanted to exclude that such effect on cell-clonogenicity actually relies on miR-205 capacity to enhance cell sensitivity to radiation, rather to on an intrinsic cytotoxic effect of the miRNA. To address this, we compared the plating efficiency of negative transfected cells with this of miR-205 transfectants, in non-irradiated cells, as any significant difference would have reflected a cytotoxic effect of the miRNA regardless of radiation involvement.

Interestingly, the PE of miR-205 (PE=0.21), measured as the ratio of counted colonies to the number of seeded cells, was almost completely identical to that of negative cells (PE=0.22). This indicated that miR-205 alone does not exert any effect on cell viability and clonogenicity. Therefore, the totality of the effect observed in miR-205 cells upon irradiation is completely imputable to miRNA ability to make cells more susceptible to radiation, which is completely compatible with its postulated role of radiosensitizer molecule. Indeed, this finding is in accordance with miR-205 involvement in PCa tumorigenesis, since the major tumour-suppressive effect of the miRNA was demonstrated to be exerted in terms of impairment of EMT/migration/invasion abilities of the cell, rather than of cell viability and proliferation capabilities.

6.1.3 miR-205 impairs radiation-induced DNA damage repair

Considering i) the crucial role of DNA damage repair in influencing cell response to radiation, and that ii) miR-205 targets pathway related to DNA repair, we sought to investigate whether miR-205-radiosensitizing effect was mediated by miRNA capacity to interfere with such mechanisms. To that aim, we assessed the kinetics of γ-H2AX foci resolution upon exposure to 4 Gy of irradiation, as previously done for miR-875-5, in order to understand whether miR-205 affect DSBs repair mechanisms.

As expected, negative transfected cells displayed a rapid accumulation and resolution of γ-H2AX foci (<20% foci within 8h from irradiation), thus confirming that DU145 cells are basally proficient in repairing radiation-induced damage. On the contrary, miR-205 transfected cells, showed a markedly delayed foci

resolution, with almost 90% of cells presenting more than 10 foci within the nucleus (Fig. 6.3). This indicates that miR-205 was able to significantly reduce DSBs clearance by interfering with cell repair mechanisms, thus ultimately extending the persistence of radiation-induced injury. This result confirms that miR-205 acts as a sensitizer molecule in PCa by enhancing the effect caused by radiation treatment.

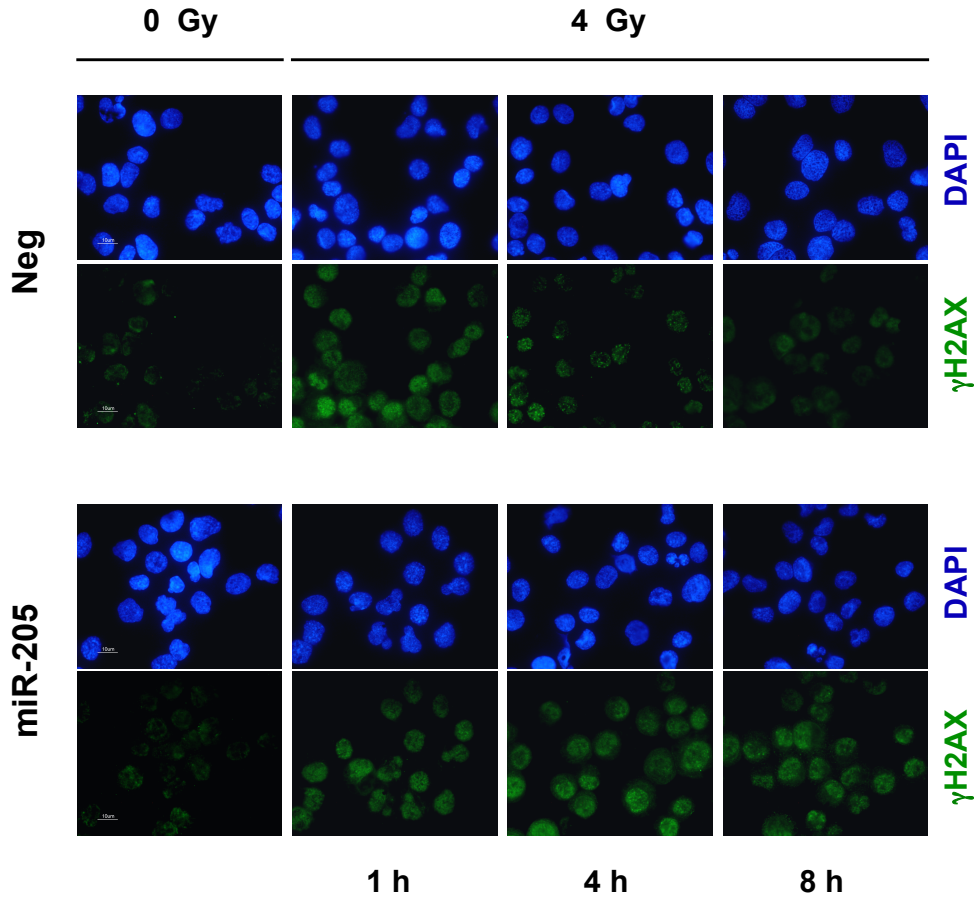

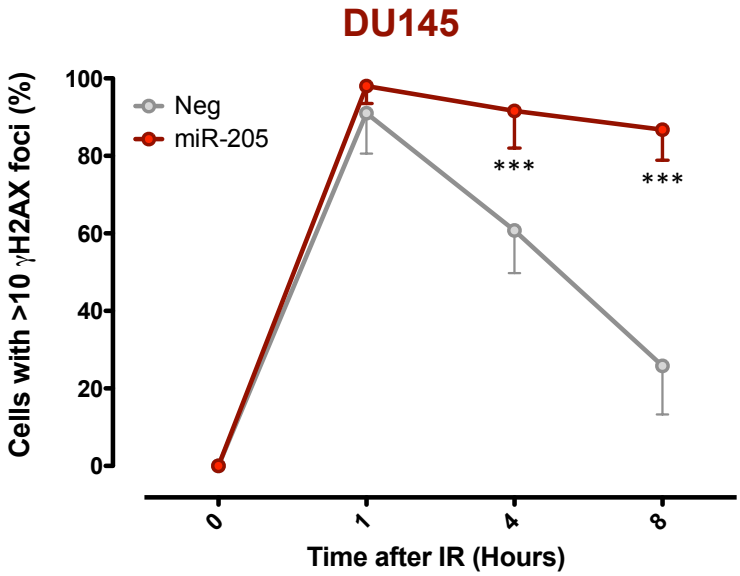

Figure 6.3 miR-205 impairs radiation-induced DNA damage repair. *(Upper panel)* Representative immunofluorescence images of nuclear γH2AX foci (cell nuclei: blue; γH2AX foci: green) of DU145 cells at 1, 4 and 8 h after exposure to 4 Gy radiation. *(Lower panel)* Kinetics of γH2AX foci resolution of miR-205 reconstituted and control DU145 cells, calculated as mean number of cells containing >10 γH2AX foci at 1, 4, 8 hours after exposure to 4 Gy of irradiation.

To assess DNA damage at a single-cell level, we performed comet assay on negative/miR-205 transfected DU145 cells after 4 h from radiation exposure (4 Gy). In line with our previous evidence that miR-205 is able to counteract the repair of radiation-induced damage, we observed that comet tail moments were markedly extended in miR-205 transfectants compared to normal cells, thus further supporting the role of miR-205 in interfering with DNA-repair processes (Fig. 6.4).

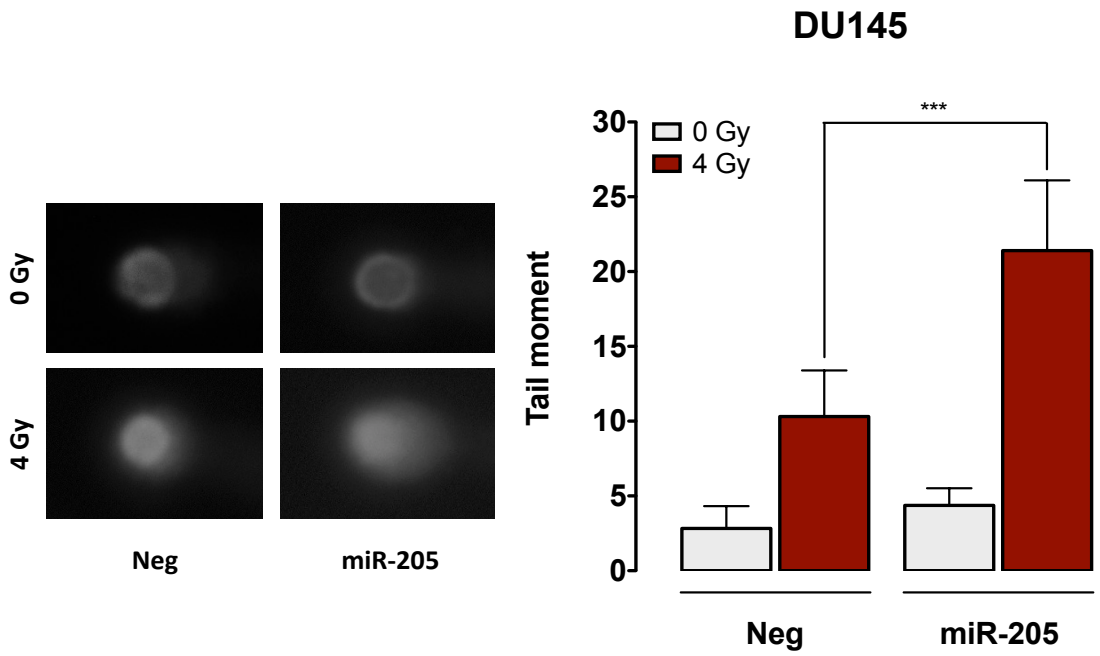

Figure 6.4 miR-205 increased radiation-induced DNA damage. (*Left panel*) Photomicrographs showing formation of Comets in Neg- or miR-205-transfected DU145 cells at 4 h after exposure to 4 Gy of γ-irradiation. (*Right panel*) Quantification of tail moments counted in at least 100 cells per group, reported as mean±SD.The level of significance was represented as ***p<0.001, Student's t-test.

6.1.4 miR-205 enhances PCa response to radiation in vivo

Considering the promising results supporting miR-205 relevance in determining PCa radiation response, and taking advantage of a previously established DU145 clone stably expressing miR-205, we tested miRNA-induced radiosensitizing effect *in vivo*. First of all we verified miR-205 overexpression in DU145 stable cells by qRT-PCR. As expected, miR-205 was consistently upregulated in DU145 stable clone with respect to the negative control harbouring an empty vector (Fig. 6.5).

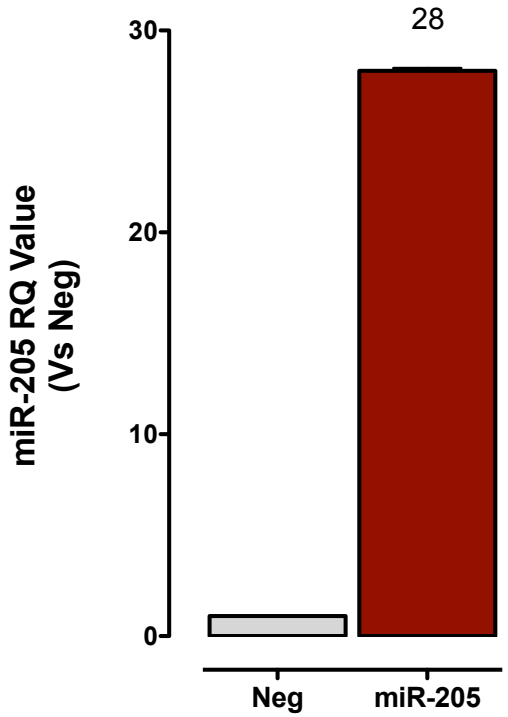

Figure 6.5 miR-205 was upregulated in a DU145 clone stably expressing the miRNA. Expression of miR-205 assessed by qRT-PCR in DU145 cells stably transfected with a vector encoding miR-205 compared to negative control cells with empty vector. Data are reported as relative quantity (RQ) ± SD with respect to Neg cells.

To assess whether the clone stably expressing miR-205 displays a higher sensitivity to radiation treatment than control clone as observed for transient transfected cells, we exposed clones to increasing doses of radiation (from 2 to 8 Gy) and evaluated their clonogenic ability. Interestingly, the stable expression of miR-205 was still able to influence cell sensitivity to radiation, as demonstrated by the decreased clonogenic cell survival (Fig. 6.6).

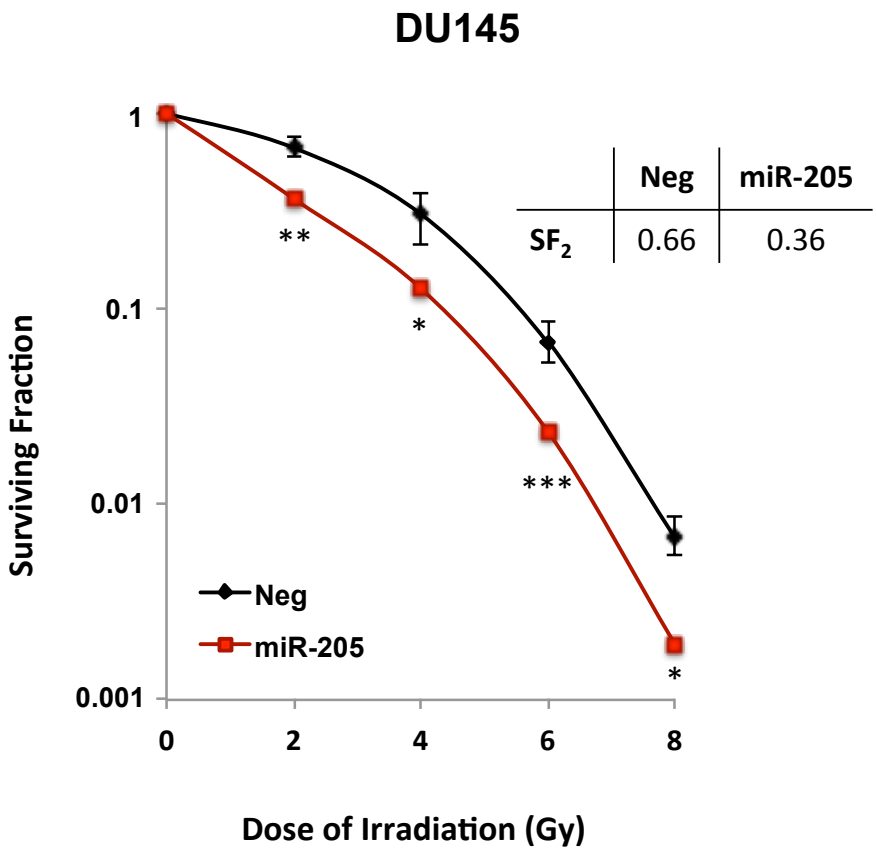

Figure 6.6 miR-205 stably expression enhanced DU145 cell sensitivity to radiation. Clonogenic cell survival of DU145 stably transfected with miR-205- or Neg-vector, exposed to increasing doses of γ-irradiation (2, 4, 6 and 8 Gy). The surviving fraction is reported as mean±SD, n=3.

Once the suitability of the cell model for *in vivo* experiment was verified, the DU145 clone stably expressing miR-205 and the respective negative control were injected into the right flank of SCID mice, and let to engraft and grow thus leading to the onset of subcutaneous PCa tumours. Tumour growth was monitored to determine when to administer radiation treatment. Noteworthy, a delay in tumour growth was observed in miR-205 xenografts compared to matched negative controls, indicating that the miRNA was *per se* able to impact on tumour growth, unlike what observed *in vitro*. Despite what it might seem, this finding is not that surprising in light of miR-205 known role in PCa. As anticipated, miR-205 is well known to play a relevant role in PCa tumourigenesis, with particular reference to EMT impairment. Although EMT final outcome is mainly appreciable in terms of tumour migration and invasion potential, it should be taken into account that preliminary transition steps occur within the tumour, manifesting in different tumour behaviour changes, conceivably also influencing tumour growth rate. Moreover, despite the established role of miR-205 in EMT/migration/invasion, and considering that a miRNA modulates multiple target processes, we can not exclude that miR-205 is implicated in other mechanisms that take place only in the complex tumour context (such as interaction with the microenvironment) and that are not perceivable in the *in vitro* settings, thus manifesting only *in vivo*.

As a result, it is not that unexpected that miR-205 exerts an effect on in vivo tumour growth, yet not displaying a cytotoxic effect in *in vitro* settings.

For this reason we decided to deliver radiation treatment when tumours reached a comparable volume (~150 mm^3), without waiting them to reach a pre-established volume (generally ~300 mm^3) in order to avoid to administer treatment on different starting points.

Mice were exposed to 5 Gy single dose of irradiation by conformational radiotherapy. Tumour volumes were determined at fixed intervals by direct measurement with a Vernier caliper. In consonance with what observed before starting the treatment, xenografts deriving from DU145 clone expressing miR-205 showed tumour growth delay, thus confirming that miR-205 exerts toxic effects on tumours. However, upon radiation, miR-205 xenografts showed a markedly increased sensitivity to the treatment, suggesting that, despite its *in vivo* toxicity, miR-205 is still able to act as a radiosensitizer. (Fig. 6.7).

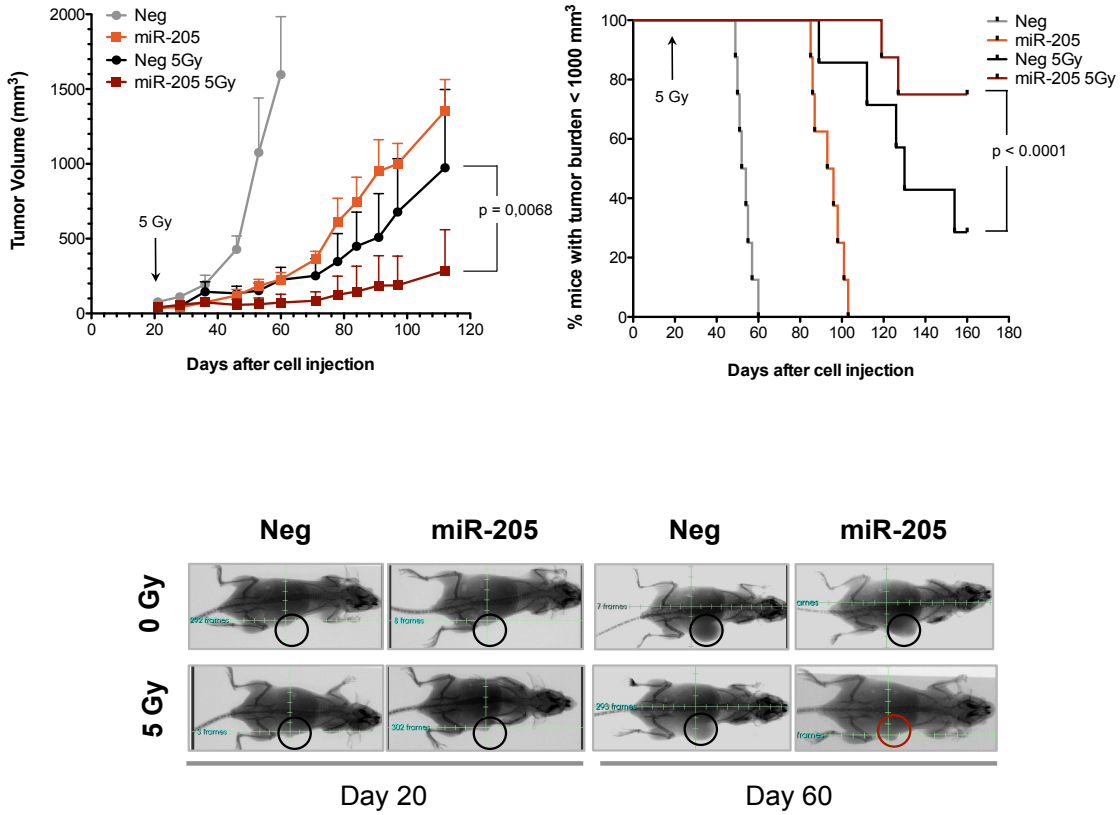

Figure 6.7 miR-205 significantly enhanced tumour growth delay induced by irradiation. DU145 cells stably transfected with miR-205 or Neg empty vector were implanted subcutaneously into the right flank of SCID mice. When tumours reached similar volumes (~150 mm3), mice were randomly separated into four groups (8 mice/group) and were treated with 5 Gy single dose irradiation locally delivered to the tumour area. (*Upper panel*) Tumour growth volume (mm3) measured with a Vernier caliper on indicated days after cell injection and Kaplan-Meier plot of mouse tumor growth to 1000 mm3. (*Lower panel*) Representative X-ray images of the subcutaneous tumour masses at the day of radiation treatment and after 40 days.

6.2 miR-205 mediated radiosensitivity: role of putative targets

6.2.1 miR-205 targets genes related to autophagy and EMT

miR-205 was demonstrated to enhance PCa sensitivity to radiation both *in vitro* and *in vivo*. According to literature data and to the results obtained in our previous studies, miR-205 is known to regulate pathways associated to radiation response, including autophagy and EMT. miR-205 involvement in autophagy is supported by miRNA ability to target RAB27A and LAMP3. As for EMT, miR-205 is largely implicated in regulating this process by targeting important EMT-related genes, such as ZEB1 and PKC-ε. To understand which of these targets is actually responsible of mediating miR-205-induced radiosensitization, we sought to perform a phenocopy experiment, by silencing those targets and finding out with which we are able to resemble miR-205 phenotype.

Specifically, we transfected DU145 cells with specific siRNA molecules against each of the putative mediators (RAB27A, LAMP3, ZEB1 and PKC-ε). Cells transfected with each siRNA or miR-205 were then exposed to 2 Gy of irradiation in order to calculate the surviving fraction (SF_2), and evaluate target-silencing effect of DU145 sensitivity profile (Fig. 6.8).

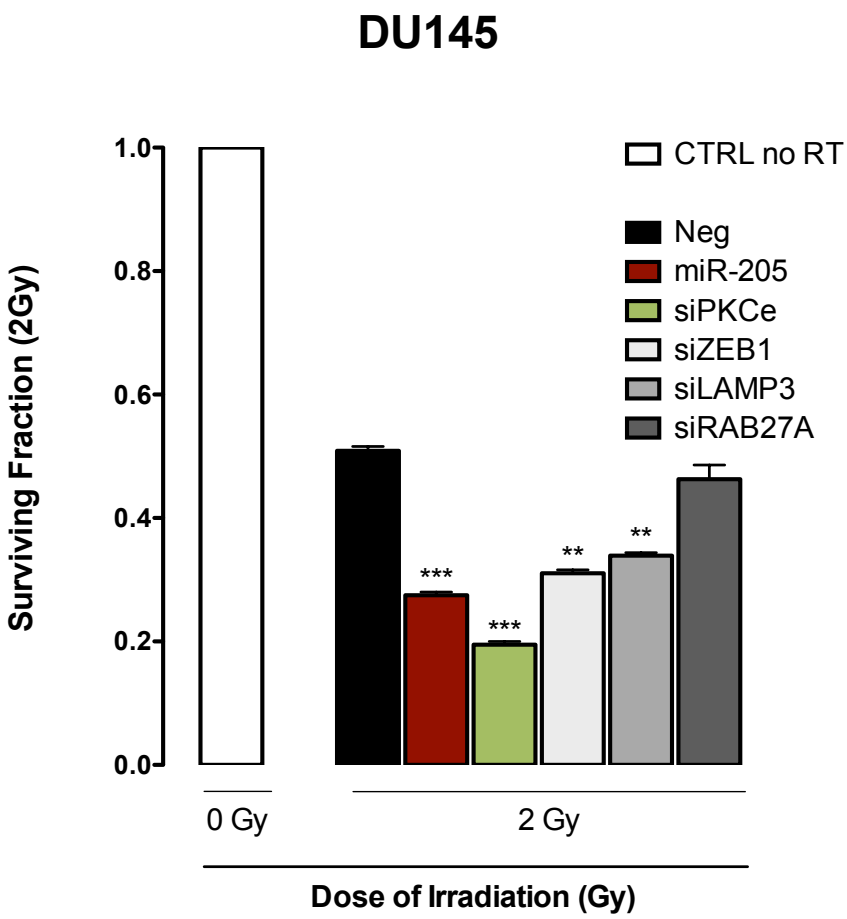

Figure 6.8 siPKC-ε enhanced DU145 radiosensitivity. Clonogenic cell survival of DU145 transfected with miR-205- or siRNA molecules against PKC-ε, ZEB1, LAMP3, and RAB27a, and exposed to 2 Gy of γ-irradiation. The surviving fraction is reported as mean±SD, n=3.

Silencing of PKC-ε, ZEB1 and LAMP3 showed a significant decrease of clonogenic cell survival at 2 Gy of irradiation, thus substantiating their putative role in influencing radiation response. However, PKC-ε silencing showed the greatest effect on radiation sensitivity, thus indicating that it could be the main mediator of miRNA-induced radiosensitization.

On these grounds, we focused our attention on PKCε to better uncover its role in miR-205-induced sensitization.

6.2.2 PKC-ε is downregulated by miR-205

To characterize PKC-ε role in mediating the radiosensitizing effect induced by miR-205, we first evaluated miRNA capacity to downregulate its target in PCa cells. For this purpose, PKC-ε expression levels were assessed upon miR-205 transfection, at both transcript and protein levels. Compatible with being miR-205 target, PKC-ε transcript was found to be significantly downregulated after 48 h from miRNA transfection (Fig. 6.9).

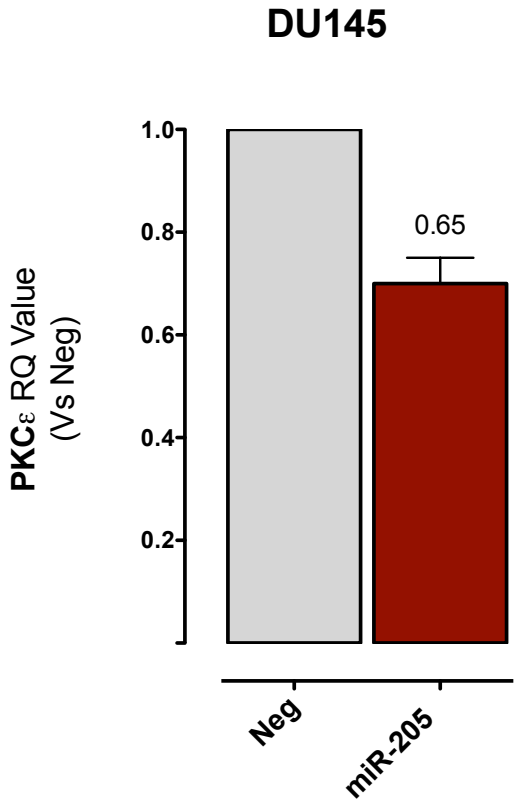

Figure 6.9 PKC-ε transcript is downregulated by miR-205. Expression levels assessed by qRT-PCR in DU145 cells transfected with miR-205 compared to negative control cells. Data are reported as relative quantity (RQ) ± SD with respect to Neg cells.

Considering that PKC-ε potential relevance in mediating miR-205 radiosensitizing effect relies on protein function implicated in EGFR nuclear translocation, to assess whether the miRNA leads to the downregulation of its protein levels is instrumental. To this aim, protein levels of PKC-ε upon transfection were assessed by western blotting analysis, revealing that actually the target is significantly downregulated at the protein level and that miR-205 mediates a functional downregulation of the target (Fig. 6.10).

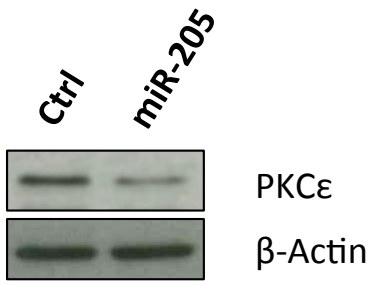

Figure 6.10 miR-205 reconstitution decreased PKC-ε protein levels. Western blot analysis showing PKC-ε protein levels upon miR-205 reconstitution in DU145 cells. Cropped images of selected proteins are shown.

Once the downregulation of PKC-ε in PCa cells has been demonstrated, we moved to further explore its ability in mediating miR-205 radiosensitizing effect, in order to implement the previous exploratory clonogenic assay.

6.2.3 PKC-ε mediates miR-205 induced radiosensitization

A previous clonogenic assay upon 2 Gy of irradiation was performed with the aim to single out the target that better recapitulates miR-205 induced radiosensitization. To confirm that PKC-ε silencing actually enhances PCa sensitivity to radiation, we performed an extended clonogenic assay by exposing cells to increasing doses of irradiation, up to 8 Gy. As previously suggested by the evaluation of SF_2, siPKC-ε was able to completely reproduce the radiosensitizing effect of miR-205, thus supporting our hypothesis that PKC-ε could be the main mediator of miRNA effect (Fig. 6.11).

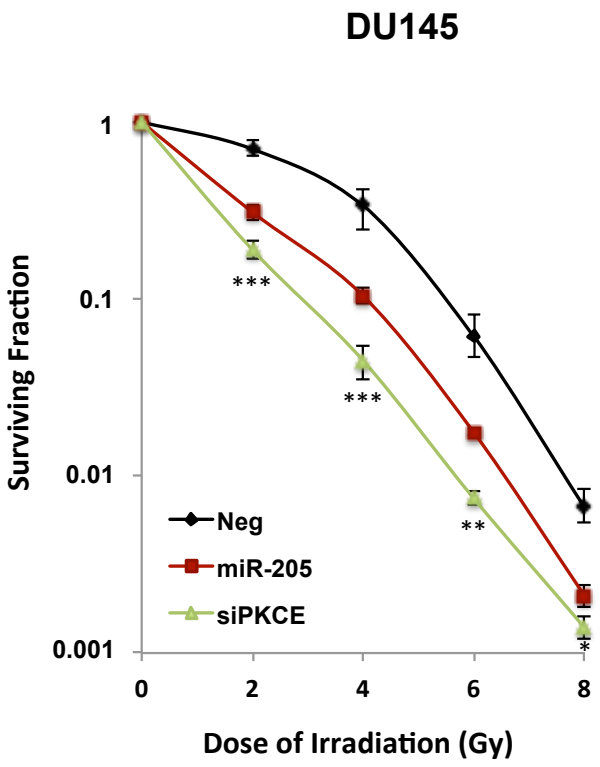

Figure 6.11 siPKC-ε recapitulated miR-205 radiosensitizing effect. Clonogenic cell survival of DU145 cells transfected with miR-205 or siPKC-ε. The surviving fractions following the indicated doses of γ-irradition are reported as mean±SD, n=3.

To verify that the silencing obtained by the use of the siRNA molecule is not far greater than that induced by the miRNA, and also to test siRNA ability to efficiently silence the target, we evaluated PKC-ε expression levels upon miR-205 and siRNA transfection. Interestingly, the downregulation levels induced by the two molecules were almost identical (RQ=0.65 Vs RQ=0.60), thus indicating that the siRNA and the miRNA were able to downregulate the target to a similar degree (Fig. 6.12).

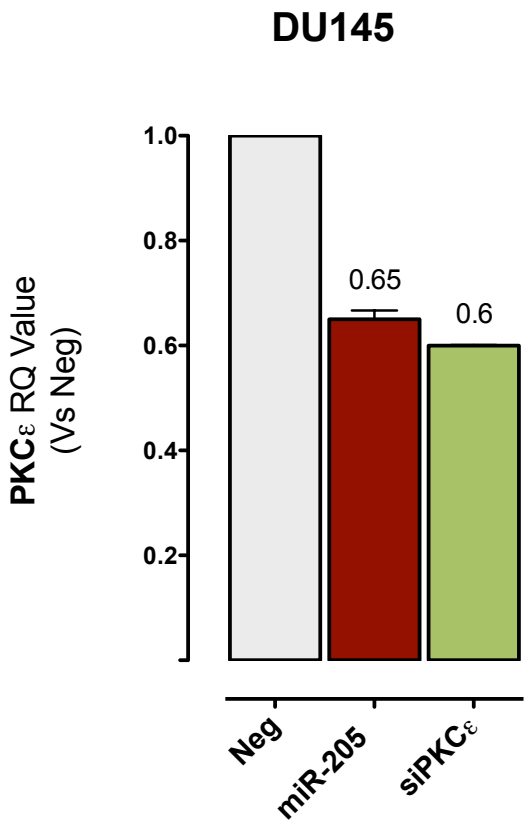

Figure 6.12 PKC-ε downregulation upon transfection with miR-205 or siPKC-ε. Expression levels assessed by qRT-PCR in DU145 cells transfected with miR-205 or siRNA compared to negative control cells. Data are reported as relative quantity (RQ) ± SD with respect to Neg cells

The evidence that PKC-ε silencing leads to a radiosensitization that is comparable to that induced by miR-205 does not *per se* demonstrate that PKC-ε is actually responsible of such radiosensitizing effect. The most specific way to ascertain PKC-ε implication is target protection experiment.

To this aim, we designed a miR-Mask molecule fully complementary to miR-205 binding site within PKC-ε 3'UTR, able to protect the site from miRNA binding. First of all, we tested whether the designed miR-Mask was actually able to prevent miRNA-mRNA interaction, by evaluating PKC-ε expression levels upon co-transfection with both miR-205 and miR-Mask molecules. We found that the miR-Mask was able to significantly recover PKC-ε expression at both mRNA and protein level in miR-205-reconstituted cells (Fig. 6.13). This result gave us the proof of miR-Mask ability to protect PKC-ε from miRNA targeting and consequent downregulation.

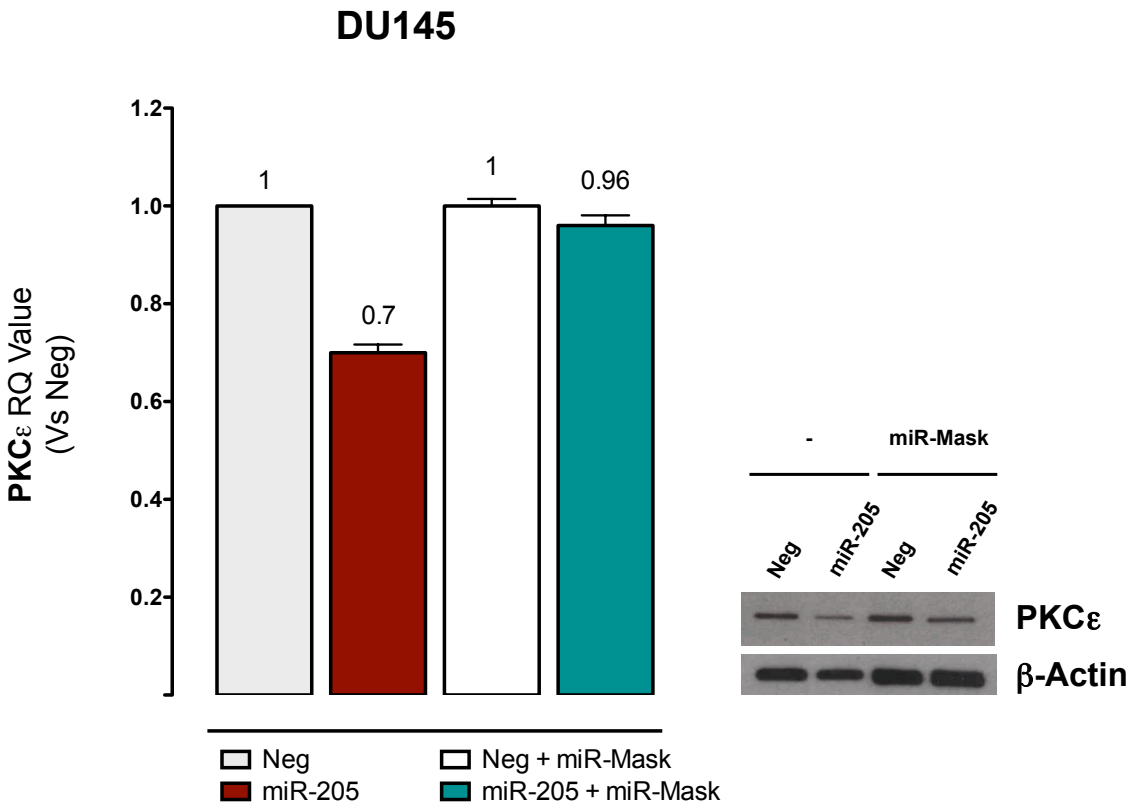

Figure 6.13 PKC-ε miR-Mask recovered PKC-ε expression levels in miR-205 cells. (*Left panel*) qRT-PCR showing PKC-ε mRNA amount in DU145 cells after miR-205 reconstitution in the presence or absence of miR-Mask, normalized to GAPDH. Data are reported as relative quantity (RQ) ± SD with respect to Neg cells. (*Right panel*) Western blot analysis showing PKC-ε protein amount in DU145 cells upon Neg or miR-205 transfection, in presence or absence of PKC-ε miR-Mask, normalized to β-actin. Cropped images of selected proteins are shown.

To investigate whether PKC-ε is the main mediator in determining the radiosensitizing effect induced by miR-205, we transfected miRNA-reconstituted DU145 cells with the miR-Mask, with the aim of testing whether the abrogation of PKC-ε downregulation influences miR-205-induced radiosensitization. Strikingly, we found that the miR-Mask molecule was able to almost completely abrogate the radiosensitizing effect induced by miRNA reconstitution (Fig. 6.14). This result indicates that, upon PKC-ε recovering, miR-205 is no longer able to boost cell response, suggesting that the downregulation of PKC-ε is actually essential for determining miR-205 radiosensitization.

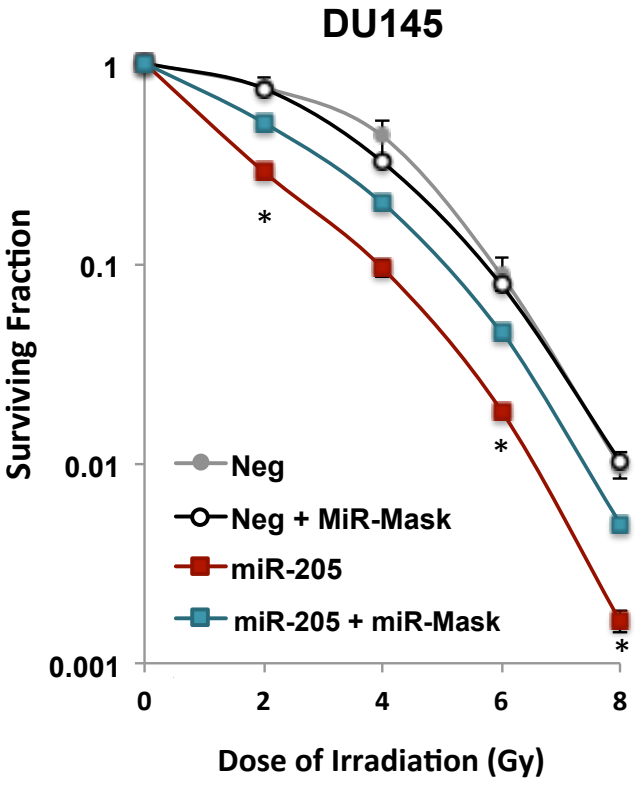

Figure 6.14 PKC-ε contributes to mediate miR-205-induced radiosensitization. Clonogenic cell survival of DU145 cells transfected with miR-205 alone or co-transfection with miR-Mask. The surviving fractions following the indicated doses of radiation are reported as mean±SD, n=3. The level of significance was represented as *p<0.05, Student's t-test.

6.2.4 miR-205 reduces DNA-PK activation via PKC-ε downregulation

As previously reported, PKC-ε role in radiation response relies on its ability to phosphorylate EGFR in the tyrosine residue T654. Consequent to phosphorylation, EGFR is internalized into the nucleus where it binds and activates DNA-PK, thus leading to NHEJ DNA-repair mechanism. The activation of DNA-PK occurs by phosphorylation of a specific residue (S2056), which is therefore considered an indicator of DNA-PK active status. To assess whether PKC-ε implication in miR-205-induced radiosensitization relies on EGFR nuclear translocation and consequent DNA-PK activation [170], we evaluated i) phospho-EGFR (pEGFR) levels with the purpose to monitor whether, following irradiation, PKC-ε promotes its phosphorylation and ii) DNA-PK specific phosphorylation to investigate whether PKC-ε downregulation leads to a decreased activation of DNA-PK.

To address these aims, we first assessed EGFR specific phosphorylation (T654) in siPKC-ε cells upon 30 or 60 minutes of 4 Gy irradiation. In keeping with the premise that EGFR is known to be specifically phosphorylated by PKC-ε upon radiation exposure, we observed that pEGFR levels increased at 60 minutes from irradiation, with total EGFR levels being equal. Interestingly, such increase was abrogated upon PKC-ε silencing, thus suggesting that EGFR phosphorylation relies, at least in part, on PKC-ε activity (Fig. 6.15, *upper panel*). This was paralleled by a slightly reduced activation of DNA-PK, as detected by the lower expression levels of the phosphorylated form of the enzyme at S2056 (DNA-PK2056) observed following irradiation of PKC-ε-silenced compared to control cells (Fig. 6.15, *lower panel*).

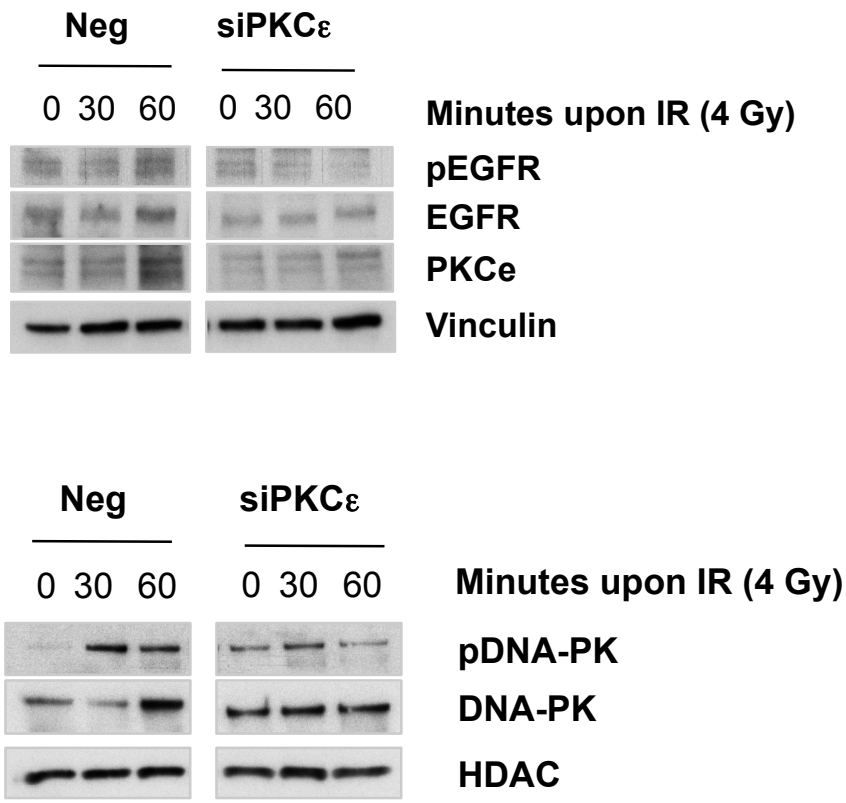

Figure 6.15 EGFR and DNA-PK phosphorylation is reduced by PKC-ε silencing. Western blot analysis showing EGFR (*upper panel*, total protein extract) and DNA-PK *(lower panel*, nuclear fractionation) phosphorylated levels in DU145 cells transfected with Neg or miR-205. Forty-eight hours after transfection, cells were irradiated at 4 Gy and harvested 30 and 60 minutes later for Western blot assay. Vinculin and HDAC were used as control for loading. Cropped images of selected proteins are shown.

DISCUSSION

7. CONCLUSIONS AND DISCUSSION

7.1 miRNAs modulated in PCa cells upon radiotherapy

7.1.1 Photon irradiation

Radiotherapy is one of the gold standard treatments for organ-confined and locally advanced PCa [171]. In the last decades, several advancements have been made in both treatment planning and delivery, specifically with the introduction of 3D-conformal radiation therapy (CRT) and the intensity modulated radiation therapy (IMRT). However, development of radioresistance significantly limits treatment effectiveness and a fraction of patients, approximately 30%, still experience biochemical failure [172].

One promising approach to improve the likelihood of durable tumour control is to combine radiotherapy with targeted agents able to interfere with molecular pathways relevant to radiation response, thus ultimately resulting in an enhanced sensitivity to the treatment [91].

Various genetic and epigenetic alterations have been associated with the onset of radioresistance, including deregulation of miRNAs, small endogenous RNA molecules endowed with regulatory functions. This ability of miRNAs to act as negative gene regulators allow them to modulate signalling pathways that control multiple cellular processes [34], including those involved in response to radiation [34]. In keeping with this, results from experimental models of different

human tumour types showed that miRNAs directly affect radiosensitivity [92]. Consequently, they have the potential to be used as radiosensitizers.

The aim of this project was to identify specific miRNAs, if any, functionally involved in influencing PCa response to radiation, with the final goal of characterizing them as promising radiosensitizing molecules to be exploited for the design of miRNA-based approaches aimed at increasing radiotherapy effectiveness.

As a very first step, we established the strategy to pursue in order to pick-up all the miRNAs potentially matching our query. We therefore proposed to follow two complementary approaches of miRNA sorting. The first approach consisted of the identification of miRNAs modulated upon radiation exposure, since modulation after the radiation stimulus can likelihood reflect an involvement in radiation response processes.

However, it is worth mentioning that the modulation upon treatment does not intrinsically and definitely reflect a functional involvement in influencing the response to radiation, as it is conceivable that treated cells undergo molecular changes, as a mere consequence of the induced-injury, that are not all actively influencing the final outcome in terms of treatment response. Hence, among all miRNAs found to be modulated upon radiation, we focused on those that are known, by literature data as well as prediction analysis, to target genes implicated in pathways relevant to radiation. This criterion was instrumental for increasing the reliability of our selection approach, as miRNAs regulating this kind of pathways are more likely to be endowed with a functional role in the response phase. Moreover, to characterize selected modulated miRNAs from a functional perspective, their expression has been artificially modulated through transfection of PCa cells with specific miRNA modulators (i.e.: miRNA mimics).

Transfected cells were then exposed to radiation and assessed for changes in their sensitivity profile. Finally, to dissect the underlying mechanisms, miRNAs showing ability in enhancing cell response to radiation were studied from a mechanistic point of view, by the identification of their targets relevant to radiation.

By following this first approach, we exposed all the four PCa cell lines (DU145, PC-3, LNCaP and 22RV1) to 10 Gy of irradiation, and collected total RNA, including miRNAs, at different time points (4, 8 and 24 h), in order to obtain a kinetics of miRNome modulation. As a result of miRNA profiling, we observed that several miRNAs showed significant changes in their expression in all cell lines, even if different miRNA were modulated at different extents across cell lines and over time. Therefore, to select specific miRNAs that could be reliably relevant, we focused on miRNAs consistently modulated (up or down) by photon irradiation in both DU145 and LNCaP cells, the two cell lines that showed a higher number of consistently modulated miRNAs (Figg. 4.1 and 4.5). As a result, we obtained a list of 9 up-regulated and 15 down-regulated miRNAs (Table 4.1 and Fig. 4.6). Among downregulated ones, we focused on miR-23a-3p and miR-24-3p, since, according to literature data, they are known to be associated with radiation-response related pathways. Specifically, miR-23a-3p was reported to negatively regulate the IL-6 pathway, by downregulation of IL-6 receptor (IL-6R) in PCa [158]. The relevance of this finding is based on the evidence that the IL-6 pathway was reported to be associated with radioresistance in PCa [156]. In this study, Wu and collaborators demonstrated that IL-6 is important in the biological sequelae following irradiation, since i) IL-6 expression was found to be positively linked to radiation resistance and, conversely, ii) IL-6 inhibition enhanced the radiation sensitivity of prostate

cancer. In accordance with this evidence, we observed that reconstitution of miR-23a-3p in PCa cells led to a significant downregulation of various components of IL-6 pathway, including IL-6 (Fig. 4.10). This result prompted us to further investigate whether the interleukin itself, and not only its receptor, could be a direct target of the miRNA. According to initial assessments, IL-6 was not included in the list of miR-23a-3p predicted targets. However, extending the analysis to genes with a poorly conserved site, IL-6 emerged as a predicted target of the miRNA, presenting a 7mer site for miRNA recognition in its 3' UTR region. Encouraged by these findings, we pursued the investigation of miR-23a-3p as a potential radiosensitizer in PCa. Interestingly, miR-23a-3p reconstitution was able to significantly enhance DU145 sensitivity to radiation, showing a radiosensitizing effect that was not biased by an intrinsic cytotoxic effect of the miRNA (Fig. 4.8, *left panel* and Fig. 4.9, *upper panel*). To substantiate the hypothesis that miR-23a-3p induced radiosensitization was actually imputable to IL-6 downregulation, we counteracted IL-6 modulation caused by the miRNA, through ectopic supplementation of interleukin with a recombinant IL-6 molecule. Indeed, the restoration of IL-6 levels endorsed by supplementation, almost completely abrogated the radiosensitizing effect assigned to the miRNA (Fig. 4.11), thus persuasively supporting a central role of IL-6 in mediating miR-23a-3p radiosensitizing effect.

Along with miR-23a-3p, miR-24-3p was also picked-up as a possible radiosensitizer miRNA in PCa. The potential relevance of miR-24-3p was based on the evidence that this miRNA was reported to be upregulated as a consequence of IL-6 downregulation in plasma cells [155], thus suggesting that it could be somehow influenced by miR-23a-3p-IL-6 axis. Accordingly, miR-24-3p expression levels were expected to be consistent with those of miR-23a-3p,

thus being both concomitantly down-regulated upon irradiation. Indeed, both miRNAs were in the list of down-regulated ones among those considered. Moreover, when miR-23a-3p was reconstituted, miR-24-3p levels were increased (data not shown), further supporting a correlation between the two miRNAs. Based on this evidence, we assessed miR-24-3p ability to actively influence PCa sensitivity profile, and observed that miRNA reconstitution significantly enhanced DU145 cell response to radiation. However, unlike what observed with miR-23a-3p, miR-24-3p displayed an intrinsic cytotoxic effect as suggested by the impact on plating efficiency (Fig.4.9). On account of this evidence, we decided not to pursue the study of miR-24-3p, since an ideal sensitizer should exert an effect only when combined with the treatment intended to be enhanced. Noteworthy, miR-23a-3p and miR-24-3p belong to the same miRNA cluster, namely miR-23a~27a~24-2 cluster, therefore being the regulation of their expression subjected to the control of the same promoter. This information could further substantiate the relevance of miR-23a-3p and miR-24-3p in the response of radiation, as they are included in the same primary transcript, which allows the concomitant modulation of both miRNAs upon the same stimulus, with their interdependent regulation suggesting that they might work in combination to accomplish their function in response to radiation exposure [173].

Overall, by following the first strategy of miRNA identification we could single-out miR-23a-3p as a potential radiosensitizer in PCa.

7.1.2 Carbon ion irradiation

Conventional radiation therapy, either alone or combined with surgery, can produce enduring loco-regional disease control in a wide variety of cancers. The chance of tumour eradication with radiation depends on various factors related to the tumour, such as radiosensitivity, volume and location, as well as factors related to the irradiation modality, such as the treatment plan and targeting accuracy. Intuitively, the higher is the dose delivered to the tumour, the better is the local control and the related disease-free survival [174]. However, a balance should be maintained to ensure that the radiation tolerance of adjacent normal tissues is not exceeded.

Impressive developments have been achieved through the introduction of CRT and IMRT, thus ameliorating treatment planning and delivery. The adoption of these techniques ultimately allowed the delivering of higher doses of photon radiation to a more precisely defined target volume, while leaving adjacent normal tissues and organs relatively unscathed [174]. However, despite these improvements, because of the intrinsic physics of photon beams, the treatment doses are still maintained at sub-optimal levels, in order to counterbalance the benefit and the harm of the treatment, thus limiting the potential of radiation-associated benefits. To address these limits that constraint the application of radiotherapy, a novel radio-therapeutic approach based on heavy charged particles has emerged. These particles have physical and radiobiological characteristics differing from those of photon beams, which offer a number of advantages over conventional radiotherapy [20]. Specifically, protons and carbon ions interact more readily with matter allowing well-defined distribution of

the dose in depth, depositing a large fraction of their energy at the end of their track, resulting in intense local ionisation that is considered highly effective against radiation-resistant tumours [175].

Taking advantage of an established collaboration with the National Centre for Oncological Hadrontherapy (CNAO), equipped with a synchrotron able to produce and deliver protons and carbon ions, we had the opportunity to perform an exploratory experiment aimed at investigating carbon ion capacity to influence PCa miRNome, a study never pursued before. In particular, we sought to compare miRNA modulation induced by carbon ions with that obtained upon photon irradiation, in order to unravel commonalities and differences between the two sources. To that aim, comparable treatment settings were maintained between the two modalities of irradiation, for both time points of RNA collection and dose delivery, taking into account the definition of RBE, based on the knowledge that different radiation sources need different doses to reach the same extent of a certain biological effect [20]. Hence, considering that DU145 and LNCaP were the two cell lines with the major number of consistently modulateted miRNAs, and also due to the high costs of carbon ion experiments, we evaluated miRNA modulation only in these two cell lines. Despite expectations, we found that only 14 miRNAs were modulated by both photon and carbon ion irradiation (Fig. 4.13). Moreover, all of these miRNAs displayed opposite direction of modulation, meaning that those found to be downregulated by photons were upregulated by carbon ions, and *vice versa*. This curious result can be justified by the notion that the two sources of irradiation have different impact on cells, being the ionization of carbon ions more intense than that produced by photons. Hence, it is reasonable that, still inducing the same type of DNA damage (i.e.: predominantly DSBs), the two

sources trigger diverse mechanisms of cell response, thus implying the modulation of different miRNAs. In keeping with this hypothesis is our finding that different pathways were found to be associated with miRNAs modulated by carbon ions compared to those linked to photons (Fig. 4.15). Moreover, it is also conceivable that a distinct kinetics in inducing DNA damage is associated with the two irradiation sources. In particular, it is likely that carbon ions do exert a certain effect in a shorter period of time than what took to photons, implying that at the same time point, different steps of repair mechanisms are occurring, which is paralleled by different patterns of miRNA modulation. This consideration entails that, as well as for doses, different time points should be considered in order to carry out comparative analysis between photons to carbon ions. To that aim, it would be informative to stretch and extend the timing of RNA collection following exposure to both sources, in order to investigate whether the same pathways, and then likely the same miRNAs, are modulated by both treatments at different time points. So far, because of the limited accessibility to the synchrotron, and due to the unaffordable costs related to the use of the accelerator, we had not the possibility to test these hypotheses in the context of this project.

7.2 The role of miR-875-5p and miR-205 in PCa radiation response

As anticipated, two different approaches were followed for the identification of miRNAs potentially involved in determining PCa response to radiation. In the framework of the first approach of miRNA sorting, we considered those miRNAs that i) are downregulated in PCa compared to normal tissues, thus suggesting an oncosuppressive role of the miRNA, and ii) target genes known to be involved in pathway relevant to radiation.

The first criterion of selection is based on the assumption that tumour cells reasonably downregulate molecules endowed with an oncosuppressive function, in order to promote and sustain tumour progression. In line with this scenario, a miRNA able to confer resistance to conventional treatments, including radiotherapy, is expected to be down-modulated in tumour tissues compared to normal ones, thus prompting to consider the downregulation as a reliable selection criterion. However, this feature is not enough to conclude that the downregulated miRNA is actually involved in mechanisms relevant to radiation response. To ascertain this link, among downregulated miRNAs we focused on those targeting genes belonging to pathways linked to radiation response, as a proof of their engagement in such processes. By combining these two criteria, we were able to pick-up two miRNAs: miR-875-5p and miR-205.

7.2.1. miR-875-5p

No information was available on miR-875-5p function in cancer when we pursued the present study. However, the potential relevance of this miRNA was supported, first of all, by the evidence that miR-875-5p was found to be downregulated in PCa cell lines (Fig. 5.1) and tissues (Table 5.1) compared to non-neoplastic tissues, thus accomplishing the first criterion of selection. Moreover, as obtained by correlation analysis carried out in a previous study, miR-875-5p was the first miRNA in the list of 18 miRNAs directly correlated with E-Cadherin, an epithelial biomarker of the mesenchymal-to-epithelial transition (Table 5.1). Such correlation was instrumental for taking into consideration miR-875-5p as a potential radiosensitizer in PCa, since it was reported that EMT is associated with radioresistance [176]. Moreover, we were encouraged to consider the correlation with E-Cadherin as a suggestion of a possible involvement in radiation response also based on our previous observation of a direct correlation between E-Cadherin mRNA levels and miR-205, a miRNA that we demonstrated to exert a prominent role in repressing EMT in PCa cells [81] and that was successively found to act as a tumour radiosensitizer in other tumour types [113].

On this basis, we investigated the biological impact of miR-875-5p reconstitution in PCa cell lines by transfecting cells with miR-875-5p mimic. miR-875-5p was able to revert EMT in DU145 cells, promoting a more epithelial-like phenotpye (Fig. 5.2). Moreover, an increased E-cadherin and β-catenin expression, at both mRNA and protein levels (Fig. 5.3), was observed in miR-875-5p-reconstituted cells, which were also characterized by intense immunoreactivity

for both markers and enhanced co-localization at cell-cell adhesions compared to control cells (Fig.5.4). Altogether, these changes are compatible with a shift from a mesenchymal to a more epithelial and less motile phenotype, consistent with the results of wound healing assay (Fig. 5.5), indicating the capability of miR-875-5p to revert EMT of PCa cells.

Once the ability of miR-875-5p to counteract EMT was ascertained, we tested miRNA impact on PCa cell sensitivity profile. In line with the solid premises that led us to focus on miR-875-5p, miRNA reconstitution resulted in an enhanced radiation response in both *in vitro* and *in vivo* PCa models (Figg. 5.6 and 5.10), thus supporting the role of miR-875-5p as a radiosensitizer molecule in PCa.

miRNAs are able to impact on cell mechanisms by post-transcriptionally regulating the expression of specific genes that, in turn, are involved in such mechanisms. To explore the molecular mechanism underlying miR-875-5p radiosensitization, we tried to figure out its relevant targets, by intersecting i) genes found to be downregulated in miR-875-5p-reconstitute PCa cells and ii) genes predicted to be targeted by the miRNA. As a result, we obtained a list of 19 genes, among which was EGFR (Table 5.2). Luciferase assay (Fig. 5.13) and expression analysis (Fig. 5.14) confirmed EGFR as a direct target of miR-875-5p. Strikingly, a very recent publication by Zhang and collaborators [176] reported that miR-875-5p is remarkably decreased in human colorectal cancers and that its ectopic expression inhibits growth and promotes apoptosis in colorectal cancer cell lines via downregulation of EGFR, which, in line with our observation, was also validated as a direct target of the miRNA. Conversely to what observed in colorectal cancer cells, we found that miR-875-5p *per se* failed to affect PCa cell growth as a consequence of EGFR downregulation, thus corroborating the notion that the receptor tyrosine kinase is not a central

player in the onset of PCa and that the specific function of a given miRNA needs to be contextualized with respect to the disease.

EGFR is one of the major players in determining radiation response in different tumour types [177,178], although the precise underlying mechanisms are still not fully understood. Most of the earlier studies linking EGFR and radioresistance focused on the prosurvival signaling induced by EGFR after ligand-independent activation in response to irradiation [179]. However, recent literature suggests that, following irradiation, EGFR translocates to the nucleus, where it directly contributes to the development of radioresistance by increasing DNA repair through the activation of DNA-PK, which is a regulator of NHEJ [160,170,180].

Given such established role of EGFR in inducing radioresistance by activating DNA-PK-mediated DNA repair, we investigated whether miR-875-5p was able to interfere with such cascade via EGFR downregulation. Indeed, once validated EGFR as a direct target of miR-875-5p, we demonstrated that protecting EGFR from miRNA binding, and therefore from the consequent downregulation, the radiosensitizing effect associated with miR-875-5p was almost completely voided, thus ultimately providing a convincing evidence of EGFR relevance in mediating miR-875-5p radiosensitizing effect in PCa. However, investigating the most common mechanism underlying EGFR involvement in radiation response, we found out that DNA-PK activation upon miR-875-5p-induced EGFR downregulation was walmost neglectible, thus prompting us to suppose that other downstream molecules were presumably involved. In keeping with this, a possible role of EGFR in homologous recombination (HR) repair can be also hypothesized, based on the evidence that the EGFR inhibitor gefitinib was able to radiosensitize non small cell lung

cancer cells through inhibition of radiation-induced ATM activation, although the possibility that such an effect relies on gefitinib targets other than EGFR cannot be excluded [160]. In this study, we found that, in spite of the marked reduction of nuclear EGFR levels following irradiation in miR-875-5p reconstituted PCa cells, a very modest inhibitory effect on ATM activation, as determined by the expression of active, phosphorylated forms of the proteins, was observed.

EMT was reported to be related to radioresistance in many cancers [159] and wealth of literature suggests a role of EGFR in this process [177,180]. As a consequence, the ability of miR-875-5p-mediated EGFR down-regulation to counteract EMT in PCa cells appears to significantly contribute to the observed radiosensitizing effect. In addition, inhibition of the EMT inducer ZEB1 may be a primary underlying mechanism for miR-875-5p-induced radio- sensitization, as demonstrated by the phenocopy experiment where siRNA-mediated ZEB1 silencing recapitulated the miRNA effect on radiation response (Fig. 5.23). Indeed, it has been previously shown that ZEB1 promotes HR repair and tumour radioresistance [166]. Specifically, it was found that, following irradiation, ATM phosphorylates and stabilizes ZEB1. ZEB1, in turn, directly interacts with the deubiquitinase USP7 and enhances its ability to deubiquitinate and stabilize CHK1, thereby promoting HR-dependent DNA repair [166]. Consistent with this pathway, we found that miR-875-5p-induced radiosensitization was paralleled by a decreased CHK1 expression (Fig. 5.21). However, the small impact of miRNA reconstitution on ATM activation we observed in PCa cells (Fig 5.20) would suggest that such ZEB1 down-regulation does not rely on ATM but is, at least in part, dependent on EGFR knock-down, as indicated by the recovery of ZEB1 expression observed when cells where transfected with a miRNA mask specifically blocking the interaction between

miR-875-5p and EGFR mRNA (Fig. 5.18). In keeping with this are previous data indicating the ability of EGFR inhibitors to suppress ZEB1 expression [164,165]. Interestingly, it has recently been reported that other miRNAs able to counteract EMT, such as miR-200c [111], miR-204 [112] and miR-205 [113], act as radiosensitizers by directly targeting ZEB1. In addition, miR-205 inhibits DNA damage repair by directly targeting the ubiquitin-conjugating enzyme Ubc13 that also promotes HR-mediated repair of DNA double strand breaks [113]. Altogether these findings pose ZEB1 at the crossroad of EMT and radiation resistance and suggest that its activity can be mediated by different targets and different interacting proteins.

The relevance of EMT-related miRNAs in radiation response has been also corroborated by a recent study that analysed global miRNA expression profile in a large panel of head and neck squamous cell carcinoma cell lines showing that low expression of miRNAs involved in EMT inhibition was an important radioresistance determinant [181]. Moreover, low expression of miR-203, which emerged as the most important miRNA in cell lines, was shown to correlate with local disease recurrence after radiotherapy in laryngeal cancer patients [181].

Overall, the study on miR-875-5p role in PCa response to radiation, provided evidence that miR-875-5p acts as a promising radiosensitizer in PCa cell and animal models, by inhibiting EGFR-ZEB1 axis (Fig. 7.1).

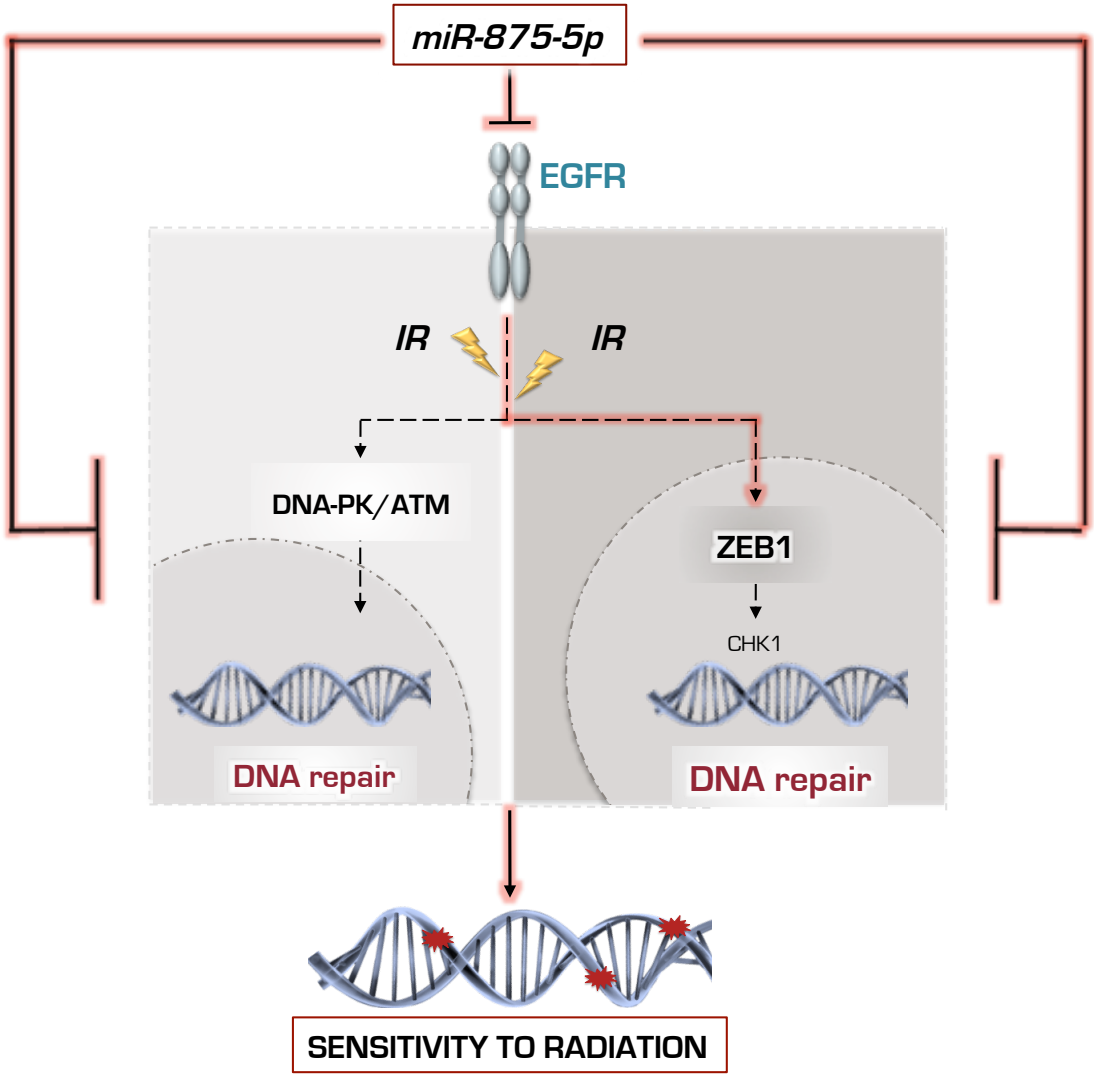

Figure 7.1 Schematic representation of miR-875-5p mechanism of radiosensitization in PCa

7.2.2. miR-205

In the framework of miRNAs sorted by following the second approach, along with miR-875-5p we singled out miR-205.

Previous studies undertaken by our group reported that miR-205 is a tumour-suppressor miRNA, the expression of which is reduced or lost in prostate tumours compared to normal tissues, with a particularly pronounced reduction in carcinomas from patients with disseminated disease. In this contest, Gandellini and collaborators demonstrated that miR-205 restoration in prostate cancer cells resulted in cell rearrangements consistent with a reversion of mesenchymal-to-epithelial transition, such as up-regulation of E-cadherin and reduction of cell locomotion and invasion [80]. Interestingly, results from this study suggested that these events were driven by the concurrent repression of specific predicted miR-205 targets, including protein kinase Cepsilon (PKC-ε). Strikingly, the latter seemed to play a direct role in regulating epithelial-to-mesenchymal transition. In fact, its down-regulation led to a cell phenotype largely reminiscent of that of cells ectopically expressing miR-205. These findings provided the first evidence supporting a role of miR-205 in counteracting PCa EMT. A role of miR-205 in regulating EMT was unravelled for the very first time by Gregory and collaborators [167]. In this study, they found that miR-205 was markedly downregulated in cells that had undergone EMT in response to transforming growth factor (TGF)-beta. Together with miR-200 family, miR-205 cooperatively regulated expression of the E-cadherin transcriptional repressors ZEB1 (also known as deltaEF1) and SIP1 (also known as ZEB2), factors previously implicated in EMT and tumour metastasis.

Inhibition of the microRNAs was sufficient to induce EMT in a process requiring upregulation of ZEB1 and/or SIP1. Conversely, ectopic expression of these microRNAs in mesenchymal cells initiated mesenchymal to epithelial transition (MET). Consistent with their role in regulating EMT, expression of these microRNAs was found to be lost in invasive breast cancer cell lines with mesenchymal phenotype.

EMT phenotypic switch is known to enhance resistance to conventional therapies, including chemo- and radiotherapy [159]. However, besides such well-known role of EMT in radioresistance, the relevance of PKC-ε in determining cell response to radiation-induced injury is also supported by the study of Wanner et al [168]. The authors demonstrated that the activation of PKC-ε stimulates DNA-repair by promoting the nuclear accumulation of EGFR. It is known that irradiation causes EGFR translocation into the nucleus, where it is involved in the activation of DNA-PK, a protein kinase essential for DNA-repair [170]. Specifically, they demonstrated that EGFR nuclear translocation is consequent to a phosphorylation in the tyrosine residue T654, which is operated by PKC-ε [168].

Moreover, as for miR-875-5p, the direct correlation of miR-205 with E-cadherin is another evidence supporting a potential role of miR-205 in radiation response via EMT-counteracting.

Furthermore, miR-205 was successively found to act as a tumour radiosensitizer in breast cancer [113]. Here the authors found that miR-205 promotes radiosensitivity and is downregulated in radioresistant subpopulations of breast cancer cells, and that loss of miR-205 is highly associated with poor distant relapse-free survival in breast cancer patients. Mechanistically, radiation

suppresses miR-205 expression through ATM and ZEB1. Moreover, miR-205 inhibits DNA damage repair by targeting ZEB1 and the ubiquitin-conjugating enzyme Ubc13. Altogether these findings demonstrate that miR-205 acts as a tumour radiosensitizer by targeting ZEB1.

Finally, the possible relevance of miR-205 in radiation response is also suggested by its role in autophagy [153]. In these regards, miR-205 was observed to induce downregulation of RAB27A, a member of RAS oncogene family, and LAMP3, the lysosomal-associated membrane protein 3. miR-205-dependent down-regulation of these lysosome-associated proteins leaded to an impairment of autophagy. Such constraints on the autophagic flux, in turn, resulted in an enhancement of cisplatin cytotoxic activity, thus ultimately indicating that miR-205 replacement sensitizes PCa cells to cisplatin treatment [153].

On this promising basis, we were strongly encouraged to pursue the investigation of miR-205 as a radiosensitizer in prostate cancer. In keeping with our hypothesis, we found that miR-205 reconstitution was actually able to significantly enhance PCa sensitivity to radiation, in both cell (Fig. 6.2) and animal models (Fig. 6.6). Compatible with its radiosensitizing ability, we observed that miR-205 was able to interfere with cell repair mechanisms aimed at resolving the injury caused by radiation exposure. Specifically, miR-205 reconstitution was found to delay γ-H2AX foci resolution, indicating an impairment of cell proficiency in repairing radiation-induced DSBs (Fig. 6.3). Accordingly, extended comet tail moments were observed in miR-205 cells compared to controls upon exposure to γ-irradiation (Fig. 6.4), thus confirming that the extent of DNA damage is increased in presence of the miRNA.

Considering that the implication of miRNAs in specific pathways relies on their capacity to regulate target genes belonging to those pathways, we sought to identify miR-205 relevant targets with the final aim to dissect the molecular mechanism underlying its radiosensitizing potential. In particular, taking into account the targets that we found in literature to be potentially relevant in supporting a postulated role of miR-205 in radiation response [81,113,153], we investigated LAMP3, RAB27A, ZEB1 and PKC-ε. After an exploratory investigation, we concluded that PKC-ε could be the target mainly responsible of miR-205 radiosensitizing effect, as its silencing via an alternative strategy (siRNA molecule) was able to successfully resemble the radiosensitizing effect associated with miR-205, supporting the hypothesis that the miRNA exerts its effect via PKC-ε downregulation. This assumption was actually substantiated and definitely corroborated when the use of a miR-Mask molecule able to specifically interfere with the interaction between miR-205 and PKC-ε resulted in a strong abrogation of miRNA radiosensitizing effect, thus demonstrating that miR-205 effect relies on its capacity to target PKC-ε.

This finding is in line with the well-established role of PKC-ε in cell mechanisms of DNA damage repair [168]. Consistent with this, we found that pEGFR, and consequently pDNA-PK, levels were significantly reduced by miR-205 reconstitution (Fig. 6.15).

miR-205 is an emblematic example of how intricate is the network of targets modulated by a single miRNA. miR-205 involvement in radiation response process was postulated starting from the evidence of miRNA engagement in a variety of related pathways, centred on diverse genes and mechanisms, including PKC-ε, autophagy, EMT and ZEB1. In this study we demonstrated that

miR-205 radiosensitized PCa via PKC-ε downregulation (Fig. 7.2), However, it cannot be excluded that other targets can contribute to the final outcome. In keeping with this, ongoing experiments are focused on investigating whether the downregulation of ZEB1, which is the target demonstrated to mediate miR-205 radiozensitization in Breast [113], is also implicated in PCa miRNA sensitization. Preliminary results (data not shown) support this hypothesis, indicating that ZEB1 is downregulated upon miR-205 transfection and that ZEB1 silencing is able to partially recapitulate miR-205-sensitized phenotype, as well as observed for PKC-ε silencing (Fig. 6.8).

Conversely, it is also conceivable that other miR-205 targets act, directly or indirectly, counteracting this radiosensitizing effect, thus counterbalancing the overall outcome. This consideration can be inferred from the effect of PKC-ε silencing compared to that of the miRNA (Fig. 6.11). siPKC-ε induced a more enhanced radiosensitization than that of miR-205, suggesting that silencing only this specific target could lead to a greater sensitization than acting concomitantly on multiple targets as the miRNA does. At a first-sight consideration, this would prompt to prefer the exploitation of siRNA molecules rather that miRNA-based approaches in order to reach a higher sensitizing effect. However, it is worth noting that the greatest and most peculiar feature of miRNAs is precisely their ability to endogenously orchestrate the regulation of multiple target mechanisms, in an extraordinary balanced fashion, which is an exclusive property of physiological settings. On one hand, the study of the effect of a specific miRNA could help uncovering the underlying mechanisms in order to exploit such information for the design of diverse intervention strategies: for instance, the evidence that miR-205 acts as a radiosensitizer in

PCa via PKC-ε downregulation, would support the use of PKC-ε small inhibitors to reach the same, and even more enhanced, effect.

On the other hand, considering the importance of not exceeding in inducing a supra-physiological effect, it should be more appropriate to go for a more physiologic solution, by preferring the use of endogenous strategies, like miRNAs, also taking into account that these small molecules display the particular feature of simultaneously regulating multiple processes. In keeping with this is our finding that miR-205, likely due to its prominent role in EMT, was able to exert *per se* an oncosuppressive role *in vivo*, thus further impacting on the overall shrinkage of treated tumours. This toxic effect of the miRNA was not expected according to *in vitro* data, where the miRNA did not show any effect on cell viability and clonogenicity (as indicated by plating efficiency values in section 6.1.2). However, the ability of a miRNA to intervene in a multiplicity of mechanisms, including those that are not appreciable in cell model settings (e.g.: interaction with tumour microenvironment), could reasonably justify this result, further sustaining the choice of a miRNA-based multi-target strategy rather then one-target approaches.

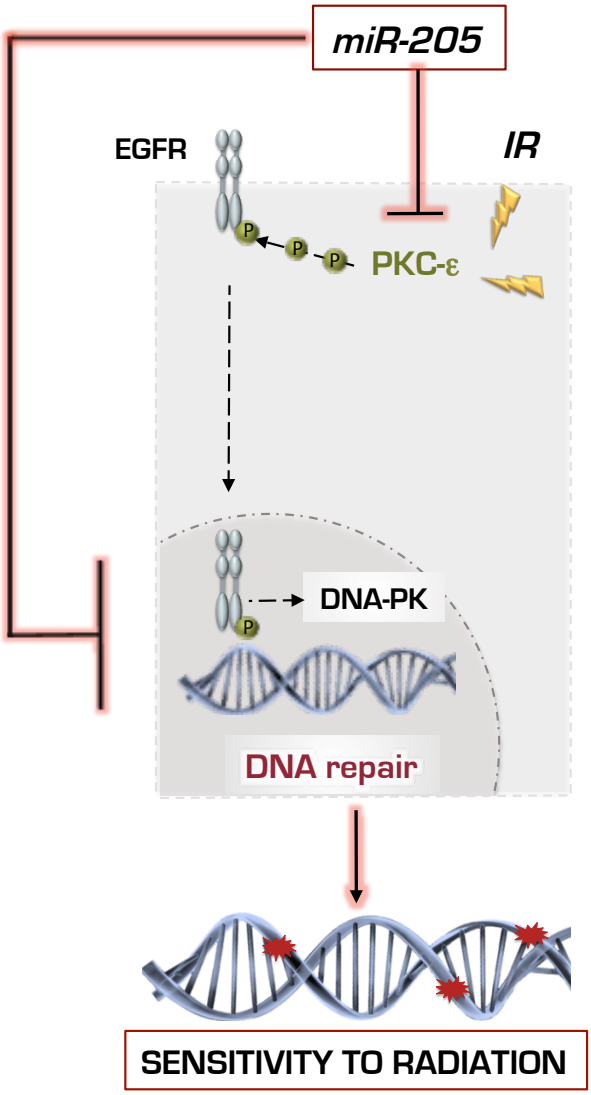

Figure 7.2 Schematic representation of miR-205 mechanism of radiosensitization in PCa

Overall, the results of this project support the clinical interest in developing novel therapeutic approaches for PCa based on miRNA reconstitution (miR-23a-3p, miR-875-5p and miR-205) to increase response to radiotherapy, based on their ability to concomitantly inhibit multiple processes, such as EMT and DNA damage repair, involved in radioresistance. Despite the indisputable advantage of using miRNAs to achieve a specific biological goal, including radiosensitization, it is worth mentioning that miRNA delivery represents a demanding challenge that still need to be addressed. In these regards, the applicability of strategies aimed at increasing specific miRNA expression in the clinical setting have been already investigated as the first liposomal nanoparticle-formulated mimic of the tumour suppressor miR-34a (MRX34) recently concluded the phase I clinical study for patients with different tumour types (https://clinicaltrials.gov/ct2/show/NCT01829971). Unfortunately, the trial terminated due to the onset of severe immune related adverse events in five patients.

miRNA	Identification Strategy	Modulation	Relevant Target
miR-23a-3p	1st	Downregulated (after IR)	IL-6
miR-24-3p	1st	Downregulated (after IR)	-
miR-875-5p	2nd	Downregulated (in PCa Vs normal)	EGFR
miR-205	2nd	Downregulated (in PCa Vs normal)	PKC-ε

Table 7.1. Table reporting the list of miRNAs identified throughout this study as candidate radiosensitizers in PCa and their respective targets demonstrated to mediate, at least in part, miRNA-induced radiosensitization.

7.3 Future perspectives

7.3.1 Fractionated radiotherapy

External beam radiation therapy is the most diffused radiotherapy treatment modality for patients with prostate cancer. A conformal delivery of treatment is ideally adopted in order to spare as much as possible the amount of radiation received by the surrounding normal tissues [182]. To address this challenging issue, fractionated radiotherapy is used. Fractionation consists of dividing the total dose of radiation into several, smaller doses over a period of several days, thus reducing the toxic effects on healthy cells. Nowadays, conventionally fractionated radiation therapy (CFRT, a single 1.8–2.0 Gy fraction lasting one hour per day, five days per week, for about eight weeks) to a total dose of 76–80 Gy represents the most adopted treatment modality [183]. Such CFRT schemes are based upon the premise that tumours typically are less responsive to fraction size than are late-responding normal tissues. Few years ago, John-Aryankalayil and collaborators investigated the alteration of miRNA profile upon fractionated radiation in prostate cancer [100]. Interestingly, they found that fractionated radiation significantly altered more miRNAs as compared to single-dose radiation. Encourage by these data and considering the increasing interest in fractionated radiotherapy in clinics, we propose to evaluate the impact of fractionated radiotherapy on PCa miRNome. Results will be compared with miRNA modulation profiles deriving from single-dose irradiation (results from section 4) in order to find out commonalities and differences between the two modalities of irradiation. For the sake of completeness, results deriving from our analysis will be also compared with data reported in literature so far.

7.3.2 Circulating miRNAs

The documented possibility to detect miRNAs in peripheral blood has raised the interest in defining their potential as novel biomarkers for treatment monitoring. Both cell-free miRNAs, that are released in the blood circulation from necrotic and apoptotic cells of different origin – and exosome/oncosomes-associated miRNAs [184] have been reported to be secreted from prostate cells. Specifically, functional miRNAs, which are different depending on the cells of origin (tumorigenic vs non-tumorigenic), were found to be released [184]. As far as radiation treatment is concerned, the only information currently available indicates that radiation increases the abundance of exosomes released by glioblastoma cells and normal astrocytes, and specifically alters their molecular composition [185], and that radiochemotherapy induces changes in circulating miRNAs in head and neck cancer patiens [186].

Based on these findings and taking advance of the availability of longitudinal plasma samples, collected before, during (after 8 Gy and 50 Gy) and at the end of treatment, from 20 PCa patients who underwent radical radiotherapy (78 Gy IMRT) at our Institute, we propose to identify miRNAs (cell-free or vescicle-associated) sensitive to radiation-induced modulation. Results should allow i) to determine the extent of overlap between the information generated with the 2 types of circulating miRNAs (cell-free vs vescicle-associated) and provide new insight into their role in the biology of PCa; ii) to define miRNAs significantly modulated by radiotherapy, which could be exploited as novel biomarkers for treatment monitoring. Radiation-modulated miRNAs in patient plasma will be compared with those identified in cell models (Results from section 4) to see

whether (and to what extent) *in vitro* findings can be predictive of the clinical situation.

REFERENCES

8. References

1. PubMed Health Glossary, NIH - National Cancer Institute, PMHT0025017

2. Schröder FH, Hugosson J, Roobol MJ, Tammela TLJ, Ciatto S, Nelen V, et al. Screening and Prostate-Cancer Mortality in a Randomized European Study. N Engl J Med. 2009;

3. Siegel RL, Miller KD, Jemal A. Cancer statistics, 2018. CA Cancer J Clin. 2018;

4. Patel VH. Nutrition and prostate cancer: An overview. Expert Rev. Anticancer Ther. 2014.

5. Rosato V, Edefonti V, Bravi F, Bosetti C, Bertuccio P, Talamini R, et al. Nutrient-based dietary patterns and prostate cancer risk: a case-control study from Italy. Cancer Causes Control. 2014;

6. Stangelberger A, Waldert M, Djavan B. Prostate cancer in elderly men. Rev Urol. 2008;

7. Mitra A V., Bancroft EK, Barbachano Y, Page EC, Foster CS, Jameson C, et al. Targeted prostate cancer screening in men with mutations in BRCA1 and BRCA2 detects aggressive prostate cancer: Preliminary analysis of the results of the IMPACT study. BJU Int. 2011;

8. Nakai Y, Nonomura N. Inflammation and prostate carcinogenesis. Int. J. Urol. 2013.

9. Thompson IM, Pauler DK, Goodman PJ, Tangen CM, Lucia MS, Parnes HL, et al. Prevalence of Prostate Cancer among Men with a Prostate-Specific Antigen Level ≤4.0 ng per Milliliter. N Engl J Med [Internet]. 2004 [cited 2018 Jun 26];350:2239–46. Available from:

http://www.ncbi.nlm.nih.gov/pubmed/15163773

10. Barry MJ. Prostate-Specific–Antigen Testing for Early Diagnosis of Prostate Cancer. N Engl J Med. 2001;

11. Matoso A, Epstein JI. Grading of Prostate Cancer: Past, Present, and Future. Curr. Urol. Rep. 2016.

12. Epstein JI, Egevad L, Amin MB, Delahunt B, Srigley JR, Humphrey PA. The 2014 international society of urological pathology (ISUP) consensus conference on gleason grading of prostatic carcinoma definition of grading patterns and proposal for a new grading system. Am J Surg Pathol. 2016;

13. Magi-Galluzzi C, Montironi R, Epstein JI. Contemporary Gleason grading and novel Grade Groups in clinical practice. Curr. Opin. Urol. 2016.

14. Gordetsky J, Epstein J. Grading of prostatic adenocarcinoma: Current state and prognostic implications. Diagn. Pathol. 2016.

15. Garisto JD, Klotz L. Active Surveillance for Prostate Cancer: How to Do It Right. Oncology (Williston Park). 2017;

16. Klotz L. Active surveillance: Patient selection. Curr. Opin. Urol. 2013.

17. Ballantyne GH, Moll F. The da Vinci telerobotic surgical system: The virtual operative field and telepresence surgery. Surg. Clin. North Am. 2003.

18. Yilmaz H, Aksu G, Dillioglugil O. External beam radiotherapy for localized prostate cancer. Asian J Androl. 2015;

19. Shioyama Y, Tsuji H, Suefuji H, Sinoto M, Matsunobu A, Toyama S, et al. Particle radiotherapy for prostate cancer. Int. J. Urol. 2015.

20. Brumm J. Brachytherapy as a treatment option for prostate cancer: overview and nursing considerations. Proc (Bayl Univ Med Cent) [Internet]. Baylor University Medical Center; 2000 [cited 2018 Jun 26];13:227–9. Available from: http://www.ncbi.nlm.nih.gov/pubmed/16389386

21. Mendes LO, Scarano WR, Rochel-Maia SS, Fioruci-Fontaneli BA, Chuffa LGA, Anselmo-Franci JA, et al. Androgen therapy reverses injuries caused by ethanol consumption in the prostate: Testosterone as a possible target to ethanol-related disorders. Life Sci. 2015;

22. Ryan CJ, Cheng ML. Abiraterone acetate for the treatment of prostate cancer. Expert Opin Pharmacother. 2013;

23. Zhang S, Wang Y, Chen Z, Kim S, Iqbal S, Chi A, et al. Genistein enhances the efficacy of cabazitaxel chemotherapy in metastatic castration-resistant prostate cancer cells. Prostate. 2013;

24. Cheever MA, Higano CS. PROVENGE (sipuleucel-T) in prostate cancer: The first FDA-approved therapeutic cancer vaccine. Clin. Cancer Res. 2011.

25. INTERNATIONAL ATOMIC ENERGY AGENCY, Radiation Biology: A Handbook for Teachers and Students, Training Course Series No. 42, IAEA, Vienna (2010)

26. Icrp. The 2007 Recommendations of the International Commission on Radiological Protection. Icrp 103. 2007;

27. Lomax ME, Folkes LK, O'Neill P. Biological consequences of radiation-induced DNA damage: Relevance to radiotherapy. Clin Oncol. 2013;

28. Paull TT, Rogakou EP, Yamazaki V, Kirchgessner CU, Gellert M, Bonner WM. A critical role for histone H2AX in recruitment of repair factors to nuclear foci after DNA damage. Curr Biol. 2000;

29. Firsanov D V., Solovjeva L V., Svetlova MP. H2AX phosphorylation at the sites of DNA double-strand breaks in cultivated mammalian cells and tissues. Clin. Epigenetics. 2011.

30. Maluf SW. Monitoring DNA damage following radiation exposure using cytokinesis-block micronucleus method and alkaline single-cell gel

electrophoresis. Clin. Chim. Acta. 2004.

31. Shibata A, Jeggo PA. DNA Double-strand Break Repair in a Cellular Context. Clin Oncol. 2014;

32. Lans H, Marteijn JA, Vermeulen W. ATP-dependent chromatin remodeling in the DNA-damage response. Epigenetics and Chromatin. 2012.

33. Palacios DA, Miyake M, Rosser CJ. Radiosensitization in prostate cancer: Mechanisms and targets. BMC Urol. 2013.

34. Gandellini P, Rancati T, Valdagni R, Zaffaroni N. miRNAs in tumor radiation response: bystanders or participants? Trends Mol. Med. 2014.

35. Bartel DP. MicroRNAs: Genomics, Biogenesis, Mechanism, and Function. Cell. 2004.

36. Zhong X, Coukos G, Zhang L. miRNAs in human cancer. Methods Mol Biol [Internet]. 2012 [cited 2018 Jun 26];822:295–306. Available from: http://link.springer.com/10.1007/978-1-61779-427-8_21

37. Calin GA, Sevignani C, Dumitru CD, Hyslop T, Noch E, Yendamuri S, et al. Human microRNA genes are frequently located at fragile sites and genomic regions involved in cancers. Proc Natl Acad Sci. 2004;

38. Gregory RI, Shiekhattar R. MicroRNA biogenesis and cancer. Cancer Res. 2005.

39. Brennecke J, Stark A, Russell RB, Cohen SM. Principles of microRNA-target recognition. PLoS Biol. 2005.

40. Eulalio A, Huntzinger E, Nishihara T, Rehwinkel J, Fauser M, Izaurralde E. Deadenylation is a widespread effect of miRNA regulation. RNA. 2009;

41. Ambros V. The functions of animal microRNAs. Nature. 2004.

42. Bentwich I, Avniel A, Karov Y, Aharonov R, Gilad S, Barad O, et al. Identification of hundreds of conserved and nonconserved human microRNAs.

Nat Genet. 2005;

43. Bartel DP. MicroRNAs: Target Recognition and Regulatory Functions. Cell. 2009.

44. Winter J, Jung S, Keller S, Gregory RI, Diederichs S. Many roads to maturity: MicroRNA biogenesis pathways and their regulation. Nat. Cell Biol. 2009.

45. Viswanathan SR, Daley GQ, Gregory RI. Selective blockade of microRNA processing by Lin28. Science (80-). 2008;

46. Lugli G, Torvik VI, Larson J, Smalheiser NR. Expression of microRNAs and their precursors in synaptic fractions of adult mouse forebrain. J Neurochem. 2008;

47. Liu J, Valencia-Sanchez MA, Hannon GJ, Parker R. MicroRNA-dependent localization of targeted mRNAs to mammalian P-bodies. Nat Cell Biol. 2005;

48. Kedde M, Strasser MJ, Boldajipour B, Vrielink JAFO, Slanchev K, le Sage C, et al. RNA-Binding Protein Dnd1 Inhibits MicroRNA Access to Target mRNA. Cell. 2007;

49. Eulalio A, Huntzinger E, Izaurralde E. Getting to the Root of miRNA-Mediated Gene Silencing. Cell. 2008.

50. Lewis BP, Burge CB, Bartel DP, Often , Pairing, RNA ,. Conserved Seed by Adenosines, Indicates that Thousands of Human Genes are Micro Cell; Cell. 2005;

51. Calin GA, Dumitru CD, Shimizu M, Bichi R, Zupo S, Noch E, et al. Nonlinear partial differential equations and applications: Frequent deletions and down-regulation of micro- RNA genes miR15 and miR16 at 13q14 in chronic lymphocytic leukemia. Proc Natl Acad Sci [Internet]. 2002 [cited 2018 Jun 26];99:15524–9. Available from:

http://www.pnas.org/cgi/doi/10.1073/pnas.242606799

52. Cimmino A, Calin GA, Fabbri M, Iorio M V., Ferracin M, Shimizu M, et al. miR-15 and miR-16 induce apoptosis by targeting BCL2. Proc Natl Acad Sci. 2005;

53. Calin GA, Liu C-G, Sevignani C, Ferracin M, Felli N, Dumitru CD, et al. MicroRNA profiling reveals distinct signatures in B cell chronic lymphocytic leukemias. Proc Natl Acad Sci USA. 2004;

54. Iorio M V, Ferracin M, Liu C, Veronese A, Spizzo R, Sabbioni S, et al. MicroRNA gene expression deregulation in human breast cancer. Cancer Res. 2005;

55. Ciafrè SA, Galardi S, Mangiola A, Ferracin M, Liu CG, Sabatino G, et al. Extensive modulation of a set of microRNAs in primary glioblastoma. Biochem Biophys Res Commun. 2005;

56. Murakami Y, Yasuda T, Saigo K, Urashima T, Toyoda H, Okanoue T, et al. Comprehensive analysis of microRNA expression patterns in hepatocellular carcinoma and non-tumorous tissues. Oncogene. 2006;

57. He H, Jazdzewski K, Li W, Liyanarachchi S, Nagy R, Volinia S, et al. The role of microRNA genes in papillary thyroid carcinoma. Proc Natl Acad Sci U S A. 2005;

58. Yanaihara N, Caplen N, Bowman E, Seike M, Kumamoto K, Yi M, et al. Unique microRNA molecular profiles in lung cancer diagnosis and prognosis. Cancer Cell. 2006;

59. Michael MZ, O' Connor SM, van Holst Pellekaan NG, Young GP, James RJ. Reduced accumulation of specific microRNAs in colorectal neoplasia. Mol Cancer Res. 2003;

60. Bloomston M, Frankel WL, Petrocca F, Volinia S, Alder H, Hagan JP, et al.

MicroRNA expression patterns to differentiate pancreatic adenocarcinoma from normal pancreas and chronic pancreatitis. J Am Med Assoc. 2007;

61. Hanahan D, Weinberg RA. Hallmarks of cancer: The next generation. Cell. 2011.

62. Esquela-Kerscher A, Slack FJ. Oncomirs - MicroRNAs with a role in cancer. Nat. Rev. Cancer. 2006.

63. Calin GA, Croce CM. MicroRNAs and chromosomal abnormalities in cancer cells. Oncogene. 2006.

64. Lujambio A, Esteller M. CpG island hypermethylation of tumor suppressor microRNAs in human cancer. Cell Cycle. 2007.

65. Calin GA, Ferracin M, Cimmino A, Di Leva G, Shimizu M, Wojcik SE, et al. A MicroRNA signature associated with prognosis and progression in chronic lymphocytic leukemia. N Engl J Med. 2005;

66. Nakamura T, Canaani E, Croce CM. Oncogenic All1 fusion proteins target Drosha-mediated microRNA processing. Proc Natl Acad Sci. 2007;

67. Karube Y, Tanaka H, Osada H, Tomida S, Tatematsu Y, Yanagisawa K, et al. Reduced expression of Dicer associated with poor prognosis in lung cancer patients. Cancer Sci. 2005;

68. He L, He X, Lim LP, De Stanchina E, Xuan Z, Liang Y, et al. A microRNA component of the p53 tumour suppressor network. Nature. 2007;

69. He L, Thomson JM, Hemann MT, Hernando-Monge E, Mu D, Goodson S, et al. A microRNA polycistron as a potential human oncogene. Nature. 2005;

70. Lu J, Getz G, Miska EA, Alvarez-Saavedra E, Lamb J, Peck D, et al. MicroRNA expression profiles classify human cancers. Nature. 2005;

71. Tong AW, Fulgham P, Jay C, Chen P, Khalil I, Liu S, et al. MicroRNA profile analysis of human prostate cancers. Cancer Gene Ther. 2009;

72. Schaefer A, Jung M, Mollenkopf H-J, Wagner I, Stephan C, Jentzmik F, et al. Diagnostic and prognostic implications of microRNA profiling in prostate carcinoma. Int J cancer. 2010;

73. Mitchell PS, Parkin RK, Kroh EM, Fritz BR, Wyman SK, Pogosova-Agadjanyan EL, et al. Circulating microRNAs as stable blood-based markers for cancer detection. Proc Natl Acad Sci. 2008;

74. Ambs S, Prueitt RL, Yi M, Hudson RS, Howe TM, Petrocca F, et al. Genomic profiling of microRNA and messenger RNA reveals deregulated microRNA expression in prostate cancer. Cancer Res. 2008;

75. Ozen M, Creighton CJ, Ozdemir M, Ittmann M. Widespread deregulation of microRNA expression in human prostate cancer. Oncogene. 2008;

76. Porkka KP, Pfeiffer MJ, Waltering KK, Vessella RL, Tammela TLJ, Visakorpi T. MicroRNA expression profiling in prostate cancer. Cancer Res. 2007;

77. Sun T, Du S-Y, Armenia J, Qu F, Fan J, Wang X, et al. Expression of lncRNA MIR222HG co-transcribed from the miR-221/222 gene promoter facilitates the development of castration-resistant prostate cancer. Oncogenesis [Internet]. 2018 [cited 2018 Jun 26];7:30. Available from: http://www.nature.com/articles/s41389-018-0039-5

78. Goto Y, Kojima S, Nishikawa R, Kurozumi A, Kato M, Enokida H, et al. MicroRNA expression signature of castration-resistant prostate cancer: the microRNA-221/222 cluster functions as a tumour suppressor and disease progression marker. Br J Cancer [Internet]. 2015 [cited 2018 Jun 26];113:1055–65. Available from: http://www.nature.com/articles/bjc2015300

79. Spahn M, Kneitz S, Scholz CJ, Stenger N, R??diger T, Str??bel P, et al. Expression of microRNA-221 is progressively reduced in aggressive prostate cancer and metastasis and predicts clinical recurrence. Int J Cancer. 2010;

80. Li T, Li RS, Li YH, Zhong S, Chen YY, Zhang CM, et al. MiR-21 as an independent biochemical recurrence predictor and potential therapeutic target for prostate cancer. J Urol. 2012;

81. Gandellini P, Folini M, Longoni N, Pennati M, Binda M, Colecchia M, et al. MiR-205 exerts tumor-suppressive functions in human prostate through down-regulation of protein kinase Cε. Cancer Res. 2009;

82. Verdoodt B, Neid M, Vogt M, Kuhn V, Liffers ST, Palisaar RJ, et al. MicroRNA-205, a novel regulator of the anti-apoptotic protein Bcl2, is downregulated in prostate cancer. Int J Oncol. 2013;

83. Wan Y, Zeng Z, Xi M, Wan S, Hua W, Liu Y, et al. Dysregulated microRNA-224/apelin axis associated with aggressive progression and poor prognosis in patients with prostate cancer. Hum Pathol [Internet]. 2015 [cited 2018 Jun 26];46:295–303. Available from: http://linkinghub.elsevier.com/retrieve/pii/S0046817714004729

84. FU H, He H chan, Han Z dong, Wan Y ping, Luo H wei, Huang Y qiang, et al. MicroRNA-224 and its target CAMKK2 synergistically influence tumor progression and patient prognosis in prostate cancer. Tumor Biol. 2015;

85. Al-Kafaji G, Al-Naieb ZT, Bakhiet M. Increased oncogenic microRNA-18a expression in the peripheral blood of patients with prostate cancer: A potential novel non-invasive biomarker. Oncol Lett. 2016;

86. Sun X, Liu Z, Yang Z, Xiao L, Wang F, He Y, et al. Association of microRNA-126 expression with clinicopathological features and the risk of biochemical recurrence in prostate cancer patients undergoing radical prostatectomy. Diagn Pathol. 2013;

87. Forno I, Ferrero S, Russo MV, Gazzano G, Giangiobbe S, Montanari E, et al. Deregulation of MIR-34b/Sox2 predicts prostate cancer progression. Culig Z,

editor. PLoS One [Internet]. 2015 [cited 2018 Jun 26];10:e0130060. Available from: http://dx.plos.org/10.1371/journal.pone.0130060

88. Zidan HE, Abdul-Maksoud RS, Elsayed WSH, Desoky EAM. Diagnostic and prognostic value of serum miR-15a and miR-16-1 expression among egyptian patients with prostate cancer. IUBMB Life [Internet]. 2018 [cited 2018 Jun 26];70:437–44. Available from: http://doi.wiley.com/10.1002/iub.1733

89. Doldi V, Pennati M, Forte B, Gandellini P, Zaffaroni N. Dissecting the role of microRNAs in prostate cancer metastasis: implications for the design of novel therapeutic approaches. Cell. Mol. Life Sci. 2016.

90. Hu H, Gatti RA. MicroRNAs: New players in the DNA damage response. J. Mol. Cell Biol. 2011.

91. Zhao L, Lu X, Cao Y. MicroRNA and signal transduction pathways in tumor radiation response. Cell. Signal. 2013.

92. Metheetrairut C, Slack FJ. MicroRNAs in the ionizing radiation response and in radiotherapy. Curr Opin Genet Dev. 2013;

93. Templin T, Paul S, Amundson SA, Young EF, Barker CA, Wolden SL, et al. Radiation-induced micro-RNA expression changes in peripheral blood cells of radiotherapy patients. Int J Radiat Oncol Biol Phys. 2011;

94. Simone NL, Soule BP, Ly D, Saleh AD, Savage JE, DeGraff W, et al. Ionizing radiation-induced oxidative stress alters miRNA expression. PLoS One. 2009;

95. Weidhaas JB, Babar I, Nallur SM, Trang P, Roush S, Boehm M, et al. MicroRNAs as potential agents to alter resistance to cytotoxic anticancer therapy. Cancer Res. 2007;

96. Ni J, Bucci J, Chang L, Malouf D, Graham P, Li Y. Targeting microRNAs in prostate cancer radiotherapy. Theranostics. 2017.

97. Petrocca F, Vecchione A, Croce CM. Emerging role of miR-106b-25/miR-17-92 clusters in the control of transforming growth factor beta signaling. Cancer Res [Internet]. 2008 [cited 2018 Jun 26];68:8191–4. Available from: http://cancerres.aacrjournals.org/cgi/doi/10.1158/0008-5472.CAN-08-1768

98. Li B, Shi XB, Nori D, Chao CKS, Chen AM, Valicenti R, et al. Down-regulation of microRNA 106b is involved in p21-mediated cell cycle arrest in response to radiation in prostate cancer cells. Prostate. 2011;

99. Gong P, Zhang T, He D, Hsieh J-T. MicroRNA-145 Modulates Tumor Sensitivity to Radiation in Prostate Cancer. Radiat Res. 2015;

100. John-Aryankalayil M, Palayoor ST, Makinde AY, Cerna D, Simone CB, Falduto MT, et al. Fractionated Radiation Alters Oncomir and Tumor Suppressor miRNAs in Human Prostate Cancer Cells. Radiat Res. 2012;

101. Josson S, Sung SY, Lao K, Chung LWK, Johnstone PAS. Radiation modulation of microRNA in prostate cancer Cell Lines. Prostate. 2008;

102. Hatano K, Kumar B, Zhang Y, Coulter JB, Hedayati M, Mears B, et al. A functional screen identifies miRNAs that inhibit DNA repair and sensitize prostate cancer cells to ionizing radiation. Nucleic Acids Res. 2015;

103. Mao A, Zhao Q, Zhou X, Sun C, Si J, Zhou R, et al. MicroRNA-449a enhances radiosensitivity by downregulation of c-Myc in prostate cancer cells. Sci Rep. 2016;

104. Mueller AC, Sun D, Dutta A. The miR-99 family regulates the DNA damage response through its target SNF2H. Oncogene. 2013;

105. Rane JK, Erb HHH, Nappo G, Mann VM, Simms MS, Collins AT, et al. Inhibition of the glucocorticoid receptor results in an enhanced miR-99a/100-mediated radiation response in stem-like cells from human prostate cancers. Oncotarget. 2016;

106. Gu H, Liu M, Ding C, Wang X, Wang R, Wu X, et al. Hypoxia-responsive miR-124 and miR-144 reduce hypoxia-induced autophagy and enhance radiosensitivity of prostate cancer cells via suppressing PIM1. Cancer Med. 2016;

107. Wang W, Liu M, Guan Y, Wu Q. Hypoxia-Responsive Mir-301a and Mir-301b Promote Radioresistance of Prostate Cancer Cells via Downregulating NDRG2. Med Sci Monit. 2016;

108. Wang W, Liu J, Wu Q. MiR-205 suppresses autophagy and enhances radiosensitivity of prostate cancer cells by targeting TP53INP1. Eur Rev Med Pharmacol Sci. 2016;

109. Liao H, Xiao Y, Hu Y, Xiao Y, Yin Z, Liu L. microRNA-32 induces radioresistance by targeting DAB2IP and regulating autophagy in prostate cancer cells. Oncol Lett. 2015;

110. Palena C, Hamilton DH, Fernando RI. Influence of IL-8 on the epithelial-mesenchymal transition and the tumor microenvironment. Futur. Oncol. 2012.

111. Cortez MA, Valdecanas D, Zhang X, Zhan Y, Bhardwaj V, Calin GA, et al. Therapeutic delivery of mir-200c enhances radiosensitivity in lung cancer. Mol Ther. 2014;

112. Lu Y, Li T, Wei G, Liu L, Chen Q, Xu L, et al. The long non-coding RNA NEAT1 regulates epithelial to mesenchymal transition and radioresistance in through miR-204/ZEB1 axis in nasopharyngeal carcinoma. Tumor Biol. 2016;

113. Zhang P, Wang L, Rodriguez-Aguayo C, Yuan Y, Debeb BG, Chen D, et al. MiR-205 acts as a tumour radiosensitizer by targeting ZEB1 and Ubc13. Nat Commun. 2014;

114. Calin GA, Croce CM. MicroRNA signatures in human cancers. Nat. Rev. Cancer. 2006.

115. Johnson SM, Grosshans H, Shingara J, Byrom M, Jarvis R, Cheng A, et al. RAS is regulated by the let-7 microRNA family. Cell. 2005;

116. Morris JP, McManus MT. Slowing Down the Ras Lane: miRNAs as Tumor Suppressors? Sci Signal. 2005;

117. Rosenfeld N, Aharonov R, Meiri E, Rosenwald S, Spector Y, Zepeniuk M, et al. MicroRNAs accurately identify cancer tissue origin. Nat Biotechnol. 2008;

118. Foekens JA, Sieuwerts AM, Smid M, Look MP, de Weerd V, Boersma AWM, et al. Four miRNAs associated with aggressiveness of lymph node-negative, estrogen receptor-positive human breast cancer. Proc Natl Acad Sci. 2008;

119. Schepeler T, Reinert JT, Ostenfeld MS, Christensen LL, Silahtaroglu AN, Dyrskjøt L, et al. Diagnostic and prognostic microRNAs in stage II colon cancer. Cancer Res. 2008;

120. Lanza G, Ferracin M, Gafà R, Veronese A, Spizzo R, Pichiorri F, et al. mRNA/microRNA gene expression profile in microsatellite unstable colorectal cancer. Mol Cancer. 2007;

121. Aharonov R, Lebanony D, Benjamin H, Gilad S, Ezagouri M, Dov A, et al. Diagnostic assay based on hsa-miR-205 expression distinguishes squamous from nonsquamous non-small-cell lung carcinoma. J Clin Oncol. 2009;

122. Guo Y, Chen Z, Zhang L, Zhou F, Shi S, Feng X, et al. Distinctive microRNA profiles relating to patient survival in esophageal squamous cell carcinoma. Cancer Res. 2008;

123. Li J, Smyth P, Flavin R, Cahill S, Denning K, Aherne S, et al. Comparison of miRNA expression patterns using total RNA extracted from matched samples of formalin-fixed paraffin-embedded (FFPE) cells and snap frozen cells. BMC Biotechnol. 2007;

124. Mattie MD, Benz CC, Bowers J, Sensinger K, Wong L, Scott GK, et al. Optimized high-throughput microRNA expression profiling provides novel biomarker assessment of clinical prostate and breast cancer biopsies. Mol Cancer. 2006;

125. Ng EKO, Chong WWS, Jin H, Lam EKY, Shin VY, Yu J, et al. Differential expression of microRNAs in plasma of patients with colorectal cancer: a potential marker for colorectal cancer screening. Gut. 2009;

126. Resnick KE, Alder H, Hagan JP, Richardson DL, Croce CM, Cohn DE. The detection of differentially expressed microRNAs from the serum of ovarian cancer patients using a novel real-time PCR platform. Gynecol Oncol. 2009;

127. Taylor DD, Gercel-Taylor C. MicroRNA signatures of tumor-derived exosomes as diagnostic biomarkers of ovarian cancer. Gynecol Oncol. 2008;

128. Rabinowits G, Gerçel-Taylor C, Day JM, Taylor DD, Kloecker GH. Exosomal microRNA: A diagnostic marker for lung cancer. Clin Lung Cancer. 2009;

129. Slaby O, Svoboda M, Fabian P, Smerdova T, Knoflickova D, Bednarikova M, et al. Altered expression of miR-21, miR-31, miR-143 and miR-145 is related to clinicopathologic features of colorectal cancer. Oncology. 2008;

130. Takamizawa J, Konishi H, Yanagisawa K, Tomida S, Osada H, Endoh H, et al. Reduced expression of the let-7 microRNAs in human lung cancers in association with shortened postoperative survival. Cancer Res. 2004;

131. Raponi M, Dossey L, Jatkoe T, Wu X, Chen G, Fan H, et al. MicroRNA classifiers for predicting prognosis of squamous cell lung cancer. Cancer Res. 2009;

132. Chen Y, Stallings RL. Differential patterns of microRNA expression in neuroblastoma are correlated with prognosis, differentiation, and apoptosis.

Cancer Res. 2007;

133. Nakajima G, Hayashi K, Xi Y, Kudo K, Uchida K, Takasaki K, et al. Non-coding microRNAs hsa-let-7g and hsa-miR-181b are associated with chemoresponse to S-1 in colon cancer. Cancer Genomics and Proteomics. 2006;

134. Ji J, Shi J, Budhu A, Yu Z, Forgues M, Roessler S, et al. MicroRNA expression, survival, and response to interferon in liver cancer. N Engl J Med. 2009;

135. Mishra PJ, Humeniuk R, Mishra PJ, Longo-Sorbello GSA, Banerjee D, Bertino JR. A miR-24 microRNA binding-site polymorphism in dihydrofolate reductase gene leads to methotrexate resistance. Proc Natl Acad Sci U S A. 2007;

136. Goto Y, Yue L, Yokoi a, Nishimura R, Uehara T, Koizumi S, et al. A novel single-nucleotide polymorphism in the 3'-untranslated region of the human dihydrofolate reductase gene with enhanced expression. Clin Cancer Res. 2001;

137. Chin LJ, Ratner E, Leng S, Zhai R, Nallur S, Babar I, et al. A SNP in a let-7 microRNA complementary site in the KRAS 3′ untranslated region increases non-small cell lung cancer risk. Cancer Res. 2008;

138. Tili E, Michaille JJ, Gandhi V, Plunkett W, Sampath D, Calin GA. miRNAs and their potential for use against cancer and other diseases. Futur Oncol. 2007;

139. Stenvang J, Silahtaroglu AN, Lindow M, Elmen J, Kauppinen S. The utility of LNA in microRNA-based cancer diagnostics and therapeutics. Semin. Cancer Biol. 2008.

140. Elmén J, Thonberg H, Ljungberg K, Frieden M, Westergaard M, Xu Y, et

al. Locked nucleic acid (LNA) mediated improvements in siRNA stability and functionality. Nucleic Acids Res. 2005;

141. Krützfeldt J, Rajewsky N, Braich R, Rajeev KG, Tuschl T, Manoharan M, et al. Silencing of microRNAs in vivo with “antagomirs.” Nature. 2005;

142. Bonci D, Coppola V, Musumeci M, Addario A, Giuffrida R, Memeo L, et al. The miR-15a-miR-16-1 cluster controls prostate cancer by targeting multiple oncogenic activities. Nat Med. 2008;

143. Fontana L, Fiori ME, Albini S, Cifaldi L, Giovinazzi S, Forloni M, et al. Antagomir-17-5p abolishes the growth of therapy-resistant neuroblastoma through p21 and BIM. PLoS One. 2008;

144. Creighton CJ, Nagaraja AK, Hanash SM, Matzuk MM, Gunaratne PH. A bioinformatics tool for linking gene expression profiling results with public databases of microRNA target predictions. RNA. 2008;

145. Yang Y, Chaerkady R, Beer MA, Mendell JT, Pandey A. Identification of miR-21 targets in breast cancer cells using a quantitative proteomic approach. Proteomics. 2009;

146. Blow N. Small RNAs: Delivering the future. Nature. 2007;

147. Pirollo KF, Zon G, Rait A, Zhou Q, Yu W, Hogrefe R, et al. Tumor-targeting nanoimmunoliposome complex for short interfering RNA delivery. Hum Gene Ther. 2006;

148. McNamara JO, Andrechek ER, Wang Y, Viles KD, Rempel RE, Gilboa E, et al. Cell type-specific delivery of siRNAs with aptamer-siRNA chimeras. Nat Biotechnol. 2006;

149. Blower PE, Chung J-H, Verducci JS, Lin S, Park J-K, Dai Z, et al. MicroRNAs modulate the chemosensitivity of tumor cells. Mol Cancer Ther. 2008;

150. Meng F, Henson R, Lang M, Wehbe H, Maheshwari S, Mendell JT, et al. Involvement of Human Micro-RNA in Growth and Response to Chemotherapy in Human Cholangiocarcinoma Cell Lines. Gastroenterology. 2006;

151. Cunningham D, You Z. In vitro and in vivo model systems used in prostate cancer research. J Biol Methods. 2015;

152. Nchinda G, Überla K, Zschörnig O. Characterization of cationic lipid DNA transfection complexes differing in susceptibility to serum inhibition. BMC Biotechnol. 2002;

153. Pennati M, Lopergolo A, Profumo V, De Cesare M, Sbarra S, Valdagni R, et al. MiR-205 impairs the autophagic flux and enhances cisplatin cytotoxicity in castration-resistant prostate cancer cells. Biochem Pharmacol. 2014;

154. Clarkson R, Lindsay PE, Ansell S, Wilson G, Jelveh S, Hill RP, et al. Characterization of image quality and image-guidance performance of a preclinical microirradiator. Med Phys. 2011;

155. Gabler J, Wittmann J, Porstner M, Renz H, Jäck HM, Abram M, et al. Contribution of microRNA 24-3p and Erk1/2 to interleukin-6-mediated plasma cell survival. Eur J Immunol. 2013;

156. Wu C Te, Chen MF, Chen WC, Hsieh CC. The role of IL-6 in the radiation response of prostate cancer. Radiat Oncol. 2013;

157. Aghaee-Bakhtiari SH, Arefian E, Naderi M, Noorbakhsh F, Nodouzi V, Asgari M, et al. MAPK and JAK/STAT pathways targeted by miR-23a and miR-23b in prostate cancer: computational and in vitro approaches. Tumor Biol. 2015;

158. Zhu LH, Liu T, Tang H, Tian RQ, Su C, Liu M, et al. MicroRNA-23a promotes the growth of gastric adenocarcinoma cell line MGC803 and downregulates interleukin-6 receptor. FEBS J. 2010;

159. Zhang P, Sun Y, Ma L. ZEB1: At the crossroads of epithelial-mesenchymal transition, metastasis and therapy resistance. Cell Cycle. 2015.

160. Javvadi P, Makino H, Das AK, Lin Y-F, Chen DJ, Chen BP, et al. Threonine 2609 Phosphorylation of the DNA-Dependent Protein Kinase Is a Critical Prerequisite for Epidermal Growth Factor Receptor-Mediated Radiation Resistance. Mol Cancer Res. 2012;

161. Shelly M, Mosesson Y, Citri A, Lavi S, Zwang Y, Melamed-Book N, et al. Polar expression of ErbB-2/HER2 in epithelia: Bimodal regulation by Lin-7. Dev. Cell. 2003.

162. Kaech SM, Whitfield CW, Kim SK. The LIN-2/LIN-7/LIN-10 complex mediates basolateral membrane localization of the C. elegans EGF receptor LET-23 in vulval epithelial cells. Cell. 1998;

163. Kim YM, Park S-Y, Pyo H. Cyclooxygenase-2 (COX-2) negatively regulates expression of epidermal growth factor receptor and causes resistance to gefitinib in COX-2-overexpressing cancer cells. Mol Cancer Res. 2009;

164. Sato F, Kubota Y, Natsuizaka M, Maehara O, Hatanaka Y, Marukawa K, et al. EGFR inhibitors prevent induction of cancer stem-like cells in esophageal squamous cell carcinoma by suppressing epithelial-mesenchymal transition. Cancer Biol Ther. 2015;

165. Nambiar DK, Rajamani P, Deep G, Jain AK, Agarwal R, Singh RP. Silibinin Preferentially Radiosensitizes Prostate Cancer by Inhibiting DNA Repair Signaling. Mol Cancer Ther. 2015;

166. Zhang P, Wei Y, Wang L i., Debeb BG, Yuan Y, Zhang J, et al. ATM-mediated stabilization of ZEB1 promotes DNA damage response and radioresistance through CHK1. Nat Cell Biol. 2014;

167. Gregory PA, Bert AG, Paterson EL, Barry SC, Tsykin A, Farshid G, et al.

The miR-200 family and miR-205 regulate epithelial to mesenchymal transition by targeting ZEB1 and SIP1. Nat Cell Biol. 2008;

168. Wanner G, Mayer C, Kehlbach R, Rodemann HP, Dittmann K. Activation of protein kinase Cepsilon stimulates DNA-repair via epidermal growth factor receptor nuclear accumulation. Radiother Oncol. 2008;

169. Chang L, Graham PH, Hao J, Bucci J, Cozzi PJ, Kearsley JH, et al. Emerging roles of radioresistance in prostate cancer metastasis and radiation therapy. Cancer Metastasis Rev. 2014;

170. Dittmann K, Mayer C, Kehlbach R, Rodemann HP. Radiation-induced caveolin-1 associated EGFR internalization is linked with nuclear EGFR transport and activation of DNA-PK. Mol Cancer. 2008;

171. Alongi F, De Bari B, Campostrini F, Arcangeli S, Matei DV, Lopci E, et al. Salvage therapy of intraprostatic failure after radical external-beam radiotherapy for prostate cancer: A review. Crit. Rev. Oncol. Hematol. 2013.

172. Thariat J, Hannoun-Levi J-M, Sun Myint A, Vuong T, Gérard J-P. Past, present, and future of radiotherapy for the benefit of patients. Nat Rev Clin Oncol. 2013;

173. Chhabra R, Dubey R, Saini N. Cooperative and individualistic functions of the microRNAs in the miR-23a~27a~24-2 cluster and its implication in human diseases. Mol Cancer [Internet]. 2010 [cited 2018 Jun 27];9:232. Available from: http://www.ncbi.nlm.nih.gov/pubmed/20815877

174. Orecchia R, Zurlo A, Loasses A, Krengli M, Tosi G, Zurrida S, et al. Particle beam therapy (hadrontherapy): Basis for interest and clinical experience. Eur. J. Cancer. 1998.

175. Denekamp J. Neutron radiobiology revisited. Acta Oncol [Internet]. 1994 [cited 2018 Jun 26];33:233–40. Available from:

http://www.ncbi.nlm.nih.gov/pubmed/8018351

176. Smith B, Bhowmick N. Role of EMT in Metastasis and Therapy Resistance. J Clin Med. 2016;

177. Brand TM, Iida M, Luthar N, Starr MM, Huppert EJ, Wheeler DL. Nuclear EGFR as a molecular target in cancer. Radiother. Oncol. 2013.

178. Chen DJ, Nirodi CS. The epidermal growth factor receptor: a role in repair of radiation-induced DNA damage. Clin Cancer Res. 2007;

179. Schmidt-Ullrich RK, Mikkelsen RB, Dent P, Todd DG, Valerie K, Kavanagh BD, et al. Radiation-induced proliferation of the human A431 squamous carcinoma cells is dependent on EGFR tyrosine phosphorylation. Oncogene. 1997;

180. Minjgee M, Toulany M, Kehlbach R, Giehl K, Rodemann HP. K-RAS(V12) induces autocrine production of EGFR ligands and mediates radioresistance through EGFR-dependent Akt signaling and activation of DNA-PKcs. Int J Radiat Oncol Biol Phys. 2011;

181. De Jong MC, Ten Hoeve JJ, Grénman R, Wessels LF, Kerkhoven R, Te Riele H, et al. Pretreatment microRNA expression impacting on epithelial-to-mesenchymal transition predicts intrinsic radiosensitivity in head and neck cancer cell lines and patients. Clin Cancer Res. 2015;

182. Mangoni M, Desideri I, Detti B, Bonomo P, Greto D, Paiar F, et al. Hypofractionation in prostate cancer: Radiobiological basis and clinical appliance. Biomed Res. Int. 2014.

183. Nakamura K, Sawada K, Yoshimura A, Kinose Y, Nakatsuka E, Kimura T. Clinical relevance of circulating cell-free microRNAs in ovarian cancer. Mol. Cancer. 2016.

184. Morello M, Minciacchi VR, De Candia P, Yang J, Posadas E, Kim H, et al.

Large oncosomes mediate intercellular transfer of functional microRNA. Cell Cycle. 2013;

185. Arscott WT, Tandle AT, Zhao S, Shabason JE, Gordon IK, Schlaff CD, et al. Ionizing Radiation and Glioblastoma Exosomes: Implications in Tumor Biology and Cell Migration. Transl Oncol. 2013;

186. Summerer I, Niyazi M, Unger K, Pitea A, Zangen V, Hess J, et al. Changes in circulating microRNAs after radiochemotherapy in head and neck cancer patients. Radiat Oncol. 2013;

9. Publications

Publication on the thesis project

El Bezawy R, Cominetti D, Fenderico N, Zuco V, Beretta GL, Dugo M, Arrighetti N, Stucchi C, Rancati T, Valdagni R, Zaffaroni N, Gandellini P. **miR-875-5p counteracts epithelial-to-mesenchymal transition and enhances radiation response in prostate cancer through repression of the EGFR-ZEB1 axis.** Cancer Lett. 2017 Jun 1;395:53-62. doi: 10.1016/j.canlet.2017.02.033. Epub 2017 Mar 6. PubMed PMID: 28274892.

Other publication during the PhD period

El Bezawy R, De Cesare M, Pennati M, Deraco M, Gandellini P, Zuco V, Zaffaroni N. **Antitumor activity of miR-34a in peritoneal mesothelioma relies on c-MET and AXL inhibition: persistent activation of ERK and AKT signaling as a possible cytoprotective mechanism.** J Hematol Oncol. 2017 Jan 18;10(1):19. doi: 10.1186/s13045-016-0387-6. PubMed PMID: 28100259; PubMed Central PMCID: PMC5242015.

10. Contributorship

I declare that I was actively engaged in the realization of the project, including participation in the concept and design of the study, acquisition and analysis of the data, writing and revision of the related manuscript.

In particular, I was first hand involved in the execution of all experiments included in the project, except for:

- ***In vivo* experiments** (animal manipulation): performed by Dr. Denis Cominetti
- **miRNA-Profiling analyses**: carried out by the institutional genomics core facility
- **Bioinformatic analysis**: carried out by Dr. Paolo Gandelini and Dr. Ivan Salido

Persons acknowledged in the “acknowledgement” section also contributed to the execution of some experiments.

The concept/design of the study and the drafting/revising of the manuscript were carried out under the supervision and with the intellectual contribution of my director of studies Dr. Nadia Zaffaroni.